Volume 10, Number 1
January–February 2002

ISSN: 0869-5938

STRATIGRAPHY AND GEOLOGICAL CORRELATION

English Translation of *Stratigrafiya. Geologicheskaya Korrelyatsiya*

Editor-in-Chief
Boris S. Sokolov

http://www.maik.ru

Journal of the Fundamental and Applied Aspects of Stratigraphy and the Correlation of Geologic Events and Processes in Time and Space

МАИК "НАУКА/INTERPERIODICA" PUBLISHING

Stratigraphy and Geological Correlation

(Stratigrafiya. Geologicheskaya Korrelyatsiya)

ISSN: 0869-5938

Editor-in-Chief
Boris S. Sokolov
Member of the Russian Academy of Sciences,
Counsellor of the Presidium of the Russian Academy of Sciences (RAS)
Address for correspondence:
Staromonetnyi per. 22, Moscow, 109180 Russia
Phones: 7 (095) 951-2164; Fax: 7 (095) 953-5590.

Deputy Editor-in-Chief
Mikhail A. Semikhatov
Member of the Russian Academy of Sciences
Head of Laboratory, Geological Institute, RAS
E-mail: semikhatov@ginran.msk.su

Assistant Editor
Aleksei B. Herman
Senior Scientist,
Geological Institute, RAS
E-mail: herman@ginran.msk.su

EDITORIAL BOARD

Mikhail A. Akhmet'ev
Dr. Sci. (Geol.–Min.),
Head of Laboratory, Geological Institute, RAS
akhmetev@ginran.msk.su

Aleksandr S. Alekseev
Professor, Dr.Sci. (Geol.–Min.),
Department of Paleontology,
Moscow State University
aaleks@geol.msu.ru

Mikhail N. Alekseev
Dr. Sci. (Geol.–Min.),
Chief Scientist, Geological Institute, RAS
alekseev@ginran.msk.su

Ivan A. Basov
Dr. Sci. (Geol.–Min.), Laboratory Chief,
Institute of the Lithosphere, RAS
basov@ilsan.msk.ru

Michael G. Basset
Professor, National Museum of Wales,
Cardiff, UK

William A. Berggren
Professor, Department of Geology and Geophysics,
Woods Hole Oceanographic Institute, USA

Elena V. Bibikova
Dr. Sci. (Geol.–Min.), Chief Scientist,
Vernadsky Institute of Geochemistry
and Analytical Chemistry, RAS
sergei@bibikov.genebee.msu.su

Nikita A. Bogdanov
Corresponding Member of
RAS, Director, Institute of the Lithosphere, RAS
bogdanov@ilsan.msk.ru

Kiyotaka Chinzei
Professor, Institute of Geology,
University of Tokyo,
Tokyo, Japan

Nikolai M. Chumakov
Dr. Sci. (Geol.–Min.),
Chief Scientist, Geological Institute, RAS
chumakov@ginran.msk.su

Yurii B. Gladenkov
Dr. Sci. (Geol.–Min.),
Head of Laboratory, Geological Institute, RAS
gladenkov@ginran.msk.su

Mikhail A. Fedonkin
Corresponding Member of RAS, Laboratory Chief,
Paleontological Institute, RAS
mfedon@paleo.ru

Dmitrii L. Kaljo
Professor, Institute of Geology, Tallinn, Estonia

Kirilla I. Kuznetsova
Dr. Sci. (Geol.–Min.), Chief Scientist,
Geological Institute, RAS
kuznetsova@ginran.msk.ru

Victor E. Khain
Member of RAS, Chief Scientist,
Institute of the Lithosphere, RAS

Evgenii E. Musatov†
Dr. Sci. (Geol.–Min.), Chief of St. Petersburg
Division, Institute of the Lithosphere, RAS
musatov@gocean.spl.su

Lidiya A. Nevesskaya
Dr. Sci. (Biol.), Laboratory Chief,
Institute of Paleontology, RAS
lenin33@paleo.ru

Aleksandr G. Ponomarenko
Dr. Sci. (Biol.), Chief Scientist,
Institute of Paleontology, RAS
vtopor@paleo.ru

Jurgen Remane
Professor, Institute de Géologie,
Université de Neuchâtel, Switzerland

Aleksei Yu. Rozanov
Corresponding Member of RAS,
Director, Institute of Paleontology, RAS
aroza@paleo.ru

Boris A. Sokolov
Corresponding Member of RAS, Professor, Dean,
Faculty of Geology, Moscow State University
mfedon@paleo.ru

Otto Walliser
Professor, Göttingen University, Göttingen,
Germany

Sun Weigo
Professor, Nanjing Institute of Geology
and Paleontology, Academia Sinica, China

Victor A. Zakharov
Dr. Sci. (Geol.–Min.), Head of Laboratory, Institute
of Geology, Geophysics, and Mineralogy, Siberian
Division, RAS, Novosibirsk

Aleksandr I. Zhamoida
Corresponding Member of RAS,
Russian Geological Institute, St. Petersburg

Staff Editor Tamara V. Trishkina

Editor of the English Translation Anatolii Ya. Sharas'kin, Dr. Sci. (Geol.–Min.)

SCOPE

Stratigraphy and Geological Correlation (*Stratigrafiya. Geologicheskaya Korrelyatsiya*) is the only journal in the world designed to provide comprehensive coverage of the fundamental and applied aspects of stratigraphy and the correlation of geological events and processes in time and space. Articles are based on the results of multidisciplinary research and are directed toward researchers, university professors, students, and geologists interested in understanding stratigraphy and the chronological features of the world's geological record.

Stratigraphy and Geological Correlation is abstracted and/or indexed in *Petroleum Abstracts*, *Research Alert*, *SciSearch*, *Current Contents* (*Physical, Chemical*, and *Earth Sciences*) and *World Translations Index*.

SUBSCRIPTION OFFICE
INTERPERIODICA
P.O. BOX 1831, BIRMINGHAM, AL 35201-1831 USA
PHONE: (800) 633-4931; (205) 995-1567 (outside US and Canada)
FAX: (205) 995-1588

PUBLISHER
INTERNATIONAL ACADEMIC PUBLISHING
COMPANY "NAUKA/INTERPERIODICA"
PROFSOYUZNAYA UL. 90, MOSCOW, 117997 RUSSIA
PHONE: 7 (095) 336-1600; FAX: 7 (095) 336-0666
E-mail: compmg@maik.ru
Web Site: http://www.maik.ru

SUBSCRIPTION PRICES (2002, Volume 10, 6 issues)
US $1165.00 (North America), $1335.00 (elsewhere). A 5% discount is given on 2-year orders. Subscriptions may be entered at any time. Orders may be placed at agencies or directly. There is a 5% discount to all subscription agencies. Cancellations not allowed except for duplicate payment. Prepayment required. Advance payment required in US$/US bank. MasterCard/Visa accepted. Make checks payable to *Stratigraphy and Geological Correlation* or Interperiodica.

Stratigraphy and Geological Correlation (ISSN: 0869-5938) is published bimonthly for US $1165.00 (North America), outside North America for $1335.00 per year by MAIK "Nauka/Interperiodica", 5724 Hwy. 280 East, Birmingham, Alabama 35242-5724 USA. Periodical postage paid at Birmingham, Alabama, and additional mailing offices. POSTMASTER: Send address changes to *Stratigraphy and Geological Correlation*, P.O. Box 1831, Birmingham, Alabama 35201 USA.

The journal was founded in 1993.

Original Russian Edition Copyright © 2002 by the Russian Academy of Sciences
and Division of Geology, Geophysics, Geochemistry, and Mining Sciences, RAS.
English Translation Copyright © 2002 by MAIK "Nauka/Interperiodica" (Russia).
Printed in the USA by Pleiades Publishing, Inc.

Contents

Vol. 10, No. 1, 2002

Simultaneous English language translation of the journal is available from MAIK "Nauka/Interperiodica" (Russia).
Stratigraphy and Geological Correlation ISSN 0869-5938.

Low $^{87}Sr/^{86}Sr$ Ratios in Seawater of the Grenville and post-Grenville Time: Determining Factors
M. A. Semikhatov, A. B. Kuznetsov, I. M. Gorokhov, G. V. Konstantinova, N. N. Mel'nikov, V. N. Podkovyrov, and E. P. Kutyavin 1

Stratigraphy of Lower Horizons in the Siberian Hypostratotype of the Riphean (the Southeastern Siberian Platform)
L. P. Karsakov, V. A. Gur'yanov, and M. V. Goroshko 42

The Famennian Stage of the Southern Transcaucasia
A. B. Mamedov 57

Correlation of Albian Radiolarian Assemblages from the Greater Caucasus, Europe, and Mediterranean
L. I. Kazintsova 69

New Data on Paleogene Biostratigraphy of the Eastern Crimea
E. M. Bugrova, E. Yu. Zakrevskaya, and I. P. Tabachnikova 77

The Holocene Dynamics of Vegetation in Buryatia
P. E. Tarasov, N. I. Dorofeyuk, and P. B. Vipper† 88

Personalia

Academician M.A. Semikhatov and Proterozoic Geology (on the Occasion of His 70th Birthday) 97

Stratigraphy and Geological Correlation, Vol. 10, No. 1, 2002, pp. 1–41. Translated from Stratigrafiya. Geologicheskaya Korrelyatsiya, Vol. 10, No. 1, 2002, pp. 3–46.
Original Russian Text Copyright © 2002 by Semikhatov, Kuznetsov, Gorokhov, Konstantinova, Mel'nikov, Podkovyrov, Kutyavin.
English Translation Copyright © 2002 by MAIK "Nauka/Interperiodica" (Russia).

Low $^{87}Sr/^{86}Sr$ Ratios in Seawater of the Grenville and post-Grenville Time: Determining Factors

M. A. Semikhatov*, A. B. Kuznetsov, I. M. Gorokhov**, G. V. Konstantinova**, N. N. Mel'nikov**, V. N. Podkovyrov**, and E. P. Kutyavin****

**Geological Institute, Russian Academy of Sciences, Pyzhevskii per. 7, Moscow, 109017 Russia*

***Institute of Precambrian Geology and Geochronology, Russian Academy of Sciences, nab. Makarova 2, St. Petersburg, 199034 Russia*

Received February 20, 2001

Abstract—The results obtained contribute much to the reconstruction of secular Sr isotope variations in seawater of the late Middle–early Late Riphean and elucidate factors that determined low values of the $^{87}Sr/^{86}Sr$ ratios in the World Ocean at the formation time of Rodinia (Grenville orogenic cycle). The new curve that depicts the Sr isotope variations in seawater 1050–1000 Ma ago is much more detailed than others characterizing the Precambrian. It is plotted after investigation of limestones collected from the Kerpyl' and Lakhanda groups of the East Siberian Uchur–Maya region and of correlative limestones from the Turukhansk region of Central Siberia. In order to obtain the confident analytical data determining the curve configuration, the selection of limestone samples was controlled by petrographic and strict geochemical criteria ($Mn/Sr \le 0.20$, $Fe/Sr \le 5.0$, $Mg/Ca \le 0.024$) that ensure the least alteration degree of rocks. In addition, all the selected samples were preliminary treated in 1N solution of ammonium acetate for the partial removal of epigenetic carbonate phases. We took into consideration the lowest $^{87}Sr/^{86}Sr$ ratios obtained for dolomites only as evaluating the maximum limit of this parameter in the sedimentation medium. After generalization of all Sr-isotopic data available for the Middle–early Late Riphean, we established that the $^{87}Sr/^{86}Sr$ ratios in seawater did not exceed 0.70490 about 1300 Ma ago and began to rise afterward to become as high as 0.70518–0.70549 approximately 1200 Ma ago. At the end of the Middle Riphean (1050–1030 Ma), the ratios reached a relative peak of values corresponding to 0.70563–0.70592, after which they decreased. During the earliest Late Riphean (1030–1000 Ma), they varied between 0.70519 and 0.70569, generally decreasing with time, and became equal to 0.70523–0.70527 1000 Ma ago. Within the time span of 900–800 Ma, the $^{87}Sr/^{86}Sr$ ratios were likely not greater than 0.70525–0.70585. The following factors and events appear to be responsible for the persistently low $^{87}Sr/^{86}Sr$ ratios in seawater of the Grenville and post-Grenville time: a high proportion of the pre-Grenvillide mantle rocks in the crust of Grenvillides; peculiar features of metamorphism, exhumation, and unroofing of different lithotectonic units in the Grenville orogens; an active influx of fresh juvenile material into oceans of the Grenville time; the Late Grenville sea-level rise; and, possibly, the partial locking up of the continental runoff in inner continental depressions at the beginning of the Late Riphean.

Key words: strontium, $^{87}Sr/^{86}Sr$ ratio in seawater, Riphean, carbonate rocks, Grenville orogenic cycle, Rodinia, Laurentia, Siberia.

INTRODUCTION

Generation of the supercontinent Rodinia during the Grenville orogenic cycle 1250–980 Ma ago (McMenamin and McMenamin, 1990; Hoffman, 1991; Powell *et al.*, 1993) and its subsequent breakup in the period of 830–750 Ma (Powell *et al.*, 1993; Wingate *et al.*, 1998) were the most significant geodynamic events of the Riphean. By analogy with the Pan-African orogeny that resulted in origin of Gondwana (Hurley *et al.*, 1967; de Almeida, 1968; Trompete, 1994, and references in the last work) and in unprecedented rise of $^{87}Sr/^{86}Sr$ ratios in seawater 600–520 Ma ago, it seems reasonable to expect that the Grenville events should also give rise to a sudden increase of this parameter for a long time.

Such an expectation is rooted in the fact that the $^{87}Sr/^{86}Sr$ ratios, which are constant in the World Ocean at a given moment, change with time being dependent on variable proportions between two main geochemical fluxes into the terminal drainage basins: the mantle one that contains the low-radiogenic Sr and the continental flux that is enriched to a different extent in ^{87}Sr. The former includes components extracted by seawater from the mantle-derived rocks, and the latter corresponds to the weathering products curried by surface and ground waters from the continental crust into the basins. At present, the average $^{87}Sr/^{86}Sr$ ratio in the continental flux is estimated to be within the range of 0.7105–0.7115 and varies from 0.7095 to 0.7384 in largest rivers depending on the rock composition in provenances (Wadleigh *et al.*, 1985; Goldstein and

Jacobsen, 1988; Palmer and Edmond, 1989). In the mantle flux, this parameter is currently equal to 0.7030–0.7035 (Albarede *et al.*, 1981; Palemer and Edmond, 1989; Veizer *et al.*, 1989, 1992). About 1 Ga ago, it was close to 0.7028 in accord with isotopic evolution of the upper mantle (Faure, 1986; Goldstein and Jacobsen, 1988; Mirota and Veizer, 1994). One is able to determine the Sr isotope composition of seawater in paleooceans, because the carbonate, sulfate, and phosphate sediments of marine origin inherit the $^{87}Sr/^{86}Sr$ ratio of their sedimentation medium and may retain this isotopic signature until the present under particular conditions.

First models explaining the Sr isotopic variations in the Precambrian oceans was based on limited data that implied the progressive and considerable increase of $^{87}Sr/^{86}Sr$ ratios during the entire Proterozoic (Veizer and Compston, 1976). The more extensive database obtained after investigations in North America and Arctic regions confirmed this general tendency of the $^{87}Sr/^{86}Sr$ ratio growth in the Riphean seawater (Derry *et al.*, 1989, 1992, 1994; Asmerom *et al.*, 1991; Kaufman *et al.*, 1993, 1996) except for two short-term episodes, when this ratio decreased owing to the enhanced contribution of the mantle flux during the Adrar (Veizer *et al.*, 1983) and Shaler (Asmerom *et al.*, 1991) events that happened about 900 and 800–750 Ma ago, respectively.

Later on, Gorokhov and his colleagues (1995a) who analyzed the Sr isotope composition in the Middle–Upper Riphean boundary deposits of Siberia obtained the results conflicting with the above conclusions of the 1980s and initial 1990s. Using the strict geochemical criteria of secondary alteration of the analyzed carbonate rocks, and a special procedure that removed the secondary carbonate phases, these researchers demonstrated that, in the period of 1100–850 Ma, the $^{87}Sr/^{86}Sr$ ratios in seawater did not increase but somewhat decreased against the general background of their low values. The subsequent investigations of materials from Siberia (Khabarov *et al.*, 1998, 2000; Semikhatov *et al.*, 1998; Vinogradov *et al.*, 1998; Kuznetsov *et al.*, 2000; Bartley *et al.*, 2001) confirmed the low level (< 0.7062) of $^{87}Sr/^{86}Sr$ ratios in seawater of the late Middle–early Late Riphean and elucidated some factors responsible for this phenomenon. As it was shown in a series of works (Gorokhov *et al.*, 1996; Kuznetsov *et al.*, 1997, 2000; Kuznetsov, 1998), the low $^{87}Sr/^{86}Sr$ ratios corresponding to 0.7053–0.7061 were characteristic of paleooceans almost until the end of the Late Riphean.

Not long ago, Jacobsen and Kaufman (1999) generalized data on the Sr isotope composition in the Neoproterozoic carbonate rocks and plotted the new reference curve of $^{87}Sr/^{86}Sr$ variations in seawater during the period of 800–530 Ma. In the Late Riphean part of the curve, they noted the interval of low $^{87}Sr/^{86}Sr$ ratios decreasing down to 0.7056 and characterizing the Shaler event (800–750 Ma), after which this parameter varied between 0.7063 and 0.7075. Discussing the older Riphean horizons, Jacobsen and Kaufman mentioned some indications of low-radiogenic Sr isotope composition that was characteristic of seawater 1100–800 Ma ago, but they did not consider this issue in detail.

In this work, our objectives were as follows: (1) to enlarge the database on the $^{87}Sr/^{86}Sr$ initial ratios in carbonate rocks that accumulated during and after the Grenville orogeny of the late Middle–early Late Riphean; (2) to plot the refined version of the reference curve depicting the Sr isotope variations in the global ocean of that time; and (3) to consider possible reasons, which may explain a contradiction between the high intensity of Grenville orogeny and the low-radiogenic Sr isotope composition in seawater of the Grenville and post-Grenville time. In order to solve the first problem, we studied the Rb–Sr systematics of those limestones from the Kerpyl' and Lakhanda groups of the Uchur–Maya region in East Siberia, which fit the strict criteria ensuring their geochemical retentivity. The second one was solved using a synthesis of new and earlier data on the Sr isotope composition in the Middle–Upper Riphean deposits of the Uchur–Maya and Turukhansk regions of Siberia, where their sections are studied in this respect much better than any other Riphean succession, and a comparison with relevant data on the underlying and overlying strata. The third problem kept us at the analysis of those factors, which influenced the Sr isotope composition in the Riphean oceans.

CARBONATES SUITABLE FOR ASSESSMENT OF Sr ISOTOPE COMPOSITION IN PALEOOCEANS

Several versions of $^{87}Sr/^{86}Sr$ variation curves in the Riphean seawater are known from publications (Veizer and Compston, 1976; Asmerom *et al.*, 1991; Derry *et al.*, 1992; Gorokhov *et al.*, 1995a, 1996; Jacobsen and Kaufman, 1999; Melezhik *et al.*, in press), and this is to a great extent a consequence of different criteria that have been used for selection of materials substantiating those curves. Accordingly, we feel it necessary to stress here that carbonate rocks appropriate for the Sr isotope analysis must meet three requirements: (1) age of samples must be substantiated on the basis of precise recent data; (2) independent control methods must be used to show that rocks selected for analysis are pristine in geochemical aspect, and (3) secondary carbonate phases, if they present, must be removed as completely as possible.

To meet the first requirement, we should study the continuous rock successions of predominantly carbonate composition, which are well investigated in geochronological, C-isotope chemostratigraphic, and paleontological aspects. In this case, we have a good opportunity for the age calibration of Sr isotope variations in a single section and also for the realistic correlation of

several individual sections, where these variations are established.

The second requirement means that it is necessary to give priority to the preliminary geochemical investigation of rocks in order to select the "best" samples affected by secondary alterations to a minimum extent. Selecting them, we can use the known redistribution patterns of trace elements (Mn, Fe, and Sr) in the course of rock alterations under influence of basinal brains, ground or meteoric waters and the pertinent covariation of these elements concentrations and $^{87}Sr/^{86}Sr$ ratios in the carbonate rocks (Brand and Veizer, 1980; Banner and Hanson, 1990; Gorokhov *et al.*, 1995a; Gorokhov, 1996; Kuznetsov *et al.*, 1997, 2000). Having geological and geochemical data for a given region, we are able to understand reasons of secondary alterations in carbonate rocks and to determine threshold values of geochemical criteria, which indicate the applicability of selected rocks for the assessment of Sr isotope composition in seawater. Unfortunately, such an approach is now appropriate for the Precambrian limestones only, because we inadequately know the behavior of trace elements in the course of formation and alteration of dolomites. The above approach is likely applicable only to some dolomitic formations of uniform lithology (Kuznetsov, 1998; Kuznetsov *et al.*, 1998), in which the necessary covariation of Mn/Sr and Fe/Sr on the one hand, and $^{87}Sr/^{86}Sr$ ratios on the other hand is established.

As for usability of $\delta^{18}O$ values for the assessment of secondary alterations in carbonate rocks, they are of a low informative potential because of a strong difference between the O and Sr concentrations in carbonates and epigenetic fluids, and between the water/carbonate distribution coefficients of both elements. As is known (Banner and Hanson, 1990; Jacobsen and Kaufman,1999), the oxygen isotopic systems can be transformed easier than those of strontium, and the difference in water/rock ratios by their transformations is as high as one–two orders of magnitude.

Using the procedure of sequential dissolution (leaching) of samples in NH_4OAc solution, we can decrease the impact of secondary alterations on the $^{87}Sr/^{86}Sr$ ratios (McArthur, 1994; Gorokhov *et al.*, 1995a; Gorokhov, 1996; Montanez *et al.*, 1996; Kuznetsov *et al.*, 1997; Ovchinnikova *et al.*, 1998, 2000; Bailey *et al.*, 2000; Bartley *et al.*, 2001). The procedure enables separation or, at least, concentrates the noncogenetic carbonate phases that differ from each other in their Sr isotope composition and trace elements concentration. Phases of this kind are common in Precambrian limestones and dolomites, but only one of them is of the early diagenetic genesis, whereas others originate in the course of secondary (catagenetic) processes and compose outer zones of carbonate grains.

It is important as well that $^{87}Sr/^{86}Sr$ initial ratios calculated from analytical data on the bulk carbonate material of limestone and dolomite samples can be either higher or lower than this parameter characterizing the primary carbonate phase left after the sample treatment in NH_4OAc (Gorokhov *et al.*, 1995a; Kuznetsov *et al.*, 1997). This is a result of improper correction for the radiogenic ^{87}Sr gain, when the same age values and Rb/Sr ratios are assumed for all heterogeneous carbonate phases, although they are different in these parameters. The preliminary treatment in NH_4OAc solution is therefore the necessary procedure for obtaining the correct data on the Sr isotope composition in paleooceans. It decreases to a good extent the systematic errors that reside in many data sets at present, even in those used for plotting the so-called reference curves of $^{87}Sr/^{86}Sr$ variations in Precambrian oceans.

For the sake of uniform selection of materials, which may yield data on $^{87}Sr/^{86}Sr$ variations in seawater of the Middle–early Late Riphean, we fulfilled both requirements to all samples, which were either studied in this work, or analyzed by our precursors. Accordingly, the presented reference curve of Sr isotope variations in paleooceans is plotted without some data published earlier.

GEOLOGY, STRUCTURE, AND AGE OF STUDIED SECTIONS

Two major structural zones of the Uchur–Maya region are separated by the thrust fault of submeridional orientation (Fig. 1). One corresponds to the Uchur–Maya plate with the subhorizontal attitude of Riphean, Vendian, and Cambrian beds, and the other one on the east is attributed to the Yudoma–Maya belt, where the same beds are thicker and form large open folds that are locally faulted (Nuzhnov, 1967; Semikhatov and Serebryakov, 1983). The regional stratigraphic scale of the Riphean includes the Uchur, Aimchan, Kerpyl', Lakhanda, and Ui groups separated one from another by unconformities of variable significance. The studied samples were collected from the Kerpyl' and Lakhanda groups characterizing the Middle–Upper Riphean boundary beds.

The Kerpyl' Group discordantly rests on the older Riphean or pre-Riphean rocks. It is divided into the siliciclastic Totta (450–1100 m), limy Malgina (60–420 m), and dolomitic Tsipanda (190–450 m) formations, which are interrelated via gradual transition zones. The analyzed samples of carbonate rocks were collected from three sections of the Malgina and Tsipanda formations, which are exposed in the Talakh-Khaya Cliffs on the east of the Uchur–Maya plate and in the Yudoma–Maya belt along the Belaya River near the Kurun-Mastakh Creek mouth and upstream of the Svetlyi Creek mouth. These localities and sampling levels in the sections are shown in Figs. 1 and 2.

The Malgina Formation is composed of fine-bedded micrites and subordinate calcisiltites, which locally show the microbial lamination and enclose sporadic

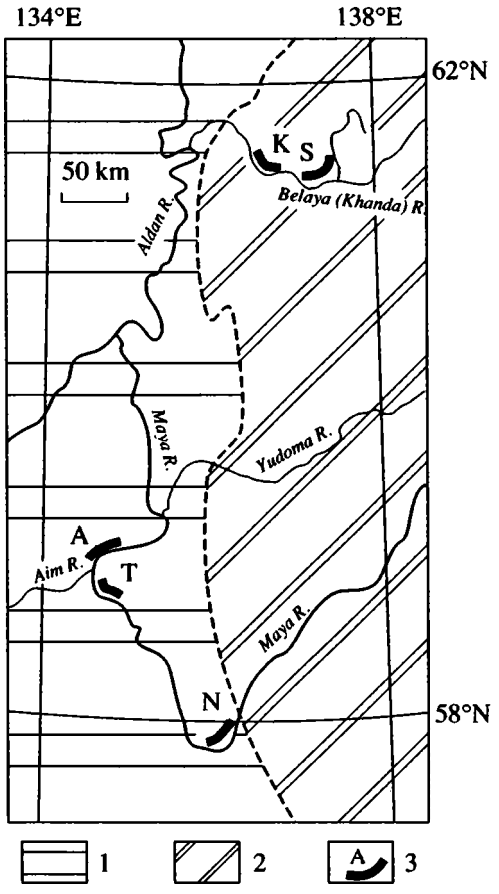

Fig. 1. Structural zones of the Uchur–Maya region and localities of studied section: (1) the Uchur–Maya plate, (2) Yudoma–Maya Belt, (3) location of the sections. Sections by names: (A) Aim (Maya River near the Aim River mouth); (K) Kurun-Mastakh (Belaya River upstream of the Kurun-Mastakh Creek mouth, western limb of the Gornostakh anticline); (N) Nel'kan (Maya River downstream of the Nel'kan Settlement); (S) Svetlyi (Belaya River upstream of the Svetlyi Creek mouth, eastern limb of the Gornostakh anticline; (T) Talakh-Khaya Cliffs (Maya River upstream of the Aim Creek mouth).

flakestone lentils and interlayer of bituminous carbonates near the top. Siliciclastic admixture (almost always clayey) is variably abundant in the rocks that are variegated in the basal part, pale-yellow in the middle, and gray in the upper one. In the Talakh-Khaya section (95–100 m), the content of siliciclastic fraction varies from 6.7 to 18% decreasing upward. In the Yudoma–Maya belt, the Malgina deposits are thicker, variegated rocks are less frequent among them, and clayey impurity is less abundant. In the Svetlyi section (400–420 m) at the eastern limb of the Gornostakhskii anticline, the siliciclastic fraction represents usually 0.6–2.2% of the rock volume, and only some basal beds contain 7.3–13% of this material. Flakestone interlayers are confined here to the middle part of the section, and black cherty lentils appear in upper horizons. In the Kurun-Mastakh section (380–400 m) at the western anticline limb, the formation is of the same structure, but its rocks experienced the epigenetic dolomitization down to the depth of 50–55 m below the contact with the overlying Tsipanda Formation (Fig. 29 in Semikhatov and Serebryakov, 1983).

Except for the dolomitic varieties mentioned above, all rocks of the Malgina Formation show insignificant signs of recrystallization and scarce thin (2–5 mm) veinlets of late calcite generation. Cathodoluminescence is untypical of micrites. Some vague patches in microsparites are weakly luminescent, and more distinct luminescence characterizes the fissure-filling calcite. Sediments of the Malgina Formation accumulated below and above the storm wave base in the proximal (Uchur–Maya plate) and distal (Yudoma–Maya belt) shelf zones.

The Tsipanda formation is well distinguishable owing to its dolomitic composition, insignificant admixture of siliciclastic material, and light-gray color of rocks, which are recrystallized to a considerable extent. Dolosparites containing less than 7.8% of siliciclastic components are its dominant rocks in the Talakh-Khaya section (280–300 m). In the lower part (80–85 m), dolomite beds frequently retain the microbial lamination. Above this level, they contain stratocolumnar and less frequent columnar stromatolites. Karst breccias formed during the pre-Lakhanda hiatus are widespread in dolomites around the Talakh-Khaya and Malgina Cliffs of the Uchur–Maya plate (Semikhatov and Serebryakov, 1983). In the Svetlyi and Kurun-Mastakh sections of the Yudoma–Maya belt, the Tsipanda Formation decreases in thickness and retains the same structure in general, although columnar stromatolites are more abundant here and rare bituminous dolosparites with cherty lentils appear among its rocks, which have low content of siliciclastic admixture (usually less than 2.5%). These sediments were deposited in mobile shallow settings of a vast carbonate platform, but their upper horizons accumulated close to the fair weather wave base.

The cathodoluminescence is almost untypical of the microbial and stromatolitic dolomites. The dim patchy luminescence is detected only within the recrystallized areas of these rocks. Luminescence of inequigranular dolosparites is more homogeneous but also dim. These features presumably reflect the peculiar distribution of Mn and Fe in the rocks under consideration.

The Lakhanda Group is separated from the Tsipanda Formation by a hiatus that is marked by development of the kaolinite-illite weathering crust in the Uchur–Maya plate, where that crust is up to 3–4 m thick (Nevolin *et al.*, 1978; *Litologiya...*, 1980). It is a common practice to unite local lithostratigraphic units of the group in two regional subdivisions: the Neryuen and Ignikan formations conformably overlying one another (Semikhatov and Serebryakov, 1983). Samples of carbonate rocks were collected from both formations in the Svetlyi section of the Yudoma–Maya belt and in

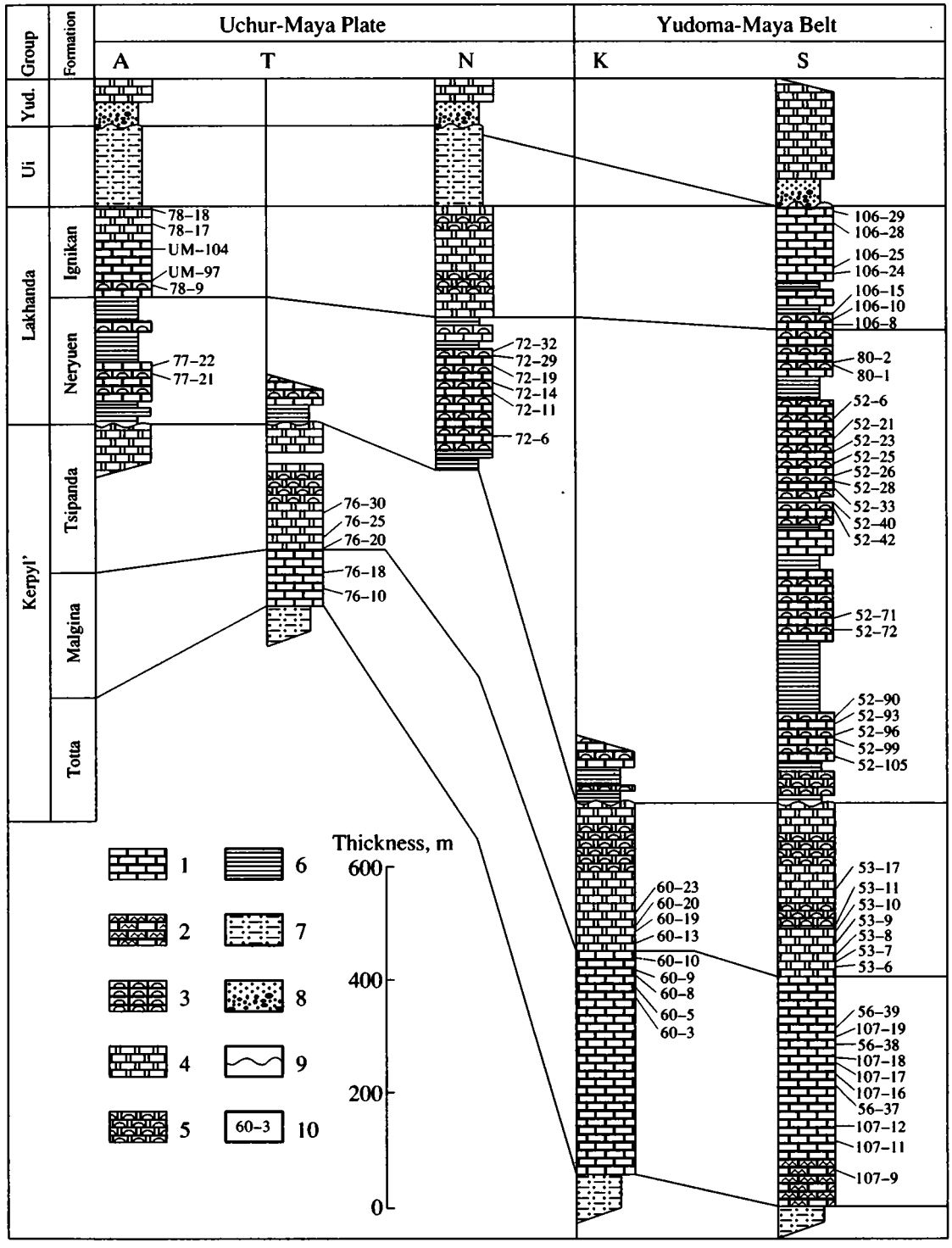

Fig. 2. Lithostratigraphy of studied sections, the Kerpyl' and Lakhanda groups: (1) limestone; (2) striate *Malginella* limestone; (3) stromatolitic limestone; (4) dolomite; (5) stromatolitic dolomite; (6) shale; (7) sandy-clayey deposits; (8) sandstone with gravelstone interlayers; (9) stratigraphic unconformity; (10) sample nos. and sampling levels. Sections by names: (A) Aim; (T) Talakh-Khaya; (N) Nel'kan; (K) Kurun-Mastakh; (S) Svetlyi.

the Aim section of the Uchur–Maya plate. In addition, the Neryuen Formation was sampled in the Nel'kan section (Figs. 1 and 2).

The Neryuen Formation of the Uchur–Maya plate consists of three members. The lower and upper members are composed of gray, predominantly clayey rocks.

The middle member of variegated carbonate rocks (Mil'kon Subformation) includes stromatolitic, subordinate microphytolitic or clastic limestones, and rare dolomites. Between the Aim and Nel'kan sections, the formation grows in thickness from 220–240 to 320–340 m toward the Yudoma–Maya belt. The parallel thickness bulge of the Mil'kon Subformation is from 70–72 to 175–180 m. In the Svetlyi section, the formation is 800–830 m thick and includes six members (60 to 180 m) of gray carbonate rocks intercalated with thinner members of gray to red shales, the latter representing in total only 25% of the entire section. The lower carbonate member is composed of stromatolitic and subordinate clastic to micritic dolomites. Other members consist of micritic and less frequent stromatolitic limestones. In the Yudoma–Maya belt, these sediments accumulated in the open shelf close to the storm wave base (carbonates) or in the relatively deep protected settings (shaly members). In the Uchur–Maya plate, they were deposited in the proximal shelf zone that was shallower and experienced the short-term episodes of subaerial exposition.

The insignificant patchy recrystallization resulted in formation of secondary calcite and Fe-dolomite in the matrix and veinlets of dolomitic limestones of the Neryuen Formation. These secondary carbonates usually constitute 5 to 8% of the studied samples. Luminescence is untypical of these samples except for the fissure-filling calcite that is clearly luminescent and for the secondary Fe-dolomite microporphyroblasts, which emit the dim reddish brown light.

The Ignikan Formation mostly consists of clastic to microphytolite-clastic carbonates intercalated with rare members and interlayers of stromatolitic varieties, and with thin (0.5–3 m) sporadic shaly beds. The rocks are usually colored gray to brownish gray; red coloration appears locally in their lower horizons only. In the Svetlyi section, the formation is composed almost entirely of limestones, which enclose thin members (20–40 m) and individual beds of dolomites and dolomitic limestone. The Ignikan deposits exposed in this section are 220–230 m thick. They are discordantly overlain by sediments of the Vendian Yudoma Group. In the Aim section, limestones are constituent rocks of the lower 20-m-thick member only, and higher beds (170–180 m thick in total) conformably overlain by sediments of the Ui Group are dolomitic in composition. The described deposits characterize sedimentation under active hydrodynamic conditions of the upper subtidal to intertidal zone.

Limestones and dolomites of the Ignikan Formation are recrystallized into micro(dolo)sparites and (dolo)sparites, which retain the relic sedimentary structures. Cathodoluminescence of microsparites is variable in intensity, generally weak, with brighter luminescence of grained matrix in the clastic and microphytolitic varieties. The bright patchy luminescence against the dim background of groundmass is characteristic of late diagenetic sparites and dolosparites.

The time range of the Kerpyl' and Lakhanda groups is established on the basis of mutually consistent paleontological and geochronological data. Paleontological data show that taxonomic composition of stromatolites and organic-walled microfossils renews across the boundary between the groups. Stromatolites of the Kerpyl' Group are represented by local endemics and transit Middle–Upper Riphean form genera and species, whereas basal beds of the Lakhanda Group show a higher diversity of transit taxa and enclose *Inzeria tjomusi* Kryl., *Jurusania cylindrica* Kryl., and *Baicalia lacera* Semikh., the form species typical of the lower Upper Riphean (Krylov, 1975; Semikhatov and Serebryakov, 1983; Semikhatov, 1995). Microstructure of the last form that is widespread in basal Upper Riphean horizons exemplifies the particular stage in evolution of cyanobacterial ecosystems and global environments of carbonate accumulation (Knoll and Semikhatov, 1998).

Renewals among the organic-walled microfossils from basal beds of the Lakhanda Group are even more impressive (German, 1990; Veis and Vorob'eva, 1993; Veis *et al.*, 1998). In addition to remains of simple cyanobacteria, which are common in all Proterozoic deposits, the Totta Formation of the Kerpyl' Group yields a series of large and complex morphotypes. These are acritarchs *Chuaria*, thalluses of coccoidal *Ostiana*, wide filaments *Asperatofilum* and *Taenitrichoides*, multiserial sheaths *Polytrichoides* and *Eomycrocoleos*, branching thalluses *Ulophyton* and *Majaphyton*, and others. Some researchers (Veis *et al.*, 1998, 2000, and references therein) interpreted their occurrence as evidence in favor of the Late Riphean age of the Totta Formation. This viewpoint can be discarded however owing to finds of all Totta microfossils in deposits predating the Upper Riphean in the southern Urals and cis-Uralian region (Veis *et al.*, 2000; *Stratigraficheskaya...*, 2000). They also occur in those deposits of the Anabar massif, which belong to the Lower Riphean according to geochronological dates and occurring stromatolite taxa (Komar, 1966; Semikhatov and Serebryakov, 1983; Gorokhov *et al.*, 1997; 2001). All microfossils of the Totta Formation transit into the Lakhanda Group, but the latter yields in addition the following taxa: acanthomorphic acritarchs *Trachyhystrichosphaera aimica* Herm., *T. stricta* Herm., and *Prolatoforma*; spiral-cylindrical *Obruchevella*; thalluses of multicellular algae *Archaeoclada* and *Varioclada*; remains of lower fungi and their reproductive structures *Eosaccharomyces, Mucorites*, and other forms characteristic of the lower Upper Riphean even in its stratotype (Veis *et al.*, 2000).

The U–Pb dates available at present define the age limits of the Kerpyl and Lakhanda groups in a wide diapason only. The youngest population of clastic zircons separated from the Totta Formation is 1300 ± 5 Ma old (Khudoley *et al.*, 1999, 2001), whereas baddeleyite

from diabase sills and flows in boundary horizons between the Lakhanda and Ui groups yielded the age values of 1005 ± 4 and 974 ± 7 Ma (Rainbird *et al.*, 1998). These magmatic rocks are interesting in several aspects (Volkodav *et al.*, 1978; Sukhorukov, 1986; Khudoley *et al.*, 2001). First, they are localized in the lower part of the Ui Group, the upper graywacke beds of which contain diabase fragments of similar petrographic composition. Second, some of diabase sills deformed during their emplacement the unconsolidated sediments in the lower part of the group. Third, some of these bodies have only lower chilled margins suggesting their extrusive origin. In other words, the basic magmatism in question was likely of synsedimentary type, and the obtained age values (1000–975 Ma) correspond, as we believe, to the accumulation time of basal beds of the Ui Group. At the same time, the Pb–Pb isochron dates obtained for limestones in the middle part of the Malgina Formation and in the lower part of the Lakhanda group are equal to 1043 ± 14 and 1025 ± 40 Ma, respectively (Semikhatov *et al.*, 2000; Ovchinnikova *et al.*, 2001). In addition, the Pb–Pb age of carbonate rocks from the middle of the Sukhaya Tunguska Formation of the Turukhansk region is 1035 ± 60 Ma (Ovchinnikova *et al.*, 1995). In terms of formal statistical criteria, difference between the listed dates is insignificant, but the succession of their values (probabilistic averages) well accords with the stratigraphic succession of the dated formations. So, the dates seem solid from this viewpoint and allow us to suggest that the boundary between the Kerpyl' and Lakhanda groups is about 1030 Ma old (Semikhatov *et al.*, 2000).

Mineralogically unstudied glauconites from the Totta Formation yielded an ordered series of K–Ar age values decreasing from 1170–1070 Ma in the lower formation part to 1070–1000 Ma in its middle interval, and then to 1020–970 Ma in the upper interval (Semikhatov and Serebryakov, 1983, and references therein). The K–Ar dates for glauconites from the Lakhanda and Ui groups (960–870 and 760–700 Ma, respectively), which continue the above series of age values, are "rejuvenated" according to the U–Pb dates obtained for the lower Ui diabases. The considerable dispersion of age value characterizing the Totta glauconites also suggests that isotopic systems of these minerals were somehow disturbed. Nevertheless, it seems reasonable to suggest that the maximum age values obtained for glauconites represent an approximation to the accumulation time of the Totta Formation. Hence, according to paleontological data, the Middle–Upper Riphean boundary corresponds in the Uchur–Maya region to the boundary between the Kerpyl' and Lakhanda groups, and geochronological dates imply that it is ~1030 Ma old, and that the upper Kerpyl' and Lakhanda deposits accumulated within the time range of 1050–1000 Ma.

PROCEDURE AND RESULTS OF SEQUENTIAL DISSOLUTION OF STUDIED SAMPLES

Among 210 samples of carbonate rocks collected from the Kerpyl' and Lakhanda groups, we selected those 69 for further investigation, which were macroscopically homogeneous, lacking obvious signs of recrystallization. We sawed them in two parts, one of which was examined by petrographic and cathodoluminescence methods, and the other one was used for chemical and isotopic analyses. Petrography of the rocks was studied in thin sections. The cathodoluminescence characteristics are obtained using the "Camebax" microprobe at the Laboratory of Electronic Microscopy and Microanalysis of the "MEKHANOBR-ANALIT" Center, St. Petersburg. Chemical composition of rocks was analyzed at the Analytical Laboratory of the Geological Institute, Russian Academy of Sciences, where the powdered weighings of samples were used, after dissolution in 1N HCl under the room temperature, for the determination of Ca and Mg contents with the help of wet chemical method, and the atomic absorption spectroscopy was applied to determine the Mn and Fe concentrations. The mineral composition of siliciclastic components in carbonates was analyzed using the X-ray diffractometry.

Samples of carbonate rocks affected by epigenetic recrystallization to the minimum extent were selected according to results of petrographic investigation and chemical analysis. We studied their Rb–Sr systematics applying the procedure of sequential dissolution (leaching). At first, the powdered material was treated in 1N solution of ammonium acetate (NH_4OAc) by ultrasonic machining during 15 minutes under the room temperature. The carbonate material that entered the acetate leachate is further designates as the AMA-phase. The leachate and residue after leaching were separated one from another by means of centrifuging, after which the residue was rinsed two times in the twice-distilled water. Washing waters and leachate were evaporated, and the residue was treated in the 10% acetic acid (CH_3COOH). We consider the carbonate material that entered the solution at this stage as the ACA-phase. Different dissolution procedures used for chemical analysis and for investigation of Rb–Sr systematics are responsible for the diversity of data characterizing contents of insoluble residue (silicate fraction) in some samples (Tables 1 and 2).

The Rb and Sr concentrations are measured using the isotopic dilution method and mixed ^{87}Rb–^{84}Sr spike. Isotopic analyses are performed on the MI 1320, 20 cm radius, 90° sector, single-collector mass spectrometer using a triple Re filament ion source. Sr was separated from solutions using the ion-exchange method, cation exchanger Dowex AG50W × 8 (200–400 mesh), and 2.5N HCl solution as eluent. Sr isotope composition was determined on the multi-collector Finnigan MAT 261 mass spectrometer using a regime of simultaneous measurements of all isotope currents

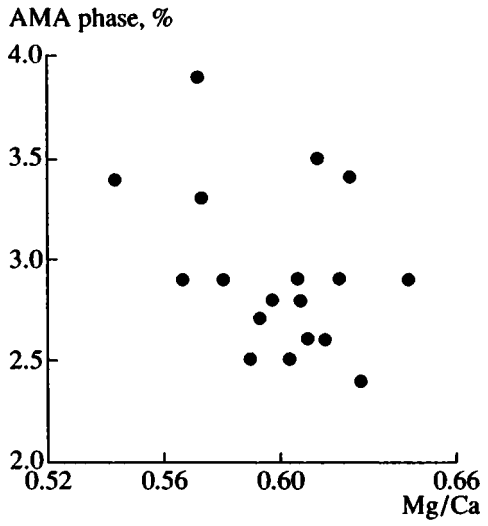

Fig. 3. Diagram showing percentage of soluble AMA phase versus Mg/Ca ratios in the studied carbonate samples (see text for explanation).

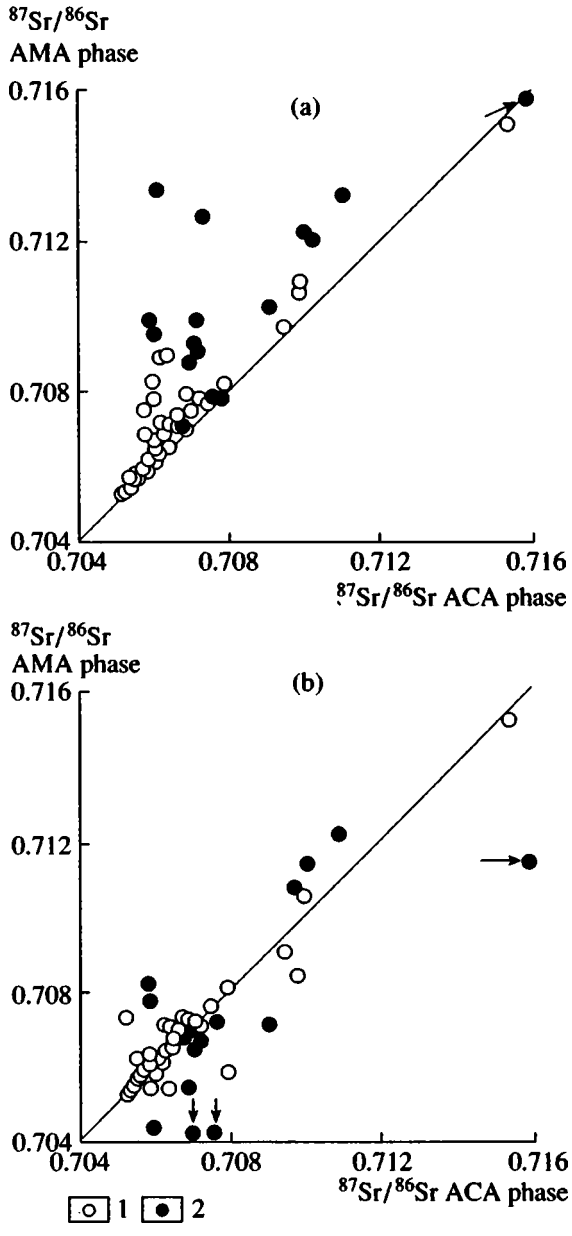

Fig. 4. Correlation diagrams for measured (a) and initial (b) $^{87}Sr/^{86}Sr$ ratios in AMA and ACA phases of limestone and dolomite samples from the Kerpyl' and Lakhanda groups: (1) limestone; (2) dolomite (see text for explanation).

and the Re-filament ion source. The laboratory averages of 0.710256 ± 0.000012 (n = 16) and 0.709187 ± 0.000010 (n = 2) were determined for the NIST SRM 987 and USGS EN-1 standard carbonates, respectively, during the period of data gathering. The uncertainties are quoted at the 2σ level.

Analytical data for the studied carbonate samples, their AMA- and ACA-phases included, are presented in Tables 1 and 2. Table 2 shows that calcite is soluble in 1N NH_4OAc better than dolomite, because the share of AMA phase varies from 3.9 to 7.6% (4.9% in average) in limestones and from 2.4 to 3.9% (2.9% in average) in dolomites. Its maximum percentage (~13%) is characteristic of fissure-filling calcite in Sample 80-2. Limestone samples 107-11, 107-12, and 76-10 do not fit this general tendency, but this is an artifact, because the decreased (down to 1.8%) content of AMA-phase in samples 107-11 and 107-12 is a result of insufficient grinding, and the higher proportion of this phase (9.9%) in Sample 76-10 was obtained owing to the material dissolution in 1N NH_4OAc under an elevated temperature. Sr concentrations in the bulk carbonate material are calculated as weighted averages for this element concentrations in corresponding AMA- and ACA-phases taking into account proportions of both phases (Table 2). Concentrations estimated in this manner are used for calculation of Mn/Sr and Fe/Sr ratios (Table 1).

Paired AMA- and ACA- phases are essentially different in their Rb–Sr characteristics. In average, concentrations of rubidium and strontium in AMA-phases of limestones are, respectively, 20 and 1.4 times higher than in ACA-phases, whereas the corresponding ratios calculated for dolomites are equal to 35 and 2. Thus, the Sr distribution between both phases is less contrasting in limestones than in dolomites. Gorokhov *et al.* (1995a) who established the same geochemical characteristics for the Riphean carbonate rocks of the Turukhansk region suggested that AMA-phases of limestones and dolomites predominantly consist of secondary calcite. As calcite is better soluble than dolomite in 1N NH_4OAc, the inverse correlation between the percentage of AMA-phase and Mg/Ca ratio in the studied dolomites (Fig. 3) is a good argument in favor of their suggestion.

The $^{87}Sr/^{86}Sr$ ratios measured in AMA-phases of limestones and dolomites are higher than in the paired ACA-phases. The corresponding difference between

Table 1. Trace element concentrations and characteristics of silicate impurity in carbonate rocks of the Kerpyl' and Lakhanda groups

Sample no.[1]	Section[2]	Sampling level in sections[3] (m)	Rock type[4]	Percentage of silicate impurity	Mg, %	Mn, ppm	Fe, ppm	Sr, ppm	Mg/Ca	Mn/Sr	Fe/Sr	Accessory silicate minerals[5]
Ignikan Formation												
106-29	5	210	L	1.7	0.39	82	200	191	0.010	0.43	1.1	–
106-28	*5*	*190*	*L*	*5.3*	*0.81*	*63*	*520*	*734*	*0.022*	*0.09*	*0.71*	*Q, Mc*
106-25	5	110	L	1.2	1.8	77	270	375	0.048	0.21	0.72	–
106-24	5	100	L	1.1	0.89	420	460	314	0.023	1.3	1.5	–
106-15	5	30	L	3.1	0.70	340	3900	1322	–	0.26	3.0	–
106-10	5	20	L	8.4	0.49	87	1650	109	0.013	0.80	15	Q, Mc, Fsp
106-8	5	10	L	15.0	0.88	320	920	487	–	0.66	1.9	–
78-18	1	150	D	4.0	12.2	240	4400	50.6	0.572	4.6	87	Q
78-17	1	130	D	2.3	12.8	204	2450	51.0	0.606	4.0	48	–
UM-104	1	85	L	2.6	6.1	100	1450	221	0.195	0.47	6.6	–
UM-97	1	25	L	1.8	0.49	350	1550	125	0.012	2.8	12	–
78-9	1	20	L	5.0	1.01	580	2100	86.3	0.027	6.7	24	Q (Fsp)
Neryuen Formation												
52-6	5	680	L	2.4	0.13	55	2260	129	0.003	0.43	18	Q, Mc
52-21	5	640	L	6.7	0.54	170	2250	806	0.014	0.21	2.8	Q, Mc (Fsp)
52-23	5	620	L	3.3	0.74	97	890	221	0.019	0.44	4.0	–
52-25	*5*	*600*	*L*	*0.9*	*0.16*	*16*	*67*	*634*	*0.004*	*0.03*	*0.11*	–
52-26	5	580	L	3.0	0.21	26	210	531	0.005	0.05	0.40	Q, Mc
52-28	5	570	L	3.9	0.48	250	3750	497	0.012	0.50	7.5	Q, Mc
52-33	5	560	L	2.9	0.45	130	1850	193	0.012	0.69	9.5	–
52-40	5	530	L	2.7	0.63	120	720	219	0.016	0.56	3.3	–
52-42	5	520	L	1.2	1.3	35	440	452	0.035	0.08	0.97	–
52-71	5	330	L	3.0	0.29	230	710	177	0.007	1.3	4.0	Q, Mc
52-72	*5*	*300*	*L*	*2.5*	*0.76*	*37*	*350*	*607*	*0.020*	*0.06*	*0.58*	–
52-90	5	150	L	2.1	0.31	100	550	207	0.008	0.49	2.7	–
52-93	5	140	L	1.5	0.26	140	310	375	0.007	0.38	0.81	–
52-96	*5*	*120*	*L*	*2.6*	*0.81*	*38*	*840*	*840*	*0.022*	*0.05*	*1.0*	–
52-99	5	110	L	2.4	0.18	150	3550	563	0.005	0.27	6.3	Q (Mc, Fsp)
52-105	*5*	*80*	*L*	*1.2*	*0.12*	*22*	*760*	*990*	*0.003*	*0.02*	*0.77*	–
72-32	3	220	D	2.3	12.2	87	1300	33.2	0.543	2.6	40	Q
72-29	3	215	D	1.5	12.5	44	590	50.3	0.573	0.87	12	–
72-19	*3*	*200*	*L*	*0.7*	*0.62*	*44*	*530*	*360*	*0.016*	*0.12*	*1.5*	–
72-14	*3*	*160*	*L*	*5.4*	*0.11*	*73*	*320*	*478*	*0.003*	*0.15*	*0.68*	*Q (Mc, Chl)*
72-11	*3*	*140*	*L*	*0.7*	*0.12*	*39*	*350*	*607*	*0.003*	*0.06*	*0.57*	–
72-6	3	60	L	2.0	0.68	260	650	63.5	0.017	4.0	10	Q (Fsp)
77-22	1	105	L	1.7	0.39	130	870	167	0.010	0.78	5.2	–
77-21	1	95	L	3.3	1.15	190	1850	117	0.031	1.6	16	Q
80-1	5	770	D	–	12.3	210	480	61.5	0.562	3.4	7.9	–
80-2	5	770	L	–	0.33	850	730	563	0.005	1.5	1.3	–

Table 1. (Contd.)

Sample no.[1]	Section[2]	Sampling level in sections[3] (m)	Rock type[4]	Percentage of silicate impurity	Mg, %	Mn, ppm	Fe, ppm	Sr, ppm	Mg/Ca	Mn/Sr	Fe/Sr	Accessory silicate minerals[5]
Tsipanda Formation												
53-17	5	150	D	5.6	13.6	58	490	13.4	0.644	4.3	37	Q
53-11	5	80	D	1.6	13.0	24	240	9.57	0.603	2.5	25	–
53-10	5	70	D	0.3	13.2	34	270	15.7	0.619	2.2	17	–
53-9	5	50	D	0.5	13.1	25	320	15.2	0.624	1.6	21	–
53-8	5	30	D	2.3	13.0	31	550	16.3	0.612	1.9	34	Q
53-7	5	20	D	1.5	12.4	33	890	22.2	0.567	1.7	40	–
53-6	5	10	D	1.5	13.4	25	360	18.2	0.627	1.4	20	–
60-23	4	70	D	0.8	12.6	80	770	25.2	0.597	3.2	31	Q
60-20	4	40	D	1.6	12.9	45	760	33.6	0.609	1.3	23	–
60-19	4	30	D	3.6	12.7	42	790	49.2	0.580	0.85	16	Q
60-13	4	10	D	1.6	13.0	45	450	22.0	0.615	2.1	20	–
76-30	2	65	D	6.4	12.5	140	2950	38.4	0.590	3.5	76	Q
76-25	2	20	D	7.0	12.5	180	3150	54.4	0.593	3.3	58	Q, Mc
Malgina Formation												
60-10	*4*	*380*	*L*	*4.0*	*0.76*	*35*	*360*	*261*	*0.020*	*0.13*	*1.39*	*Q*
60-9	4	360	L	7.7	1.58	140	2970	230	0.044	0.60	13	Q (Mc)
60-8	4	350	L	4.5	1.41	150	2450	201	0.038	0.72	12	Mc, Q
60-5	4	330	L	5.8	2.41	76	2030	397	0.066	0.19	5.1	Mc, Q
60-3	*4*	*310*	*L*	*3.4*	*0.92*	*58*	*890*	*362*	*0.024*	*0.16*	*2.44*	*Mc, Q*
56-39	*5*	*305*	*L*	*1.3*	*0.26*	*17*	*400*	*1206*	*0.007*	*0.01*	*0.33*	–
107-19	*5*	*290*	*L*	*1.2*	*0.22*	*32*	*150*	*1198*	*0.006*	*0.03*	*0.13*	–
56-38	*5*	*280*	*L*	*2.2*	*0.58*	*33*	*320*	*936*	*0.015*	*0.04*	*0.34*	–
107-18	*5*	*260*	*L*	*0.6*	*0.11*	*31*	*130*	*1377*	*0.003*	*0.02*	*0.09*	–
107-17	*5*	*250*	*L*	*1.2*	*0.22*	*30*	*100*	*1610*	*0.006*	*0.02*	*0.06*	*Q*
107-16	*5*	*230*	*L*	*1.7*	*0.26*	*40*	*220*	*879*	*0.007*	*0.05*	*0.25*	
56-37	5	210	L	13.0	0.47	180	4600	370	0.012	0.48	12	*Mc, Q*
107-12	5	140	L	7.3	0.56	130	3530	234	0.014	0.55	15	Mc, Q, Fsp, Chl
107-11	5	110	L	9.5	0.61	210	4600	171	0.016	1.2	27	Mc, Q, Fsp, Chl
107-9	5	60	L	11.0	0.38	370	3700	165	0.010	2.2	22	Mc, Q (Fsp, Chl)
76-18	2	60	L	6.7	0.40	85	1050	194	0.010	0.44	5.4	Mc, Q, Chl
76-10	2	30	L	8.3	0.47	370	980	117	0.012	3.1	8.4	Mc, Q, Chl

Note: [1] Italicized are data obtained for samples satisfying the accepted geochemical criteria Mg/Ca ≤ 0.024, Mn/Sr ≤ 0.2, and Fe/Sr ≤ 5; [2] Aim (1), Talakh-Khaya (2), Nel'kan (3), Kurun-Mastakh (4), and Svetlyi (5) sections; [3] interval in meters from the base of corresponding section; [4] limestone (L) or dolomite (D); [5] quartz (Q), mica (Mc), feldspar (Fsp), and chlorite (Chl) listed in order of decreasing abundance, and trace of the mineral when bracketed.

Table 2. Rb–Sr analytical data characterizing carbonate phases of limestones and dolomites of the Kerpyl' and Lakhanda groups

Sample no.[1]	Rock[2]	Carbonate phase[3]	Content of the phase (%)	Rb, ppm	Sr, ppm	$^{87}Rb/^{86}Sr$	$^{87}Sr/^{86}Sr$ measured	$^{87}Sr/^{86}Sr$ initial
Ignikan Formation								
106-29	L	AMA	4.1	1.47	275	0.0157	0.70616	0.70593
		ACA	94.8	0.03	188	0.0004	0.70602	0.70601
106-28	*L*	*AMA*	*4.4*	*3.96*	*967*	*0.0099*	*0.70705*	*0.70691*
		ACA	*89.9*	*0.12*	*721*	*0.0005*	*0.70635*	*0.70634*
106-25	L	AMA	5.0	1.74	495	0.0103	0.70654	0.70639
		ACA	94.0	0.06	369	0.0005	0.70640	0.70639
106-24	L	AMA	5.4	1.26	386	0.0095	0.70703	0.70689
		ACA	93.8	0.05	310	0.0004	0.70686	0.70685
106-15	L	AMA	4.6	1.60	1602	0.0029	0.70617	0.70613
		ACA	92.8	0.11	1308	0.0003	0.70607	0.70606
106-10	L	AMA	4.0	7.24	126	0.1680	0.70823	0.70577
		ACA	87.4	0.08	108	0.0022	0.70787	0.70783
106-8	L	AMA	4.2	9.80	595	0.0483	0.70968	0.70897
		ACA	50.9	1.15	478	0.0070	0.70944	0.70935
78-18	D	AMA	3.9	11.6	81.2	0.4182	0.71266	0.70653
		ACA	91.5	0.23	49.3	0.0136	0.70730	0.70710
78-17	D	AMA	2.9	18.2	85.4	0.6230	0.71338	0.70425
		ACA	94.8	0.24	49.7	0.0144	0.70609	0.70588
UM-104	L	AMA	5.4	2.91	265	0.0321	0.70709	0.70670
		ACA	92.5	0.09	219	0.0012	0.70573	0.70572
UM-97	L	AMA	5.2	2.81	143	0.0575	0.70799	0.70715
		ACA	93.4	0.10	124	0.0022	0.70584	0.70581
78-9	L	AMA	5.4	8.74	103	0.2475	0.70898	0.70535
		ACA	89.4	0.02	85.3	0.0006	0.70633	0.70632
Neryuen Formation								
52-6	L	AMA	4.7	1.50	179	0.0246	0.70636	0.70600
		ACA	92.7	0.07	126	0.0016	0.70613	0.70610
52-21	L	AMA	5.1	5.47	1072	0.0149	0.70608	0.70586
		ACA	88.4	0.22	799	0.0001	0.70578	0.70578
52-23	L	AMA	4.9	1.43	298	0.0141	0.70740	0.70719
		ACA	93.2	0.06	217	0.0008	0.70661	0.70659
52-25	*L*	*AMA*	*4.5*	*0.62*	*934*	*0.0019*	*0.70536*	*0.70533*
		ACA	*95.2*	*0.02*	*621*	*0.0001*	*0.70527*	*0.70527*
52-26	L	AMA	4.4	2.61	837	0.0091	0.70580	0.70566
		ACA	92.1	0.14	517	0.0008	0.70555	0.70554
52-28	L	AMA	4.8	3.38	686	0.0144	0.70722	0.70701
		ACA	91.9	0.18	487	0.0011	0.70619	0.70617
52-33	L	AMA	4.9	2.71	229	0.0347	0.71094	0.71043
		ACA	93.5	0.08	191	0.0013	0.70989	0.70987
52-40	L	AMA	4.4	1.86	339	0.0161	0.70711	0.70687
		ACA	94.0	0.25	213	0.0034	0.70662	0.70657
52-42	L	AMA	4.6	1.24	667	0.0054	0.70559	0.70551
		ACA	94.7	0.03	440	0.0002	0.70546	0.70546
52-71	L	AMA	4.8	2.33	245	0.0278	0.70752	0.70711
		ACA	93.8	0.06	174	0.0011	0.70694	0.70692
52-72	*L*	*AMA*	*4.9*	*3.99*	*974*	*0.0120*	*0.70532*	*0.70514*
		ACA	*93.6*	*0.16*	*588*	*0.0008*	*0.70521*	*0.70519*

Table 2. (Contd.)

Sample no.[1]	Rock[2]	Carbonate phase[3]	Content of the phase (%)	Rb, ppm	Sr, ppm	$^{87}Rb/^{86}Sr$	$^{87}Sr/^{86}Sr$ measured.	$^{87}Sr/^{86}Sr$ initial
			Neryuen Formation					
52-90	L	AMA	4.1	2.95	346	0.0249	0.70646	0.70610
		ACA	95.1	0.09	201	0.0013	0.70603	0.70601
52-93	L	AMA	4.6	3.54	671	0.0155	0.70606	0.70583
		ACA	94.5	0.07	363	0.0006	0.70581	0.70580
52-96	*L*	*AMA*	*5.6*	*1.65*	*1050*	*0.0046*	*0.70544*	*0.70538*
		ACA	*92.7*	*0.07*	*827*	*0.0002*	*0.70542*	*0.70542*
52-99	L	AMA	4.9	2.89	692	0.0122	0.70594	0.70576
		ACA	93.1	0.06	556	0.0003	0.70575	0.70574
52-105	*L*	*AMA*	*4.6*	*1.54*	*1521*	*0.0030*	*0.70541*	*0.70537*
		ACA	*94.4*	*0.04*	*990*	*0.0001*	*0.70531*	*0.70531*
72-32	D	AMA	3.4	3.26	51.1	0.1867	0.70912	0.70638
		ACA	94.8	0.10	32.4	0.0088	0.70710	0.70697
72-29	D	AMA	3.3	1.12	106	0.0310	0.70714	0.70669
		ACA	95.2	0.06	46.3	0.0037	0.70679	0.70673
72-19	*L*	*AMA*	*6.8*	*0.46*	*181*	*0.0075*	*0.70562*	*0.70551*
		ACA	*92.8*	*0.04*	*373*	*0.0003*	*0.70551*	*0.70550*
72-14	*L*	*AMA*	*5.3*	*4.03*	*445*	*0.0265*	*0.70573*	*0.70535*
		ACA	*89.6*	*0.19*	*480*	*0.0012*	*0.70535*	*0.70533*
72-11	*L*	*AMA*	*5.6*	*0.88*	*847*	*0.0031*	*0.70545*	*0.70540*
		ACA	*93.8*	*0.05*	*593*	*0.0002*	*0.70537*	*0.70536*
72-6	L	AMA	4.1	2.83	71.1	0.1165	0.70891	0.70720
		ACA	94.2	0.11	63.1	0.0050	0.70619	0.70612
77-22	L	AMA	3.9	3.13	190	0.0484	0.70691	0.70620
		ACA	94.5	0.12	166	0.0021	0.70579	0.70575
77-21	L	AMA	4.5	5.11	125	0.1194	0.70784	0.70609
		ACA	92.6	1.65	116	0.0416	0.70601	0.70540
80-1	D	AMA	2.7	2.39	108	0.0650	0.71228	–
		ACA	96.7	0.03	60.3	0.0012	0.71000	–
80-2	L	AMA	13.0	0.68	476	0.0042	0.71515	–
		ACA	87.1	0.12	576	0.0006	0.71531	–
			Tsipanda Formation					
53-17	D	AMA	2.9	1.96	29.0	0.1979	0.72030	0.71137
		ACA	91.5	0.09	12.9	0.0203	0.72102	0.72072
53-11	D	AMA	2.5	1.22	38.6	0.0927	0.71205	0.71068
		ACA	96.9	0.12	8.83	0.0381	0.71016	0.70960
53-10	D	AMA	2.9	1.15	44.4	0.0759	0.71325	0.71212
		ACA	97.0	0.51	14.9	0.0099	0.71098	0.71083
53-9	D	AMA	3.4	1.51	27.4	0.1611	0.70917	0.70678
		ACA	96.5	0.09	14.7	0.0172	0.70706	0.70680
53-8	D	AMA	3.5	1.45	20.9	–	–	–
		ACA	94.3	0.05	16.2	0.0083	0.70954	0.70941
53-7	D	AMA	2.9	6.69	33.8	0.5796	0.70774	0.69916
		ACA	96.0	0.14	21.9	0.0186	0.70781	0.70753
53-6	D	AMA	2.4	2.10	36.6	–	–	–
		ACA	97.0	0.06	17.7	0.0091	0.70661	0.70647
60-23	D	AMA	2.8	4.38	94.2	0.2367	0.70878	0.70528
		ACA	96.0	0.08	23.2	0.0094	0.70693	0.70679
60-20	D	AMA	2.6	7.56	42.8	0.5173	0.70990	0.70224
		ACA	96.4	0.15	33.4	0.0130	0.70714	0.70694

Table 2. (Contd.)

Sample no.[1]	Rock[2]	Carbonate phase[3]	Content of the phase (%)	Rb, ppm	Sr, ppm	$^{87}Rb/^{86}Sr$	$^{87}Sr/^{86}Sr$ measured	$^{87}Sr/^{86}Sr$ initial
Tsipanda Formation								
60-19	D	AMA	2.9	3.56	209	0.0500	0.70783	0.70709
		ACA	93.5	0.12	44.2	0.0079	0.70762	0.70750
60-13	D	AMA	2.6	3.60	48.1	0.2192	0.71025	0.70701
		ACA	96.8	0.08	21.3	0.0110	0.70908	0.70891
76-30	D	AMA	2.5	1.94	49.2	0.1167	0.70986	0.70813
		ACA	90.5	0.14	38.1	0.0107	0.70591	0.70575
76-25	D	AMA	2.7	1.53	66.2	–	–	–
		ACA	90.3	0.23	54.1	0.0123	0.70645	0.70626
76-20	D	AMA	2.8	2.39	58.4	0.1299	0.70954	0.70762
		ACA	87.4	0.19	40.0	0.0136	0.70602	0.70582
Malgina Formation								
60-10	*L*	*AMA*	*5.1*	*1.85*	*442*	*0.0113*	*0.70627*	*0.70609*
		ACA	*91.5*	*0.11*	*251*	*0.0013*	*0.70594*	*0.70592*
60-9	L	AMA	6.0	4.73	372	0.0373	0.70717	0.70661
		ACA	86.5	0.14	220	0.0018	0.70643	0.70640
60-8	L	AMA	5.5	3.36	178	0.0552	0.70795	0.70712
		ACA	89.9	0.12	202	0.0018	0.70686	0.70683
60-5	L	AMA	5.1	10.3	430	0.0700	0.70673	0.70568
		ACA	89.2	0.19	396	0.0014	0.70600	0.70598
60-3	*L*	*AMA*	*5.3*	*5.79*	*445*	*0.0381*	*0.70691*	*0.70634*
		ACA	*918*	*0.21*	*357*	*0.0017*	*0.70625*	*0.70622*
56-39	*L*	*AMA*	*4.4*	*1.85*	*1816*	*0.0030*	*0.70586*	*0.70582*
		ACA	*94.5*	*0.13*	*1178*	*0.0003*	*0.70577*	*0.70576*
107-19	*L*	*AMA*	*6.1*	*1.49*	*1783*	*0.0024*	*0.70574*	*0.70574*
		ACA	*92.5*	*0.14*	*1160*	*0.0004*	*0.70563*	*0.70563*
56-38	*L*	*AMA*	*4.8*	*2.04*	*1378*	*0.0043*	*0.70588*	*0.70581*
		ACA	*93.5*	*0.11*	*913*	*0.0004*	*0.70586*	*0.70585*
107-18	*L*	*AMA*	*5.9*	*0.74*	*2304*	*0.0009*	*0.70599*	*0.70597*
		ACA	*93.6*	*0.10*	*1318*	*0.0002*	*0.70579*	*0.70579*
107-17	*L*	*AMA*	*7.6*	*2.12*	*2339*	*0.0026*	*0.70595*	*0.70591*
		ACA	*89.8*	*0.04*	*1548*	*0.0001*	*0.70575*	*0.70575*
107-16	*L*	*AMA*	*5.3*	*1.22*	*1247*	*0.0029*	*0.70585*	*0.70581*
		ACA	*93.3*	*0.10*	*858*	*0.0004*	*0.70577*	*0.70576*
56-37	L	AMA	4.5	15.3	734	0.0612	0.70784	0.70692
		ACA	83.1	0.33	358	0.0027	0.70717	0.70713
107-12	L	AMA	1.8	2.52	483	0.0154	0.70772	0.70749
		ACA	90.9	0.09	229	0.0011	0.70742	0.70741
107-11	L	AMA	1.8	1.49	431	0.0101	0.70820	0.70805
		ACA	88.7	0.08	165	0.0014	0.70787	0.70785
107-9	L	AMA	6.8	15.4	293	0.1542	0.71066	0.70835
		ACA	82.5	0.49	154	0.0093	0.70983	0.70969
76-18	L	AMA	5.6	10.0	256	0.1142	0.70756	0.70584
		ACA	87.6	0.40	190	0.0061	0.70573	0.70563
76-10	L	AMA	9.9	4.50	67.8	0.1943	0.70830	0.70538
		ACA	82.4	0.46	123	0.0108	0.70596	0.70580

Note: [1] Italicized are data obtained for samples satisfying the accepted geochemical criteria Mg/Ca ≤ 0.024, Mn/Sr ≤ 0.2, and Fe/Sr ≤ 5; [2] limestone (L) or dolomite (D); [3] carbonate material dissolved in 1N NH_4OAc (AMA) and residue after leaching dissolved subsequently in 10% CH_3COOH (ACA).

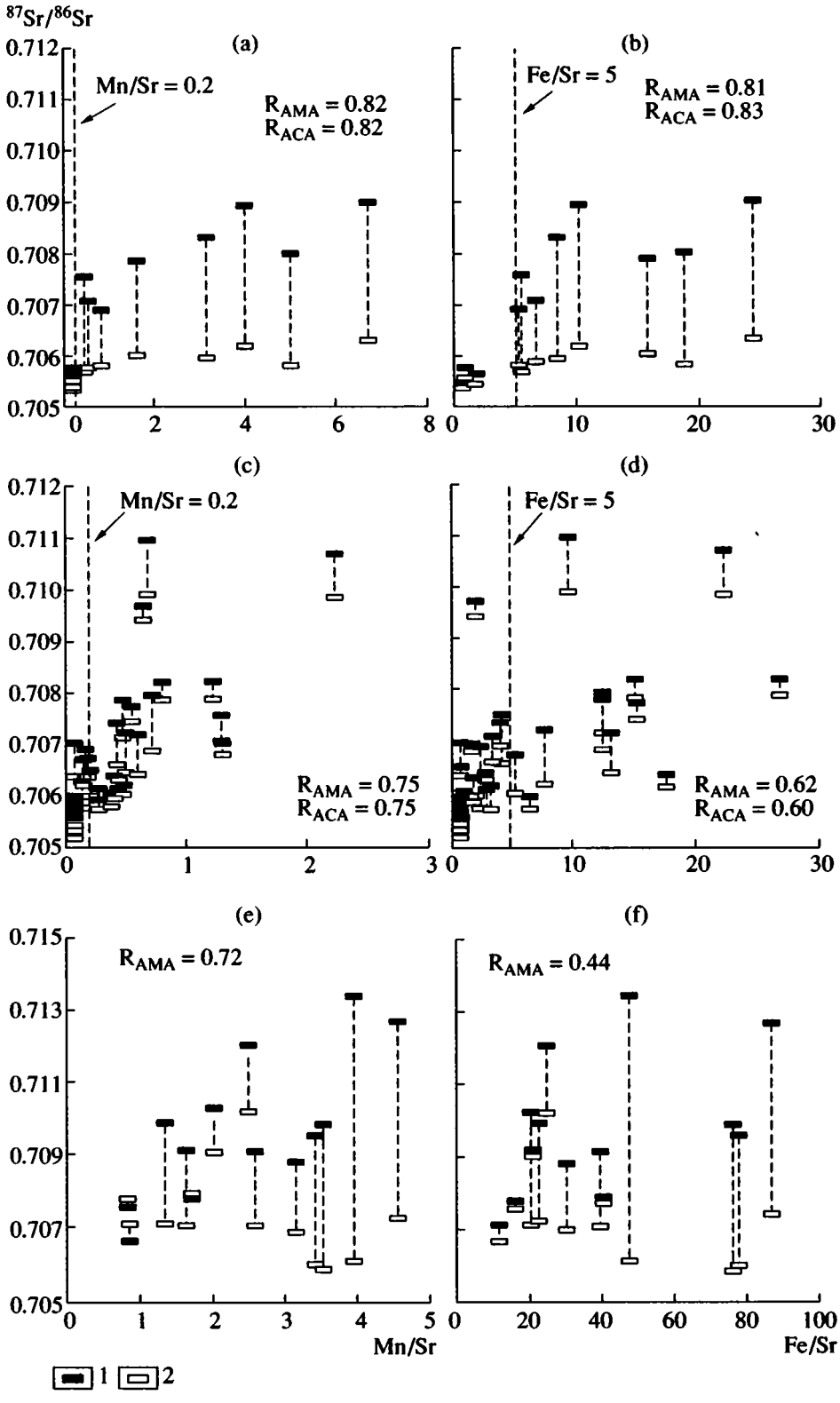

Fig. 5. $^{87}Sr/^{86}Sr$ ratios in AMA and ACA phases plotted versus Mn/Sr and Fe/Sr ratios in the bulk carbonate material of limestones from the Uchur–Maya Plate (a, b) and Yudoma–Maya Belt (c, d), and of dolomites from both structural zones (e, f): (1) ratios measured in AMA phases; (2) ratios measured in ACA phases; R_{AMA} and R_{ACA} are corresponding correlation coefficients (see text for explanation).

ratios can be as great as 0.0073 in dolomites but is not greater than 0.0027 in limestones (Table 2, Fig. 4a). Only two samples, for which the measured $^{87}Sr/^{86}Sr$ ratios are very high (>0.715), represent an exception. These are the fissure-filling calcite (Sample 80-2) and one dolomite from the Tsipanda Formation (Sample 53-17). The established difference between the $^{87}Sr/^{86}Sr$ ratios measured in AMA- and ACA-phases confirms their non-cogenetic character that was established as well for the Riphean and Vendian carbonate rocks of the Urals and Siberia (Gorokhov *et al.*, 1995a; Kuznetsov *et al.*, 1997).

The AMA-phase leached from the surface of mineral particles likely represents the latest epigenetic generation of carbonate minerals, whereas the ACA-phase, even if it experienced some epigenetic alterations, consists predominantly of primary material. The degree of epigenetic alterations in original carbonate sediments defines potentialities of sequential dissolution that leads to separation of these phases. The regional peculiarities of alterations can be elucidated when we know Mn/Sr and Fe/Sr ratios and character of their correlation with the $^{87}Sr/^{86}Sr$ ratios in carbonate material. As one can see from Fig. 5, correlation between the above parameters is not identical for AMA- and ACA-phases and depends on the mineral composition of rocks and on their position in the Uchur–Maya plate, or in the Yudoma–Maya belt.

An obvious covariation of $^{87}Sr/^{86}Sr$ ratios measured in AMA-phases, on the one hand, and Mn/Sr or Fe/Sr ratios characterizing bulk carbonate material of limestones and dolomites, on the other, implies that variability of all these ratios is caused by the same epigenetic processes. Judging from values of corresponding correlation coefficients (Figs. 5a–5d), the alterations affected to some extent the ACA-phases of limestones as well. However, the $^{87}Sr/^{86}Sr$ ratios plotted versus Mn/Sr and Fe/Sr ratios grow in the latter phases slower than in the AMA-phases. In this respect, the Rb–Sr systematics of limestones from the Uchur–Maya plate and Yudoma–Maya belt is not identical: the growth of $^{87}Sr/^{86}Sr$ ratios measured in ACA-phases is much smaller in the plate than in the belt. The considered data lead to the following conclusions:

(1) Epigenetic alterations in limestones of the Yudoma-Maya belt are more intense than in analogous rocks of the Uchur–Maya plate. In mineralogical terms, this means that outer zones of calcite grains are recrystallized deeper in the belt than in the plate.

(2) The sequential dissolution in 1N NH_4OAc turned out to be more effective for the weakly altered limestones of the Uchur–Maya plate. This procedure efficiently removes outer "layers" of calcite grains that were recrystallized in the course of epigenesis and thus considerably enriches the residue in the primary carbonate material.

(3) The $^{87}Sr/^{86}Sr$ ratios measured in AMA-phases of dolomites show covariance with Mn/Sr and Fe/Sr ratios characterizing bulk carbonate material (Fig. 5e and 5f) that is untypical of ACA-phases of these rocks. This means that precipitation of secondary calcite at the surface of carbonate grains was accompanied by Mn and Sr redistribution in the course of epigenesis. In contrast, the inner (properly dolomitic) parts of the grains may retain the Sr isotopic signature of earlier fluids.

In general, it is beyond all doubts that the Rb–Sr systems of AMA- and ACA-phases were formed at different stages of lithogenesis of limestones and dolomites in the Uchur–Maya region. Accordingly, it would be incorrect to calculate the $^{87}Sr/^{86}Sr$ initial ratio in any AMA-phase using data on the Rb and Sr concentrations in the bulk carbonate material and on the stratigraphic age of studied sample. Calculations of this kind may give much lower value of the above ratio as compared to that obtained for the ACA-phase (Fig. 4b). Each example of such calculations evidences that the Rb/Sr ratio was stabilized in a given AMA-phase much later than in the paired ACA-phase. Difference between the $^{87}Sr/^{86}Sr$ ratios measured in AMA- and ACA-phases may indicate the degree of epigenetic alterations in carbonate rocks, but this statement is applicable only to those rocks, in which the initial carbonate material retained the closed-system behavior at the earlier stages of lithogenesis.

ISOTOPIC AND GEOCHEMICAL CHARACTERISTICS OF CARBONATES FROM THE KERPYL' AND LKHANDA GROUPS

Considering below the $^{87}Sr/^{86}Sr$ ratios, we refer only to those, which characterize solely the ACA phases of carbonate rocks studied in this work or in our previous papers (Gorokhov *et al.*, 1995a; Semikhatov *et al.*, 1998). When the above ratios are quoted from other publications, they are supplemented with characteristics of the studied material.

Kerpyl' Group. The carbonate Malgina and Tsipanda formations of the group are less thick than the sandy–clayey Totta Fotmation that is likely of a greater time range as well. We studied 17 limestone and 14 dolomite samples characterizing respectively the Malgina and Tsipanda formations.

Malgina Formation. The carbonate fraction of samples from this formation consists of calcite that shows the very low Mg concentration (0.11–0.61%); limestones containing 0.72–2.41% Mg appear only in the terminal part of the Kurun-Mastakh section. Percentage of silicate fraction varies in the studied rocks from 0.6 to 13% (Table 1). This fraction predominantly consists of quartz and mica associated sometimes with accessory feldspar and chlorite. Bulk carbonate material of samples, in which percentage of silicate components is greater than 5%, is relatively richer in Mn (130–370 ppm) and Fe (2000–4600 ppm) than in samples containing 0.6–5% of these components (Mn = 17–85 ppm and Fe = 100–890 ppm). These features sug-

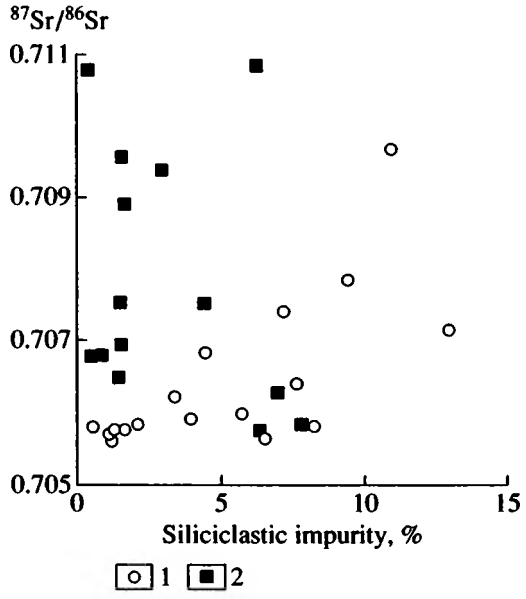

Fig. 6. $^{87}Sr/^{86}Sr$ initial ratios plotted versus percentage of siliciclastic components in carbonate rocks of the Kerpyl' Group: (1) limestone, Malgina Formation; (2) dolomite, Tsipanda Formation.

gest that carbonate material was contaminated with both elements extracted from silicate components. Sr concentrations in limestones are highly variable. The highest one (879–1610 ppm) was determined in samples from the middle part of the Svetlyi section. Lower horizons of the same section and terminal beds of the Kurun-Mastakh section are relatively depleted in Sr (201–397 ppm). The lowest Sr concentrations (117 and 194 ppm) are established in two samples from the Talakh-Khaya section.

The $^{87}Sr/^{86}Sr$ initial ratios of studied limestones fall within the interval of 0.70563–0.70969 and are covariant with the percentage of silicate impurity, and also with Mn/Sr and Fe/Sr ratios (Figs. 6 and 7). The highest $^{87}Sr/^{86}Sr$ ratios (0.70713–0.70969) are characteristic of basal interval of the Svetlyi section, where percentage of silicate components in limestones is relatively high (7.3–13%). In the middle part of the same section, limestones contain only 0.6–2.2% of silicate components and show the local minimum of $^{87}Sr/^{86}Sr$ ratios (0.70563–0.70585). These ratios in limestone samples 76-10 and 76-18 (middle part of the Talakh-Khaya section) are similarly low (0.70563 and 0.70580), but they fall out of covariation with the content of siliciclastic admixture or with Mn/Sr and Fe/Sr ratios. Comparatively higher $^{87}Sr/^{86}Sr$ ratios (0.70592–0.70683) characterize carbonates from the terminal part of the Kurun-Mastakh section. The lowest of these ratios was obtained for Sample 60-10 that defines the local minimum of Mg/Ca (0.020), Mn/Sr (0.13), and Fe/Sr (1.4) ratios and shows the lowest difference between $^{87}Sr/^{86}Sr$ ratios in AMA- and ACA-phases.

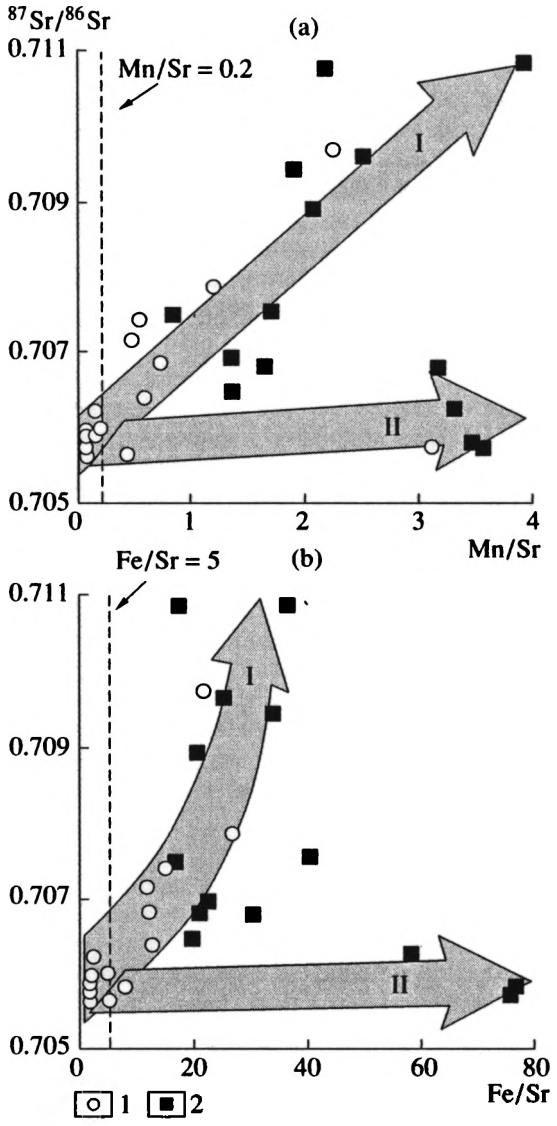

Fig. 7. $^{87}Sr/^{86}Sr$ initial ratios plotted versus Mn/Sr (a) and Fe/Sr (b) ratios in carbonate rocks of the Kerpyl' Group of Yudoma–Maya Belt (I) and Uchur–Maya Plate (II): (1) limestone, Malgina Formation; (2) dolomite, Tsipanda Formation.

The isotopic and geochemical characteristics of Malgina limestones suggest that the degree of their epigenetic alterations is variable in space and with time. A high degree of alterations in the lower horizons of these limestones presumably is a consequence of their proximity to terrigenous rocks of the Totta Formation, through which the basinal brines circulated. As for a greater alteration degree of rocks in the eastern sections, as compared to the western ones, this phenomenon may reflect not only the difference in downwarping of the Uchur–Maya plate and Yudoma–Maya belt, but also the variable clay/sand ratio characterizing the Totta deposits and growing eastward (Semikhatov and Serebryakov, 1983).

In the middle Malgina horizons, which have been sampled best of all in the Svetlyi section (Fig. 2), alterations in limestones are minimal. Rocks from upper horizons sampled in the Kurun-Mastakh section only are relatively rich in Mg, while their $^{87}Sr/^{86}Sr$ initial ratios and difference between ratios measured in AMA- and ACA-phases (0.0003–0.0011) are comparatively high. A possible explanation to these features is the proximity of the Kurun-Mastakh section to a zone of intense late dolomitization that extends along the contact with the Tsipanda Formation. An irregular character of dolomitization was responsible for a considerable variability of Mn (35–150 ppm) and Fe (360–3000 ppm) concentrations in the samples under consideration. Accordingly, among samples from the Kurun-Mastakh section, only those may retain the least altered Rb–Sr isotopic systems, which show the minimal Mg/Ca ratios.

Tsipanda Formation. In dolomites of this formation, Mg/Ca ratios vary from 0.567 to 0.644. Rocks of the Kurun-Mastakh and Svetlyi sections usually contain less than 2.5% of silicate impurity predominantly consisting of quartz. Only in two samples (nos. 53-8 and 53-17), which have been collected from a member that encloses the early diagenetic cherty concretions, percentage of silicate material equals to 3.6 and 5.6%. In the Talakh-Khaya section, dolomites contain up to 7.8% of silicate components represented by quartz and accessory mica. In general, Mn, Fe, and Sr are irregularly distributed in the Tsipanda dolomites. In the Kurun-Mastakh and Svetlyi sections, the bulk carbonate material of dolomites is less rich in Mn and Fe than in the Talakh-Khaya section (Mn 24–80 versus 140–180 ppm; Fe 240–890 versus 2900–3200 ppm). The lowest Sr concentrations (9.6–22.2 ppm) are characteristic of rocks in the Svetlyi section, where they decrease upward in the rock succession. In the Kurun-Mastakh section, concentrations of this element are somewhat higher (22.0–49.2 ppm), and their maximum values (38.4–54.4 ppm) are established in the Talakh-Khaya section.

The $^{87}Sr/^{86}Sr$ initial ratio varies in the Tsipanda dolomites from 0.70575 to 0.72072 without noticeable correlation with either Mn/Sr and Fe/Sr ratios, or with percentage of silicate impurity in the rocks (Figs. 5 and 6). The highest $^{87}Sr/^{86}Sr$ initial ratios are characteristic of rocks from the Gornostakhskii anticline, especially from the Svetlyi section, where they increase from 0.70647 in lower beds to 0.72072 in the upper ones. In dolomites from the lower part of the Talakh-Khaya section (samples 76-20, 76-25, and 76-30), these ratios are lower (0.70582, 0.70626, and 0.70575, respectively). In the neighboring Aim section that is situated on the plate, the $^{87}Sr/^{86}Sr$ ratios measured in ACA-phases of dolomites from the middle and upper part of the Tsipanda Formation are noticeably higher (0.70702–0.70915), growing toward the section top (Bartley *et al.*, 2001).

The intense secondary alterations that are recorded in textural, isotopic, and geochemical characteristics of the Tsipanda dolomites were likely caused by migration of meteoric waters during the pre-Lakhanda break in sedimentation. This conclusion is inferable from the following observations: the $^{87}Sr/^{86}Sr$ ratios grow upward in the rock successions sampled in the plate (Bartley *et al.*, 2001) and Gornostakhskii anticline (this work); the top of the Tsipanda Formation is marked by development of the weathering crust, and karst breccias are characteristic of the whole formation range in the Uchur–Maya plate (Nevolin *et al.*, 1978; Sklyarov, 1981; Semikhatov and Serebryakov, 1983). The lowest $^{87}Sr/^{86}Sr$ initial ratios (0.70575 and 0.70582) observed in the Tsipanda Formation and elevated Sr concentration are characteristic of the lower dolomite horizons in the Talakh-Khaya section.

Lakhanda Group. Concise data on the Rb–Sr systematics of the Lakhanda limestones in the Svetlyi section were published not long ago (Semikhatov *et al.*, 1998). Below, we present their extended characteristic and new data on Rb–Sr systematics of 13 samples from the Nel'kan and Aim sections of the Uchur–Maya plate.

Neryuen Formation. Among 24 studied samples, 22 are of limestones (Mg = 0.1–1.3%) and 2 of dolomites (Mg = 12.2–12.5%). In addition, we studied calcite (Sample 80-2) filling thin (0.1–0.3 mm) veins and epigenetic dolomite (Sample 80-1) from the exocontact zone of a dolomite vein near the top of the Svetlyi section.

In most samples, percentage of siliciclastic admixture (silty grains of quartz, mica, and feldspar) is below 4%, and only two samples showed values as high as 5.4 and 6.7%. Concentration ranges of Mn and Fe in carbonate material of limestones and dolomites are 16–260 and 67–3750 ppm, respectively, but 13 limestone samples contain less than 100 ppm Mn. These are samples from the lower–middle interval of the Svetlyi section and from the middle portion of the Nel'kan section. Limestones of the Svetlyi section are slightly richer in Sr (129–990 ppm) than rocks of the Nel'kan and Aim sections (61.5–607 ppm). The higher Mn and/or Fe contents and simultaneously lover Sr concentrations are characteristic of dolomites, on the one hand, and of limestones occurring close to clayey members, on the other. The epigenetic perivein dolosparites and calcite filling thin fissures in upper horizons of the formation are rich in Mn (210–850 ppm) and Sr (61.5–563 ppm), bur are relatively depleted in Fe (480–730 ppm).

In most limestones of the Svetlyi section, the $^{87}Sr/^{86}Sr$ initial ratios vary from 0.70519 to 0.70692, reaching their maximum near the shale interlayers. In one sample that was collected in the same section near a zone of interstratal tectonic dislocations this ratio is significantly higher (0.70987), approaching ratios measured in the perivein dolosparite (0.71000) and fissure-filling calcite (0.71531). It was difficult to calculate the $^{87}Sr/^{86}Sr$ initial ratio for the last two samples, because

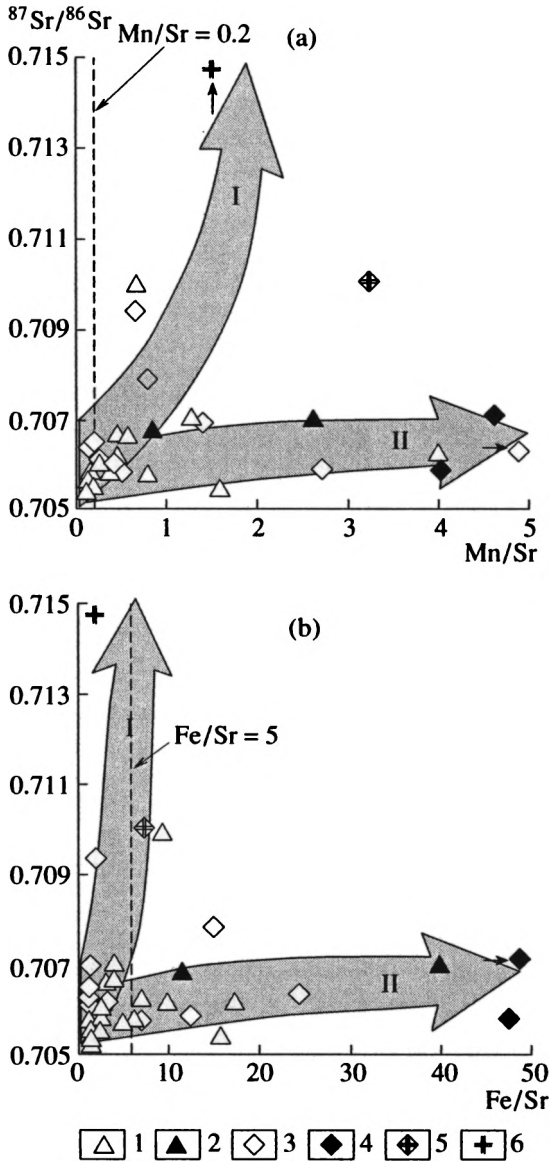

Fig. 8. $^{87}Sr/^{86}Sr$ initial ratios plotted versus Mn/Sr (a) and Fe/Sr (b) ratios in carbonate rocks of the Lakhanda Group of Yudoma–Maya Belt (I) and Uchur–Maya Plate (II): (1) limestone, Neryuen Formation; (2) dolomite, Neryuen Formation; (3) limestone, Ignikan Formation; (4) dolomite, Ignikan Formation; (5) perivein dolosparite; (6) fissure-filling calcite.

the formation time of their calcite and dolomite components is unclear. In the Aim and Nel'kan sections, this ratio ranges from 0.70533 to 0.70612 in limestones and from 0.70673 to 0.70697 in dolomites increasing in rocks adjacent to clayey members.

The $^{87}Sr/^{86}Sr$ ratio in carbonates of the Neryuen Formation is covariant with Mn/Sr and Fe/Sr ratios, and corresponding data points show two different trends in Fig. 8. One of the trends characterizing limestones of the Svetlyi section is steeply inclined and directed toward the data point of fissure-filling calcite. The other one refers to rocks of the Aim section and is directed to data points of dolomites. Difference between the trends points to the variable degree and, probably, to different conditions of alterations that affected the rocks. The variability of conditions could be related to the dissimilar downwarping of the Uchur–Maya plate and Yudoma–Maya belt during the Lakhanda–Ui period, and also to siliciclastic rocks present in the plate sections, where they could produce basinal brines.

Ignikan Formation. We studied 12 samples from this formation, 7 of which were collected from the Svetlyi section and 5 from the Aim section. Two topmost samples from the last section (nos. 78-17 and 78-18) are dolomitic in composition, and others characterize limestones. Concentration ranges of Mn and Sr in limestones are broad, corresponding to 63–580 and 200–3900 ppm, respectively. Maximum concentrations of both elements are established in basal beds of the formation, which are intercalated with and/or rest on the upper siliciclastic member of the Neryuen Formation. The upper limit of Mn concentrations in dolomites is lower (200–240 ppm), but Fe concentration is generally high (2450–4400 ppm), and concentration ranges of both elements are narrower than in limestones.

The Sr concentration ranges are 86.3–1322 ppm in limestones and 50.6–51.0 in dolomites. The $^{87}Sr/^{86}Sr$ initial ratio varies from 0.70572 to 0.70935 in limestones and from 0.70588 to 0.70710 in dolomites. The maximum values of this ratio are established in two limestone samples 106-8 and 106-10 collected from the Svetlyi section in a thin carbonate member that is intercalated with shales near the formation base. The content of siliciclastic impurity in these samples is high (8.4 and 15.0%), Fe concentration is elevated, but their Mn/Sr and Fe/Sr ratios are of a moderate level. Covariation of $^{87}Sr/^{86}Sr$ ratios with Mn/Sr and Fe/Sr values is untypical of other Ignikan limestones from the Svetlyi section (Fig. 7). The Sr isotopic ratios characterizing these rocks are higher than in limestones of the Aim section (0.70601–0.70685 versus 0.70572–0.70632). The difference is likely a consequence of a more intense circulation of meteoric waters though the Ignikan deposits in the northeast of the region, where the erosion level is deeper (see Fig. 2). Two dolomite samples 78-17 and 78-18 from the Aim section yielded the very contrast $^{87}Sr/^{86}Sr$ ratios (0.70588 and 0.70710), the greater of which characterizes a dolomite bed near the formation top. This result and $^{87}Sr/^{86}Sr$ ratios in the bulk carbonate material of Ignikan limestones, which grow upward in this section (Bartley *et al.*, 2001), suggest that the Rb–Sr isotopic systems of carbonates occurring in the upper interval of the Lakhanda Group were reset under influence of meteoric waters, which percolated through siliciclastic rocks of the Ui Group during the pre-Yudoma upwarping of the study region.

RECONSTRUCTION OF $^{87}Sr/^{86}Sr$ INITIAL RATIO IN THE MIDDLE–UPPER RIPHEAN BOUNDARY DEPOSITS

The reconstruction is based on the Rb-Sr data, which were obtained for the Kerpyl' and Lakhanda groups and their analogues in the Turukhansk region of Central Siberia in this and previous works (Gorokhov *et al.*, 1995a, 1996; Semikhatov *et al.*, 1998; Bartley *et al.*, 2001). Unlike the other Middle–lower Upper Riphean deposits, rocks of indicated successions are altered by epigenetic processes to the least extent and are characterized by plentiful analytical data on the Sr isotope composition (more than 160 analyses).

Materials presented above define the following threshold values of geochemical criteria that imply the "isotopic retentivity" of limestone samples applicable for reconstruction of Sr isotope composition in the Riphean seawater: Mn/Sr ≤ 0.20; Fe/Sr ≤ 5.0; and Mg/Ca ≤ 0.024. The results obtained for samples fitting these criteria and italicized in Tables 1 and 2 are used to plot the reference curve of $^{87}Sr/^{86}Sr$ variations in the paleoocean. We failed to define similar criteria for dolomites, because covariation of Mn/Sr or Fe/Sr ratios in the bulk carbonate material, on the one hand, and $^{87}Sr/^{86}Sr$ ratio in the AMA-phase, on the other hand, is untypical of these rocks. Nevertheless, data considered above convincingly show that $^{87}Sr/^{86}Sr$ ratios are increased in any altered carbonate rocks. Accordingly, the minimum values of this ratio in dolomites, although they do not correspond in general to this parameter in sedimentation medium, define a maximum limit of the latter parameter.

Uchur–Maya Region

The Malgina and Neryuen formations of the region are most important for reconstruction of the Sr isotope composition in sedimentation medium.

Malgina Formation. Only 7 of 17 analyzed limestone samples (nos. 56-38, 56-39, 107-16, 107-17, 107-18, 107-19, and 60-10) fit the accepted geochemical criteria. Except for the last one, they all were collected from a member (~80 m thick) located slightly above the middle of the Svetlyi section (Fig. 2). The variation range of $^{87}Sr/^{86}Sr$ initial ratios in these rocks is narrow (0.70563–0.70585), and difference between Sr isotopic ratios measured in their AMA- and ACA-phases is below 0.0002. A higher ratio of 0.70592 is established for Sample 60-10 that was collected from the terminal part of the Kurun-Mastakh section near a zone of epigenetic dolomitization. The difference between ratios measured in carbonate phases of this sample is low (0.0003) and excludes a possibility of considerable alterations in the rock. Accordingly, the $^{87}Sr/^{86}Sr$ initial ratio calculated for that sample may also characterize the sedimentation medium. $^{87}Sr/^{86}Sr$ ratios of 0.70580 and 0.70563 were obtained for two samples of altered limestones (Mn/Sr = 0.44–3.1; Fe/Sr = 5.4–8.1) from the middle third of the Talakh-Khaya section. They fall actually in the range characterized by the "best" samples from the correlative and higher horizons of the formation in the Svetlyi section. Thus, data presented above show that the variation range of $^{87}Sr/^{86}Sr$ ratios during the Malgina time corresponded to 0.70563–0.70592 (Fig. 9)

Bartley *et al.* (2001) published data on the Sr isotope composition in nine limestones of the Malgina Formation, which characterize intervals of the unit unstudied in this work: its basal beds in the Aim section and the lower–middle portion of the Kurun-Mastakh section. These workers also used the sequential dissolution of samples in 1N NH_4OAc, but the studied limestones showed high Mn/Sr (3.7–7.3) and Fe/Sr (19–33) ratios, and, as a consequence, the high values of $^{87}Sr/^{86}Sr$ ratios measured in ACA-phases (0.70651–0.71762). One more determination of Sr isotope composition in basal Malgina limestones of the Aim section was published by Vinogradov *et al.*, (1998) without any data on composition and geochemical parameters of the studied sample. Recalculated for 1050 Ma, the value is 0.70607. In view of considerable secondary alterations of rocks in the lower part of the section (Bartley *et al.*, 2001), we exclude their Sr isotopic characteristics from the further consideration.

Tsipanda Formation. In the studied dolomites of this formation, Mn/Sr ratios are moderate (commonly 1.3–4.3, and 0.85 in one sample), but Fe/Sr ratios are comparatively high (16–77). The $^{87}Sr/^{86}Sr$ initial ratio is highly variable in these rocks (0.70575–0.72072), and, as was mentioned, it grows upward in the stratigraphic succession, reflecting an impact of meteoric diagenesis during the pre-Lakhanda break in sedimentation. The minimum values of this ratio (0.70575–0.70582) are characteristic of the lower part of the Talakh-Khaya section, and they presumably determine the maximum $^{87}Sr/^{86}Sr$ ratios in seawater of the early Tsipanda time. According to results obtained by Bartley *et al.* (2001), the $^{87}Sr/^{86}Sr$ ratios measured in ACA-phases of three dolomite samples, which were collected from the middle and upper part of Tsipanda Formation in the Aim section, are equal to 0.70702, 0.70866, and 0.70915. Vinogradov *et al.* (1998) obtained somewhat lower values for the bulk carbonate material of two dolomite samples from the lower part of the same section. Provided that the formation is 1040 Ma old, the initial ratios calculated for these samples correspond to 0.70548 and 0.70594, but they cannot be correctly interpreted, because the necessary lithological and geochemical characteristics have not been published. In addition, we should mention that the Tsipanda carbonates in the lower part of the Aim section show variable Mn/Sr (3.8–7.0) and Fe/Sr (19–176) ratios, and also the Sr concentration range of 40–73 ppm (Bartley *et al.*, 2001).

Neryuen Formation. The most representative data on the Sr isotope composition of limy and dolomitic

rocks of this formation are obtained in the Svetlyi section, three fourth of which is composed of carbonates (Semikhatov *et al.*, 1998). Five of 18 limestone samples collected here (nos. 52-25, 52-26, 52-72, 52-96, and 52-105) are the least altered according to accepted geochemical criteria and characterize the lower and middle part of the formation (Fig. 2). For these samples, the variation range of $^{87}Sr/^{86}Sr$ initial ratios in ACA-phases is narrow, corresponding to 0.70519–0.70554. The same criteria imply that limestones in higher horizons of the Svetlyi section are noticeably altered. Among eight samples, which were collected from the middle part of the Mil'kon Subformation in the Nel'kan section of the Uchur–Maya plate, only three (nos. 72-11, 72-14, and 72-19) passed the geochemical test. Their $^{87}Sr/^{86}Sr$ initial ratios are 0.70536, 0.70533, and 0.70550. Close values (0.70540 and 0.70575) are obtained for limestone samples 77-21 and 77-22 from the upper part of the same subformation exposed in the Aim section, but their Mn/Sr and Fe/Sr ratios are higher than the accepted threshold values.

The correlation of the Svetlyi and Nel'kan sections, if we assume that their proportional intervals are coeval, elucidates variations of the $^{87}Sr/^{86}Sr$ ratios in the Late Riphean seawater. At the very beginning of the early Neryuen time this parameter fluctuated around 0.70531–0.70542 and decreased to 0.70519 at the end of that time. Afterward, it gradually increased to 0.70533–0.70536 and then to 0.70554–0.70555; it lowered again to 0.70527 by the end of the Neryuen time (Fig. 9).

Studying rocks of the Aim section, Bartley *et al.* (2001) obtained the $^{87}Sr/^{86}Sr$ initial ratios (0.70577 and 0.70573) for the bulk carbonate material of two limestones (samples UM-87 and UM-89) from the middle part of the Mil'kon Subformation, which are slightly altered (Mn/Sr 0.2 and 0.3; Fe/Sr 3 and 4). Their ratios are somewhat higher than ours established for the correlative horizons of the section, but this is not surprising, because Bartly and her coauthors analyzed the bulk carbonate material in contrast to ACA-phases studied in this work. Two very different ratios (0.70650 and 0.70553) were reported by Vinogradov *et al.* (1998) for limestone samples of the Mil'kon Subformation collected from the same section, but their data are published without characterization of the analyzed material. However, all carbonate rocks studied in this interval of the Aim section, except for samples UM-87 and UM-89, show extremely wide variation ranges of Mn/Sr (0.7–38.3) and Fe/Sr (11–428) ratios (Bartley *et al.*, 2001).

Ignikan Formation. Only one limestone sample (no. 106-28) of 12 studied and characterizing the Ignikan Formation of the Svetlyi section is satisfactory in terms of geochemical criteria used in this work. The $^{87}Sr/^{86}Sr$ initial ratio calculated for its ACA-phase is 0.70634. At the same time, the Mg/Ca ratio (0.022) obtained for this sample is close to the threshold value, and difference between $^{87}Sr/^{86}Sr$ ratios measured in its AMA- and ACA-phases (0.0007) is grater than in other samples from the same section. In addition, we obtained much lower $^{87}Sr/^{86}Sr$ initial ratios (0.70601 and 0.70609 versus 0.70634) for ACA-phases of samples 106-15 and 106-29, which were collected close to Sample 106-28 and showed worse geochemical parameters. Taking into account these data and stratigraphic position of Sample 106-28 that is only 50 m below the pre-Vendian disconformity, we feel it impossible to use isotopic parameters of this sample for reconstruction of the Sr isotope composition in seawater. Data on the Aim section lead to the same decision. Even lower $^{87}Sr/^{86}Sr$ initial ratios equal to 0.70581, 0.70572, and 0.70588 were obtained for ACA-phases of two evidently altered limestones (samples UM-97 and UM-104), which have high Mn/Sr (4.4 and 1.8) and Fe/Sr (21 and 28) ratios, and of one dolomite sample (no. 78-17) characterizing the lower, middle, and upper parts of the Ignikan Formation in this section.

Bartley *et al.* (2001) studied the bulk carbonate material of two Ignikan limestones from the lower 35 m of the Aim section. This material was obviously recrystallized, as one can judge from the reported geochemical parameters (Mn/Sr = 4.0–6.4; Fe/Sr = 27–32). Nevertheless, the $^{87}Sr/^{86}Sr$ initial ratio calculated for one of these samples is 0.70575 and falls within the range of 0.70572–0.70581 obtained in this work for ACA-phases of altered limestones from higher horizons of this section (samples UM-97 and UM-104). Vinogradov *et al.* (1998) also analyzed one carbonate sample from the Aim section. This one is enriched in Rb (2.15 ppm) and difference between the measured and initial $^{87}Sr/^{86}Sr$ ratios equals to 0.00170, if we take into account that the formation is 1010 Ma old. It is very likely that Rb concentrated in the rock at the late stage of lithogenesis, and this sample is inappropriate for calculation of the $^{87}Sr/^{86}Sr$ ratio in sedimentation medium.

Thus, the isotopic and geochemical characteristics of dolomite and limestone samples, which have been collected from the Ignikan Formation in the Svetlyi and Aim sections, show that these rocks are variably altered. Consequently, the minimum values of $^{87}Sr/^{86}Sr$ initial ratios characteristic of these rocks (0.70572–0.70588) may define only the upper limit of this parameter in the paleoocean.

Turukhansk Region

The siliciclastic–carbonate succession of the Kerpyl' and Lakhanda groups of the Uchur–Maya region is stratigraphically and, to some extent, lithologically correlative with the Riphean subdivisions exposed in the Turukhansk region of Central Siberia. The basal portion of the Riphean deposits exposed in the last region is represented by the siliciclastic Bezymyannyi Formation (apparent thickness up to 950 m) that underlies a thick (up to 3400 m) succession that consists almost entirely of carbonate rocks. This car-

bonate succession is divided into the Linok, Sukhaya Tunguska, Derevnya, Burovaya, Shorikha, Miroedikha, and Turukhansk formations (Serebryakov, 1975; Semikhatov and Serebryakov, 1983; Shenfil', 1991), which represent two sedimentary complexes separated by the pre-Derevnya disconformity. Data on stromatolites and microfossils (Semikhatov and Serebryakov, 1983; Semikhatov, 1995; Sergeev, 1999) show that the Middle–Upper Riphean boundary coincides in the Turukhansk region with the aforementioned unconformity. The results of C-isotopic chemostratigraphy and of paleomagnetic and geochronological investigations (Semikhatov, 1995; Ovchinnikova *et al.*, 1995, 2001, Knoll *et al.*, 1995; Podkovyrov and Vinogradov, 1996; Vinogradov *et al.*, 1998; Rainbird *et al.*, 1998, Semikhatov *et al.*, 2000; Gallet *et al.*, 2000; Bartley *et al.*, 2001) enable a fair correlation between the Turukhansk and Uchur–Maya successions so that the Sr-isotopic data obtained for both can be integrated into a single series of stratigraphically successive values. Our analysis showed the following: (1) The Malgina and Tsipanda formations correspond to the terminal part of the Bezymyannyi Formation coupled with the Linok Formation and lower portion of the Sukhaya Tunguska Formation. The upper part of the latter has, most likely, no analogues in the Uchur–Maya region, where they apparently were eroded during the pre-Lakhanda event. (2) The Derevnya and Byrovaya formations are equivalent to the Lakhanda Group. This is evident from a short-term negative excursion of $\delta^{13}C$ values that is recorded in the middle of the Derevnya Formation and near the base of the Mil'kon Subformation of the Neryuen Formation, and also from a series of synphase positive $\delta^{13}C$ undulations in the upper horizons of the Burovaya Formation and Lakhanda Group. These observations elucidate some necessary details of correlation between the indicated subdivisions. (3) The lower part of the Ui Group (1000–970 Ma) seems to be correlative with lower horizons of the Shorikha Formation, but higher Riphean strata of the Turukhansk region, which are probably 950–900 Ma old, have no analogues in the Uchur–Maya region.

Turning now to analysis of Sr-isotopic data, which characterize carbonate rocks of the Turukhansk section (Gorokhov *et al.*, 1995a; Bartley *et al.*, 2001), we should mention that even the least altered of these rocks have higher Fe and, sometimes, Mn concentrations than correlative rocks of the Uchur–Maya region. This is especially characteristic of the Linok Formation. The minimal Mn/Sr and Fe/Sr ratios in limestones from the upper part of this formation (samples T-30, T-31, and T-33) are relatively high, corresponding to 0.53–0.70 and 14.1–16.6, respectively. The $^{87}Sr/^{86}Sr$ initial ratio calculated for ACA-phases of these samples ranges from 0.70601 to 0.70652. A close ratio (0.70621) was obtained for Sample T-8 that was collected in the middle part of the formation and showed higher Mn/Sr and Fe/Sr ratios (1.19 and 37.9, respectively). The $^{87}Sr/^{86}Sr$ ratios measured in the bulk carbonate material of the Linok limestones fall in the interval of 0.70611–0.70924, and corresponding variation ranges of Mn/Sr and Fe/Sr ratios are 0.69–1.76 and 26–32, respectively (Bartley *et al.*, 2001). The considered geochemical parameters imply that limestones of the Linok Formation are inappropriate for calculation of their initial isotopic signature.

Data on less altered rocks of the overlying Sukhaya Tunguska Formation are more informative with respect to reconstruction of Sr isotope composition in seawater. In limestone samples from this formation, variation ranges of Mn/Sr and Fe/Sr ratios are 0.04–1.1 and 0.7–32.3, respectively (Gorokhov *et al.*, 1995a; Bartley *et al.*, 2001). The $^{87}Sr/^{86}Sr$ initial ratios of 0.70567 and 0.70585 are calculated for ACA-phases of samples T-37 and T-38, in which both geochemical ratios are minimal (0.04–0.05 and 0.7–0.8). These samples were collected from the middle and upper members of the lower Sukhaya Tunguska Subformation (Petrov *et al.*, 1995).Despite the higher values of Mn/Sr and Fe/Sr ratios (1.1 and 32.3), a similar value of 0.70581 is obtained for Sample T-39 adjacent in the section to Sample T-38. Dolomites from the upper part of the formation show very broad ranges of elevated Mn/Sr and Fe/Sr ratios (0.59–3.0 and 9.5–42.8, respectively), the peak of which is recorded exactly below the pre-Derevnya unconformity. In ACA-phases of four of six studied dolomite samples, the $^{87}Sr/^{86}Sr$ initial ratios range from 0.70565 to 0.70584. For two other dolomite samples, this parameter is either above (0.70606, Sample T-40) or below (0.70532, Sample T-42) the indicated range. In contrast to other rocks of the formation, the ACA-phase of the last sample is enriched in Rb (0.83 ppm) that could be a consequence of incomplete removal of secondary carbonates at the proper stage of laboratory treatment. Accordingly, the isotopic parameters of this sample are excluded from further consideration.

Thus, variation ranges of the $^{87}Sr/^{86}Sr$ initial ratio, which characterize ACA-phases of limestones (0.70567–0.70585) and most dolomites (0.70565–0.70584) from middle and upper parts of the Sukhaya Tunguska Formation, are rather low and close to each other (Gorokhov *et al.*, 1995a). Bartley *et al.* (2001) obtained comparable values of this parameter for the bulk carbonate material of seven limestone samples from the lower part of the unit, which showed lower Mn/Sr (0.05–0.11) but higher Fe/Sr (5.8–10) ratios. The $^{87}Sr/^{86}Sr$ initial ratio in this material ranges from 0.70564–0.70586 to 0.70611 in the lower 180 m of one formation section, and is equal to 0.70588 near the base of another. Applying the accepted criteria of geochemical retentivity, we selected only two of the above values as indicative of the Sr isotopic composition in sedimentation medium. These values (0.70567 and 0.70585) characterize ACA-phases of samples T-37 and T-38 from an upper part of the lower Sukhaya Tunguska Subformation (Fig. 9) and accord well with other data on the Sr isotopic composition in the formation.

The Derevnya Formation is predominantly composed of dolomites, which experienced to a various extent the epigenetic dedolomitisation. The $^{87}Sr/^{86}Sr$ ratios in ACA-phases of these rocks are variable (0.70584–0.70762). In one dolomite sample collected near the formation base, Mg/Ca ratio is maximal, and Mn/Sr (4.2) and Fe/Sr (29.3) ratios are relatively low. The $^{87}Sr/^{86}Sr$ initial ratio in ACA-phase of this sample can be considered as defining the maximum limit of this parameter in seawater. According to geochemical criteria, limestones sporadically occurring in the Derevnya Formation are badly altered, and their $^{87}Sr/^{86}Sr$ ratios are high.

Within the Burovaya Formation, geochemical characteristics of limestones and dolomites are notably variable. The variation ranges of Mn/Sr and Fe/Sr ratios for four limestone samples collected in representative sections are 0.02–1.79 and 0.2–12.6, respectively. The $^{87}Sr/^{86}Sr$ initial ratio in their ACA-phases ranges from 0.70523 to 0.70599. In samples T-96 and T-64, which fit the criteria of geochemical retentivity (Mn/Sr equals to 0.02 and 0.11; Fe/Sr to 0.2 and 3.0), these ratios are 0.70569 and 0.70523. The first sample is collected at the level of 40 m above the formation base, and the second one is from basal level of the upper third of the unit. One more low value of the Sr isotopic ratio (0.70537) was obtained for the more altered sample (Mn/Sr = 0.54, Fe/Sr = 12.6) that characterizes level of 28 m above the formation base (Gorokhov *et al.*, 1995a). The bulk carbonate material of limestone having similar geochemical characteristics (Mn/Sr = 0.23; Fe/Sr = 12) and sampled near the formation base in another section yielded the $^{87}Sr/^{86}Sr$ initial ratio of 0.70551 (Bartley *et al.*, 2001).

Dolomites that are confined predominantly to the lower Byrovaya Subformation show high variation ranges of Mn/Sr (1.3–10.5) and Fe/Sr (6.0–165) ratios, which do not correlate with $^{87}Sr/^{86}Sr$ initial ratio in ACA-phases (0.70593–0.70699). These data imply a high degree of post-diagenetic alterations in dolomites, because sediments of the lower Burovaya Subformation appear to be frequently experienced subaerial exposition that led to development of initial karstification (Petrov and Semikhatov, 1998). Thus, only basal and upper limestone horizons of the formation retained isotopic signatures characterizing the Sr isotope composition in seawater. The corresponding ratios are equal to 0.70569 and 0.70523.

Dolomites of the Shorikha Formation were recrystallized in a medium with high $^{87}Sr/^{86}Sr$ ratio, and even minimal initial values of this parameter, which were established in the formation (0.70570–0.70594), are inappropriate for reconstruction of the Sr isotopic composition in seawater (Gorokhov *et al.*, 1995a). Limestones and dolomites of the Miroedikha and Turukhansk formations, which are terminal in the regional succession of Riphean deposits, are also considerably altered, as it is evident from their high Mn/Sr (1.5–145) and Fe/Sr (1–191) ratios. The minimum $^{87}Sr/^{86}Sr$ initial ratio in the bulk carbonate material of the Miroedikha limestones (Mn/Sr = 2.91) is 0.70679 (Bartley *et al.*, 2001). In the ACA-phase of dolomite sample from the Turukhansk Formation it is 0.70622 (Gorokhov *et al.*, 1995a)

Thus, only two of seven carbonate formations of the Turukhansk region contain rocks that satisfy the criteria of geochemical retentivity. The $^{87}Sr/^{86}Sr$ initial ratios, which were obtained for these subdivisions (0.70567–0.70585 and 0.70523–0.70569 for Sukhaya Tunguska and Burovaya formations, respectively), are used below to substantiate the reference variation curve of Sr isotopic parameters in the Riphean ocean (Figs. 9 and 10). Isotopic characteristics of altered carbonates from other formations of the Turukhansk region define the upper limit of these variations and imply that $^{87}Sr/^{86}Sr$ ratios in seawater of that time were not greater than 0.7057–0.7062. It seems reasonable to remain that exactly data on the Turukhansk region initially stimulated the revision of traditional viewpoint on variations of Sr isotopic ratios in the Middle–Upper Riphean boundary deposits (Gorokhov *et al.*, 1995a, 1996).

Sr ISOTOPE COMPOSITION IN SEAWATER OF THE MIDDLE–INITIAL LATE RIPHEAN

Data on the Sr isotope composition in carbonates and sulfates of the Middle–initial Late Riphean (1350–800 Ma) are still fragmentary, obtained with the help of different analytical procedures. As for the Middle–Upper Riphean boundary beds (1050–1000 Ma), the corresponding $^{87}Sr/^{86}Sr$ ratio is determined for more than 160 samples from the well-correlated rock successions of the Turukhansk and Uchur–Maya regions. The alteration degree of 125 samples was checked with the help of geochemical criteria, and the analyzed material was preliminary treated in ammonium acetate solution in order to remove secondary carbonate phases. About a hundred of published $^{87}Sr/^{86}Sr$ ratios was also obtained for the remaining Middle–initial Late Riphean strata, which span 90% of this stratigraphic interval. These results characterize discrete lithostratigraphic units of various regions, many of which have inadequate geochronological calibration. Most of the results are obtained either for the bulk carbonate material with high Mn/Sr and Fe/Sr ratios, or for samples lacking the necessary geochemical characteristics, except for Sr isotopic ratio.

The indicated database for the Middle–Upper Riphean boundary deposits of the Uchur-Maya and Turukhansk regions, includes 19 values of $^{87}Sr/^{86}Sr$ initial ratio characterizing ACA-phases of limestones, which satisfy the strict criteria of geochemical retentivity ($Mn/Sr \le 0.2$; $Fe/Sr \le 5$; $Mg/Ca \le 0.024$). These ratios are principal ones for the new reference curve of $^{87}Sr/^{86}Sr$ ratio variations in seawater 1050 to 1000 Ma ago. About forty minimal $^{87}Sr/^{86}Sr$ ratios, which are obtained either for associated dolomites, or for ACA-

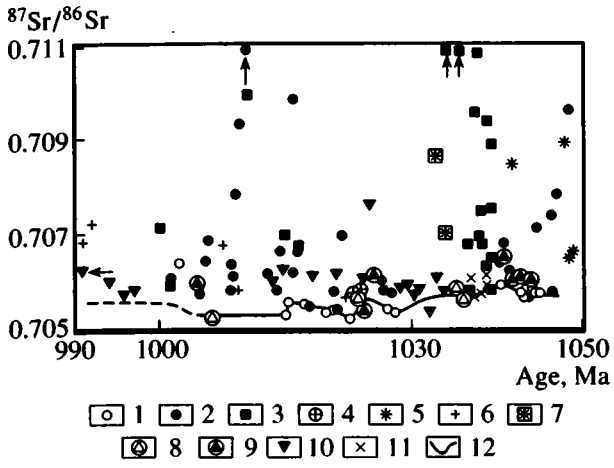

Fig. 9. Variations of $^{87}Sr/^{86}Sr$ ratios in carbonate rocks from the Middle–Upper Riphean boundary horizons of the East Siberian Uchur–Maya and Central Siberian Turukhansk regions. Rocks of the Uchur–Maya region: (1) preliminary leached limestone satisfying the accepted geochemical criteria; (2) ditto, geochemical criteria are unsatisfied; (3) preliminary leached dolomite; (4) limestone satisfying the geochemical criteria, preliminary leaching has not been applied (Bartley *et al.*, 2001); (5) limestone unsatisfying the geochemical criteria despite the preliminary leaching (Bartley *et al.*, 2001); (6) ditto, geochemical criteria are unsatisfied and preliminary leaching has not been applied (Bartley *et al.*, 2001); (7) preliminary leached dolomite (Bartley *et al.*, 2001). Rocks of the Turukhansk region: (8) preliminary leached limestone satisfying the geochemical criteria are satisfied (Gorokhov *et al.*, 1995a); (9) ditto, geochemical criteria are unsatisfied (Gorokhov *et al.*, 1995a); (10) preliminary leached dolomite (Gorokhov *et al.*, 1995a); (11) limestone unsatisfying the geochemical criteria, preliminary leaching has not been applied (Bartley *et al.*, 2001); (12) line connecting data points of least altered samples and depicting variations of Sr isotopic parameters in seawater of the terminal Middle–initial Late Riphean time.

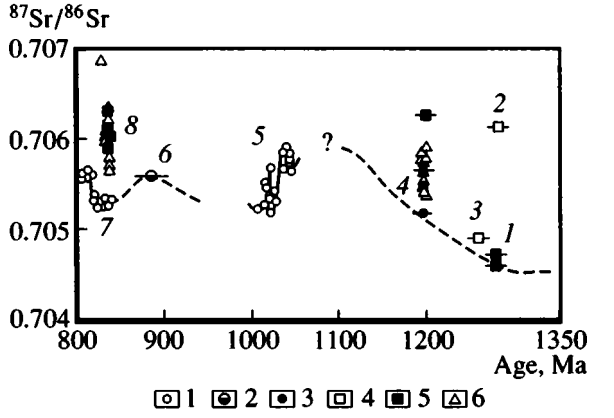

Fig. 10. Sr isotope composition in seawater of the Middle–early Late Riphean time: (1) preliminary leached limestone satisfying the accepted geochemical criteria; (2) limestone, geochemical characteristics are known, but preliminary leaching has not been applied; (3) ditto, geochemical characteristics are unavailable, and preliminary leaching has not been applied; (4) preliminary leached dolomite, geochemical characteristics are known; (5) dolomite, geochemical characteristics are unavailable, and preliminary leaching has not been applied; (6) sulfate. Stratigraphic units by numbers: (*1*) Yusmastakh Formation of the Anabar massif (Pokrovskii and Vinogradov, 1991); (*2*) Arymas Formation of the Olenek Uplift (Gorokhov *et al.*, 1995a); (*3*) Debengda Formation of the Olenek Uplift (Gorokhov *et al.*, 1995a); (*4*) limestone and gypsum beds of the Society Cliffs Formation, northern Canada (Kah *et al.*, 2001); (*5*) Riphean limestones of the Uchur–Maya and Turukhansk regions, Siberia (this work); (*6*) Member I_6 of the Atar Group, northern Africa (Viezer *et al.*, 1983); (*7*) Inzer Formation, southern Urals (Kuznetsov *et al.*, 1997); (*8*) Bitter Springs Formation, central Australia (Hill *et al.*, 2000; Hill and Walter, 2000).

phases and bulk carbonate material of limestones unsatisfying the above criteria, define the upper limitation of the curve. As compared to the curve that was recently published for the same stratigraphic interval by Bartley *et al.* (2001), the new one is of a different configuration, since it is plotted on the basis of more representative data for rock samples that passed the stricter geochemical control.

The initial part of the curve is plotted using the $^{87}Sr/^{86}Sr$ initial ratios calculated for eight least-altered limestone samples from middle and upper horizons of the Malgina Formation. These ratios varying from 0.70563 to 0.70592 show the tendency to grow up-section (Fig. 9). The subsequent gentle decline of $^{87}Sr/^{86}Sr$ ratio is substantiated by data on the bulk carbonate material of the least-altered samples from the lower part of the lower Sykhaya Tunguska Subformation of the Turukhansk region (0.70564–0.70586) and on ACA-phases of two "best" limestone samples from the upper part of this subformation (0.70567 and 0.70585). The $^{87}Sr/^{86}Sr$ initial ratio of dolomite samples from the upper subformation of the same formation (0.70565–0.70584) point to the low-radiogenic Sr isotope composition in seawater of the corresponding time.

The Sr isotopic characteristics of "best" limestones of the Neryuen and Burovaya formations indicate that the $^{87}Sr/^{86}Sr$ value in seawater of the earliest Late Riphean (~1030–1000 Ma ago) were within the range of 0.70519–0.70569 gradually rising up two times and suddenly decreasing after the relative peak values. The first cycle of variations, when they grew from 0.70531 to 0.70569 and drop down to 0.70519, is inferable from data on the lower part of the Neryuen Formation and basal horizons of the Burovaya Formation (increasing trend) and on the middle of the former unit (decreasing trend). The next increase from 0.70519 to 0.70554 and subsequent decline down to 0.70527 are recorded in middle and upper horizons of the Neryuen Formation. After this decline, i.e., by the end of the Lakhanda time (about 1010–1000 Ma ago), the $^{87}Sr/^{86}Sr$ ratio in paleoocean was rather stable (0.70523), as it is evident from data on the terminal part of the Burovaya Formation. The lower $^{87}Sr/^{86}Sr$ initial ratios (0.70500–0.70515) were reported for the carbonate Dzhura Formaition of the Yenisei Ridge (Khabarov *et al.*, 2000), which is cor-

relative with Derevnya Formation of the Turukhansk region (Semikhatov and Serebryakov, 1983), and also for some other Upper Riphean deposits of that ridge (Khabarov *et al.*, 2001). Data on rocks from the Yenisei Ridge are published however without necessary analytical data, and we omit them from further consideration. Thus, the valid data suggest that the $^{87}Sr/^{86}Sr$ ratio in seawater varied in a narrow range from 0.70519 to 0.70592 about 1050–1000 Ma ago and in general had a tendency of decreasing with time.

The Middle Riphean deposits that predate the considered Kerpyl'–Lakhanda succession are poorly characterized by data on their Sr isotope composition, which have been obtained for deposits of six widely separated regions. The relevant oldest deposits constitute the Yusmastakh Formation of the Anabar massif. Gorokhov *et al.* (2001) showed that this formation accumulated 1280–1270 Ma ago (Rb–Sr isochron dates for fine illite subfractions) and belongs to the lower Middle Riphean. The Sr isotopic data were published for the bulk carbonate material of 10 dolomite samples from this formation (Pokrovskii and Vinogradov, 1991) without supplementary geochemical characteristics, which may shed light on the degree of secondary alterations in the studied rocks. In view of high Rb concentration in these dolomites and unknown character of this element distribution between non-cogenetic carbonate phases, significance of corresponding $^{87}Sr/^{86}Sr$ initial ratios is doubtful. For the assessment of Sr isotope composition in seawater, it is possible to use conditionally only data on three samples from the lower part of the Yusmastakh Formation, which contain less than 0.25 ppm Rb and are comparable in this respect with "best" samples from the Uchur–Maya and Turukhansk regions (Table 2; Gorokhov *et al.*, 1995a, Table 3). For these three samples, the $^{87}Sr/^{86}Sr$ initial ratios recalculated for the age of 1300 Ma correspond to 0.70458, 0.70459, and 0.70471.

A much higher $^{87}Sr/^{86}Sr$ initial ratio of 0.70613 was obtained for the ACA-phase of dolomite from the Arymas Formation of the Olenek Uplift, but this rock is badly altered, as one can judge from high Mn/Sr (3.1) and Fe/Sr (52) ratios (Gorokhov *et al.*, 1995a). The Arymas Formation, basal one in the Middle Riphean succession of the region, is correlated with the Yusmastakh Formation of the Anabar massif (Komar, 1966; Semikhatov and Serebryakov, 1983) and contains the mineralogically unstudied glauconite that yields K–Ar age of 1220–1170 Ma. However, the isochron Rb–Sr and K–Ar ages of glauconite from the basal part of overlying Debengda Formation correspond to 1262 ± 13 and 1287 ± 16 Ma, respectively. The Mössbauer spectrum of the last glauconite indicates the closed-system behavior of its isotopic systems (Gorokhov *et al.*, 1995b), and dates obtained for glauconite of the Arymas Formation are therefore "rejuvenated." The Sr isotope composition is also determined for the ACA-phase of one dolomite sample from a lower horizon of the Debengda Formation, but the calculated $^{87}Sr/^{86}Sr$ initial ratio of 0.70490 appears to be insufficiently reliable owing to the high Mn/Sr (12) and Fe/Sr (20) ratios in the studied rock (Gorokhov *et al.*, 1995a).

Plentiful data on the Sr isotope composition characterize carbonate and gypsum beds of the Society Cliffs Formation of the Bylot Supergroup in the Baffin Island. Volcanics of the Bylot Supergroup are well correlated with volcanic rocks in adjacent areas, where the latter are confidently dated, and these results indicate, together with data of C-isotope chemostratigraphy, that the Supergroup is younger than 1270 Ma and older than 1000 Ma. The isochron Pb–Pb age of carbonates from the Society Cliffs Formation is 1199 ± 24 Ma (Kah *et al.*, 1999, 2001, and references therein). The $^{87}Sr/^{86}Sr$ values measured in three limestone and one dolomite samples from the lower part of this formation correspond to 0.70518, 0.70549, 0.70564, and 0.70627 (Kah, 2000), but additional geochemical characteristics have not been published for these rocks. The same ratios for gypsum beds intercalated with carbonates show the variation range of 0.70540–0.70858, but in the lower part of the formation they fall between 0.70540 and 0.70594 (Kah *et al.*, 2001). Among all these ratios, only the minimum ones obtained for limestone (0.70518–0.70549) and gypsum (0.70540–0.70555) appear to be appropriate for assessment of Sr isotopic parameters in seawater of the corresponding time.

The $^{87}Sr/^{86}Sr$ initial ratios falling in the range of 0.70404–0.70600 (including those obtained after the preliminary leaching of samples) are reported for the Riphean carbonates of the Baikit anteclise in Siberia (Khabarov *et al.*, 1998, 2000, 2001), but their positions in the stratigraphic scale are far from being unambiguously defined, and other analytical results characterizing the studied rocks have not been published. One more reported value of 0.7055 characterizes the Sr isotope composition in the bulk carbonate material of the Grenville Marble in Canada (Hoff *et al.*, 1984), the age of which falls in the range of 1280–1220 Ma (Corriveau and Morin, 2000). A high metamorphic grade of the rock and absence of its geochemical characteristics imply that the above value must be omitted from consideration.

Carbonate rocks that accumulated 1200–1050 Ma ago and fill the gap between the Society Cliffs Formation and the upper Kerpyl'–Lakhanda succession (1050–1000 Ma) have no reliable Sr isotope characteristics. During the formation time of the mentioned succession, the $^{87}Sr/^{86}Sr$ ratios in seawater smoothly fluctuated, as is shown above, in the range of 0.70592–0.70519 gradually decreasing with time. After this time, we have another gap in the Sr-isotopic record that is as long as 100 m.y. approximately. Only few data on three formations terminating the Riphean section in the Turukhansk region suggest that the Sr isotopic ratio was below 0.7057–0.7068 in the period of 1000–900 Ma.

For younger deposits of the lower Upper Riphean (900–800 Ma), the Sr isotope composition is deter-

mined in 57 samples from the Atar Group of northern Africa, Inzer Formation of southern Urals, and Bitter Springs Formation of central Australia.

The studied limestones and dolomites of the Atar Group (16 samples) showed the wide variation ranges of Mn/Sr, Fe/Sr, and measured $^{87}Sr/^{86}Sr$ ratios, which correspond to 0.34–86, 3.3–1680, and 0.70562–0.72134 (Veizer *et al.*, 1983). An intense disturbance of geochemical and isotopic systems in these rocks was favored by alternation of carbonate and siliciclastic members in the section and by strong meteoric diagenesis at the time of Pan-African events (Fairchild *et al.*, 1990). The $^{87}Sr/^{86}Sr$ ratio is sufficiently low only in one limestone sample that was collected close to the base of predominantly sandy–shaly Member I_6 and showed the lowest Mn/Sr and Fe/Sr ratios. When recalculated to the age of 890 Ma, the $^{87}Sr/^{86}Sr$ initial ratio is equal to 0.70558, and exactly this value was interpreted as indicative of "a mantle event at 900 Ma ago" (Veizer *et al.*, 1983). The Member I_6 is of a roughly known age. Stromatolites from the underlying Member I_5 (Bertrand-Sarfati, 1972; Knoll and Semikhatov, 1998) are characteristic of the lower Upper Riphean (~1030–850 Ma), and the Rb–Sr isochron dates for illite fractions ~2 μm separated from both members are 890 ± 37 and 874 ± 23 Ma, respectively (Clauer, 1981). However, these dates are applicable only for the approximate evaluation of the age, because the fraction ~2 μm usually contains, as is established now (Gorokhov *et al.*, 2001, and references therein), the non-cogenetic illite generations. In this study, we tentatively accept the age of 890 Ma for the Member I_6.

The isotopic age of the Inzer Formation in the lower part of the Upper Riphean stratotype is defined with confidence. The Pb–Pb isochron date of 836 ± 25 Ma that characterizes limestones of the lower Inzer Subformation is interpreted as indicating the age of early diagenesis (Ovchinnikova *et al.*, 1998), and the burial diagenesis of these sediments took place 805–835 Ma ago (the Rb–Sr isochron ages of fine illite subfractions; Gorokhov *et al.*, 1995c). These dates blend well with sequential K–Ar dates obtained for glauconite from the middle part of the Upper Riphean stratotype (*Stratotip...*, 1982) and suggest that the Inzer Formation accumulated 835–810 Ma ago. Among 20 limestone samples from this formation, 13 satisfy the accepted criteria of geochemical retentivity (Kuznetsov *et al.*, 1997). The $^{87}Sr/^{86}Sr$ initial ratios of their ACA-phases are in the range of 0.70525–0.70566. Beginning from the value of 0.70534 that is characteristic of basal horizon of the lower subformation, they smoothly decrease to 0.70525 in its middle part and then grow to 0.70566 in the middle of the upper subformation. Finally, they decline again to 0.70555 near the top of the latter unit.

Age limits of the Bitter Springs Formation are established quite confidently. Volcanics of this unit and basic dikes in southerly areas of Australia are comagmatic (Zhao *et al.*, 1992), and the U–Pb age of the latter is 827 ± 6 Ma (Wingate *et al.*, 1998). In the middle and upper parts of the Gillen Member, the basal unit of the formation, the $^{87}Sr/^{86}Sr$ ratios measured in dolomites fall in the range of 0.70592–0.70633, varying in alternating gypsum and anhydrite beds from 0.70568 to 0.70636 (Fanning, 1986; Hill *et al.*, 2000). The higher $^{87}Sr/^{86}Sr$ ratios (0.7069 and 0.7072) in two gypsum samples from the base of the overlying Loves Creek Member reflect the progressive isolation of the basin (Hill *et al.*, 2000; Hill and Walter, 2000). The minimal of obtained values are comparable with the $^{87}Sr/^{86}Sr$ initial ratios in ACA-phases of the Inzer Formation that is close in age.

Data considered above show that the $^{87}Sr/^{86}Sr$ ratios in seawater were very low (not greater than 0.7046–0.7047) at the beginning of the middle Riphean (1280–1270 Ma ago; the Yusmastakh Formation), actually comparable with those of the Early Riphean ocean (Gorokhov *et al.*, 1995a; Hall and Veizer, 1996). Available fragmentary data suggest that the ratios could be slightly greater later on, but they were still not higher than 0.70490 about 1260 Ma ago (the Debengda Formation). Judging from data on the Society Cliffs Formation, the ratio approached the range of 0.7052–0.7056 about 1200 Ma ago. Ratios that were maximal in the Middle Riphean (0.70563–0.70592) are recorded in sediments deposited 1050–1040 Ma ago (the Malgina time). Afterward, during the Sukhaya Tunguska time and at the very beginning of the Late Riphean (1030–1000 Ma; the Lakhanda time), this parameter slowly decreased to 0.70523–0.70527. Very similar $^{87}Sr/^{86}Sr$ initial ratios are typical of "best" samples from successive lithostratigraphic units of the initial Late Riphean, namely from the Lakhanda Group and Burovaya Formation (070519–0.70569; 1030–1000 Ma), and then from Member I_6 of the Atar Group (0.70558; >890 Ma), Inzer Formation (0.70525–0.70566; ~835–810 Ma), and Gillen Member of the Bitter Springs Formation (0.70568–0.70592; 827 ± 6 Ma). These convincing data imply that the $^{87}Sr/^{86}Sr$ values were steadily low in oceans of the Grenville and post-Grenville time, i.e., during the first half of the Late Riphean (1030–800 Ma).

GEOLOGICAL FACTORS THAT DETERMINED THE Sr ISOTOPIC COMPOSITION IN SEAWATER OF THE GRENVILLE AND POST-GRENVILLE TIME

The Grenville orogenic cycle responsible for origin of the Rodinia supercontinent was of a global significance. Structures that were formed at that time extend from Labrador to Adirondack along the eastern edge of North America, westward of the Appalachian frontal thrust, and are traceable below the cover of younger deposits up to Georgia and New Mexico and are exposed in the Llano uplift and Van Horn area of Texas (Davidson, 1995; Roback, 1996; Rivers, 1997; Mosher, 1998; Rivers and Corrigan, 2000; Hynes *et al.*, 2000).

These structures are also known in Mexico (Ortega-Gutierrez *et al.*, 1995), exposed in the Folkland Plateau (Warenham *et al.*, 1998; Jacobsen *et al.*, 1999), and mapped in Andes from Columbia to Bolivia and northwestern Argentine (Orinoco orogeny; Kay *et al.*, 1996; Restrepo-Pace *et al.*, 1997). They are investigated in western Brazil (Condie, 2001), in foldbelts surrounding and separating the San-Francisco and Amazonian cratons (Strieder and Suita, 1999; Cordani and Sato, 1999), and are described in western Greenland, Scotland, Ireland, and southwestern Scandinavia (Cosca *et al.*, 1998; Christoffel *et al.*, 1999; Anderson *et al.*, 1999). Structures of the Grenville orogeny occupy vast areas in Africa from Namibia to Natal (Namaqua orogeny; Trompette, 1994; Hartandy *et al.*, 1985) and have been observed in eastern (Mozambique and Tanzania; Kröner *et al.*, 1997) and southern (Frimmel and Frank, 1998) margins of this continent. In addition, they frame western and southern coastal zones of West Australia, western to eastern Antarctica (Jacobs *et al.*, 1998; Warenham *et al.*, 1998; Bruguer *et al.*, 1999), and are established in Madagascar, Sri Lanka, central India (Condie, 2001, and references therein), and southeastern China (Li and McCulloch, 1996; Li *et al.*, 1996; Smith *et al.*, 2000). The long succession of event, which resulted in formation of Rodinia, is reconstructed most completely in the vast (1900 × 400 km) Grenville Province in the northeast of North America, and coeval events in other aforementioned regions substantiate the global significance of corresponding tectonic cycle.

Viewpoints on the geodynamic essence, age limits, and hierarchy of events representing the Grenville orogenic cycle considerably progressed in the last years. In the current understanding, the cycle either consisted of successive Elzevirian (~1350–1220 Ma) and Ottawan (1200–1000 Ma) orogeny (Davidson, 1995; McLelland *et al.*, 1996), or represented a succession of the Shawinigan (1190–1140 Ma), Ottawan (1080–1020 Ma), and Rigolet (1000–980 Ma) collisional impulses, which developed after and partly simultaneously with the accretionary Elzevirian orogeny (1250–1190 Ma), being separated from each other by periods of crustal extension (Rivers, 1997; Carr *et al.*, 2000; Hynes *et al.*, 2000; Ketchum and Davidson, 2000; Indares *et al.*, 2000). At the same time, the reconstructed pre-Grenville history of those crustal areas, which were subsequently involved into the Grenville events, showed that Grenvillides incorporate a considerable volume of pre-Elzevirian magmatic and metamorphic rocks of the crustal and mantle origin (Li and McCulloch, 1996; Rivers, 1997; Christoffel *et al.*, 1999; Anderson *et al.*, 1999; Strieder and Suita, 1999; Cordani and Sato, 1999; Tassinarini and Macambra, 1999; Dickin, 2000; Indares *et al.*, 2000; Rivers and Corrigan, 2000; Carr *et al.*, 2000; Ketchum and Davidson, 2000; Martignol *et al.*, 2000).

The origin of the Rodinia supercontinent comprising a global system of collisional and accretionary orogens should result in a sudden increase of the continental runoff (of its siliciclastic fraction, first of all) in response to erosion of these structures. This can be illustrated by following examples. (1) The reconstruction of Grenville provenance of clastic zircons found in United States and Canada and the facies analysis of their host rocks point to existence of a pan-continental river system in Laurentia, where it extended north and northwest of the Grenville orogen foreland for a distance of 3000 km (Rainbird *et al.*, 1996). Taking into account clastic zircons of Grenville age, which were discovered from the Ui Group of the Uchur–Maya region, and recent data on the Siberia position in the Rodinia structure (Rainbird *et al.*, 1998; Gallet *et al.*, 2000; Khudoley *et al.*, 2001), we may conclude that the distribution zone of the Grenville clastic material was even wider by about 2000 km. (2) In some regions, the unmetamorphosed and unfolded Cambrian or Vendian deposits overlie granulites and eclogites of the Grenville basement metamorphosed 1.0–1.2 Ga ago, and this may point to a considerable (22–25 km deep) base level of erosion. (3) Important changes in the global biogeochemical cycle of carbon are recorded in the upper Middle–lower Upper Riphean deposits. Values of $\delta^{13}C_{carb.} = 0 \pm 1‰$ PDB, which were characteristic of the Early–early Middle Riphean time turned into lower positive values (+3.5 ± 1‰ PDB) about 1250 Ma ago to become greater (up to +6.0‰ PDB) about 1030 Ma ago (Knoll *et al.*, 1995; Kah *et al.*, 1999, 2000; Bartley *et al.*, 2001). On the basis of mass balance, it is assumed that the $\delta^{13}C$ increase was related to the progressing burial of isotopically light organic carbon, when siliciclastic sedimentation intensifies during the orogenic periods of the Earth's history (Des Marais, 1994; Galimov, 1999; Jacobsen and Kaufman, 1999, and references therein).

Nonetheless, the $^{87}Sr/^{86}Sr$ ratio in seawater of the Middle–initial Late Riphean time (1350–800 Ma) did not rise to the extent comparable with that at the time of Pan-African events, which created Gondwana, or after the Eurasia formation, when collision with Hindustan rose up the Tibet–Himalayas plateau (Raymo *et al.*, 1988; Hodell *et al.*, 1990; Richter *et al.*, 1992).

The precise data on the $^{87}Sr/^{86}Sr$ ratio in seawater of the initial Middle Riphean are unknown so far. Nevertheless, the above-considered data on the Sr isotope composition in feebly altered carbonate and gypsum beds, which were deposited at that time, allow us to suggest with some reservations that this ratio began to grow slowly 1280–1200 Ma ago (Fig 10). This tendency is agreeable with geodynamic environments inferable for that time, i.e., with the development of Elzevirian orogeny that commenced ca. 1250 Ma ago and resulted in a widespread accretion of island arcs and some continental terranes to Laurentia and in closure of back-arc basins of variable maturity (McLelland *et al.*, 1996; Rivers, 1997; Corriveau and van Breemen, 2000; Carr *et al.*, 2000; Van Schimus, 2000; Rivers and Corrigan, 2000). As McLelland and his colleagues (1996) stated, data available for various regions of

North America, Ireland, and Baltia imply a subglobal significance of events under consideration. At the first glance, their conclusion is incompatible with the weak increase of $^{87}Sr/^{86}Sr$ ratios in seawater of the Elzevirian time (from 0.7046–0.7047 to 0.7052–0.7056). A possible explanation to this apparent discordance is a relatively high proportion of mantle-derived rocks in island arcs and back-arc basins accreted to Laurentia during the Elzevirian orogeny (Dikin, 2000; Rivers and Corrigan, 2000).

Data on the Sr isotope composition in seawater at the time of the Shawinigan collisional impuls (1190–1140 Ma) are on the way to being elucidated. The collision of southeastern (in modern coordinates) Laurentia with either another continent, or the microcontinent and/or island arc (McLelland *et al.*, 1996; Rivers, 1997; Rivers and Carrigan, 2000; Carr *et al.*, 2000) was able to increase however the $^{87}Sr/^{86}Sr$ ratios in the World Ocean.

The Sr-isotopic record of seawater during the more intense and widespread Ottawan (1080–1020 Ma) and initial Rigolet (1000–980 Ma) collisional impulses are clearer. Data on ACA-phases of "best" limestones of the Malgina Formation record the Middle Riphean (about 1040 Ma) maximum of $^{87}Sr/^{86}Sr$ ratios (0.70563–0.70592) that terminates the trend of their gentle rising since the period of 1280–1200 Ma. In addition, data on the Lakhanda Group of the Uchur–Maya region (1030–1000 Ma) and on the Burovaya Formation of the Turukhansk region imply that afterward, in the initial Late Riphean, the ratios decreased in a similar gentle manner. In the last period, they ranged from 0.70519 to 0.70569 generally decreasing with time (Fig. 9). Thus, the recent data (Gorokhov *et al.*, 1995a; Semikhatov *et al.*, 1998; Bartley *et al.*, 2001; and this work) show that the terminal period of the Grenville orogenic cycle and Rodinia formation was characterized not only by low $^{87}Sr/^{86}Sr$ ratios in seawater (0.70519–0.70585), but also by stability with time.

Materials available in publications allowed us to distinguish and evaluate several alternative or complimentary factors, which reconcile two contraries: the low $^{87}Sr/^{86}Sr$ ratios in seawater of the terminal Middle–initial Late Riphean time and the high continental runoff triggered by termination of the Grenville tectogenesis and Rodinia formation. Our analysis of these factors is based first of all on materials of the Grenville Province that is studied much better than other regions of Grenvillides.

1. Impulses of juvenile crust increment. Analyzing time distribution of well-dated juvenile crustal complexes, Condie (1998) came to the conclusion that the continental growth during the Precambrian was periodical, divisible into three large impulses. About 36% of the present-day continental crust formed 3.0–2.5 Ga ago; 39% are accreted about 2.15–1.65 Ga ago and 12% about 1.32–1.0 Ga ago. Peaks of the juvenile crust accretion were 2.7, 1.9, and 1.2 Ga ago, and each of them (Superevent in Condie's terminology) is considered as a consequence of the mantle superplume development. The Rodinia formation and Grenville tectogenesis, both coinciding in time with one of the continental growth peaks and superplume development (Condie, 1998, Fig. 1), were also marked by a considerable increment of juvenile crust 1.32–1.2 Ga ago that remarkably declined 1.0–0.9 Ga ago.

A similar analysis in South America (Cordani and Sato, 1999) showed that nearly 34% of the crust was formed in this continent by the end of Archean, and up to 80% in total originated here by the end of the Trans-Amazonian orogeny (2.15–1.9 Ga), while the subsequent impuls of noticeable accretion took place 1.3–1.0 Ga ago. Close age limits (2.1–2.0 and 1.2–1.0 Ga) are established for the statistical maximums of model Sm–Nd ages calculated for granitoids and volcanics of the Amazonian craton (Tassinari and Macambra, 1999).

The time coincidence of three extraordinary events: (1) one of the accretion peaks of juvenile continental crust (Superevent 1.2); (2) the formation of supercontinent; and (3) the mantle superplume development, gave rise to the assumption that their combined influence was able to change the global Sr-isotopic balance. As was assumed, the intensified hydrothermal activity in mid-ocean ridges and oceanic plateaus could decrease, with partial contribution of the juvenile crust erosion in collisional and accretionary orogens, the $^{87}Sr/^{86}Sr$ ratio in seawater.

However, the modernized method to calculate the juvenile crust accretion (histograms of its volume increment with time) led to a surprising result (Condie, 2001). As it turned out, the Superevent 1.2 or peak accretion of juvenile crust formerly postulated for the period of 1.35–1.0 Ga (Condie, 1998) did not exist, because the increment in that period was equal to 7–13% only. According to new results (Condie, 2001, Fig. 3), the juvenile crust that was accreted 1.35–0.9 Ga ago represents not more than 0.1–0.5% of the total crust volume in large regions, which were affected by the Grenville orogeny. In three regions only (southern part of the Grenville Province, Latin America, and Antarctica), its increment was greater, equal to 1.2–1.7%. It is clear therefore that erosion that affected the Grenville orogens, which had such a percentage of juvenile material, and older continental areas was unable to maintain steadily the low $^{87}Sr/^{86}Sr$ ratio in seawater. In other words, the original conclusion turned out to be incorrect.

2. Abundance of pre-Grenville mantle-derived materials in the crust of Grenvillides. Like other Grenvillides, the Grenville Province proper corresponds to the deeply eroded collisional–accretionary orogen that is composed of structurally interrelated lithotectonic units, which are different in composition, metamorphic grade, and age. Their age range is from the Archean to early Late Riphean. Among the pre-Grenville rocks of Grenvellides, most widespread are

Late Paleoproterozoic complexes (younger than 1.79 Ma), which originated, according to Condie (1998), during the Superevent 1.9 (2.15–1.65 Ga) of the continental growth and are relatively rich in the mantle-derived material. This is clearly evident in the Grenville Province.

The province bounded in the northwest by the Grenville front includes two major crustal blocks: (1) one corresponding to the para-autochthonous belt that extends along its northwestern border is a reworked margin of the Laurentia foreland composed of Paleoproterozoic and some Archean rocks, and (2) the other one consisting of terranes accreted to the Laurentia edge, which have different composition, age, thermal history, and Sm–Nd systematics of constituent rocks. In the south of the province, there are distinguished three structural subdivisions: (1) the Central Gneiss Belt that includes para-autochthon in the north and a considerable part of the allochthon in the south, which are separated by a narrow granulite–eclogite zone; (2) the allochthonous Central Metasedimentary Belt that is of imbricated structure, consists of age-variable para- and orthorocks of different metamorphic grade, and represents the uppermost structural unit; and (3) the lower structural unit of the Adirondack Mountains, where rocks of variable metamorphic grade had different protoliths (Davidson, 1995; Rivers, 1997; Ketchum and Davidson, 2000; Indares *et al.*, 2000). The improved understanding of the Grenville Province evolution and the refined position of boundary between the para-autochthon and allochthon (Ketchum and Davidson, 2000) allowed Carr *et al.* (2000) to suggest a somewhat different structural scheme for the southern part of the province, where they distinguished (1) the Laurentia and its reworked margin that is partially overridden by younger complexes and is up to 350 km wide (White *et al.*, 2000) according to geophysical data, (2) the composite Island-Arc Belt that is thrust over the reworked Laurentia margin and approximately corresponds in area to the Central Metasedimentary Belt, and (3) the Frontenac–Adirondack Belt of western areas that is equivalent to the Adirondack Highland and eastern margin of the Central Metasedimentary Belt.

The Paleoproterozoic basement of the reworked Laurentian margin was formed 1.98–1.79 Ga ago at the terminal stage of Laurentia formation (Hoffman, 1988). Major events, which affected this margin later on, were as follows: accretion (with partial overthrusting) of volcanic island arcs and back-arc basins at the time of the Labradorian (1680–1630 Ma) and Pinvarian (1500–1450 Ma) orogenies; emplacement of Killarney granites (1740–1700 Ma), small bodies of which show either negative (–7) or low positive (up to +3) $\varepsilon_{Nd}(T)$ values, respectively northward and southward of the Grenville front; sequential intrusions of large Trans-Labradorian juvenile batholith of basic composition (1654–1648 Ma), of mantle-derived gabbro–anorthosite magma (1650–1620 Ma), and basic dike swarms (1459–1426 Ma) widespread over a considerable area; and formation of granite gneisses in Ontario (1.5–1.4 Ga), which are characterized by positive $\varepsilon_{Nd}(T)$ values (Rivers, 1997; Hynes *et al.*, 2000; Indares *et al.*, 2000; Rivers and Corrigan, 2000; Dickin, 2000).

Plentiful Sm–Nd (over 500) and U–Pb characteristics of rocks from the Grenville Province (Carr *et al.*, 2000; Dickin, 2000; Hynes *et al.*, 2000; Indares *et al.*, 2000; Martignol, 2000; Rivers and Corrigan, 2000) show that a number of sizeable island arcs, which were accreted together with others to the Laurentia margin in the terminal Paleoproterozoic and initial Riphean time, are composed of juvenile rock complexes dated back to 1740, 1660, and 1450 Ma. In lesser island arcs (50 × 400 km in size), the $\varepsilon_{Nd}(T)$ values range from +1.0 to +3.0. In central segments of the greater ones (more than 100 000 km^2), this parameter ranges from +2.9 to +4.0 decreasing to +2.2 or +2.5 toward their marginal zones, where the rocks are contaminated with the older crustal material. The $\varepsilon_{Nd}(T)$ values from –0.3 to +1.0 were calculated for metasediments associated with volcanics of the island arcs under consideration. Among Paleoproterozoic (1.9–1.75 Ga) terranes of the Grenville Province, there are two medium-sized (200 × 300 and 50 × 60 km) island arcs, which have been strongly contaminated with anatectic magmas derived 1.68–1.63 and 1.6–1.3 Ga ago from the older crust but still retain low positive $\varepsilon_{Nd}(T)$ values (Dickin, 2000). We also should note that a fragment of Mesoproterozoic juvenile crust is distinguished in the Central Metasedimentary Belt (Martignol *et al.*, 2000). In addition, the island-arc magmatism in southeastern Laurentia was accompanied by the intense hydrothermal activity 1.4–1.3 Ga ago, and two episodes of eruption (1.16 and 1.06 Ga ago) of younger mantle-derived magmas are recorded in the Middle Riphean succession of western Quebec (Corriveau and Morin, 2000). Thus, there were several Late Paleoproterozoic to Early Riphean stages of the juvenile crust formation in the Grenville Province. They resulted in accretion of pre-Grenville and Grenville island arcs to the southeastern Laurentia (Dickin, 2000; Corriveau and Morin, 2000) and were associated with accretion of continental terranes and with development of back-arc basins.

Summarizing recent data on the southeastern Laurentia evolution in the Early–Middle Riphean, Rivers and Corrigan (2000) came to the conclusion that the marginal magmatic arc of the Andean type, which existed here ~1500–1230 Ma ago, extended for a distance of 4000 km from Labrador to Arizona and New Mexico. The southeastern zone of the arc was involved into the Grenville orogeny to be deformed and metamorphosed 1190–990 Ma ago, whereas its greater northwestern part remained intact. The latter part known in publications as the Granite–Rhyolite Belt represents an assembly of comagmatic volcanics and hypabyssal A-granites associated with rare siliciclastic sediments (Muehlenberger *et al.*, 1967; Van Schimus, 2000). In the Grenville Province and outside it, the northern arc zone is predominantly composed of quartz

monzonites and granodiorites in contrast to the tonalite–granodiorite association typical of the southern part. The Sm–Nd and U–Pb characteristics show that northern rocks are of crustal origin, whereas the calc-alkaline tonalites and granodiorites from southern zone represent the mantle-derived rocks displaying insignificant signs of crustal contamination. The belt extended to the Llano Uplift, where, as is established, the juvenile island-arc magmatic complex that is 1.33–1.27 Ga old was accreted to Laurentia (Mosher, 1998; Rivers and Corrigan, 2000).

Back-arc basins, which developed at that time along the Laurentia border, were of non-simultaneous opening and diverse maturity, thus being related in origin to separate impulses of crustal extension. Some of them accumulated only continental sediments and evaporites, while others were sites of bimodal volcanism. Those, which were more mature, hosted anorthosite intrusions (1.23–1.28 Ga old), $\varepsilon_{Nd}(T)$ values of which are positive, or represented root zones of ophiolites (1230 Ma) and other rock complexes of oceanic crust (Rivers and Corrigan, 2000). The back-arc basins closed at the time of the Pinvarian (1500–1450 Ma) and Elzevirian (1250–1190 Ma) orogenic events, or in response to collision events of the Grenville orogeny proper. At the Elzevirian time, their closure in the Central Metasedimentary Belt was accompanied by the suprasubduction magmatism and by formation of imbricated thrust sheets (Rivers and Corrigan, 2000; Martignol *et al.*, 2000).

All events considered above emplaced large volumes of mantle-derived rocks into outer shells of the Earth, and these rocks influenced the Sr isotope composition of seawater in two ways. First, they interacted with seawater, enriching it with low-radiogenic Sr, at the stage of island arcs development. Second, they decreased the $^{87}Sr/^{86}Sr$ ratio in the continental runoff, when orogens experienced erosion at the later stages of their evolution.

We suggest as well that there was an additional factor of the Middle Riphean time, which activated the seawater interaction with the mantle-derived rocks. The giant Midcontinent rift system developed at that time (1109–1087 Ma ago) in the middle of Laurentia as a result of changes in configuration of plates, which composed Rodinia, and over 2000000 km^3 of volcanic rocks, mostly of olivine tholeiites similar to MORB in geochemical parameters, accumulated in this system during 20–22 m.y. Being of the intracontinental type, the system was unable to influence directly the Sr isotope composition in paleoocean, but its origin was likely connected with concurrent development of oceanic rift systems, where fresh mantle-derived basalts were in contact with seawater.

The juvenile magmatism predated the major phase of collisional deformations in other areas of Grenvillides as well, for instance, in the Tocantins Province of South America (Strieded and Suita, 1999), around the Amazonian craton (Tassinari and Macambra, 1999), and in northern Andes (Restrepo-Pace *et al.*, 1997). A good example is a successive accretion of three island arcs to the southwestern edge of the Amazonian craton. The oldest arc (1790–1750 Ma) was composed of juvenile acid volcanics and granitoids ($\varepsilon_{Nd}(T)$ from +2.2 to +2.6; T_{DM} = 2.0–1.8 Ga). Tonalite–granite series ($\varepsilon_{Nd}(T)$ from –1.3 to +3.7; T_{DM} = 2.0–1.7 Ga) was predominant in the second arc (1560–1530 Ma), and association of the same rocks with slightly different isotopic parameters ($\varepsilon_{Nd}(T)$ from +2.6 to +4.1; T_{DM} = 1.7–1.5 Ga) was characteristic of the third one (1460–1420 Ma; Geraldes *et al.*, 2000). Magmatic island arcs, which had age of 1.5–1.4 Ga and were partially dislocated later on, at the time of Rodinia formation, are also distinguished in the western Amazonia (Fuck and Pimental, 2000). In addition, the juvenile granites of the Grenville age, which show positive $\varepsilon_{Nd}(T)$ values, are established in eastern and western Antarctica, South Africa, Mozambique, Folkland Plateau, and Cordillera piedmonts of Argentine (Kay *et al.*, 1996; Kröner *et al.*, 1997; Jacobs *et al.*, Trimmel *et al.*, 1998; Wareham *et al.*, 1998; Condie, 2001). In opinion of some researchers (Warenham *et al.*, 1998), their occurrence may indicate that the juvenile crust of the Grenville age was widespread in South Atlantics.

Thus, the Sr isotope composition in seawater of the terminal Paleoproterozoic and Early–Middle Riphean times was under influence of considerable masses of juvenile mantle-derived rocks and associated hydrothermal systems. Later on, during the erosion of Grenville orogens, the same rocks supplied paleoocean with the low-radiogenic Sr thus decreasing the $^{87}Sr/^{86}Sr$ ratio in seawater of the Late Riphean.

3. Time-and space distinctive features of metamorphism, exhumation, and unroofing of the Grenville lithotectonic units. Using isotopic dates obtained for mineral thermobarometers, which have different closing temperatures of U–Pb and $^{40}Ar/^{39}Ar$ systems, one can define the time and dynamics of post-metamorphic cooling of metamorphic complexes, and consequently, the rate of their ascent in the crust in response to gravitational redistribution of material, tectonic exhumation, or erosional unroofing. This approach is of a high resolution ability with respect to main domains, terranes, and some tectonic slices of imbricated nappes of the Grenville Province.

The earliest Shawinigan phase of high-T metamorphism and convergent dislocations affected the greater part of the Grenville Province 1190–1140 Ma ago (Rivers, 1997; Corriveau and van Breemen, 2000; Carr *et al.*, 2000). The phase took place close to the termination time of the Elzevirian orogeny but differed from the latter in its essence. It marked collision of southeastern Laurentia either with other continent or, what is more likely, with an island arc and/or microcontinent, whereas the Elzevirian orogeny resulted in amalgamation of island arcs and back-arc basins with the Lau-

rentia edge (McLelland *et al.*, 1996; Rivers, 1997; Rivers and Corrigan, 2000; Carr *et al.*, 2000). In the Central Metasedimentary Belt of Quebec, metamorphism of amphibolite to granulite facies took place 1140–1120 Ma ago (Martignol *et al.*, 2000), but principal distribution patterns of rock complexes different in age and metamorphic grade appeared in the course of the Ottawan orogeny (1080–1020 Ma ago) that was caused by collision of two continents and included two impulses of crustal contraction separated by a period of extension (Rivers, 1997; Carr *et al.*, 2000).

The U–Pb dates available for zircon and monazite fractions from metamorphic complexes show that peaks of metamorphism were asynchronous in different domains and terranes of the Grenville province (Martignol *et al.*, 2000; Corriveau and van Breemen, 2000; Carr *et al.*, 2000; Rivers and Corrigan, 2000; Ketchum and Davidson, 2000). This clearly evident from the following observations. (1) The Archean crust of para-autochthon experienced thermal reworking 50–160 m.y. after the peak metamorphic events in various zones of allochthon. (2) In western Quebec, ages of peak metamorphism decrease in the northeastern direction from 1190–1160 to 1170 Ma for the Shawinigan period, from 1080–1050 to 1070–1045 Ma for the Ottawan time, and correspond to 1020–990 Ma for the Rigolet time. (3) The peak granulite metamorphism in northern Quebec (1.02 Ga) took place not only after a similar event in adjacent terrane (1.18 Ga), but also after the terrane cooling below 450°C (1.4 Ga). This and aforementioned lateral migration of thermal events were likely connected with the collision progradation, on the one hand, and with localization of huge volumes of anorthosite–mangerite–granite magma, on the other, because the latter yielded first injections 1650–1620 Ma ago (Rivers, 1997) and main intrusions 1190–1140 Ma ago (Carr *et al.*, 2000; Corriveua and van Breemen, 2000; Martignol *et al.*, 2000). (4) The time difference between the K–Ar system closure (450 ± 50°C) in hornblendes from neighboring terranes of the Central Metasedimentary Belt can be as great as 20–40 m.y. in the western Quebec and Ontario, and as 5–25 m.y. in the northern Quebec.

Plentiful isotopic dates obtained for zircon, monazite, rutile, apatite (U–Pb method), amphibole, muscovite, and biotite ($^{40}Ar/^{39}Ar$ method) elucidate many important features of tectono-thermal evolution of the Grenville Province during terminal stages of its evolution (Mezger *et al.*, 1993; MvLelland *et al.*, 1996; Rivers, 1997; Ketchum *et al.*, 1998; Indares *et al.*, 1998, 2000; Carr *et al.*, 2000; Corriveau and Morin, 2000; Corriveau and van Breemen, 2000; Hynes *et al.*, 2000; Ketchum and Davidson, 2000; Martignol *et al.*, 2000). Let us mention several examples. (1) In various domains of the Central Gneiss Belt, the time gap between the peak metamorphic event and domain cooling to the closing temperature of K–Ar system in hornblende varies from 30 to 180 m.y., and these variations reflect difference in the burial depth and in the unroofing or exhumation rate of individual domains. (2) Against the background of very slow post-metamorphic cooling of lithotectonic units in the Grenville Province, some of them reveal the relatively short (10–20, sometimes 30 m.y.) episodes of quick (up to 10–15°C/m.y.) cooling and uprising. These episodes followed immediately the metamorphic peaks and developed under conditions of crustal extension that favored the uplift of hot lithotectonic units to the upper crustal levels. (3) As is established for some deeply metamorphosed complexes, their exhumation occurred during short (~10–12 m.y.) episodes of crustal extension in the major detachment zones. Processes of this kind were most active ~1200 to ~1000 Ma ago and led to an irregular cooling of high-grade metamorphic complexes and their thrusting over the less altered rocks. (4) The present-day erosion surface of para-autochthon crossed the isotherm of K–Ar system closure in hornblende 50–80 m.y. after the same event in the allochthon. (5) During the Rigolet impuls (1010–980 Ma) that was terminal one in the Grenville òrogeny, the extension and cooling of orogen led to subsidence of weakly metamorphosed rocks down to lower crustal levels, where they became juxtaposed with high-grade metamorphic complexes. During the subsequent unroofing, the cooling dynamics of compositionally contrast domains, separated by thick (up to 10 km) zones of foliation or mylonitization, was independent of their position in the present-day thrust-and-fold structure of the province. Uprising of concrete lithotectonic units in the course of cooling was essentially controlled by their rheologic properties, and this was especially typical of intrusions and their frames (Corriveau and van Breemen, 2000; Ketchum *et al.*, 2000). Horizontal displacements were also irregular. Transverse displacements after the peak metamorphism developed 1.07–1.00 Ma ago as discrete impulses propagating from the central part of orogen toward the Grenville front (Martignol *et al.*, 2000).

Other collisional orogens of the Grenville age went though a similar thermal history. In different areas of the Sveconorwegian Belt (Cosca *et al.*, 1998; Christoffel *et al.*, 1999; Andersson *et al.*, 1999), high-grade metamorphism ranged in age from 1190–1150 (granulites of the Bamble sector) to 970 Ma (amphibolite facies); in Columbian Andes, similar events took place 1090 Ma ago (Restrepo-Pace *et al.*, 1997) and migrated with time in Australia from the Albany (1190 Ma) to Darling (1080 Ma) belts thus emphasizing the diachronous development of collision (Bruguier *et al.*, 1999). The last event of high-T metamorphism that affected structures of Kibaran orogeny in the Gariep Belt of Africa is dated back to 1030 Ma (Trimmel *et al.*, 1998). In South China, some researchers attributed the Sibaoan folding and concurrent granite intrusions (Sm-Nd isochron age of 1060 Ma) to the Grenville events (Smith *et al.*, 2000), but more precise data show that juxtaposition of the Yangtze and Huainan blocks happened not earlier than 970 Ma ago (Li, 1999).

All these regions are similar to the Grenville Province in the rate of post-metamorphic cooling and, accordingly, of the Grenvillides unroofing. In the Sveconorwegian Belt, this rate changed in space and with time. In the greater part of the belt, it was equal to 5–11°C/m.y. during a short period (~12 m.y.) after the peak of metamorphism and decreased to 4–7 or 2.5–5°C/m.y. later on, as it is estimated for the period of 930–880 Ma (Christoffel *et al.*, 1999; Andersson *et al.*, 1999). In the Bamble sector of the belt, where cooling began 100 m.y. earlier, the initial cooling rate of 3–8°C/m.y. subsequently decreased to 2–4°C/m.y. (Cosca *et al.*, 1998). The initial cooling rate of this sector is one of the most rapid in Grenvillides, but it was much slower than that estimated for the last 15–20 m.y. of development of the Alps and Himalayas (Bernet *et al.*, 2000; Brandon *et al.*, 2000). The noticeably higher values (15 ± 2°C/m.y.) were estimated in Grenvillides for a short (20–25 m.y.) period that followed the terminal metamorphic event in the Gariep Belt of southern Africa (Trimmel *et al.*, 1998). In Australia, the corresponding parameter declined to 1°C/m.y. immediately after the relatively brief episode of quick cooling after the last metamorphic peak (Bruguier *et al.*, 1999).

The average unroofing rate of the Grenville Province is estimated to be very low in general. Cosca *et al.* (1991a, 1991b, 1992) calculated values of 30–80 to 30–140 m/m.y. for various zones of the province, and the assessment of Mezger *et al.* (1993) is equal to 120 ± 40 m/m.y. As is accepted in mentioned works, the initial cooling rate under conditions of crustal extension that lasted 20–30 m.y. after the peak of metamorphism might be as high as 10°C/m.y. and decreased to 1–4°C/m.y. afterward. It is assumed as well that the thrust faulting and protrusive tectonics could be responsible for the higher cooling and unroofing rates of some deep-seated lithotectonic units as compared to the shallower ones. For instance, variable unroofing rates are established for terranes of the Central Metasedimentary Belt (Martignol *et al.*, 2000). For the time interval from the peak metamorphism to the cooling down to 450 ± 50°C, the calculated rate values are 330 m/m.y. and 6°C/m.y. for some high-grade terranes versus 50 m/m.y. and 1.5°C/m.y. for the others. Using the erosion rates considered above, Cosca *et al.* (1992) calculated that the original tectonic relief of Grenvillides must be denuded about 920 Ma ago, and Carr *et al.* (2000) obtained the close value of 980 Ma. Cosca, Martignol, and their colleagues also pointed out that the considered unroofing (and cooling) rates, except for their extreme values, were at least one order of magnitude lower than rates (400–700 m/m.y.) calculated for the last 15–20 m.y. of development of the Alps and Himalayas (Garver *et al.*, 1999; Bernet *et al.*, 2000; Brandon *et al.*, 2000). In this connection, we should mention here that exactly the uplift of Tibet–Himalayan structures was responsible for the extreme growth of $^{87}Sr/^{86}Sr$ ratios in seawater of the Late Tertiary time (Raymo *et al.*, 1988; Hodell *et al.*, 1990; Richter *et al.*, 1992). In other words, the asynchronous uplift and low rising rates of various zones in Grenvillides cardinally differ the latter from Alpides. According to average rates of cooling and unroofing of metamorphic terranes in Grenvillides, the ascent of the latter is comparable with isostatic uprising in response to erosion.

Thus, Grenvillides represent tectonic assemblies of large lithotectonic units of various metamorphic grade, composition, age, and geochemical parameters of their protoliths, $\varepsilon_{Nd}(T)$ included, which went through different histories of the post-metamorphic cooling. The asynchronous rate-variable cooling and uprising of these units consisting of contrasting rocks controlled proportions and volume of diverse erosion products, which entered the Riphean ocean. Rocks with high $^{87}Sr/^{86}Sr$ ratios apparently were subordinate in composition of these lithotectonic units, as it follows from the established low level of Sr isotopic ratios in seawater of the Grenville and post-Grenville time.

Considering factors that determined the $^{87}Sr/^{86}Sr$ ratios in seawater, we should keep in mind that in general they do not depend directly on the continental erosion rate only (on continental runoff). As it is convincingly shown for the Late Tertiary oceans, this parameter of seawater depends on both the Sr mass delivered by the continental runoff and the ^{87}Sr abundance in the latter (Richter *et al.*, 1992). Consequently, the low level of $^{87}Sr/^{86}Sr$ ratios in the Middle–Late Riphean ocean was maintained not only by the low erosion rate and asynchronous movements of particular Grenvillide domains and terranes, but also by the low Sr isotopic ratios in magmatic and metamorphic rocks of the provenance areas. For the sake of correct formulation, it is necessary to state therefore that $^{87}Sr/^{86}Sr$ in seawater depends on three, but not on two variables usually referred to (mantle flux and continental runoff). The additional variable is the $^{87}Sr/^{86}Sr$ ratio in the latter, first of all, in the river water (Richter *et al.*, 1992; Jacobson and Kaufman, 1999; Godders and Veizer, 2000).

4. Flux of fresh juvenile components in seawater of the Grenville and post-Grenville time. Some very symptomatic variations in the Sm–Nd systematics of shales are established at present in several Upper Riphean sections. In the Transbaikal region, for instance, metabasites that have the isochron Sm–Nd age of 1035 ± 92 Ma and $\varepsilon_{Nd}(T)$ value of +7.1 underlie metasediments, which also show mantle values of the last parameter ranging from +4.8 to +4.7 (Rytsk *et al.*, 1999). In the middle of the Danzhou Group of South China that is constrained between 1050 and 830 Ma (Li and McCulloch, 1996; Li, 1999), there is established a transition from the relatively old (1.9–1.7 Ga) to younger (1.6–1.4 Ga) T_{DM} values, which is interpreted as indicating a considerable influx of fresh mantle components in sediments. Variations of this kind are also characteristic of the Kerpyl' and Lakhanda groups of the Uchur–Maya region being most distinct in the latter group (Podkovyrov *et al.*, 2001, and in press). Shales of

the Talyn Formation that is basal one in the regional Middle Riphean succession (Semikhatov and Serebryakov, 1983) and shales of the Totta Formation of the Yudoma–Maya belt have negative $\varepsilon_{Nd}(T)$ parameters (from –4.3 to –7.1) and Early Proterozoic values of T_{DM} (2.3–2.1 Ga). In contrast, the low positive $\varepsilon_{Nd}(T) = +0.3$ and "younger" $T_{DM} = 1.8$ Ga are characteristic of the Totta shales of the Uchur–Maya plate. In the Yudoma–Maya belt, low negative $\varepsilon_{Nd}(T) = -1.9$ and pre-Riphean $T_{DM} = 1.9$ Ga are established for shales near the base of the Neryuen Formation of the Lakhanda Group, and the first parameter increases here to +2.2 upward in the section, while the second one decreases to 1.4 Ga. The other values $\varepsilon_{Nd}(T) = +4.3$ and $T_{DM} = 1.6$ Ga are obtained for shales of the same formation in the Uchur–Maya plate. In shales of the overlying Ui Group (Ust'-Kirba Formation), $\varepsilon_{Nd}(T)$ decreases to –2.2 and T_{DM} increases to 2.1 Ga. Data mentioned above are interpreted as indications of the fresh juvenile material influx that was repeated twice, in the accumulation period of the Totta Formation and afterward, within the time range of the Neryuen Formation (Podkovyrov *et al.*, in press). Basic dikes with MORB geochemical parameters appeared later on in the Yudoma–Maya trough at the base of the Ui Group (Sukhorukov, 1986; Rainbird *et al.*, 1998).

The conclusion about fresh mantle material flux in the Late Riphean ocean is well agreeable with current data on the Paleo-Asiatic ocean opening at the very beginning of the Late Rivean, about 1 Ga ago or slightly before (V. Khain *et al.*, 1997, 1999; Khomentovskii and Postnikov, 2001; Sklyarov *et al.*, 2001; Rytsk *et al.*, 2001; E. Khain *et al.*, in press). This inference is based on data characterizing the newly formed oceanic crust in the structure of Early Baikalides and on reconstructions of the circum-Siberian ophiolite belt, along which the age of constituent ophiolite massifs progressively changes from 1100–1000 to 720–500 Ma (V. Khain *et al.*, 1997; E. Khain *et al.*, in press).

Putting aside the reconstructions of Rodinia, which leave the rest of the globe to the giant Monrovia Ocean (Weil *et al.*, 1998), we should mention here some clear evidences for the intense development of oceanic crust beginning from the earliest Late Riphean. Par example, ophiolites interrelated with a system of Late Riphean and younger island arcs are widespread in the vast Nubian Shield. The oldest island-arc volcanics with high $\varepsilon_{Nd}(T)$ values (up to +7.0) erupted here 887 ± 2 Ma ago and had the $^{87}Sr/^{86}Sr$ initial ratios that fall in the range of 0.70221–0.70295 (Reschmann, 2000). The Gaios Ocean that started evolution ~1280 Ma ago developed in the Late Riphean at the site of future Gondwana and closed about 900 Ma ago as a consequence of collision between the San-Franciscan and Amazonian cratons. In the Middle Riphean, this was a site of intense bimodal intrusive to extrusive magmatism that gave place to development of an island-arc system at the beginning of the Late Riphean. These island arcs now composed of metarhyolites and metabasalts with $\varepsilon_{Nd}(T) = +5.3$ erupted 928–900 Ma ago and later on (Strieded and Suita, 1999). Some researchers believe that island-arc complexes of South America, which range here in age from 930 to 900–850 Ma or less, signify the commencement of Rodinia breakup and opening of an ocean that was closed at the time of the Brazilian orogeny (Fuck and Pimentol, 2000).

Thus, a considerable new mass of low-radiogenic Sr entered the outer shells of the Earth at the beginning of the Late Riphean as a result of seawater interaction with oceanic magmatic rocks and of associated hydrothermal activity.

5. Transgression of the Late Grenville time. The early Late Riphean (from 1030 to 850–800 Ma) is known as a period of intense sea transgression that left intact only the central Africa, a part of South-American platform, Australia, Antarctica, and Midcontinent of North America (Ronov *et al.*, 1984; Semikhatov and Raaben, 1994, 1996; Trompète, 1994, and references therein). As that transgression flooded the former vast provenances of clastic material, its trivial significance for the problem under consideration consists in the continental runoff decrease.

The calculated global number of the carbonate lithostratigraphic units (formations and their equivalents), which accumulated in the late Middle and early Late Riphean (1200–1030 and 1030–850 Ma ago), shows that they are twice more abundant in the last stratigraphic interval (Semikhatov and Raaben, unpublished data). This intensification of carbonate sedimentation well accords with the idea that the greater part of Rodinia was situated during the early Late Riphean in the low near-equatorial latitudes (Weil *et al.*, 1998; Gallet *et al.*, 2000). Such a position of supercontinent does not deny, however, the concurrent development of intense terrigenous sedimentation that was characteristic, for instance, of the East European platform (*Stratigraficheskaya...*, 2000) and southern Rocky Mountains (Link *et al.*, 1993). Nonetheless, the considerable peak of carbonate accumulation in the early Late Riphean is likely reflecting the decreased continental runoff the more so as the tectonic relief in the Grenville province is thought to be denuded about 980–920 Ma ago (Cosca *et al.*, 1991a, 1991b, 1992; Carr *et al.*, 2000). It worth to mention in this connection that the high sea-level stand at that time triggered formation of new (in North to Arctic Canada and Greenland) or favored further development (in North Africa, Mexico, central to northeastern Siberia, Tarim, Beishan, northern Tien Shan, Spitsbergen, and other regions) of former carbonate platform (Raaben, 1975; Harland *et al.*, 1979; Semikhatov and Serebryakov, 1983; Brezhnev and Raaben, 1992; Semikhatov and Raaben, 1994, 1996; Rainbird *et al.*, 1996; Kah *et al.*, 1999, 2001; Kah, 2000; and references therein).

It seems reasonable to think that the transgression was interrelated as well with some other events impor-

tant for our considerations. The analysis of eustatic sea-level fluctuations during the Phanerozoic shows that they were dependent on the spreading rate, appearance of lava plateaus in oceans, and some other factors (Larson, 1991, 1997; Milanovskii *et al.*, 1992; Yakubchuk and Nikishin, 1992; Nikishin 1994). Accordingly, we may assume that the intense transgression of the early Late Riphean time was also connected somehow with activation of the mid-ocean ridge system that naturally "worked" for the $^{87}Sr/^{86}Sr$ ratio decrease in seawater at that time.

6. Locking up of continental runoff in inner basins of Laurentia. It is well known that events of this kind strongly influenced the Sr isotope composition in seawater during the Sakmarian–Early Triassic stage of Gondwana evolution. Ending of this supercontinent formation has not been associated with the increase of $^{87}Sr/^{86}Sr$ in seawater. On the contrary, that ratio was at the very end of the Permian (Tatarian Age) the minimal one among others of the Phanerozoic time (Smalley *et al.*, 1994; Denison *et al.*, 1994; Denison and Koepnick, 1995), although this time corresponded to the most geocratic Phanerozoic epoch (Ronov *et al.*, 1984) remarkable owing to the intense siliciclastic sedimentation (Zharkov and Chumakov, 2001). There was an attempt to explain this paradox by the *assumed* activation of the low-radiogenic Sr flux from mantle sources (Denison *et al.*, 1994), but the *established* paleogeographic and paleoclimatic factors undoubtedly contributed much to the appearance of that paradoxical situation. Zharkov and Chumakov (2001) clearly demonstrated that principal volumes of siliciclastic material, mobilized during the Sakmarian–Early Triassic time, accumulated in inner basins of Gondwana, which were isolated from the ocean. Moreover, the extremely arid climate of that time decreased the total mass of continental Sr dissolved in meteoric and ground waters (Francois and Walker, 1992). The outer edges of Gondwana were rimmed in this time by shelf zones of variable width, which accumulated predominantly the carbonate sediments. A similar situation could be characteristic of the post-Grenville Laurentia that was surrounded almost everywhere by collisional orogens in the early Late Riphean time (Condie, 2001, Fig. 2), which represented potential barriers for the terrestrial material transported by rivers from land areas. In other words, paleogeography and climate of a supercontinent were able to correct essentially the Sr-isotopic record: these factors could diminish the mass of dissolved high-radiogenic Sr of continental origin, which plays first violin in determination of the Sr isotope composition in seawater, or even could fully shelter the terrestrial material from oceanic sedimentation settings.

The aforementioned factors, which appear to be able to control the $^{87}Sr/^{86}Sr$ ratio in seawater, are of differing validity. The first of them (increment of juvenile crust) that seemed recently as most convincing (Condie, 1998) did not bear the test of time. Among five others, four are inferable from factual data and can be accepted for influential, whereas the fifth one (the continental runoff imprisonment in inner basins) is assumed by a probable analogy.

The relative significance of each factor cannot be correctly evaluated at present. We suspect however the prime importance of the second and third factors (abundance of juvenile rocks in Grenvillides and activated seawater interaction with mantle-derived rocks), whereas others (exhumation and unroofing rates of lithotectonic units, the early Late Riphean sea transgression, and paleogeography of Laurentia at that time) were likely not as important as these two. The selection of a leading factor is not so important though, because they all acted in alike manner decreasing the $^{87}Sr/^{86}Sr$ ratio in seawater that was, as is established, steadily low during the Grenville and post-Grenville time.

CONCLUSION

The data obtained and discussed in this work led us to the following conclusions.

(1) Plotting the reference curve of the $^{87}Sr/^{86}Sr$ ratio variations in the Riphean seawater, one should use analytical data obtained only for those samples, which are well calibrated in geochronological aspect, least altered, and preliminary treated (leached) in 1N solution of ammonium acetate in order to remove epigenetic carbonate phases from the surface of carbonate particle and to separate them from primary phases displaying the other Rb–Sr systematics.

(2) The degree of secondary alterations in carbonate rocks should be evaluated from their structural and textural features, and also from cathodoluminescent data, but most indicative in this case are regularities of Mn, Fe, and Sr redistribution in the course of epigenesis, on the one hand, and the analyzed correlation between these elements concentrations and $^{87}Sr/^{86}Sr$ ratio in carbonate phases, on the other. As is shown, the threshold values of geochemical criteria discriminating the least altered ("best") samples, which are applicable for reconstruction of Sr isotope composition in seawater, from those, which are more altered and inapplicable therefore for this purpose are presently known for limestones only. Like before (Kuznetsov *et al.*, 1997; Kuznetsov, 1998; Semikhatov *et al.*, 1998), we used in this work the following threshold values of geochemical parameters: $Mn/Sr \le 0.2$, $Fe/Sr \le 5.0$, and $Mg/Ca \le 0.024$. The same approach to discrimination of dolomite samples is impossible at present, because their geochemistry at the time of sedimentation and subsequent transformation is inadequately understood and Mn/Sr and Fe/Sr ratios of dolomitic rocks (except for few examples reported by Kuznetsov *et al.*, 1998) are out of covariation with their $^{87}Sr/^{86}Sr$ ratios. Accordingly, the lowest level of these ratios calculated for dolomitic samples defines only the maximum limit of this parameter in seawater, because the epigenesis of carbonate rocks increases it in most cases.

(3) Carbonate rocks of the Kerpyl' and Lakhanda groups (~1050–1000 Ma), which represent principal objects in the first part of this study, are insignificantly altered. The alterations are less intense in the stable Uchur–Maya plate that subsided slowly, than in the Yudoma–Maya belt, where Riphean deposits are thicker, folded, and experienced thrust faulting. Isotopic systems of the Uchur–Maya carbonates were disturbed in the course of rocks interaction with basinal brines, which originated in associated siliciclastic deposits during the subsidence, and with meteoric waters, which influenced the rocks during the pre-Lakhanda and pre-Yudoma breaks in sedimentation. The impact of basinal brines is predominantly recorded in the Malgina limestones overlying the sandy–clayey Totta Formation throughout the study region and in the Neryuen carbonates of the Uchur-Maya plate, where they are intercalated with clayey members. The meteoric catagenesis significantly affected the Tsipanda dolomites during the pre-Lakhanda hiatus and the Ignikan Formation at the time of the pre-Yudoma disconformity. Nonetheless, the Malgina and Neryuen formations of both structural zones still retain slightly altered limestones, which satisfy the accepted geochemical criteria of "best" samples.

(4) More than 160 determination of $^{87}Sr/^{86}Sr$ ratios are published for the Middle–Upper Riphean boundary deposits of the Uchur–Maya and Turukhansk regions, and 125 of them are obtained for rock samples which possess geochemical criteria of alteration degree and which were treated in ammonium acetate in order to remove their secondary carbonate phases. In the last group, 19 analytical results are obtained for ACA-phases of limestones enriched in primary carbonate material (Gorokhov *et al.*, 1995a; Semikhatov *et al.*, 1998; and this work) and fitting the strict criteria of geochemical retentivity. The corresponding 19 data points for limestones represent the basis of new reference curve of the $^{87}Sr/^{86}Sr$ ratio variations in seawater 1050–1000 Ma ago (Fig. 9). Over forty lowest values of that ratio, which are obtained for associated dolomites, bulk carbonate material, and limestone phases unfitting the aforementioned criteria define the upper limitation of the curve. The new curve differs in configuration from the other one recently plotted for the same time interval by Bartley *et al.* (2001) owing to the more representative database, stricter criteria of selecting "best" samples, and obligatory removing of secondary carbonate phases by preliminary leaching. At present, the suggested curve is most detailed among all others published for the Precambrian.

(5) The $^{87}Sr/^{86}Sr$ ratios in seawater were somewhat higher 1050–1030 Ma ago (0.70563–0.70592 in the Malgina Formation and 0.70567–0.7085 in the Sukhaya Tunguska Formation) than during the subsequent 30 m.y. (0.70519–0.70569 in the Lakhanda Group and its analogues corresponding to the lower Upper Riphean in the Turukhansk region). About 1000 Ma ago, that ratios ranged from 0.70523 to 0.70527 (upper horizons of the Neryuen and Burovaya formations).

(6) Nearly a hundred of $^{87}Sr/^{86}Sr$ initial ratios is known from publications for carbonate and sulfate rocks constituting other intervals of the Middle–early Late Riphean (from 1350 to 1050 and from 1000 to 800 Ma), though they are of different reliability being obtained harnessing variable methodical approaches. Nonetheless, generalization of all available data elucidates the main trend of $^{87}Sr/^{86}Sr$ ratio variations in seawater of the Middle–early Late Riphean time. At the beginning of the Middle Riphean (~1.3 Ga ago), this ratio was not higher than 0,7046–0.7047 thus being close to that characteristic of the Early Riphean (Gorokhov *et al.*, 1995a; Hall and Veizer, 1996). Afterward, it grew slowly and reached the range of 0.7052–0.7056 about 1.2 Ga ago. Leaving aside a considerable gap in the Sr-isotopic records, we see then, in the Malgina Formation, the Middle Riphean peak of $^{87}Sr/^{86}Sr$ ratios (0.70563–0.70592) that is followed by the descending trend of their values characterizing the Sukhaya Tunguska and Lakhanda time (0.70523–0.70527 about 1000 Ma ago). Later on, in the first half of the Late Riphean (900–800 Ma), the $^{87}Sr/^{86}Sr$ ratios in seawater were steadily low and presumably ranged from 0.70525 to 0.70568.

(7) The steadily low level of $^{87}Sr/^{86}Sr$ ratios in seawater of the Grenville and post-Grenville time was controlled by combination of several factors. Judging from all data, we assume that the high abundance of older mantle-derived rocks in the Grenvillide crust and considerable volumes of fresh mantle material that arrived at the oceanic floor in the early Late Riphean were most important among these factors, whereas specific features of exhumation and unroofing of Grenvillide lithotectonic units, as well as the early Late Riphean transgression and paleogeography of Laurentia at that time, were of subordinate significance. The accelerated river runoff and continental erosion at the final stages of Rodinia assembling were unable to increase considerably the $^{87}Sr/^{86}Sr$ ratio in seawater, because the Grenvillide crust subjected to erosion was enriched in low-radiogenic Sr of the juvenile origin.

(8) All available data imply that secular variations of $^{87}Sr/^{86}Sr$ ratios in seawater reflect the mutual influence of three variables: (a) the Sr flux from the mantle, where the Sr isotope composition was approximately constant during the Riphean and Phanerozoic; (b) the continental runoff (continental erosion rate); and (3) changeable Sr isotope composition in the latter. In some cases, the above variations were likely dependent on the climate and paleogeography of supercontinents as well, e.g., of the Late Permian Gondwana and, presumably, of the Late Riphean Laurentia. The paleogeographic factor seems to be able in particular situations to decrease and cease the flux of eroded sialic material into the ocean.

ACKNOWLEDGMENTS

We are grateful to J. K. Bartley, M.A. Zharkov, Yu.D. Pushkarev, and A.B. Kotov for the fruitful discussion of problems considered in this work. We appreciate the contribution of I.V. Kislova who analyzed Mn and Fe concentrations in the studied samples using atomic absorption spectrometry and the invaluable technical assistance of O.V. Artemova. Information on stratigraphic position of rock samples from the Kerpyl' and Lakhanda groups, the Rb–Sr systematics of which was earlier studied by V.I. Vinogradov, was kindly provided by A.F. Veis. The work was supported by the Russian Foundation for Basic Research, project nos. 99-05-64054, 99-05-65181, 00-05-72011, 01-05-06084.

Reviewer B.S. Sokolov

REFERENCES

Albarede, F., Michard, A., Minster, J.F., and Michard, G., $^{87}Sr/^{86}Sr$ Ratios in Hydrothermal Waters and Deposits from the East Pacific Rise at 21°N, *Earth Planet. Sci. Lett.*, 1981, vol. 55, no. 2, pp. 229–236.

Almeida de, F.F.M., Precambrian Geology of North-Eastern Brazil and Western Africa and the Theory of Continental Drift, *Proc. Symp. Granites West Africa*, UNESCO Natur. Resources, 1968, vol. 8, pp. 151–162.

Andersson, J., Söderlund, U., Cornell, D., *et al.*, Sveconorwegian (Grenvillian) Deformation, Metamorphism and Leucosome Formation in SW Sweden, SW Baltic Shield: Constraints from a Mesoproterozoic Granite Intrusion, *Precambrian Res.*, 1999, vol. 98, no. 1/2, pp. 151–171.

Asmerom, Y., Jacobsen, S.B., Knoll, A.H., *et al.*, Strontium Isotopic Variations of Neoproterozoic Seawater: Implications for Crustal Evolution, *Geochim. Cosmochim. Acta*, 1991, vol. 55, no. 10, pp. 2883–2894.

Bailey, T.R., McArthur, J.M., Prince, H., and Thirlwall, M.F., Dissolution Methods for Strontium Isotope Stratigraphy: Whole Rock Analysis, *Chem. Geol.*, 2000, vol. 167, nos. 3–4, pp. 313–319.

Banner, J.L. and Hanson, G.N., Calculation of Simultaneous and Trace Element Variations during Water–Rock Interaction with Applications of Carbonate Diagenesis, *Geochim. Cosmochim. Acta*, 1990, vol. 54, no. 11, pp. 3123–3137.

Bartley, J.K., Semikhatov, M.A., Kaufman, A.J., *et al.*, Global Events across the Mesoproterozoic-Neoproterozoic Boundary: C and Sr Isotopic Evidence from Siberia, *Precambrian Res.*, 2001, vol. 111, nos. 1–4, pp. 165–202.

Bernet, M., Zattin, M., Garver, J.I., *et al.*, Steady-State Exhumation of the European Alps, *Geology*, 2000, vol. 29, no. 1, pp. 35–38.

Bertrand-Sarfati, J., Stromatolites Columnaries du Precambrian Superior du Sahara Nord-Occidental, *CRNS, Ser. Geol. Paris*, 1972, no. 14.

Brand, U. and Veizer, J., Chemical Diagenesis of a Multicomponent Carbonate System. 1. Trace Elements, *J. Sed. Petrol.*, 1980, vol. 50, no. 4, pp. 1219–1236.

Brandon, M.T., Garver, J.I., Bernet, M., and Vance, J.A., Exhumation Histories from Detrital Zircon Thermochronometry, *Abstracts, 9th International Conference on Fission Track Dating and Thermochronology*, Geol. Soc. Austral., 2000, no. 58, pp. 41–42.

Brezhnev, V.D. and Raaben, M.E., The Proterozoic of Northwestern and Northern China: Correlation and Geodynamic Reconstructions, *Izv. Akad. Nauk SSSR, Ser. Geol.*, 1992, no. 10, pp. 97–110.

Bruguier, O., Bosch, D., and Pidgeon, R.T., U–Pb Chronology of the Northampton Complex, Western Australia—Evidence for Grenvillian Sedimentation, Metamorphism and Deformation and Geodynamic Implications, *Contrib., Mineral. Petrol.*, 1999, vol. 136, pp. 258–272.

Cannon, W.F. and Nicholson, S.W., Middle Proterozoic Midcontinent Rift System, *US Geol. Surv. Prof. Pap.*, 1996, no. 1556, pp. 60–67.

Carr, S.D., Easton, R.M., Lamieson, R.A., and Gulshaw, N.G., Geologic Transect Across the Grenville Orogen of Ontario and New York, *Can. J. Earth Sci.*, 2000, vol. 37, nos. 2–3, pp. 193–216.

Christoffel, C.A., Connelly, J.N., and Ahäll, K.-I., Timing and Characterization of Recurrent Pre-Sveconorwegian Metamorphism and Deformation in the Varberg-Halmstad Region of SW Sweden, *Precambrian Res.*, 1999, vol. 98, nos. 3–4, pp. 173–195.

Clauer, N., Rb–Sr and K–Ar Dating of Precambrian Clays and Glauconites, *Precambrian Res.*, 1981, vol. 15, nos. 3–4, pp. 331–352.

Condie, K.C., Episodic Continental Growth and Supercontinents: a Mantle Avalanche Connection?, *Earth and Planetary Sci. Letters*, 1998, vol. 163, nos. 1–4, pp. 97–108.

Condie, K.C., *Continental Growth during Formation of Rodinia at 1.35–0.9 Ga*, Gondwana Res., 2001, vol. 4, no 1, pp. 5–16.

Cordani, U.G. and Sato, K., Crustal Evolution of the South American Platform, Based on Nd Isotopic Systematics on Granitoid Rocks, *Episodes*, 1999, vol. 22, no. 3, pp. 167–173.

Corriveau, L. and Morin, D., Modeling 3D Architecture of Western Grenville from Surface Geology, Xenoliths, Styles of Magma Emplacement, and Lithoprobe Reflectors, *Can. J. Earth Sci.*, 2000, vol. 37, nos. 2–3, pp. 235–251.

Corriveau, L. and van Breemen, O., Docking of the Central Metasedimentary Belt to Laurentia in Geon 12: Evidence from the 1.17–1.16 Ga Chevreuil Intrusive Suite and Host Gneisses, Quebec, *Can. J. Earth Sci.*, 2000, vol. 37, nos. 2–3, pp. 253–269.

Cosca, M.A., Sutter, J.F., and Essene, E.J., Cooling and Inferred Uplift/Erosion History of the Grenville Orogen, Ontario: Constraints from $^{40}Ar/^{39}Ar$ Thermochronology, *Tectonics*, 1991a, vol. 10, no. 5, pp. 959–977.

Cosca, M.A., Essene, E.J., and Bowman, J.R., Major Element, FeO/Fe_2O_3, and H_2O Measurements of Metamorphic Hornblendes: Implications for Amphibole Normalizations and Calculated Metamorphic H_2O Activities, *Contrib. Mineral. Petrol.*, 1991b, vol. 108, pp. 472–484.

Cosca, M.A., Essene, E.J., Kunk, M.J., and Sutter, J.F., Differential Unroofing Within the Central Metasedimentary Belt of the Grenville Orogen: Constraints from $^{40}Ar/^{39}Ar$ Thermochronology, *Contrib. Mineral. Petrol.*, 1992, vol. 110, pp. 211–225.

Cosca, M.A., Mezger, K., and Essene, E.J., The Baltica–Laurentia Connection: Sveconorwegian (Grenvillian) Metamorphism, Cooling, and Unroofing in the Bamble Sector, Norway, *J. Geol.*, 1998, vol. 106, pp. 539–552.

Davidson, A., A Review of the Grenville Orogen in Its North American Type Area, *J. Austral. Geol. Geophys.*, 1995, vol. 16, pp. 3–24.

Denison, R.E. and Koepnik, R.B., *Variation in $^{87}Sr/^{86}Sr$ of Permian Seawater: An Overview*, Scholle, P.A., Peryt, T.M., and Ulmer-Scholle, D.S., Eds., Berlin: Springer, 1995, vol. 1, pp. 124–132.

Denison, R.E., Koepnick, R.B., Burke, W.H., *et al.*, Construction of the Mississippian, Pennsylvanian and Permian Seawater $^{87}Sr/^{86}Sr$ Curve, *Chem. Geol.*, 1994, vol. 112, no. 1/2, pp. 145–167.

Derry, L.A., Keto, L.S., Jacobsen, S.B., *et al.*, Sr Isotopic Variations in Upper Proterozoic Carbonates from Svalbard and East Greenland, *Geochim. Cosmochim. Acta*, 1989, vol. 53, no. 9, pp. 2331–2339.

Derry, L.A., Kaufman, A.J., and Jacobsen, S.B., Sedimentary Cycling and Environmental Change in the Late Proterozoic: Evidence from Stable and Radiogenic Isotopes, *Geochim. Cosmochim. Acta*, 1992, vol. 56, no. 3, pp. 1317–1329.

Derry, L.A., Brasier, M.D., Corfield, R.M., *et al.*, Sr and C Isotopes in the Lower Cambrian Carbonates from the Siberian Craton: a Paleoenvironmental Record during the Cambrian Explosion, *Earth Planet. Sci. Lett.*, 1994, vol. 128, nos. 3–4, pp. 671–681.

Des Marais, D.J., Tectonic Control of the Crustal Organic Carbon Reservoir during the Precambrian, *Chem. Geol.*, 1994, vol. 114, no. 3/4, pp. 303–314.

Dickin, A.P., Crustal Formation in the Grenville Province: Nd-Isotope Evidence, *Can. J. Earth Sci.*, 2000, vol. 37, nos. 2–3, pp. 165–181.

Fairchild, I.J., Marshall, J.D., and Bertrand-Sarfati, J., Stratigraphic Shifts in Carbon Isotopes from Proterozoic Stromatolitic Carbonates (Mauritania): Influence of Primary Mineralogy and Diagenesis *Am. J. Sci.*, 1990, vol. 290–A, pp. 46–79.

Fanning, C.M., *$^{87}Sr/^{86}Sr$ of Gypsum/Anhydrite and Carbonate Samples*, Austral. Mineral. Develop. Lab. Rep., 1986.

Faure, G., *Principles of Isotope Geology*, 2nd Edition, New York: Willey & Sons, 1986.

Francois, L.M. and Walker, J.C.G., Modeling the Phanerozoic Carbon Cycle and Climate: Constraints from the $^{87}Sr/^{86}Sr$ Isotopic Ratio of Seawater, *Am. Geol. Sci.*, 1992, vol. 292, no. 2, pp. 136–148.

Frimmel, H.E. and Frank, W., Neoproterozoic Tectono-Thermal Evolution of the Gariep Belt and Its Basement, Namibia and South Africa, *Precambrian Res.*, 1998, vol. 90, nos. 1–2, pp. 1–28.

Fuck, R. and Pimentol, M., Archean and Proterozoic Geology of Brazil: an Overview, *31st Int. Geol. Congr., Rio de Janeiro, Aug. 6–17, 2000: Congr. Program*, Rio de Janeiro, 2000.

Galimov, E.M., Nature of Global Variations in Isotopic Composition of Carbon in the Biosphere, *Geokhimiya*, 1999, no. 8, pp. 787–803.

Gallet, Y., Pavlov, V.E., Semikhatov, M.A., and Petrov, P.Yu., Late Mesoproterozoic Magnetostratigraphic Results from Siberia: Paleogeographic Implications and Magnetic Field Behavior, *J. Geophys. Res.*, 2000, vol. 105, no. B7, pp. 16481–16499.

Garver, J.I., Brandon, M.T., Roden-Tice, M., and Kamp, P.J.J., Exhumation History of Orogenic Highlands Determined by Detrital Fission Track Thermochronology, *Exhumation Processes: Normal Faulting, Ductile Flow and Erosion*, Ring U., Brandon M.T., Lister, G.S., and Willett, S.D., Eds., London: Geol. Society, 1999, pp. 283–304.

Geraldes, M.C., Van Schmus, N.R., and Teixeira, W., Three Parallel Crustal Accretionary Arcs (1.79–1.49 Ga) in the SW Amazon Craton, State of Mato Grosso, Brazil, *31st Int. Geol. Congr., Rio de Janeiro, Aug. 6–17, 2000: Congr. Program*, Rio de Janeiro, 2000.

German, T.N., *Organicheskii mir milliard let nazad* (Organic World a Billion Years Ago), Leningrad: Nauka, 1990.

Godderis, Y. and Veizer, J., Tectonic Control of Chemical and Isotopic Composition of Ancient Oceans: the Impact of Continental Growth, *Am. Geol. Sci.*, 2000, vol. 300, no. 3, pp. 434–461.

Goldstein, S.J. and Jacobsen, S.B., Nd and Sr Isotopic Systematics of River Water Suspended Material: Implications for Crustal Evolution, *Earth Planet. Sci. Lett.*, 1988, vol. 87, no. 3, pp. 249–265.

Gorokhov, I.M., Diagenesis of Carbonate Sediments: Behavior of Trace Elements and Strontium Isotopes, *Litologiya i paleogeografiya* (Lithology and Paleogeography), Verba, Yu.L., Ed., St. Petersburg: St. Petersburg Gos. Univ., 1996, pp. 141–164.

Gorokhov, I.M., Melnikov, N.N., Turchenko, T.L., *et al.*, Two Illite Generations in an Upper Riphean Shale: the Rb–Sr Isotopic Evidence, *EUG 8, Strasbourg, France, 9–13 April 1995 (Terra Abstracts Supplement no. 1 to Terra Nova)*, 1995, vol. 7, pp. 330–331.

Gorokhov, I.M., Semikhatov, M.A., Baskakov, A.V., *et al.*, Sr Isotopic Composition in Riphean, Vendian, and Lower Cambrian Carbonates from Siberia, *Stratigr. Geol. Korrelyatsiya*, 1995a, vol. 3, no. 1, pp. 3–33.

Gorokhov, I.M., Yakovleva, O.V., Semikhatov, M.A., and Ivanovskaya, T.A., Rb–Sr and K–Ar Age and Mössbauer Spectra of Globular Phyllosilicates of the Glauconite Series: The Middle Riphean Debengda Formation of the Olenek Uplift, Northern Siberia, *Litol. Polezn. Iskop.*, 1995, no. 6, pp. 615–631.

Gorokhov, I.M., Semikhatov, M.A., Kuznetsov, A.B., and Melnikov, N.N., Improved Reference Curve of Late Proterozoic Seawater $^{87}Sr/^{86}Sr$, *Proceedings of the 4th Intern. Symposium on the Geochemistry of the Earth's Surface, Ilkley, Yorkshire, England, 22–28 July 1996. Theme 5. Land–Atmosphere–Hydrosphere Interactions*, Leeds, 1996, pp. 714–717.

Gorokhov, I.M., Mel'nikov, N.N., Turchenko, T.L., and Kutyavin, E.P., Rb–Sr Systematics of Pelitic Fractions from Lower Riphean Shalles: Ust'-Il'ya Formation, Anabar Massif, Northern Siberia, *Litol. Polezn. Iskop.*, 1997, no. 5, pp. 530–539.

Gorokhov, I.M., Semikhatov, M.A., Mel'nikov, N.N., *et al.*, Rb-Sr Geochronology of the Middle Riphean Shales, the Yusmastakh Formation of the Anabar Massif, Northern Siberia, *Stratigr. Geol. Korrelyatsiya*, 2001, vol. 9, no. 3, pp. 3–28.

Hall, S. and Veizer, J., Geochemistry of Precambrian Carbonates: VII. Belt Supergroup, Montana and Idaho, USA, *Geochim. Cosmochim. Acta*, 1996, vol. 60, no. 4, pp. 667–677.

Harland, W.B., Horsfield, W.T., Manby, G.M., and Morris, A., An Outline Pre-Carboniferous Evolution of Svalbard, *Norsk Polarinstitutt Skrifter*, 1979, vol. 167, pp. 119–144.

Hartnady, C., Joubert, P., and Stowe, C., Proterozoic Crustal Evolution in Southwestern Africa, *Episodes*, 1985, vol. 8, pp. 236–244.

Hill, A.C. and Walter, M.R., Mid-Neoproterozoic (850–750 Ma) Isotope Stratigraphy of Australia and Global Correlation, *Precambrian Res.*, 2000, vol. 100, no. 1, pp. 181–211.

Hill, A.C., Arouri, K., Gorjan, P., and Walter, M.R., *Geochemistry of Marine and Nonmarine Environments of a Neoproterozoic Cratonic Carbonate/Evaporite: The Bitter Springs Formation, Central Australia, Precambrian carbonates*, Grotzinger, G.P. and James, N.P., Eds., SEMP Spec. Publ., Tulsa, 2000, vol. 67, pp. 327–344.

Hodell, D.A., Mead, G.A., and Mueller, P.A., Variation in the Strontium Isotopic Composition of Seawater (8 Ma to Present): Implications for Chemical Weathering Rates and Dissolved Fluxes to the Oceans, *Chem. Geol. (Isotope Geosci. Section)*, 1990, vol. 80, no. 4, pp. 291–307.

Hoff, J.A., Grant, N.K., and Whelan, J.F., Strontium and Sulfur Isotope Variations in the Grenville Marbles of the Balmat-Edwards District, Northwestern New York, *Geol. Soc. Am.*, 1984, vol. 16, p. 541.

Hoffman, P.F., United Plates of America, the Birth of a Craton: Early Proterozoic Assembly and Growth of Laurentia, *Earth Planet. Sci. Lett.*, 1988, vol. 16, no. 5, pp. 543–603.

Hoffman, P.F., Did the Breakup of Laurentia Turn Gondwanaland Inside-Out?, *Science*, 1991, vol. 252, pp. 1409–1412.

Hurley, P.M., de Almeida, F.F.M., Melcher, G.C., *et al.*, Test of Continental Drift by Comparison of Radiometric Ages. A Pre-Drift Reconstruction Shows Matching Geologic Age Provinces in West Africa and Northern Brazil, *Science*, 1967, vol. 157, pp. 495–500.

Hynes, A., Indares, A., Rivers, T., and Gobeil, A., Lithoprobe Line 55: Integration of Out-of-Plane Seismic Results with Surface Structure, Metamorphism, and Geochronology, and the Tectonic Evolution of the Eastern Grenville Province, *Can. J. Earth Sci.*, 2000, vol. 37, nos. 2–3, pp. 341–358.

Indares, A., Dunning, G., Cox, R., *et al.*, High-Pressure, High-Temperature Rocks from the Base of Thick Continental Crust: Geology and Age Constraints from the Manicouagan Imbricate Zone, Eastern Grenville Province, *Tectonics*, 1998, vol. 17, no. 3, pp. 426–440.

Indares, A., Dunning, G., and Cox, R., Tectono-Thermal Evolution of Deep Crust in a Mesoproterozoic Continental Collision: the Manicouagan Example, *Can J. Earth Sci.*, 2000, vol. 37, nos. 2–3, pp. 325–340.

Jacobs, J., Fanning, C.M., Henjes-Kunst, F., *et al.*, Continuation of the Mozambique Belt into East Antarctica: Grenville-Age Metamorphism and Polyphase Pan-African High-Grade Event in Central Dronning Maund Land, *J. Geol.*, 1998, vol. 106, no. 3, pp. 385–406.

Jacobs, J., Thomas, R.J., Armstrong, R.A., and Henjes-Kunst, F., Age and Thermal Evolution of the Mezoproterozoic Cape Meredith Complex, West Falkland, *J. Geol. Soc.* (London), 1999, vol. 156, no. 9, pp. 917–928.

Jacobsen, S.B. and Kaufman, A.J., The Sr, C and O Isotopic Evolution of Neoproterozoic Seawater, *Chem. Geol.*, 1999, vol. 161, no. 1, pp. 37–57.

Kah, L.C., Preservation of Depositional $\delta^{18}O$ Signatures in Proterozoic Dolostones: Constraints on Seawater Chemistry and Early Diagenesis, *Precambrian Carbonates*, Grotzinger, G.P. and James, N.P., Eds., SEMP Spec. Publ., Tulsa, SEPM, 2000, no. 67, pp. 345–360.

Kah, L.C., Lyons, T.W., and Chelsey, J.T., Geochemistry of a 1.2 Ga Carbonate-Evaporate Succession, Northern Baffin and Bylot Islands: Implications for Mesoproterozoic Marine Evolution, *Precambrian Res.*, 2001, vol. 111, nos. 1–4, pp. 235–256.

Kah, L.C., Sherman, A.G., Narbonne, G.M., *et al.*, $\delta^{13}C$ Stratigraphy of the Proterozoic Bylot Supergroup, Baffin Island, Canada: Implications for Regional Lithostratigraphic Correlation, *Can. J. Earth Sci.*, 1999, vol. 36, no. 3, pp. 313–332.

Kaufman, A.J., Jacobsen, S.B., and Knoll, A.H., The Vendian Record of Sr and C Isotopic Variations in Seawater: Implications for Tectonics and Paleoclimate, *Earth Planet. Sci. Lett.*, 1993, vol. 120, no. 3, pp. 409–430.

Kaufman, A.J., Knoll, A.H., Semikhatov, M.A., *et al.*, Integrated Chronostratigraphy of Proterozoic–Cambrian Boundary Beds in the Western Anabar Region, Northern Siberia, *Geol. Mag.*, 1996, vol. 133, no. 5, pp. 509–533.

Kay, S.M., Orrell, S., and Abbruzzi, J.M., Zircon and Whole-Rock Nd–Pb Isotopic Evidence for a Grenvillian Age and a Laurentian Origin for the Basement of the Pre-Cordillera in Argentina, *J. Geol.*, 1996, vol. 104, no. 6, pp. 637–648.

Ketchum, J.W.F. and Davidson, A., Crustal Architecture and Tectonic Assembly of the Central Gneiss Belt, Southwestern Grenville Province, Canada: a New Interpretation, *Can. J. Earth Sci.*, 2000, vol. 37, nos. 2–3, pp. 217–234.

Ketchum, J.W.F., Heaman, L.M., Krogh, T.E., *et al.*, Timing and Thermal Influence of Late Orogenic Extension in the Lower Crust: a U–Pb Geochronological Study from the Southwest Grenville Orogen, Canada, *Precambrian Res.*, 1998, vol. 89, nos. 1–2, pp. 25–45.

Khabarov, E.M., Morozova, I.P., Ponomarchuk, V.A., *et al.*, Correlation and Age of Oil- and Gas-Bearing Riphean Sediments of Baikit Anteclise of the Siberian Platform: Implications of Isotopic-Geochemical Data, *Dokl. Akad. Nauk*, 1998, vol. 358, no. 3, pp. 378–380.

Khabarov, E.M., Ponomarchuk, V.A., and Morozova, I.P., Evolution of Sr Isotopic Composition and Carbonate Carbon in the Riphean Basins, the Western Margin of Siberian Craton, *Osadochnye basseiny: zakonomernosti stroeniya i evolyutsii, minerageniya* (Sedimentary Basins: Regularities in Structure and Mechanism of Evolution, Minerageny), Yekaterinburg: Ural. Otd. Ross. Akad. Nauk, 2000, pp. 156–158.

Khabarov, E.M., Ponomarchuk, V.A., and Morozova, I.P., Sr-Isotope Evidence of Breakup and Formation of Supercontinents in the Riphean (Western Margin of the Siberian Craton), *Superkontinenty v geologicheskom razvitii dokembriya. Materialy soveshchaniya, 4–6 iyunya 2001 g., Irkutsk* (Proc. of Conference on Supercontinents in the Precambrian Geological Evolution, June 4–6, 2001, Irkutsk), Irkutsk: Inst. Zemnoi Kory Ross. Akad. Nauk, 2001, pp. 279–282.

Khain, V.E., Gusev, G.S., Khain, E.V., *et al.*, Circum-Siberian Neoproterozoic Ophiolite Belt, *Ofioliti*, 1997, vol. 22, no. 2, pp. 195–200.

Khain, E.V., Bibikova, E.V., Degtyarev, K.E., *et al.*, Paleo-Asian Ocean in the Neoproterozoic and Early Proterozoic: New Radiometric Data, *Geologicheskoe razvitie proterozoiskikh perikratonnykh paleookeanicheskikh struktur Severnoi Evrazii* (Geological Evolution of Proterozoic Pericratonic Paleooceanic Structures of Northern Eurasia), St. Petersburg: Tema, 1999, pp. 175–181.

Khain, E.V., Gibsher, A.S., Didenko, A.N., *et al.*, The Paleo-Asian Ocean in the Neoproterozoic and Early Paleozoic: New Geological and Geochronological Evidence, *Precambrian Res.* (in press).

Khomentovskii, V.V. and Postnikov, A.A., Neoproterozoic History of the Baikal–Vilyui Branch of Paleo-Asian Ocean, *Geotektonika*, 2001, no. 3, pp. 3–21.

Khudoley, A.K., Rainbird, R.M., Stern, R.A., *et al.*, Sedimentary Evolution of the Riphean–Vendian Basin of Southeastern Siberia, *Precambrian Res.*, 2001, vol. 111, nos. 1–4, pp. 129–163.

Knoll, A.H. and Semikhatov, M.A., The Genesis and Time-Distribution of Two Distinctive Proterozoic Stromatolite Microstructures, *Palaios*, 1998, vol. 13, no. 4, pp. 408–422.

Knoll, A.H., Grotzinger, J.P., Kaufman, A.J., and Kolosov, P., Integrated Approaches to Terminal Proterozoic Stratigraphy: an Example from the Olenek Uplift, Northeastern Siberia, *Precambrian Res.*, 1995, vol. 73, nos. 1–4, pp. 251–270.

Komar, V.A., *Stromatolity verkhnedokembriiskikh otlozhenii severa Sibirskoi platformy i ikh stratigraficheskoe znachenie* (Stromatolites from Upper Precambrian Sediments of the North Siberian Platform and Their Stratigraphic Significance), Moscow: Nauka, 1966.

Kröner, A., Sacchi, R., Jaeckel, P., and Cosca, M., Kibaran Magmatism and Pan-African Granulite Metamorphism in Northern Mozambique: Single Zircon Ages and Regional Implication, *J. African Earth Sci.*, 1997, vol. 25, no. 4, pp. 467–484.

Krylov, I.N., *1975. Stromatolity rifeya i fanerozoya SSSR* (Riphean and Phanerozoic Stromatolites of the Soviet Union), Moscow: Nauka, 1975.

Kuznetsov, A.B., Evolution of Strontium Isotope Composition in the Late Riphean Seawater: Carbonates of the Karatau Group, the Southern Urals, *Extended Abstracts of Cand. Sc. (Geol.–Mineral.) Dissertation*, St. Petersburg: Inst. Geol. Geokhronol. Dokembriya, Ross. Akad. Nauk, 1998, p. 23.

Kuznetsov, A.B., Gorokhov, I.M., Semikhatov, M.A., *et al.*, Isotopic Composition of Strontium in Limestones of the Inzer Formation, the Upper Riphean Stratotype of Southern Urals, *Dokl. Akad. Nauk*, 1997, vol. 353, no. 2, pp. 249–254.

Kuznetsov, A.B., Gorokhov, I.M., Mel'nikov, N.N., *et al.*, Dolomitization of the Upper Riphean Carbonates in the Min'yar Formation, Karatau Group, Southern Urals, *Tez. dokl., Osadochnye formatsii dokembriya i ikh rudonosnost'*, (Abstracts, Precambrian Sedimentary Formations and Their Ore Potentials), St. Petersburg, Inst. Geol. Geochronol. Dokembriya, Ross. Akad. Nauk, 1998, p. 31.

Kuznetsov, A.B., Gorokhov, I.M., and Semikhatov, M.A., Strontium Isotope Chemostratigraphy in the Proterozoic: State of the Problem, *Izotopnoe datirovanie geologicheskikh protsessov: novye metody i rezul'taty. 1-ya Rossiiskaya konferentsiya po izotopnoi geokhronologii, 15–17 noyabrya 2000 g, Moscow, Inst. Geol. Rudn. Mest. Ross. Akad. Nauk* (Isotopic Dating of Geological Processes: New Methods and Results, 1st Russian Conference on Isotopic Geochronology, November 15–17, 2000, Moscow, IGEM RAS), Moscow: GEOS, 2000, pp. 199–202.

Larsen, R.L., Latest Pulse of Earth Evidence for Mid-Cretaceous Superplume, *Geology*, 1991, vol. 19, no. 6, pp. 547–551.

Larsen, R.L., Superplume and Ridge Interactions Between Ontong Java and Manihiki Plateaus and the Nova-Canon Trough, *Geology*, 1997, vol. 25, no. 9, pp. 779–782.

Li, X.H. and McCulloch, M.T., Secular Variation in the Nd Isotopic Composition of Neoproterozoic Sediments from the Southern Margin of the Yangtze Block: Evidence for a Proterozoic Continental Collision in Southeast China, *Precambrian Res.*, 1996, vol. 76, nos. 1–2, pp. 67–76.

Li, X.H., U–Pb Zircon Ages of Granites from the Southern Margin of the Yangtze Block: Timing of Neoproterozoic Jinning Orogeny in SE China and Implications for Rodinia Assembly, *Precambrian Res.*, 1999, vol. 97, nos. 1–2, pp. 43–57.

Li, Z.X., Zhang, L., and Powell, C.Mc.A., Position of the East Asia in the Neoproterozoic Supercontinent Rodinia, *Austral. J. Earth Sci*, 1996, vol. 43, pp. 593–604.

Link, P.R., Christie-Blick, N., Devlin, W.J., *et al.*, Middle and Late Proterozoic Stratified Rocks of the Western US Cordillera, Colorado Plateau, and Basin and Range Province, *The Geology of North America, vol. C-2: Precambrian: Conterminous US*, Boulder: Geol. Soc. Am., 1993, pp. 463–595.

Litologiya i neftegazonosnost' yugo-vostoka Sibirskoi platformy (verkhnii dokembrii) (Lithology and Oil-and-Gas Potential of the Southeastern Siberian Platform: Upper Precambrian), Moscow: Nauka, 1980.

Martignole, J., Calvert, A.J., Friedman, R., and Reynolds, P., Crustal Evolution along a Seismic Section Across the Grenville Province (Western Quebèc), *Can. J. Earth Sci.*, 2000, vol. 37, nos. 2–3, pp. 291–306.

McArthur, J.M., Recent Trends in Strontium Isotope Stratigraphy, *Terra Nova*, 1994, vol. 6, no. 4, pp. 331–358.

McLelland, J., Daly, J.S., and McLelland, J.M., The Grenville Orogenic Cycle (ca. 1350–1000 Ma): an Adirondack Perspective, *Tectonophysics*, 1996, vol. 265, pp. 1–28.

McMenamin, M.A.S. and McMenamin, D.L.S., *The Emergence of Animals; The Cambrian Breakthrough*, New York: Columbia Univ., 1990.

Melezhik, V.A., Gorokhov, I.M., Kuznetsov, A.B., and Fallick, A.E., Chemostratigraphy of the Neoproterozoic Carbonates: Implications for 'Blind Experiments', *Terra Nova*, (in press).

Mezger, K., Essene, E.J., van der Pluijm, B.A., and Halliday, A.N., U–Pb., Geochronology of the Grenville Orogen of Ontario and New York: Constraints on Ancient Crustal Tectonic, *Contrib. Mineral. Petrol.*, 1993, vol. 114, pp. 13–26.

Milanovskii, E.E., Nikishin, A.M., Kopaevich, L.F., *et al.*, On the Correlation of Reorganization Phases in Kinematics of Lithospheric Plates and Short-Period Variations of the World Ocean Level, *Dokl. Akad. Nauk*, 1992, vol. 326, no. 2, pp. 313–318.

Mirota, M.D. and Veizer, J., Geochemistry of Precambrian Carbonates: VI. Aphabian Albanel Formations, Quebec, Canada, *Geochim. Cosmochim. Acta*, 1994, vol. 58, no. 7, pp. 1735–1745.

Montanez, I.P., Banner, J.L., Osleger, D.A., *et al.*, Integrated Sr Isotope Variation and Sea-Level History of Middle to Upper Cambrian Platform Carbonates: Implications for the Evolution of Cambrian Seawater $^{87}Sr/^{86}Sr$, *Geology*, 1996, vol. 24, no. 10, pp. 917–920.

Mosher, S., Tectonic Evolution of the Southern Laurentian Grenville Orogenic Belt, *Bull. Geol. Soc. Am.*, 1998, vol. 110, pp. 1357–1375.

Muehlberger, W.R., Denison, R.E., and Lidiak, E.G., Basement Rocks of Continental Interior of United States, *Bull. Am. Assoc. Petrol. Geol.*, 1967, vol. 51, no. 12, pp. 1211–1235.

Nevolin, B.S., Potapov, S.V., and Stavtsev, A.L., The Upper Proterozoic (Riphean) and Lower Cambrian of the Southeastern Margin of the Siberian Platform, Yudoma-Maya Belt

and Okhotsk Median Massif, *Novoe v stratigrafii i paleontologii pozdnego dokembriya vostochnykh i severnykh raionov Sibiri* (News in Stratigraphy and Paleontology of the Late Precambrian of Eastern and northern Regions of Siberia), Novosibirsk: Inst. Geol. Geophys. Sib. Otd. Akad. Nauk SSSR, 1978, pp. 21–63.

Nikishin, A.M., Comparison of Geological and Geomagnetic History of the Earth: Plate Tectonics and Pulsating Style of the Earth Evolution, *Vestn. Mosk. Univ., Ser. 4, Geol.*, 1994, no. 1, pp. 76–82.

Nuzhnov, S.V., *Rifeiskie otlozheniya yugo-vostoka Sibirskoi platformy* (Riphean Sediments of the Southeastern Siberian Platform), Moscow: Nauka, 1967.

Ortega-Gutierrez, F., Ruitz, J., and Centeno-Garcia, E., Oaxaquia, a Proterozoic Microcontinent Accreted to North America during the Late Paleozoic, *Geology*, 1995, vol. 23, no. 12, pp. 1127–1130.

Ovchinnikova, G.V., Semikhatov, M.A., Gorokhov, I.M., *et al.*, U–Pb Systematics of the Precambrian Carbonates: the Riphean Sukhaya Tunguska Formation of the Turukhansk Uplift, Siberia, *Litol. Polezn. Iskop.*, 1995, no. 5, pp. 525–536.

Ovchinnikova, G.V., Vasil'eva, I.M., Semikhatov, M.A., *et al.*, U–Pb Systematics of the Proterozoic Carbonate Rocks: the Inzer Formation of the Upper Riphean Stratotype, Southern Urals, *Stratigr. Geol. Korrelyatsiya*, 1998, vol. 6, no. 4, pp. 20–31.

Ovchinnikova, G.V., Vasil'eva, I.M., Semikhatov, M.A., *et al.*, The Pb–Pb Trail Dating of Carbonates with Open U–Pb Systems: the Min'yar Formation of the Upper Riphean Stratotype, Southern Urals, *Stratigr. Geol. Korrelyatsiya*, 2000, vol. 8, no. 6, pp. 3–19.

Ovchinnikova, G.V., Semikhatov, M.A., Vasil'eva, I.M., *et al.*, Pb–Pb Age of Limestones of the Middle Riphean Malgina Formation, the Uchur–Maya Region of Eastern Siberia, *Stratigr. Geol. Korrelyatsiya*, 2001, no. 6, pp. 3–25.

Palmer, M.R. and Edmond, J.M., The Strontium Isotope Budget of the Modern Ocean, *Earth Planet. Sci. Lett.*, 1989, vol. 92, no. 2, pp. 11–26.

Petrov, P.Yu. and Semikhatov, M.A., The Upper Riphean Stromatolite Reef Complex: the Burovaya Formation of the Turukhansk Region in Siberia, *Litol. Polezn. Iskop.*, 1998, no. 6, pp. 604–628.

Petrov, P.Yu., Semikhatov, M.A., and Sergeev, V.N., Development of the Riphean Carbonate Platform and Distribution of Silicified Microfossils (the Sukhaya Tunguska Formation, the Turukhansk Uplift, Siberia), *Stratigr. Geol. Korrelyatsiya*, 1995, vol. 3, no. 6, pp. 79–99.

Podkovyrov, V.N. and Vinogradov, D.P., Epigenesis and Preservation of Isotope System of Carbon and Oxygen from the Lakhanda and Yudoma Groups of the Upper Riphean and Vendian, the Belaya River Sections (SE Yakutia), *Litol. Polezn. Iskop.*, 1996, no. 5, pp. 541–551.

Podkovyrov, V.N., Kovach, V.P., and Kotova, L.N., Paleotectonic Models for Riphean Basins of the Siberian Type (the Uchur–Maya Region): Geochemical and ε_{Nd} Isotope Evidence from Clayey Rocks, *Materialy nauchn. soveshch. "Superkontinenty v geologicheskom razvitii dokembriya", Irkutsk, 4–6 iyunya 2001* (Proc. of Conf. on Supercontinents in the Precambrian Geological Evolution, Irkutsk, June 4–6, 2001), Irkutsk, 2001, pp. 189–192.

Podkovyrov, V.N., Kovach, V.P., and Kotova, L.N., Clayey Sediments of the Riphean–Vendian Hypostratotype in Siberia: Chemical Composition, Sm-Nd Systematics, Provenance, and Stages of Formation, *Litol. Polezn. Iskop.* (in press).

Pokrovskii, B.G. and Vinogradov, V.I., Isotopic Composition of Strontium, Oxygen, and Carbon in the Upper Precambrian Carbonates, the Western Slope of the Anabar Uplift (Kotuikan R.), *Dokl. Akad. Nauk SSSR*, 1991, vol. 320, no. 5, pp. 1245–1250.

Powell, C.McA., Li, Z.X., McElhinny, M.W., *et al.*, Paleomagnetic Constraints on Timing of the Neoproterozoic Breakup of Rodinia and Cambrian Formation of Gondwana, *Geology*, 1993, vol. 21, no. 10, pp. 889–982.

Raaben, M.E., *Verkhnii rifei kak edinitsa obshchei stratigraficheskoi shkaly* (The Upper Riphean as a Unit of the General Stratigraphic Scale), Moscow: Nauka, 1975.

Rainbird, R.H., Jefferson, C.W., and Young, G.M., The Early Neoproterozoic Sedimentary Succession B of the Northwest Laurentia: Correlation and Paleogeographic Significance, *Bull. Geol. Soc. Am.*, 1996, vol. 108, no. 4, pp. 454–470.

Rainbird, R.H., Stern, R., Khudoley, A.K., *et al.*, U–Pb Geochronology of Riphean Supracrustal Rocks from Southeastern Siberia and Its Bearing on the Laurentia-Siberia Connection, *Earth Planet. Sci. Lett.*, 1998, vol. 164, nos. 3–4, pp. 409–420.

Raymo, M.E., Ruddiman, W.F., and Froelich, P.N., Influence of Late Cenozoic Mountain Building on Ocean Geochemical Cycles, *Geology*, 1988, vol. 16, no. 7, pp. 649–653.

Reischmann, T., Ophiolites and Island Arcs in the Late Proterozoic Nubian Shield, *Ofioliti*, 2000, vol. 25, no. 1, pp. 1–13.

Restrepo-Pace, P.A., Ruiz, J., Gehrels, G., and Cosca, M., Geochronology and Nd Isotopic Data of Grenville-Age Rocks in the Colombian Andes: New Constraints for Late Proterozoic–Early Paleozoic Paleocontinental Reconstructions of the Americas, *Earth Planet. Sci. Lett.*, 1997, vol. 150, nos. 3–4, pp. 427–441.

Richter, F.M., Rowley, D.B., and De Paolo, D.J., Sr Isotope Evolution of Seawater: the Role of Tectonics, *Earth Planet. Sci. Lett.*, 1992, vol. 109, no. 1/2, pp. 11–23.

Rivers, T. and Corrigan, D., Convergent Margin on Southeastern Laurentia during the Mesoproterozoic: Tectonic Implication, *Can. J. Earth Sci.*, 2000, vol. 37, nos. 2–3, pp. 359–383.

Rivers, T., Lithotectonic Elements of the Grenville Province: Review and Tectonic Implications, *Precambrian Res.*, 1997, vol. 86, nos. 3–4, pp. 117–154.

Roback, R.C., Characterization and Tectonic Evolution of a Mesoproterozoic Island Arc in the Southern Grenville Orogen, Llano Uplift, Central Texas, *Tectonophysics*, 1996, vol. 265, no. 1, pp. 29–52.

Rodgers, J.W., A History of Continents in the Past 3 Billion Years, *J. Geol.*, 1996, vol. 104, no. 1, pp. 91–107.

Ronov, A.B., Khain, V.E., and Seslavinskii, K.B., *Atlas litologo-paleogeograficheskikh kart mira. Pozdnii dokembrii i paleozoi kontinentov* (Atlas of Lithological-Paleogeographic Maps of the World: Late Precambrian and Paleozoic Continents), Leningrad: Vses. Geol. Inst., 1984.

Rytsk, E.Yu., Amelin, Yu.V., Krymskii, R.Sh., *et al.*, Baikal–Muya Belt: Age, Formation Stages, and the Crust Evolution, *Tektonika, geodinamika i protsessy magmatizma i metamorfizma. Materialy XXXII Tektonicheskogo soveshch* (Proc. XXXII Tectonic Conference: Tectonics, Gedynamics, and Processes of Magmatism and Metamorphism), Moscow: GEOS, 1999, vol. 2, pp. 93–95.

Rytsk, E.Yu., Kovach, V.V., Shapaev, V.S., *et al.*, Two Rifting Stages of Destruction of the Ancient Continental Crust of the Siberian Craton in the Late Precambrian (Baikal Fold Region), *Superkontinenty v geologicheskom razvitii dokembriya. Materialy soveshchaniya (4–6 iyunya 2001 g., Irkutsk)* (Proc. of Conference: Supercontinents in the Precambrian Geological Evolution, June 4–6, 2001, Irkutsk), Irkutsk: Inst. Zemnoi Kory Ross. Akad. Nauk, 2001, pp. 231–243.

Semikhatov, M.A., Methodic Principles of the Riphean Stratigraphy, *Stratigr. Geol. Korrelyatsiya*, 1995, vol. 3, no. 6, pp. 33–50.

Semikhatov, M.A. and Raaben, M.E., Dynamics of the Global Diversity of Proterozoic Stromatolites. Article 1: Northern Eurasia, China, and India, *Stratigr. Geol. Korrelyatsiya*, 1994, vol. 2, no. 6, pp. 10–32.

Semikhatov, M.A. and Raaben, M.E., Dynamics of Global Diversity of Proterozoic Stromatolites. Article 2: Africa, Australia, Northern America and General Synthesis, *Stratigr. Geol. Korrelyatsiya*, 1996, vol. 4, no. 1, pp. 26–54.

Semikhatov, M.A. and Serebryakov, S.N., *Sibirskii gipostratotip rifeya* (Siberian Hypostratotype of the Riphean), Moscow: Nauka, 1983.

Semikhatov, M.A., Gorokhov, I.M., Kuznetsov, A.B., *et al.*, Sr Isotopic Composition of Seawater at the Beginning of the Riphean: Limestones of the Lakhanda Group of the Uchur-Maya Region in Siberia, *Dokl. Akad. Nauk*, 1998, vol. 360, no. 2, pp. 236–240.

Semikhatov, M.A., Ovchinnikova, G.V., Gorokhov, I.M., *et al.*, Isotopic Age of the Middle–Upper Riphean Boundary: Pb–Pb Geochronology of Carbonate Rocks of Lakhanda Group, Eastern Siberia, *Dokl. Akad. Nauk*, 2000, vol. 372, no. 2, pp. 216–221.

Serebryakov, S.N., *Osobennosti formirovaniya i razmeshcheniya rifeiskikh stromatolitov Sibiri* (Peculiarities in Formation and Distribution of Riphean Stromatolites in Siberia), Moscow: Nauka, 1975.

Sergeev, V.N., Silicified Microfossils from Transitional Meso-Neoproterozoic Deposits of the Turukhansk Uplift, Siberia, *Bull. Soc. Paleontol. Ital.*, 1999, vol. 38, nos. 2–3, pp. 287–295.

Shenfil', V.Yu., *Pozdnii dokembrii Sibirskoi platformy* (The Late Precambrian of the Siberian Platform), Novosibirsk: Nauka, 1991.

Sklyarov, R.Ya., The Late Precambrian Paleogeography in Southeastern Part of the Siberian Platform, the Kumakha Time, *Geologiya i metallogeniya dokembriya Dal'nego Vostoka* (Geology and Metallogeny of the Precambrian of the Far East), Leningrad: Nauka, 1981, pp. 77–84.

Sklyarov, E.V., Gladkochub, D.P., Donskaya, T.V., *et al.*, Most Important Marks in the Precambrian Evolution of the Southern Marginal Part of the Siberian Craton, *Superkontinenty v geologicheskom razvitii dokembriya. Materialy soveshchaniya, 4–6 iyunya 2001 g., Irkutsk)* (Proc. of Conference: Supercontinents in the Precambrian Geological Evolution, June 4–6, 2001, Irkutsk), Irkutsk: Inst. Zemnoi Kory Ross. Akad. Nauk, pp. 242–243.

Smaley, P.C., Higgins, A.C., Howarth, R.J., *et al.*, Seawater Sr Isotope Variations Through Time: a Procedure for Constructing a Reference Curve to Date and Correlate Marine Sedimentary Rocks, *Geology*, 1994, vol. 22, no. 4, pp. 431–434.

Smith, A.D., Wen, D.J., Huang, L.Y., and Wang, C.S., Constraints from Gneisses in the Qilian Fold Belt for the Position of the North China Block in the Proterozoic, *J. Geol. Soc.*, China, 2000, vol. 43, no. 1, pp. 81–93.

Stratigraficheskaya skhema rifeiskikh i vendskikh otlozhenii Volgo-Ural'skoi oblasti. Ob"yasnitel'naya zapiska (Stratigraphic Scheme for the Riphean and Vendian Sediments of the Volga–Ural Region, Explanatory Notes), Ufa: Inst. Geol. Ufim. Nauchn. Tsentr, Ross. Akad. Nauk, 2000.

Stratotip rifeya. Paleontologiya. Paleomagnetizm (Stratotype of the Riphean: Paleontology and Paleomagnetism), Keller, B.M., Ed., Moscow: Nauka, 1982.

Strieder, A.J. and de Freitas Suita, M.T., Neoproterozoic Geotectonic Evolution of Tocantins Structural Province, Central Brazil, *Geodynamics*, 1999, vol. 28, pp. 267–289.

Sukhorukov, V.I., Reference Sections of the Upper Riphean in the Ulakhan-Bam Ridge, *Pozdnii dokembrii i rannii paleozoi Sibiri. Sibirskaya platforma i vneshnyaya zona Altae-Sayanskoi skladchatoi oblasti* (The Late Precambrian and Early Paleozoic of Siberia: The Siberian Platform and External Zone of the Altai–Sayan Foldbelt), Novosibirsk: Inst. Geol. Geofiz., Sib. Otd. Akad. Nauk SSSR, 1986, pp. 23–64.

Tassinari, C.C.G. and Macambira, M.J.B., Geochronological Provinces of the Amazonian Craton, *Episodes*, 1999, vol. 22, no. 3, pp. 174–182.

Trimmel, H.E. and Frank, W., Neoproterozoic Tectono-Thermal Evolution of the Garriep Belt and Its Basement, Namibia and South Africa, *Precambrian Res.*, 1998, vol. 90, no. 1, pp. 1–28.

Trompette, R., *Geology of Western Gondwana (2000–500 Ma)*, Rotterdam: Balkema, 1994.

Van Schmus, W.R., Mesoproterozoic Orogenesis in the USA, *31st Int. Geol. Congr., Rio de Janeiro, Aug. 6–17, 2000: Congr. Program*, Rio de Janeiro, 2000, pp. 574–578.

Veis, A.F. and Vorob'eva, N.G., Microbiotas of the Kerpyl' Group in the Riphean Hypostratotype of Siberia, *Stratigr. Geol. Korrelyatsiya*, 1993, vol. 1, no. 1, pp. 41–58.

Veis, A.F., Larionov, N.N., Vorob'eva, N.G., and Lee Seong-Joo, Significance of Microfossils for Riphean Stratigraphy of the Southern Urals (Bashkirian Meganticlinorium) and Adjacent Region (Kama–Belaya Aulacogen), *Stratigr. Geol. Korrelyatsiya*, 2000, vol. 8, no. 5, pp. 3–28.

Veis, A.F., Petrov, P.Yu., and Vorob'eva, N.G., The Late Riphean Miroedikha Microbiota from Siberia. Part 1: Composition and Facial-Ecological Distribution of Organic-Walled Microfossils, *Stratigr. Geol. Korrelyatsiya*, 1998, no. 5, pp. 15–38.

Veizer, J. and Compston, W., $^{87}Sr/^{86}Sr$ in Precambrian Carbonates as an Index of Crustal Evolution, *Geochim. Cosmochim. Acta*, 1976, vol. 40, no. 8, pp. 905–914.

Veizer, J., Compston, W., Clauer, N., and Schidlowski, M., $^{87}Sr/^{86}Sr$ in Late Proterozoic Carbonates: Evidence for a "Mantle" Event at 900 Ma Ago, *Geochim. Cosmochim. Acta*, 1983, vol. 47, no. 2, pp. 295–302.

Veizer, J., Hoefs, J., Lowe, D.R., and Thurston, P.C., Geochemistry of Precambrian Carbonates: II. Archean Greenstones Belts and Archean Sea Water, *Geochim. Cosmochim. Acta*, 1989, vol. 53, no. 4, pp. 859–871.

Veizer, J., Plumb, K.A., Clayton, R.N., *et al.*, Geochemistry of Precambrian Carbonates: V. Late Paleoproterozoic Seawater, *Geochim. Cosmochim. Acta*, 1992, vol. 56, no. 7, pp. 2487–2501.

Vinogradov, V.I., Pokrovskii, B.G., Golovin, D.I., *et al.*, Isotopic Evidences of Epigenetic Transformations and the Age Problem of the Riphean Sediments in the Uchur-Maya Region of East Siberia, *Litol. Polezn. Iskop.*, 1998, no. 6, pp. 629–646.

Volkodav, I.G., Bazilevskaya, R.V., and Starnikov, A.I., Stratigraphy of the Lower Riphean in the Gornostakhskii Ridge (Southeastern Yakutia), *Novoe v stratigrafii i paleontologii pozdnego dokembriya vostochnykh i severnykh raionov Sibiri* (News in Stratigraphy and Paleontology of the Late Precambrian), Novosibirsk: Inst. Geol. Geofiz., Sib. Otd. Akad. Nauk SSSR, 1978, pp. 3–11.

Wadleigh, M.A., Veizer, J., and Brooks, C., Strontium and Its Isotopes in Canadian Rivers: Fluxes and Global Implications, *Geochim. Cosmochim. Acta*, 1985, vol. 49, no. 8, pp. 1727–1736.

Wareham, C.D., Pankhurst, R.J., Tomas, R.J., *et al.*, Pb, Nd and Sr Isotope Mapping of Grenville-Age Crustal Provinces in Rodinia, *J. Geol.*, 1998, vol. 106, no. 6, pp. 647–659.

Weil, A.B., Van der Voo, R., MacNicaiel, C., and Meert, J.G., The Proterozoic Supercontinent Rodinia: Paleomagnetically Derived Reconstructions for 1100 to 800 Ma, *Earth Planet. Sci. Lett.*, 1998, vol. 154, no. 1, pp. 13–24.

White, D.J., Forsyth, D.A., Asudeh, J., *et al.*, A Seismic Based Cross-Section of the Grenville Orogen in Southern Ontario and Western Quebec, *Can. J. Earth Sci.*, 2000, vol. 37, nos. 2–3, pp. 183–192.

Wingate, M.T.D., Campbell, I.H., Compston, W., and Gibson, G.M., Ion Microprobe U–Pb Ages for Neoproterozoic Basaltic Magmatism in South-Central Australia and Implications for Breakup of Rodinia, *Precambrian Res.*, 1998, vol. 87, no. 1, pp. 137–162.

Yakobchuk, A.S. and Nikishin, A.M., Estimated Intensity of Oceanic Crust Formation in the Phanerozoic, *Dokl. Akad. Nauk SSSR*, 1992, vol. 323, no. 5, pp. 908–911.

Zhao, W.L., Yuen, D.A., and Honda, S., Multiple Phase Trans and Style of Mantle Convection, *Phys. Earth Planet*, 1992, vol. 72, pp. 185–210.

Zharkov, M.A. and Chumakov, N.M., Paleogeography and Sedimentation Settings During Permian–Triassic Reorganization in Biosphere, *Stratigr. Geol. Korrelyatsiya*, 2001, vol. 9, no. 4, pp. 29–54.

Stratigraphy and Geological Correlation, Vol. 10, No. 1, 2002, pp. 42–56. Translated from Stratigrafiya. Geologicheskaya Korrelyatsiya, Vol. 10, No. 1, 2002, pp. 47–61.
Original Russian Text Copyright © 2002 by Karsakov, Gur'yanov, Goroshko.
English Translation Copyright © 2002 by MAIK "Nauka/Interperiodica" (Russia).

Stratigraphy of Lower Horizons in the Siberian Hypostratotype of the Riphean (the Southeastern Siberian Platform)

L. P. Karsakov*, V. A. Gur'yanov, and M. V. Goroshko*****

**Institute of Tectonics and Geophysics, Far East Division, Russian Academy of Sciences, ul. Kim Yu Chena 65, Khabarovsk, 680063 Russia*

***Federal State Unitary Mining-Geological Enterprise "Khabarovskgeologiya," ul. Karla Marksa 74, Khabarovsk, 680000 Russia*

****Federal State Geological Enterprise "Taezhgeologiya," ul. Novaya 17, Khabarovsk, 680032 Russia*

Received August 20, 1998; in final form, May 24, 1999

Abstract—A multidisciplinary approach was used to study the Lower Riphean deposits in the Siberian hypostratotype of the Riphean in the Uchur region of the southeastern Siberian platform and to clarify their relationships with the Lower Proterozoic (Upper Karelian) rocks. As is shown, the regional section of the Lower Riphean begins with the Uyan Group divisible into the Birindya, Konkula, and Adargai formations, the latter distinguished for the first time. An important unconformity is established below basal beds of the Uyan Group overlying the deeply eroded surface of weathered acid volcanics of the Elgete Formation of the Upper Karelian Ulkan Group, which are intruded by granites having the U–Pb isotopic ages of 1676–1721 Ma. The Uchur Group including the Gonam, Omakhta, and Ennin formations terminates the Lower Riphean in the Uchur–Maya region and overlies deposits of the Uyan Group with a stratigraphic hiatus and azimuthal discordance. The basal conglomerate of the Gonam Formation includes pebbles of stromatolitic dolomites derived from the underlying Adargai Formation. This geological boundary separates the Ulkan and Uyan rock complexes of contrast lithological composition. The boundary is geologically distinct and close in isotopic age to the lower boundary of the Riphean that is accepted to be 1650 ± 50 Ma old in the Precambrian stratigraphic scale of Russia.

Key words: Riphean, stratigraphy, Siberian hypostratotype of the Riphean, lower boundary of the Riphean, Uyan and Uchur groups, Birindya, Konkula, Adargai and Gonam formations.

INTRODUCTION

The Uchur–Maya section of the Riphean in the southeast of the Siberian platform is most complete and better characterized in paleontological aspect than other Upper Proterozoic reference sections of northern Eurasia. It includes the Lower, Middle, and Upper Riphean deposits. It is important as well that this section, overlain by the Vendian–Lower Cambrian deposits, reveals stratigraphic relationships between the Riphean and underlying Upper Karelian rocks crowning the Lower Proterozoic Erathem. All these features imply a high stratigraphic status of the Uchur–Maya section that stands out from the Uralian stratotype and has been properly selected for the Siberian hypostratotype of the Riphean (Semikhatov and Serebryakov, 1983). The mentioned fundamental monograph summarized the results obtained during the 50-year-long period of investigations of Riphean deposits in the southeast of the Siberian platform. Nevertheless, some principal problems of the regional Riphean stratigraphy remained unsolved here even in subsequent years despite the long investigation history. In particular, the subdivision of the Lower Riphean deposits, stratigraphic ranges of formations distinguished in the region and their reciprocal relations, as well as position of the boundary that separates the Riphean from older rocks represented important points of scientific discussion. It was impossible to solve these problems, because the distribution areas of the Lower Riphean deposits in the region are poorly exposed and inadequately studied. At the same time, the Uchur–Maya section qua standard is of a general but not of the regional significance only.

During the last 15 years, we carried out the large-scale geological and prospecting survey of the Uchur region (Fig. 1) that included the comprehensive study of various rock complexes and their interrelations, the multichannel aerial gamma-ray spectrometry, the exploration drilling, geochemical and geophysical investigations. We studied purposefully the contacts between various lithological sequences, which are favorable for localization of uranium deposits. The new materials obtained elucidate to a considerable extent the structure of the Lower Riphean deposits in the Uchur region and specify position of their lower boundary. The corresponding data are presented below.

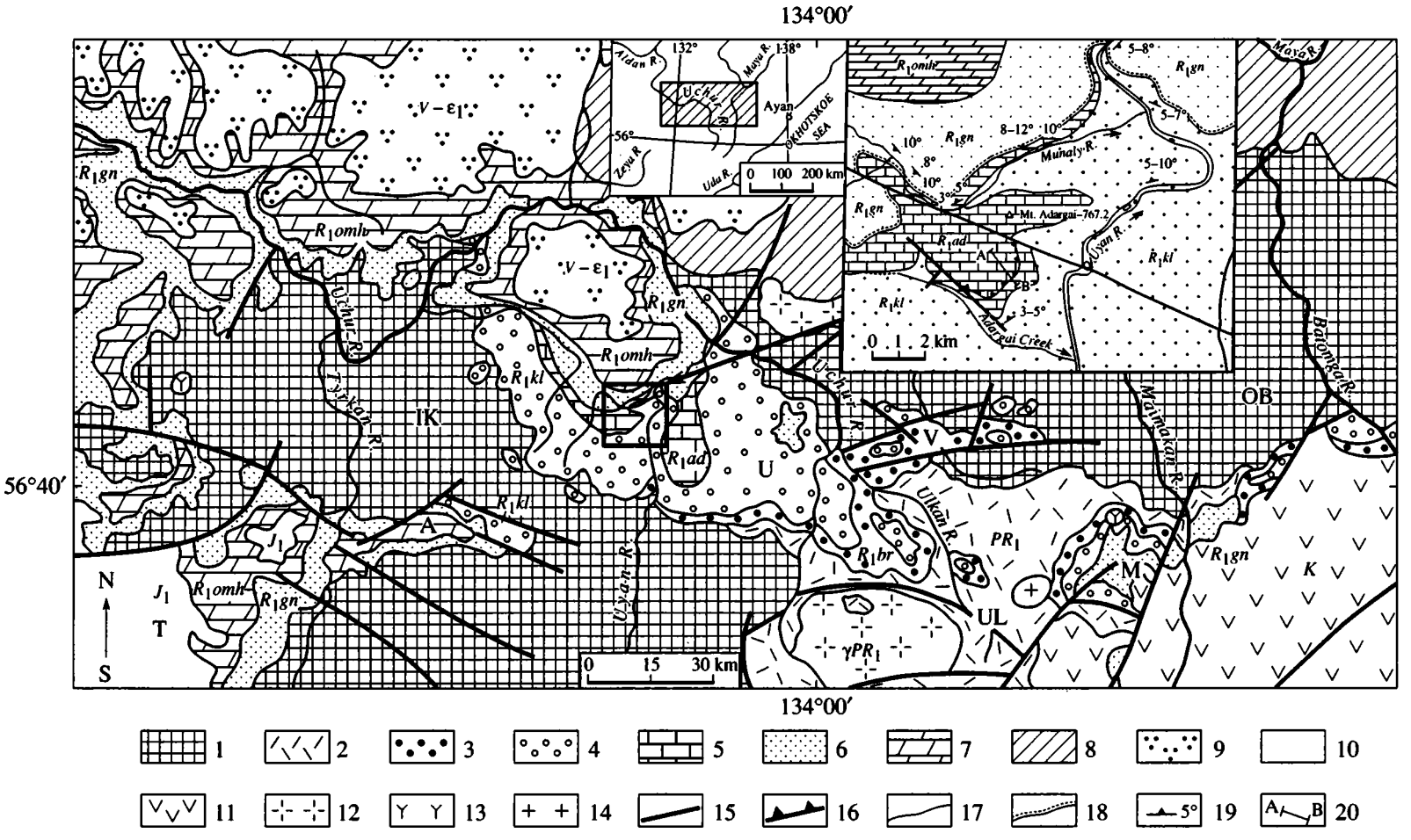

Fig. 1. Schematic geological map of the Uchur riverhead region (the inset map show structure of the Adargai area): (1) crystalline basement; (2) Ulkan Group of the Lower Proterozoic (Toporikan, Ulkachan, and Elgete formations); (3) Birindya, (4) Konkula, and (5) Adargai formations of the Lower Riphean Uyan Group; (6) Gonam and (7) undivided Omakhta and Ennin formations of the Lower Riphean Uchur Group; (8) undivided Middle and Upper Riphean; (9) Vendian–Lower Cambrian deposits; (10) Jurassic rocks; (11) Cretaceous volcanics; (12) Early Proterozoic granitoids of the Ulkan complex; (13) Proterozoic igneous rocks; (14) Cretaceous granitoids; (15) faults; (16) thrust faults; (17) conformable and (18) unconformable geological boundaries; (19) elements of bed attitude; (20) line of profile shown in Fig. 3. Structural elements: (U) Uchur, (M) Maimakan, (T) Tokin and (UL) Ulkan depressions; (A) Amulikan and (V) Verkhnii Ugayan grabens; (IK) Idyum–Khaikan and (OB) Omna–Batomga uplifts.

GENERAL GEOLOGICAL CHARACTERISTICS OF THE UCHUR REGION

The Uchur region in the southeast of the Siberian platform is one of few areas in the world, which exhibit relationships between the Lower Riphean and Lower Proterozoic (Upper Karelian) rocks (Semikhatov, 1978). The interval from the top of crystalline basement to the base of fossiliferous Lower Cambrian deposits is composed here of several rock complexes correlated with the lower Proterozoic (Upper Karelian), Riphean, and Vendian (Fig. 1). The Ulkan Group of rocks, which overlie crystalline basement of the Aldan shield that is as old as 1800–2000 Ma or older (Gamaleya, 1968; Semikhatov and Serebryakov, 1983; Gur'yanov and Karsakov, 1990), is attributed to the Upper Karelian. Deposits of the group fill in the Ulkan trough situated in the southeast of the region. The trough represents an elongated asymmetric structure, the southern wall of which is steeper than the northern one. Wedging out in the western direction until cessation at the Uyan River meridian, this structure merges with the Bilyakchan trough. The Ulkan group overlies the weathering crust (up to 35 m thick) on the top of crystalline basement and includes the Toporikan, Ulkachan, and Elgete formations up to 3090 m thick in total (Gur'yanov and Karsakov, 1990). The Toporikan Formation (200 m) consists of white quartz and feldspar-quartz sandstones intercalated with rare gravelstone and conglomerate lentils. The Ulkachan Formation (750 m) is represented by volcanics basic in composition and enclosing interlayers of terrigenous sediments. Dominant rocks of the Elgete Formation (2140 m) are trachyrhyolite, trachydacite, trachyrhyodacite, and their pyroclastic varieties; basic lavas, sediments, and tuffaceous sedimentary rocks are less abundant. Volcanic rocks of the last formation are 1687 ± 4 to 1721 ± 5 Ma old according to U–Pb ages of their zircons and 1721 Ma old according to Sm–Nd and Rb–Sr isotopic data (Larin *et al.*, 1997). The Ulkan Group encloses gabbroid and granitoid bodies of the Gekundan and Ulkan intrusive complexes. Isotopic age values obtained for various intrusive phases of the Gekundan complex are as follows: 1721.9 ± 3, 1720.7 ± 1.2 Ma (U–Pb method) and 1721 Ma (Sm–Nd and Rb–Sr methods) for the first phase; 1715.4 ± 4.8, 1716 ± 2.8 Ma (U–Pb method) and 1716 Ma (Sm–Nd and Rb–Sr methods) for the second phase; 1690 ± 8.5, 1676 ± 8.5, 1691 ± 1.4 Ma (U–Pb method) and 1703 Ma (Sm–Nd method) for the third phase (Larin *et al.*, 1997). The Ulkan Group is discordantly overlain by Riphean deposits of the platform cover.

In stratigraphic schemes accepted now, Riphean deposits of the southeastern Siberian platform are subdivided into the Uchur, Aimchan, Kerpyl', Lakhanda, and Ui groups (Semikhatov and Serebryakov, 1983; Shenfil', 1991). All researchers attribute the Uchur and Aimchan groups to the Lower and Middle Riphean, respectively, but stratigraphic equivalents of the Upper Riphean are defined controversially. Some researchers place the lower boundary of the Upper Riphean at the base of the Kerpyl' Formation, while others consider it as corresponding to the base of the Lakhanda Formation. The Uyan Group distinguished lately in the region as the new unit predating the Uchur Group is not included into current schemes. According to Semikhatov and Serebryakov (1983), glauconite fractions from different levels of the Uchur Group yielded K–Ar dates of 1450–1520 Ma for its lower part (Gonam Formation) and of 1360 Ma for the upper one (Omakhta Formation).

In the southeastern Siberian platform, the Lower Riphean deposits are structural constituents of the large Uchur depression and smaller complementary structures of the Verkhnii Ugayan and Amulikan grabens and Maimakan depression (Fig. 1). The Uchur depression of complex structure is spread nearly over the entire Uchur River basin (Nuzhnov, 1967; Semikhatov and Serebryakov, 1983). In this work, we consider its southeastern part (a gulf) probably representing one of subordinate depressions in upper courses of the Uchur River. The gulf extending from the northwest to southeast is 150 km long and 60 km wide; it is bounded by the Omna–Batomga uplift in the northeast and by the Idyum–Khaikan uplift in the southwest. The Verkhnii Ugayan graben that is bounded by sublatitudinal faults departs from the Uchur depression at the right side of the Uchur River. The studied part of the Uchur depression is filled with the Lower Riphean, Vendian, and Lower Cambrian deposits. The lowermost Riphean horizons exposed here rest on volcanic rocks of the pre-Riphean Ulkan Group. In total, sediments filling in the depression are as thick as 1200 m at least. Rocks beds that are subhorizontal in the central part of the depression have a gentle centroclinal dip near its walls.

The Maimakan depression occupying middle courses of the eponymous river in the southeast of the study region extends in sublatitudinal direction for the distance of 120 km. Near its western terminus, the depression is filled with Lower Riphean deposits overlying different horizons of the Ulkan group. In the east, within a through adjacent to the Dzhugdzhur Mountains, these deposits are concealed under Mesozoic volcanic rocks.

The sublatitudinal Amulikan Graben in the west of the study region is 50 km long and 10–15 km wide. This structure is deepening toward the west, where it disappears under Mesozoic coaliferous deposits of the Tokin through. The Lower Riphean deposits overlying volcanics of the Ulkan Group are also known in the Verkhnii Ugayan graben that is 45–50 km long and 8–15 km wide.

STRUCTURE AND CORRELATION OF LOWER RIPHEAN SECTIONS

The Lower Riphean stratigraphic scale accepted in this work is shown at the left of Fig. 2. It includes the

Uyan and Uchur groups corresponding to principal stages of sedimentation and separated by a regional hiatus.

Uyan Group

The group was originally distinguished as equivalent in range to the Konkula Formation only (Nuzhnov and Yarmolyuk, 1959), while the Birindya Formation was included into this unit later (Nuzhnov, 1967). Nuzhnov believed that the Uyan Group and underlying volcano-sedimentary rocks of the Ulkan Group represent an indivisible orogenic complex of the Early Proterozoic age that is separated from overlying deposits by a considerable hiatus in sedimentation corresponding to the emplacement time of the Ulkan intrusive complex of granosyenites and quartz porphyries. We established however that deposits of the Birindya Formation overlie the deeply eroded surface of volcanic rocks representing the Elgete Formation of the Ulkan Group. Accordingly, we had to revise the stratigraphic position of the Uyan Group in the Uchur–Maya section of the Upper Proterozoic and to correct the local stratigraphic scheme of Riphean deposits. Within the Uyan Group, we distinguish the Birindya and Konkula formations that were recognized in earlier times and the new Adargai Formation.

Birindya Formation

Zabrodin (1966) was first to distinguish this formation in exposures along the Levaya Birindya Creek at the right side of the Uchur River. According to his data, the formation consisting of sandstones intercalated with lava flows of diabases, trachyandesites, and basalts can be divided into three subformations. Gamaleya *et al.* (1969) distinguished afterward the inner regional hiatuses in this unit. They considered lower beds of the lower subformation as the individual Bitop Formation. The overlying beds along with middle subformation were regarded as the Birindya Formation proper, and the former upper subformation was attributed to the Konkula Formation.

In the stratotype area, we studied the structure of the Birindya Formation, its upper and lower boundaries, and described three complete sections of this unit (Fig. 2). We failed to recognize regional hiatus between the Bitop and Birindya formations. As we think, the misinterpretation was related to improper understanding of a fault detectable on aerial photographs and locally concealed under thick cover of diluvial-proluvial deposits. The latter were erroneously taken for the Birindya deposits. We established as well that the former Bitop Formation is an invalid unit, because it actually corresponds to that element of section, where lower beds of the Birindya Formation, as we understand it, are doubled back upon themselves.

The Birindya Formation of red sandstones and conglomerates that are intercalated with lava flows of subalkaline olivine and leucocratic amygdaloidal basalts is exposed in the Uyan–Batomga interfluve, but westward it is transgressively overlain by deposits of the Konkula Formation (Fig. 1). There is angular unconformity between the Birindya deposits and underlying rocks, as they are separated from the crystalline basement and fluidal trachyandesites of the Elgete Formation by the weathering crust up to 40 m thick. Pebbles and boulders in basal conglomerate of the Birindya Formation mostly consist of quartz, red trachydacite, trachyrhyodacite, and trachyrhyolite of the Elgete Formation; metabasalts of the Ulkachan Formation or plagiogneisses, granite gneisses, crystalline schists, quarts sandstones, and quartzites occur among them sporadically.

The weathering crust that originated prior to deposition of the Birindya Formation is predominantly autochthonous, divisible into the disintegration and leaching zones. The first zone corresponds to debris and breccias composed of Fe-hydroxides and clayey hydromica particles, whereas the second one is composed of red ferruginate clay with residual quartz grains. Being enriched in Fe-hydroxides, the weathering crust above volcanic rocks of the Elgete Formation is characteristically brick-red in contrast to lighter colored weathering products of crystalline rocks. Adularia syngenetic to the crust (Synnyar River basin) yielded the Rb–Sr isochron age of 1670 ± 40 Ma (determination of 1997 by Yu.P. Shergina, All-Russia Geological Institute). We divided the Birindya Formation into two subunits by virtue of structural and lithological features. In the type section (right side of the Toporikan River) that is described below, the unit under consideration overlies the Elgete Formation and is overlain by the Konkula Formation (Fig. 2, section 13).

Lower Birindya Subformation (from the base upward)

(1) Basal horizon consisting of alternating conglomerate (small- to medium pebbled), gravelstone, sandstone, and siltstone beds (10 to 50 cm thick); basal bed encloses pebbles and boulders of quartz, Lower Proterozoic metabasalts, trachyrhyodacite and trachyrhyolite of the Elgete Formation. The well-rounded pebbles and boulders constitute 25–75% of rock volume. The coarse-grained cement is of the feldspar-quartz composition, corresponding in grain size to sandy or gravely material. The member is 50 m thick.

(2) Alternating red beds (5–10 cm thick) of small- to medium-grained feldspar-quartz gravel with rare pebbles of milky white quartz; the member is 80 m thick.

(3) Cherry red to gray feldspar-quartz sandstones, medium- to coarse-grained, thick-bedded, bearing sporadic pebbles of quartz, trachyrhyodacite, and fine-grained sandstone of similar mineral composition; the member is 50 m thick.

(4) Cherry red to gray, fine-bedded sandy siltstones; the member is 0.5 m thick.

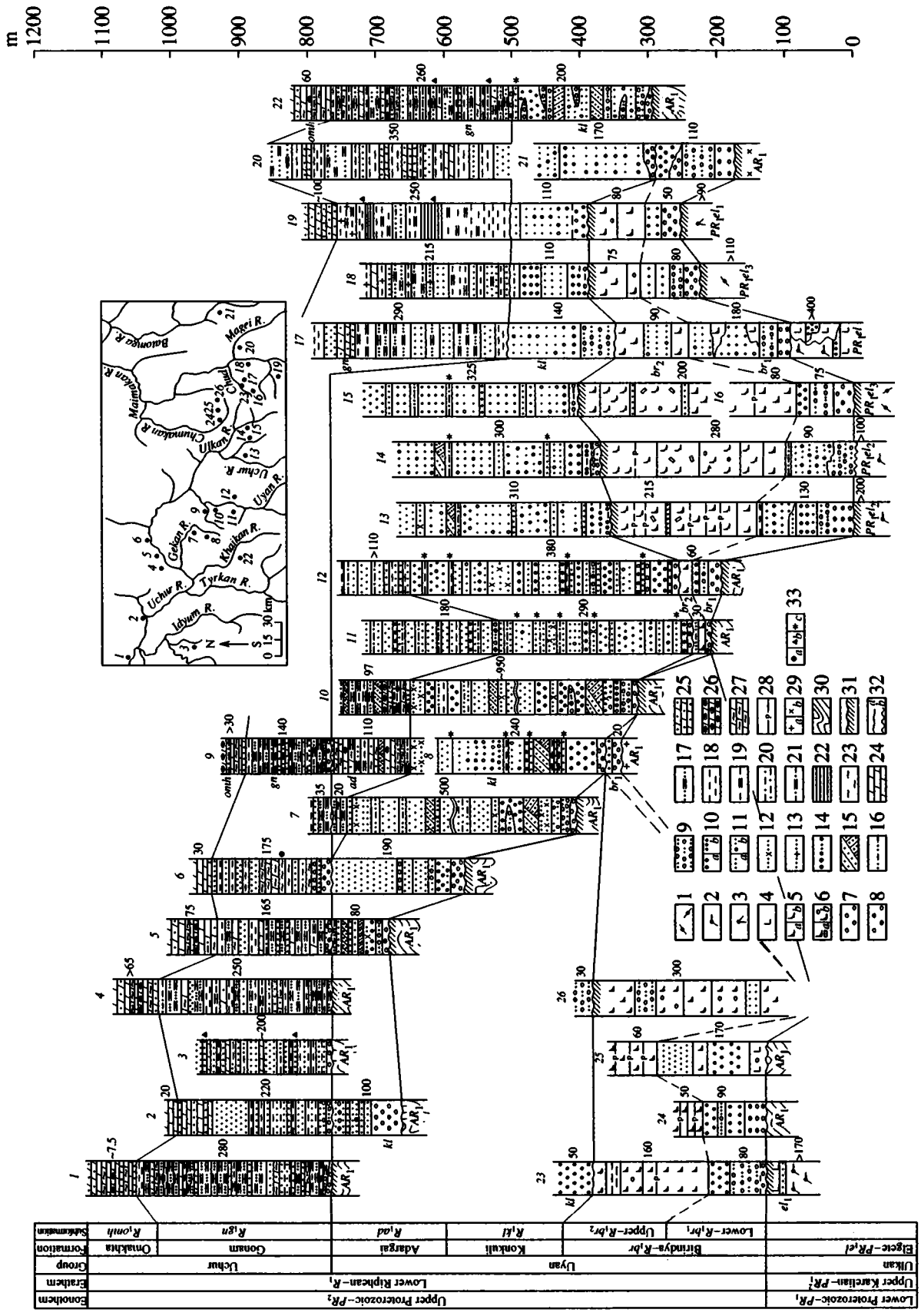
m
1200
1100
1000
900
800
700
600
500
400
300
200
100
0
Baomnga R.
Magri R.
Maimakan R.
Chuul
Chumukan R.
Ulkan R.
Uchur R.
Uyan R.
Gekon R.
Khoikon R.
Tyrkan R.
Uchur R.
Ithym R.
0 15 30 km
N
S
Lower Proterozoic–PR1
Upper Proterozoic–PR2
Lower Riphean–R1
Upper Kartalian–PR1
Eratkem
Ulkan
Uyan
Ulchur
Group
Lower–R1br1
Upper–R1br2
Birindya–R1br
Konkuli
R1ll
Adargai
R1ad
Gonam
R1gn
Omakha
R1omh
Formation
Eopaleic–PR1el
Subformation

Upper Birindya Subformation

(5) Subalkaline olivine basalts, cherry red to gray, massive, aphyric; the member is 31 m thick.

(6) Leucocratic subalkaline olivine basalts, dark gray, massive, aphyric, enclosing clasts of quartzite-like rocks near the base; the member is 3 m thick.

(7) Pinkish gray, thick-bedded and medium-grained feldspar-quarts sandstone; the bed is 0.5 m thick.

(8) Subalkaline olivine basalts, dark gray, massive, aphyric; the member is 19 m thick.

(9) Gray fine-grained feldspar-quartz sandstone; the bed is 0.3 m thick.

(10) Subalkaline olivine basalts, dark gray, massive, with rare small phenocrysts; the member is 25 m thick.

(11) Feldspar-quartz sandstone, lilac gray, fine- to medium-grained; the bed is 0.8 m thick.

(12) Subalkaline olivine basalts, dark gray, massive and phyric; the member is 32 m thick.

(13) Feldspar-quartz sandstone, cherry red to gray, thick-bedded and medium-grained; the bed is 2 m thick.

(14) Subalkaline olivine basalts, black, massive and phyric; the member is 30 m thick.

(15) Feldspar-quartz sandstone, gray, fine- to medium-grained; the bed is 0.2 m thick.

(16) Leucocratic subalkaline olivine basalts, dark green to gray, aphyric; the member is 17 m thick.

(17) Feldspar-quartz sandstone, dark lilac-gray and medium-grained; the bed is 0.2 m thick.

(18) Leucocratic subalkaline olivine basalts, aphyric, greenish to dark gray, weathered and dark brown in the upper part; the member is 34 m thick.

The Birindya Formation is about 380 m thick in total. The described section is well correlative with others (Fig. 2, sections 11–20 and 23–26).

Konkula Formation

In 1956, V.R. Alekseev and N.S. Shpak (see in Zlenko *et al.*, 1960) distinguished the Konkula Formation in the range corresponding to that of continental red beds in the scheme that was suggested by A.K. Matveev and his colleagues in 1940. They attributed to this unit the sandstone succession of uniform composition that is overlain by basal conglomerates of the Gonam Formation and overlies with a distinct angular unconformity the Archean rocks, presumably, together with volcanic lava flows. The formation stratotype is situated in the interfluve area of the Levaya and Verkhnyaya Konkula rivers (left tributaries of the Gekan River). As we established, rocks of the Konkula Formation are widespread in the study region. Their outcrops are detected in drainage areas of the Munaly, Adargai, Sargatta, Toporikan, Birindya, Yuktanda, Verkhnyaya and Nizhnyaya Konkula rivers, where we studied the unit relationships with underlying and overlying deposits (Fig. 2).

The formation is composed of dark red and lilac thick-bedded feldspar-quartz sandstones and arkoses, which enclose "floating" pebbles and sporadic gravelstone, shale, and quartz sandstone interlayers. Its rocks either unconformably overlie the Archean rocks, or transgressively overlap deposits of the Birindya Formation, resting above the weathering crusts. Above the Birindya basalts, the brick-red weathering crust up to 10 m thick is darker in coloration than that developed above crystalline rocks at the base of the Konkula and Birindya formations. The crust in question is composed of hard rocks vesicular to some extent and lacking traces of original structural and textural features. Vesicles in these red to brown aggregates of hydrogoethite, hydromica, and other clay minerals are filled with secondary quartz, carbonate, and hydromica. In the Givun, Amulikan, and Gekan river basins, the apparent thickness of weathering crust varies from 1 to 10 m. Two lev-

Fig. 2. Correlated sections of Lower Riphean deposits in the Uchur region: (1) trachyrhyolite; (2) trachyrhyodacite; (3) trachydacite; (4) basalts; (5) subalkaline olivine basalts (a) and their leucocratic varieties (b); (6) porphyritic (a) and amygdaloidal (b) subalkaline basalts; (7) quartz conglomerate; (8) polymictic conglomerate; (9) gravelstone; (10) coarse- (a) and medium-grained (b) oligomictic sandstones; (11) fine-grained (a) and inequigranular (b) oligomictic sandstones; (12) quartz sandstone; (13) glauconite-bearing sandstone; (14) sandstone with "floating" quartz pebbles; (15) cross-bedded sandstone; (16) sandstone with siltstone and shale laminae or clasts; (17) sandstone with dolomitic cement; (18) siltstone; (19) siltstone with dolomitic cement; (20) silty sandstone; (21) silty sandstone with dolomitic cement; (22) shale; (23) opoka; (24) pelitomorphic dolomite; (25) sandy dolomite; (26) oolitic dolomite; (27) stromatolitic dolomite; (28) sandstone interlayer less than 1 m thick; (29) Early Archean granites (a) and quartz diorites (b); (30) Lower Archean gneisses and crystalline schists; (31) weathering crust; (32) stratigraphic (a) and angular (b) unconformities; (33) pseudomorphs of gypsum (a), halite (b), and glauconite (c). Figures to the right indicate the unit thickness in meters.

Sections in numerical order: (*1*) Uchur River, right bank 15 km downstream of Gonam River mouth; (*2*) Lenkovaya River basin; (*3*) Dzhiendo River; (*4*) Medvezh'ya and Zoryanka river basins; (*5*) area of Givun River mouth; (*6*) altitude marks 770 and 1055, Uchur River right side; (*7*) interfluve area of Verkhnyaya and Nizhnyaya Konkula rivers; (*8*) Verkhnyaya Konkula River, left bank; (*9*) Munaly River, left bank; (*10*) Adargai Creek, left bank; (*11*)Sargatta River, left bank; (*12*) Uyan River, right bank; (*13*) Toporikan River, right bank; (*14*) Birindya River; right bank; (*15*) Tala Creek source area; (*16*) Pravyi Chad riverhead; (*17*) Mokhovoi Creek; (*18*) El'domu River, left bank; (*19*) Yuktanda River, right side; (*20*) Magei–Glukharinyi water divide; (*21*) Batomga–Bereya interfluve; (*22*) Amulikan River basin; (*23*) Chad River, right bank; (*24*) Chumikandzha River, left bank; (*25*) Chumikandzha River, right bank; (*26*) Chumikandya River, right bank.

Geologists who described sections (numbered in parentheses): M.V. Goroshko (5, 7, 9, 10, 12); V.A. Gur'yanov (13–21, 23, 26); M.K. Zheverzheeva (16, 18); V.E. Kirilov (12); A.G. Losev (24, 25); S.V. Nuzhnov (3); A.L. Osipov (4, 5, 7, 9, 10); M.A. Semikhatov (1); Ya.D. Shenkman (6, 8, 11, 12); V.M. Shmigirilov (17, 20, 26); N.S. Shpak (2); V.E. Chepygin (21).

els of weathering crust have been established in continuous Riphean sections that have been studied in detail within the Toporikan, Birindya, El'domu, Ulkan (Tala Creek), and Yuktanda river basins. In all cases, the areal distribution of weathering crust is established.

Basal conglomerates of the Konkula Formation are intercalated with gravelstone and sandstone beds. They are rich in quartz pebbles, which are much more abundant than pebbles of gray quartzite, quartzite-like sandstone, granite gneiss, granite, siltstone, weathering crust, acid Elgete volcanics, Ulkachan metabasalts, and gabbro-diabases. Pebbles are not larger than 8 cm across, but some boulders are up to 50 cm in diameter. Pebbles constitute 10 to 90% of rock volume. They are well rounded but poorly sorted.

The most representative rock succession of the Konkula Formation is detected in the left-side area of the Uyan River, where we studied its upper part (504 m) using core samples from the Adargai locality or in natural outcrops at the left side of the Munaly River. The lower part of the unit was investigated in bedrock exposures along the Verkhnyaya Konkula, Sargatta, and Ellara-El'ge rivers and in the Adargai Creek valley. The succession of distinguished rock members (Fig. 2, section 10) is as follows:

(1) Quartz gravelstones and sandstones with "floating" quartz pebbles and conglomerate lentil up to 5–6 m thick that overlie rocks of the Archean basement; all these rocks are pinkish to brown-gray. Well-rounded pebbles from 1–2 to 5–10 cm in diameter consist of milky white quartz, quartzite-like sandstones, sometimes of red Archean granites, granite gneisses, and rocks of weathering crust. The member is 25 m thick.

(2) Pinkish quartz sandstones with occasional "floating" quartz pebbles; these rocks with feldspar-quartz matrix show ripple bedding. The member is 15 m thick.

(3) Pinkish to yellowish gray oligomictic medium-grained sandstones displaying cross-lamination; the member is 25 m thick.

(4) Brownish gray to pinkish coarse-grained feldspar-quartz sandstones with rare "floating" pebbles and brownish gray interbed of intraformational gravelstone; ferruginate matrix of the rocks is of the feldspar–quartz composition. The member is 40 m thick.

(5) Pinkish white medium- to fine-grained quartz sandstones with hydromica–quartz cement; the member is 15 m thick.

(6) Coarse alternation of oligomictic and arkosic coarse- to medium-grained sandstones colored brown or pinkish gray, locally variegated; cement of the rocks is of the hydromica–quartz, ferruginate hydromica–quartz, ferruginous–siliceous, or clay–hydromica types. Bedding planes reveal ripple marks and desiccation cracks. The member is 50 m thick.

(7) Fine alternation of brick-red siltstones, shales, and sandstones; frequent desiccation cracks are characteristic of bedding planes. The member is 30 m thick.

(8) Coarse alternation of oligomictic and arkosic coarse- to medium-grained sandstones colored pinkish gray or cherry-red, locally variegated; the rocks sporadically enclose "floating" pebbles and are intercalated with red interlayers of siltstone, shale, and cross-bedded sandstones. Ripple marks at bedding planes occur throughout the member section that is 32.5 m thick.

(9) Light gray to cherry-red fine- to medium-grained oligomictic sandstones intercalated with red siltstone and shale interlayers (1–30 cm); the member is 25 m thick.

(10) Coarsely bedded fine- to medium-grained light gray, light cherry-red, and red oligomictic sandstones; the rocks enclose lenticular and angular fragments of red shales and siltstones derived from the underlying unit. Ripple marks, desiccation cracks, and cross-bedded laminae occur throughout the member section. Carbonate material is detected in the matrix composition. The member is 35 m thick.

(11) Brownish gray inequigranular or medium-grained oligomictic sandstones; the member is 20 m thick.

(12) Light gray medium- to fine-grained quartz sandstone; the bed is 7 m thick.

(13) Pinkish medium- to fine-grained cross-laminated oligomictic sandstone; the bed is 8 m thick.

(14) Pinkish and brownish gray medium-grained oligomictic sandstones; the member is 25 m thick.

(15) Reddish gray medium-grained feldspar–quartz sandstones enclosing fragments and intercalated with interlayers of red and brown siltstones and shales; the member is 15 m thick.

(16) Coarse-grained feldspar–quartz sandstones with vague pinkish and brown-gray stains; the member is 20 m thick.

(17) Pinkish and lilac fine-grained oligomictic sandstones with inclusions and thin interlayers of red to cherry-red siltstones and shales; an interlayer of reddish gray siltstone near the base is 2.5 m thick. The member is 15 m thick.

(18) Light gray and pinkish coarse- to medium-grained oligomictic sandstones enclosing rare lenticles of red siltstones; the member is 15 m thick.

(19) Pinkish and white medium- to fine-grained quartz sandstones; matrix of the rocks contains carbonate and barite. The member is 25 m thick.

In this section, the Konkula Formation is 950 m thick and overlain by carbonate–terrigenous sediments of the Adargai Formation.

Another characteristic section of the Konkula Formation has been studied in the right-bank area of the Toporikan River (Fig. 2, section 13), where this unit overlies the weathering crust above leucocratic subal-

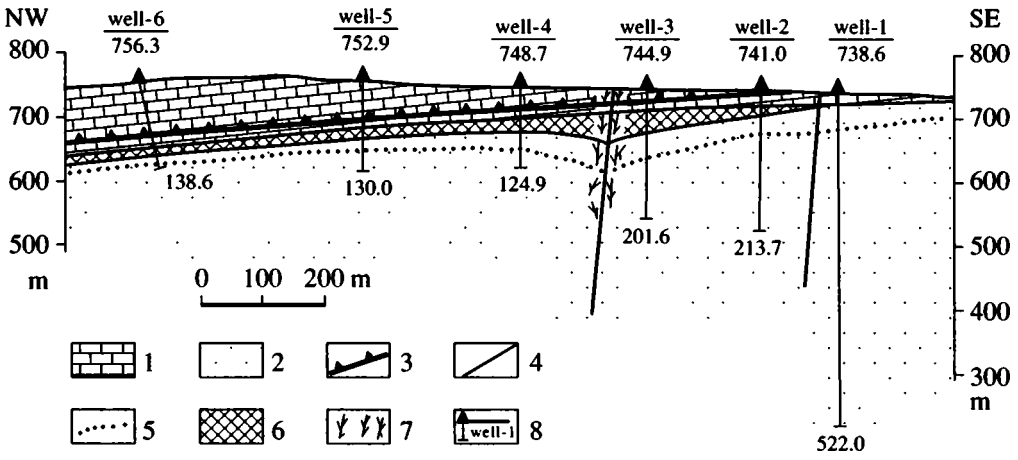

Fig. 3. Schematic geological section of the Adargai and Konkula formations (profile line is shown in the inset map to Fig. 1): (1) sandstones, siltstones, and pelitomorphic sandy, oolitic, and algal dolomites of the Adargai Formation; (2) oligomictic quartz sandstones with rare siltstone and shale interlayers of the Konkula Formation; (3) thrust fault; (4) steeply dipping faults; (5) lower boundary of argillization zone; (6) tabular body of barite deposits; (7) zone of coarse-grained barite veins; (8) wells, their numbers, altitude marks, depth of penetration.

kaline olivine basalts of the Lower Riphean Birindya Formation. Basal beds of the latter rest here on the weathering crust above acid volcanics of the Elgete Formation.

In their lithology and structure, individual sections of the Konkula Formation are well correlative to each other and with the stratotype situated in the drainage area of the Verkhnyaya and Nizhnyaya Konkula rivers (Fig. 2, sections 2, 5–23, 26). The formation consists of almost invariable facies except for appearance of rather frequent and thin interlayers of brown-gray silty sandstones and siltstones in the stratotype area or along the Sargatta Creek and Uyan River. In the upper part of the formation, sandstones are more rich in feldspar clasts (up to 40%) than below, and admixture of carbonates and barite is detected in their cement. A sandstone horizon with barite cement is traceable from the Uyan River to the Givun River mouth and further, apparently to the Tyrkan River mouth.

In general, the Konkula Formation varies in thickness from 80–100 to 380–500 m (Figs. 2, 3). Data of prospecting drilling and seismic investigations indicate however that it is 950 m thick in the right-side area of the Uyan River. Toward the northwest, e.g., near the Givun and Gekan rivers, the formation is much thinner, pinching out in proximity to the Tyrkan River mouth (Fig. 1). These observations suggest the more southern localization of corresponding sedimentation center during the Early Riphean.

Adargai Formation

We distinguished this unit for the first time. It corresponds to the succession of gray carbonate–terrigenous sediments conformably overlying red sandstones of the Konkula Formation. Red sandstones and conglomerates of the younger Gonam Formation overlie it either with hiatus (the Munaly River basin) or with azimuthal discordance (the Gekan River basin). The formation stratotype is located in the drainage area of the Adargai Creek and Munaly River (middle courses of the Uyan River). The rock succession of the Adargai Formation is most complete in proximity to the eponymous creek (left tributary of the Uyan River). Its lower part was studied here with the help of drilling data, and the upper one was investigated in bedrock outcrops along the Munaly River (Fig. 2, sections 9, 10). According to drilling results, the lower contact of the unit is conformable (Figs. 4, 5) and corresponds to the distinct transition from pinkish and lilac sandstones of the Konkula Formation to gray silty sandstones and siltstones of the Adargai Formation, which are intercalated with dolomite interlayers. We place the upper unit boundary at the base of cherry-red conglomerate and gravelstone beds of the Gonam Formation, which bear pebbles of gray stromatolitic dolomites of the Adargai Formation (Fig. 4).

In the drainage area of the Adargai Creek, the type section of the unit is of the following structure:

(1) Fine rhythmic alternation of light to yellowish gray quartz–feldspar silty sandstone laminae (0.5–2 cm) having dolomitic or clay–sericite–quartz–feldspar cement with yellow-gray sandstones and siltstones having dolomitic matrix; gray medium- to fine-grained sandstones dominant in the upper part of the bed consist of subrounded quartz and feldspar grains. Near the base, there is an interlayer of light gray siltstone with siliceous–carbonate cement. Lenticular veinlets and disseminations composed of chalcopyrite, chalcosine, malachite, azurite, hydrogoethite, limonite, psilomelane, and vernadite are confined to bedding planes in this interlayer. The bed is 7.5 m thick.

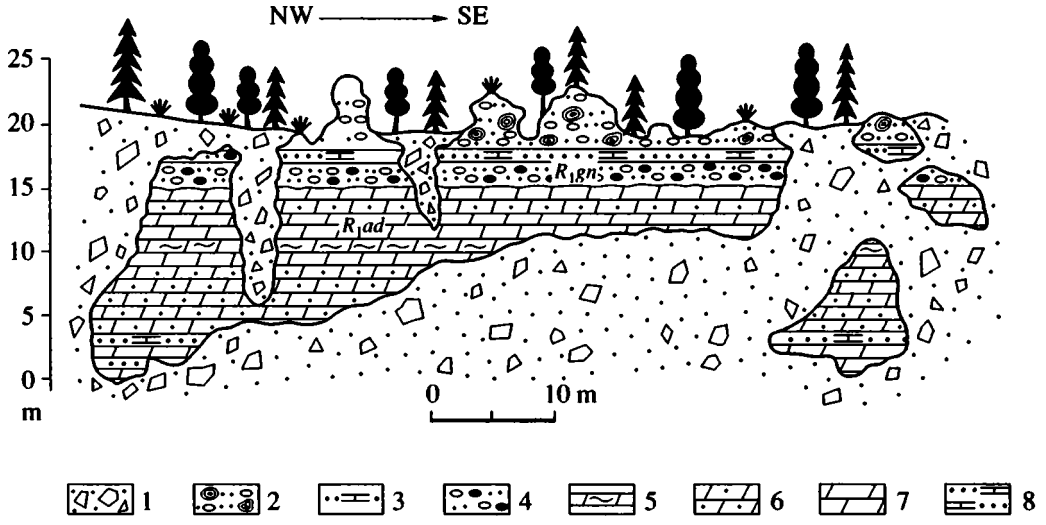

Fig. 4. Sketch of bedrock outcrop 108 at the left bank of the Munaly River characterizing contact between the Gonam and Adargai formations: (1) diluvial deposits; (2–4) Gonam Formation of (2) cherry-red gravelstone and conglomerate lentils with quartz, quartzite, stromatolitic dolomite and granite gneiss pebbles, (3) pink medium to fine-grained quartz–feldspar sandstones with dolomitic cement, and (4) cherry-red gravelstones overlying basal conglomerate with pebbles composed of quartz, quartzite, sandstone, stromatolitic dolomite, red granite, granite gneiss and brick-red argillaceous rocks of the weathering crust; (5–8) Adargai Formation of (5) stromatolitic, (6) sandy, (7) pelitomorphic dolomites and (8) coarse-grained quartz-feldspar sandstones with dolomitic cement.

(2) Stromatolitic, sometimes sandy pelitomorphic and oolitic dolomite enclosing thin interlayers of gray fine- to medium-grained quartz–feldspar sandstones that are cemented by dolomitic or siliceous–carbonate material and laminae of dark gray siltstones and silty sandstones; the bed is 6.5 m thick.

(3) Dark to light gray fine-laminated siltstones with clay–quartz–hydromica–feldspar matrix; the bed is 9 m thick.

(4) Alternating beds of light gray pelitomorphic, oolitic, or sandy dolomites; the member is 15 m thick.

(5) Ashy and light gray medium- to fine-grained feldspar–quartz sandstones that have feldspar–quartz–dolomite matrix and enclose thin (up to 1 cm) laminae of siltstone and silty sandstone. The member is 7 m thick.

(6) Alternation of light gray stromatolitic and sandy dolomite beds (2.5 m thick); the latter dominate near the member base and others prevail higher. The member is 13 m thick.

(7) Gray fine-laminated siltstones with dolomitic matrix; near the base, they enclose interlayers (up to 3.5 m thick) of light gray fine-grained quartz–feldspar sandstones cemented by dolomitic material. The member is 12.5 m thick.

(8) Light gray bedded fine-grained sandstone of quartz-feldspar composition; this sandstone with dolomitic matrix overlies the basal bed (3m thick) of gray quartz–feldspar silty sandstone with hydromica–siliceous cement. The member is 7.5 m thick.

(9) Ashy gray bedded siltstone with carbonate matrix overlying the lower bed (4.5 m thick) of light gray sandy dolomite that encloses siltstone laminae; the member is 11.5 m thick.

(10) Alternation of gray to light gray sandy and oolitic dolomites; the latter are dominant in the upper part. The member is 8.5 m thick.

(11) Light gray dolomites, sandy near the base (6.5 m) and oolitic higher; the member is 14 m thick.

(12) Sandy dolomites, locally pelitomorphic; the member is 8 m thick.

In total, the Adargai Formation is 110 m thick in this section. Southeastward, its thickness increases up to 180 m (Fig. 3). Individual sections of the formation are well correlative to each other (Fig. 2, sections 7–12). Some lenticular interlayers in carbonate beds are enriched in P_2O_5 (more than 1 wt %).

According to determinations of M.A. Semikhatov, stromatolites of the Adargai Formation are represented by *Omachtenia omachtensis* Nuzhn. and *Stratifera omachtella* (in coll.). These morphotypes are widespread in carbonate rocks of the Gonam, Ennin, and Omakhta formations. They occur as well in the upper Kotuikan and lower Yusmastakh formations of the Anabar Uplift and are known from the Mac Arthur Formation of northern Australia and from Tsipanda Formation of the Maya River basin (Semikhatov and Serebryakov, 1983; Knoll and Semikhatov, 1998). In the light of current understanding, these are abiogenous structures, which originated in particular settings of carbonate accumulation within the time range from the Late Karelian to Middle Riphean.

Uchur Group

The currently accepted stratigraphic range and structure of the Uchur Group that includes the Gonam, Omakhta, and Ennin formations were established by scientists from the Geological Institute, Russian Academy of Sciences (Komar *et al.*, 1977; Semikhatov and Serebryakov, 1983). The original term "Uchur Formation" (group, system) was introduced by Yarmolyuk (1946, 1956). In the subsequent scheme (Nuzhnov and Yarmolyuk, 1959; Nuzhnov, 1967), the group was accepted as consisting of the Gonam and Omakhta formations, and the Ennin Formation was included as terminal unit in the group later on (Komar *et al.*, 1977). In the unified regional stratigraphic scheme of the Uchur–Maya region that was authorized not long ago (*Resheniya...*, 1994), the Uchur Group also includes the Birindya Formation, and this decision was misleading, as it is evident from data presented above. We did not study the Omakhta and Ennin formations, and they are missing from subsequent considerations.

Gonam Formation

Z.G. Ushakova and Yu.K. Dzevanovskii distinguished the Gonam Formation in 1947. Its stratotype is located at the right bank of the Uchur River, 15 km downstream off the Gonam River mouth (Semikhatov and Serebryakov, 1983) and includes five members. Four lower members (up to 90 m thick in total) are composed of red quartz–feldspar sandstones intercalated with siltstone and dolomite interlayers irregularly distributed throughout this interval of the section. The upper member (100–110 m thick) consists exclusively of similar inequigranular sandstones. The basal conglomerate bed of the stratotype rests on the gneissic basement, and 90 km southeastward, basal deposits of the Gonam Formation overlie different horizons of the Uyan Group (Fig. 1).

In basal conglomerate beds, pebbles and boulders are composed of quartz, quartzite, light gray sandstone, trachyrhyolite, metabasalt, red granite, granite gneiss, and brick-red rocks exemplifying weathering crust. In the Munaly, Adargai, and Givun river basins, these beds also include pebbles of dolomite and oncolitic or dolomitic sandstones resembling rocks of the Adargai Formation (Figs. 4, 5). In places, e.g., in the Medvezh'ya and Zoryanka river basins at the right side of the Uchur River (Fig. 2, section 4), the Gonam Formation overlies the red weathering crust that originated above crystalline schists. Rocks of the crust are hard, exhibiting occasional vesicles and resembling shale. They represent aggregate of hydrogoethite, hydromica, and other clay minerals that represent matrix for disseminated quartz, feldspar, and chloritized biotite grains. Vesicles are filled with secondary quartz, carbonate, and green hydromica.

We studied the representative section of the Gonam Formation at the right bank of the Munaly River, where

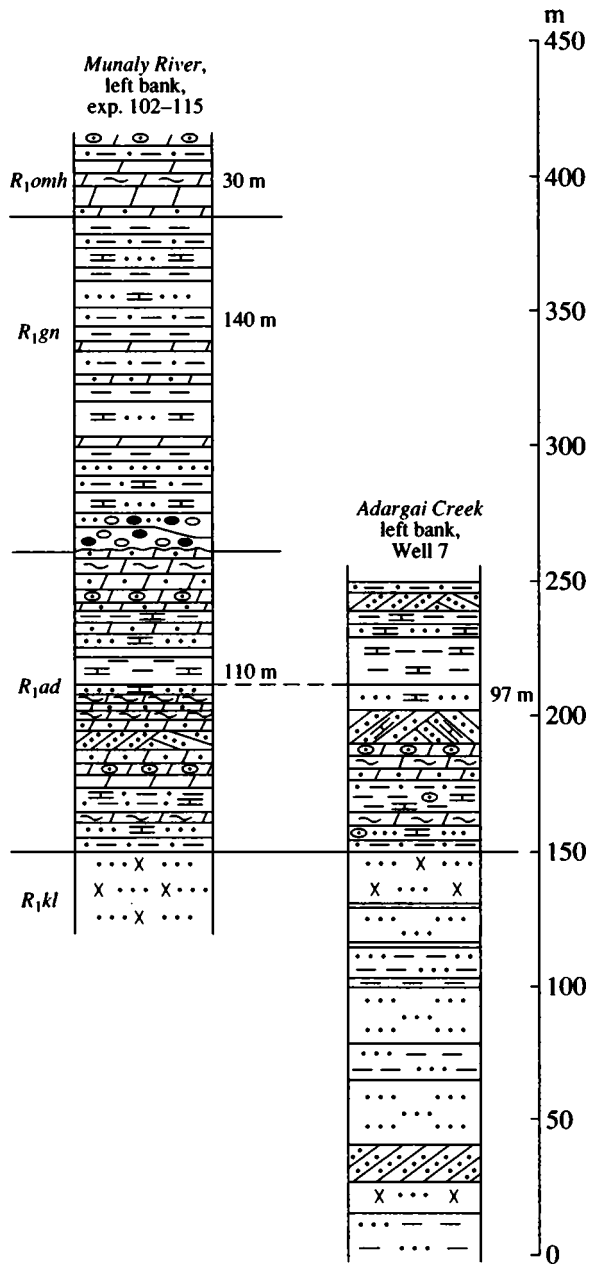

Fig. 5. Lithostratigraphy of the Adargai Formation, left-bank area of the Uyan River (symbols as in Fig. 2).

the Adargai Formation is overlain by the following rock succession (Fig. 5):

(1) Cherry-red conglomerate with boulders and pebbles (1–5 to 10–15 cm in diameter) of quartz, quartzite, silicified rocks, sandstones, red granite and granite gneisses, sandy or ripple-laminated algal dolomites, and brick-red rocks of weathering crust; the predominantly basal, slightly ferruginate cement of the rock is of the chlorite–hydromica or quartz–feldspar–dolomite composition. Local dark green stains characterize areas, where chlorite and hydromica are concentrated. The bed is 9.5 m thick.

(2) Cherry-red polymictic gravelstone; the bed is 4.5 m thick.

(3) Sandstones, coarse-grained, enclosing interlayers (up to 0.4 m thick) of pinkish gray sandy or pelitomorphic dolomite in the lower part and cherry-red to dark brown oligomictic fine- or medium-grained in the upper one; the member is 9.5 m thick.

(4) Brown-red bedded feldspar–quartz silty sandstone with interlayers of orange- or pink-red sandy and pelitomorphic dolomites; ferruginate cements of the rock is of the sericite–quartz–feldspar composition with dolomite admixture; the bed is 6.5 m thick.

(5) Dark red bedded fine-grained sandstone of the feldspar–quartz composition; the rock encloses laminae (up to 1–2.5 cm thick) of brown-red siltstone. The ferruginate cement is of the sericite–quartz–feldspar composition. The bed is 6.5 m thick.

(6) Light cherry-red to brown siltstone with ferruginate clay–feldspar–quartz cement; the bed is 6.5 m thick.

(7) Pink- to orange-gray pelitomorphic dolomite; the bed is 5 m thick.

(8) Thick-bedded fine- to medium-grained feldspar–quartz sandstone beds and intercalated dark cherry-red siltstones and silty sandstones; cement is of the dolomite–feldspar–quartz composition. The member is 15 m thick.

(9) Brown to cherry-red fine-laminated siltstone; the bed is 9 m thick.

(10) Pink- to yellow-gray sandy dolomite with siltstone laminae (up to 1 cm thick); the bed is 2 m thick.

(11) Dark red to brown feldspar–quartz silty sandstone enclosing thin interlayers (0.5–1.5 m thick) of fine-grained sandstone; the ferruginate cement of the rocks is of the clay–feldspar–quartz composition with dolomite admixture. The member is 11 m thick.

(12) Yellowish to light gray banded pelitomorphic dolomite with siltstone and fine-grained sandstone laminae (up to 1–2 cm thick); the bed is 3.5 m thick.

(13) Dark cherry-red siltstone with intercalations of silty sandstone cemented by clay–sericite–feldspar–quartz material; the bed is 6 m thick.

(14) Brown- to cherry-red bedded silty sandstone cemented by clay–feldspar–quartz material and enclosing thin interbeds (up to 10 cm thick) of reddish brown fine-grained feldspar-quartz sandstone; the bed is 6.5 m thick.

(15) Reddish brown fine-grained feldspar-quartz sandstones with interlayers (up to 10 cm thick) of silty sandstones cemented by clay–feldspar–quartz material; the bed is 11.5 m thick.

(16) Dark cherry-red fine-bedded siltstone with slightly ferruginate clay–quartz–feldspar–dolomite matrix; the bed is 6 m thick.

(17) Reddish brown fine-grained feldspar–quartz sandstone with laminae (up 1–2 cm thick) of cherry-red siltstone and yellowish gray dolomite; the bed is 8 m thick.

(18) Cherry- to pink-red fine-bedded silty sandstone with siltstone laminae (up to 1–2.5 cm thick); the bed is 6 m thick.

(19) Dark red fine-bedded siltstone; the bed is 7 m thick.

The Gonam Formation is 140 m thick in this section and concordantly underlies gray sandy dolomites of the Omakhta Formation. This and other studied sections are correlative to each other and with the formation stratotype (Fig. 2, sections 1–9). Individual distinctions depend on proportions of beds of that or other lithology; some of the beds are pinching out and displaying grain-size variations. Particular sections show presence of glauconite-bearing sandstones (Fig. 2). We cannot share the idea that considerable facies variations are characteristic of the Gonam Formation (Basharin, 1967; Komar *et al.*, 1977; Semikhatov and Serebryakov, 1983) because, as we established, the former erroneous practice was to include different beds of the Lower Riphean Konkula, Adargai, and even Birindya formations in the unit under discussion.

Dolomites of the Gonam Formation enclose stromatolites *Omachtenia omachtensis* Nuzhn., *O. utschurica* Nuzhn., *Stratifera omachtella* (in coll.) and microphytoliths *Globosites magnus* Nar., *Osagia testace* Nar., *O.* aff. *libidinosa* Z. Zhur., *Radiosus tenebricus* Z. Zhur., *R. ovale* (Volog. et Drosd.), and *Vesicularites rotunus* Z. Zhur. (Semikhatov and Serebryakov, 1983; *Resheniya...*, 1994). The K–Ar ages of glauconites from the Gonam Formation range from 1450 to 1550 Ma (Semikhatov and Serebryakov, 1983).

RELATIONSHIPS BETWEEN THE KONKULA AND GONAM FORMATIONS

Interpretation of the Konkula Formation range, stratigraphic position, and lithology changed several times since the moment of its recognition. In last decades, some researchers considered it as individualized unit predating the Gonam Formation (Alekseev *et al.*, 1962; Nuzhnov, 1967; Nevolin *et al.*, 1978), whereas others interpreted this unit as local lithofacies of the latter (Basharin, 1967; Komar *et al.*, 1977; Semikhatov and Serebryakov, 1983). The independent stratigraphic status of the Konkula Formation was questioned, when Nuzhnov mistakenly suggested that its stratotype could exemplify not this but the older Toporikan Formation (see in Mokshantsev *et al.*, 1968).

The section of principal significance that elucidates relationships between the Konkula and Gonam formation is situated at the right bank of the Uchur River opposite the Givun Creek mouth. The rock succession overlying here the crystalline basement (Fig. 2, section 5) is described below.

Konkula Formation

(1) Pinkish gray small-pebbled conglomerate grading toward the base into coarse psephite with large pebbles and rare boulders; quartz pebbles are dominant and those of quartzite, quartzite-like sandstone, cherty rocks, red granite gneisses, gneisses, and argillites (weathering crust rocks) are much less abundant. In the gravely cementing mass ferruginate sometimes, feldspar and quartz clasts are set in the kaolin–quartz matrix. Kaolinization is characteristic of the whole rock volume. The bed is 10.5 m thick.

(2) Mottled small-pebbled quartz gravelstone; coloration varies from pinkish gray to dirty orange depending, as we think, on the kaolinization degree. Rare subangular and poorly sorted pebbles consist of quartz, quartzite-like sandstone, quartzite, and red granite gneisses. The inequigranular rock matrix consists of feldspar and quartz clasts cemented by kaolin–quartz and hydromica–clay, sometime ferruginate mass. The bed is 12.5 m thick.

(3) Pinkish gray feldspar–quartz sandstones with "floating" quartz pebbles; rocks are coarse-grained, enclosing gravely interbeds (up to 10–30 cm thick) near the base and fine-grained, bearing gypsum pseudomorphs (up to 1 cm across) in the upper interval. Cementing mass consists of quartz, kaolin, hydromica, and other clay minerals. The member is 18.5 m thick.

(4) Pink to red medium-grained feldspar–quartz oligomictic sandstone displaying cross lamination and enclosing rare lenticular intercalations (up to 1–2 cm thick) of red siltstone in the upper interval; the bed is 6.5 m thick.

(5) Brown to red-brown or pink medium-grained sandstone with rare "floating" quartz pebbles and feldspar–quartz matrix; the bed is 7.5 m thick.

(6) White fine-grained quartz sandstone with regenerated quartz cement; the bed is 5 m thick.

(7) Pink feldspar-quartz and quartz cross-bedded fine-grained sandstones with lenticular interactions of siltstone and shale (up to 1 cm thick); the bed is 8.5 m thick.

(8) Medium- to fine-grained feldspar–quartz sandstone with gravely admixture; kaolinization is a characteristic feature of the bed that is 7 m thick.

(9) Light gray fine-grained feldspar–quartz sandstone grading upward into cherry-red siltstone and shale; these upper rocks presumably represent the weathering crust up to 0.5 m thick. The member is 4 m thick in total.

Gonam Formation

(10) Red-brown to cherry-red conglomerate grading upward into gravelstone; round to flattened pebbles of rocks are composed of red granite, gneiss, quartz, trachyrhyolite, and basalt. Also characteristic are rare subangular inclusions (0.5–1 to 10–15 cm across) of dark cherry-red argillite (weathering crust) derived from underlying Bed 9. Ferruginate cement in gravelstones and coarse-grained sandstones is of quartz–feldspar composition with dolomitic admixture. The member is 12.5 m thick.

(11) Brick-red bedded quartz-feldspar sandstone with coarse-grained interlayers; the rock is cemented by ferruginate–dolomitic hydromica–quartz–feldspar matrix. The member is 11 m thick.

(12) Frequently alternating cherry-red siltstone with dolomitic cement and gray pelitomorphic dolomites; the member is 13 m thick.

(13) Red medium- to fine-grained feldspar–quartz sandstone; the rock is ferruginate and dolomitic, enclosing laminae of dolomitic siltstone. The bed is 10 m thick.

(14) Beds (0.3–0.6 m thick) of brown-red siltstone and orange dolomitic fine-grained sandstone of feldspar–quartz composition alternating with rare interlayers of pelitomorphic dolomite; the member is 8.5 m thick.

(15) Alternating beds (1 m thick) of pelitomorphic dolomite and brown siltstone; the member is 9 m thick.

(16) Cherry-red fine- to medium-grained oligomictic sandstone locally cross-bedded and displaying ripple marks; the bed is 5 m thick.

(17) Cherry-red fine-grained and dolomitic feldspar–quartz sandstone with thin intercalations (10 cm thick) of brown-red dolomitic siltstone; the bed is 5.5 m thick.

(18) Cherry-red coarse- to medium-grained feldspar–quartz sandstone with ripple marks; the bed is 5 m thick.

(19) Cherry-red fine-grained feldspar–quartz dolomitic sandstone bearing glauconite and enclosing laminae of siltstone and stromatolitic dolomite; the bed is 10.5 m thick.

(20) Cherry-red laminated silty sandstone with rare siltstone lenticles; the bed is 8 m thick.

(21) Light gray pelitomorphic dolomite with rare interlayers of red feldspar–quartz sandstone and siltstone; the bed is 7 m thick.

(22) Dark red and cherry-red laminated siltstone with ferruginate clay–hydromica cement; the bed is 15 m thick.

(23) Red and brown bedded medium- to fine-grained sandstones of feldspar–quartz composition; rocks are cemented by hydromica–feldspar–quartz matrix. The member is 15.5 m thick.

(24) Alternating stromatolitic and pelitomorphic dolomites; the member is 9 m thick.

(25) Pinkish brown dolomitic medium- to fine-grained sandstone of feldspar–quartz composition; the bed is 9.5 m thick.

(26) Cherry-red to brown laminated siltstone; the bed is 11 m thick.

Average compositions of basaltic rocks from the Ulkachan and Birindya formations

Components	Trachybasalts of the Ulkachan Formation (44 analyses)	Olivine basalts of the Birindya Formation (18 analyses)
SiO_2	50.2	45.44
TiO_2	2.50	1.57
Al_2O_3	14.95	16.32
Fe_2O_3	7.34	8.29
FeO	6.28	4.03
MnO	0.17	0.14
MgO	4.60	5.43
CaO	5.50	8.36
Na_2O	3.44	3.42
K_2O	2.09	1.80
P_2O_5	0.48	0.32
SO_3	0.05	0.02
CO_2	0.75	0.87
H_2O^-	2.90	2.39
Sr $n10^{-4}$%	271	491
Rb $n10^{-4}$%	44	8
Pb $n10^{-4}$%	19	5
Y $n10^{-4}$%	32	10
Nb $n10^{-4}$%	18	7
Zr $n10^{-4}$%	321	145
Th $n10^{-4}$%	5	3
U $n10^{-4}$%	2	2

The last bed is conformably overlain by dolomites of the Omakhta Formation. The Givun section has been recurrently studied (Basharin, 1967; Nuzhnov, 1967: Semikhatov and Serebryakov, 1983) but available descriptions slightly differ from each other, because this section is concealed in places by taluses. Our description is more detailed, as we took into consideration the results of prospect excavations, aerial photographs deciphering, and radiometric investigations. We attribute beds 1–9, which are 80 m thick in total, to the Konkula Formation and overlying beds to the Gonam Formation that is 165 m thick (beds 10–26) in the described section. Like in the Munaly Creek section, basal conglomerates of the Gonam Formation enclose here pebbles of light gray oncolitic dolomites characteristic of the Adargai Formation. As we believe, the latter was completely eroded during the pre-Gonam break in sedimentation.

To a certain extent, the Konkula beds resemble in lithology the lower horizons of the Gonam Formation, and this was considered in previous works as an argument in favor of attributing them to the latter. As we established, however, these are not lithological analogues. The Konkula Formation is composed predominantly of rudaceous deposits, i.e., of coarse-, sometimes medium-grained sandstones that enclose "floating" pebbles and associate with conglomerates and gravelstones. In contrast, main rock types of the Gonam Formation are fine- to medium-grained sandstones, siltstones, and shales, which are intercalated with dolomite interlayers untypical of the Konkula Formation. The feldspar content in sandstones of the Gonam Formation is nearly twice higher (30–40%) than in the Konkula beds. In addition, matrix of the former reveals dolomitic admixture, whereas the regenerated cement of the latter is of the quartz or feldspar–quartz composition with occasional admixture of kaolin or barite. It is clear therefore that accumulation environments of the Gonam Formation differed from those of the Uyan Group. Features suggesting this are the halite pseudomorphs and glauconite grains present in rocks of the Gonam Formation, fine rhythmic alternation of terrigenous and carbonate sediments, the lesser grain size of clastic components (higher abundance of siltstone and shale interlayers), and frequent dolomitic admixture in the rock matrix.

RELATIONSHIPS BETWEEN ULKAN AND UYAN GROUPS AND LOWER BOUNDARY OF THE RIPHEAN

The Uchur River region is one of few regions in the world, where it is possible to observe how the Lower Riphean deposits overlie the upper Lower Proterozoic rocks (Semikhatov and Serebryakov, 1983). We observed relationships between the Ulkan and Uyan groups in several places. In the Ulkan depression (the Toporikan, Ulkan, and Birindya river basins), basal beds of the Uyan Group overlie older deposits with angular unconformity and truncate tectonic structures and subvolcanic bodies. At the boundary between two groups under consideration, there is a continuous horizon of weathering crust that originated above acid volcanics of the Elgete Formation and metamorphic rocks of the Aldan shield. In addition, basal conglomerates of the Uyan Group include pebbles of volcanic rocks characteristic of the Elgete and Ulkachan formations or of correlative subvolcanic rocks. The presented geological map (Fig. 1) also elucidates relationships between the Ulkan and Uyan groups, showing how the latter overlies different horizons of the former and overlaps considerable areas of the crystalline basement. As one can see, the western boundary of elongated Ulkan centrocline is sharply truncated by the superimposed Uchur depression. Both structures plunging in opposite directions have been formed under different tectonic conditions and are filled with deposits of contrast lithological composition (Semikhatov and Serebryakov, 1983).

Volcanic rocks of the Uyan and Ulkan groups are dissimilar in composition. It was formerly accepted (Basharin, 1967; Nuzhnov, 1967; Konstantinovskii, 1974; Komar *et al.*, 1977; Nevolin *et al.*, 1978; Semikhatov, 1978; Semikhatov and Serebryakov, 1983) that

the Birindya Formation of the former includes acid lava flows, and that the granitoid magmatism in the Ulkan depression ceased prior to the Uchur time (prior to deposition of the Gonam Formation). We established however that the Birindya Formation includes only olivine basalts and lacks intercalations of acid volcanics. According to chemical composition these are olivine and leucocratic basalts of the K-Na series with comparatively low TiO_2 but rather high Fe_2O_3 content (see the table). As compared to basalts of the Ulkachan Formation of the Ulkan Group, they are depleted in SiO_2, TiO_2, Fe, Mn, K, and Rb, being simultaneously enriched in MgO, CaO, Al_2O_3, and Sr. The high specific weight of rocks and low oxidation state of iron allow us to attribute these lavas to continental dolerites. At the same time, the abundance rates of Al_2O_3, Fe_2O_3, FeO, and K_2O differ these rocks from their possible counterparts in the Siberian trap formation (Efremova and Stafeev, 1985). The rocks under discussion also reveal the superclarke concentrations of Be, Th, and U, being relatively depleted in Co, Ni, and Zn. Their structures vary from ophitic to microlitic, and occasionally to intersertal. Plagioclase (0–30%), olivine (1–5%), clino- and orthopyroxene (0–5%) occur as phenocrysts, and magnetite, apatite, spinel, and titanomagnetite represent accessory minerals.

Melanocratic silica-saturated trachybasalts of the Ulkachan Formation are moderately rich in aluminum but depleted in alkalies, calcium, and magnesium. They resemble rocks of the continental trachybasalt formation but differ from platform-type basalts, in comparison with which they have higher contents of titanium, magnesium, alkalies and lower concentrations of aluminum, calcium, and ferrous iron (Efremova and Stafeev, 1985). Tin, zirconium, and beryllium concentrations in these rocks are above the clarke values. Plagioclase (0–30%), augite (0–15%), orthopyroxene (single crystals), and titanomagnetite are characteristic phenocryst minerals, and ilmenite (up to 10%), leucoxene (0–5%), and apatite represent the accessory group.

All the data discussed above clarify position of the lower Riphean boundary in the Uchur River region. Formerly, it was placed at the base of the Gonam Formation of the Uchur Group, because the Birindya Formation was thought to be enclosing acid volcanic rocks coeval to the pre-Uchur (pre-Gonam) granitoid magmatism in the Ulkan graben. Accordingly, the Birindya Formation was considered as a part of volcano-sedimentary succession accumulated in the graben prior to deposition of the Gonam Formation that was accepted for the lowermost subdivision of the Riphean (Nuzhnov, 1967; Konstantinovskii, 1974; Komar *et al.*, 1977; Nevolin *et al.*, 1978; Semikhatov and Serebryakov, 1983). The new data obtained show however that we should displace the lower Riphean boundary downward to the level separating the Uyan and Ulkan groups, because it marks the principal turning point in the geological history of the Uchur River region. This level remarkable in geological aspect is close in age to the Riphean base that is accepted to be 1650 ± 50 Ma old in the Precambrian stratigraphic scale of Russia (Semikhatov *et al.*, 1991).

CONCLUSION

Summarizing the results of this study, we can state the following:

(1) The Lower Riphean rock succession in the Uchur River region consists of the Uyan and Uchur groups, the former divisible into the Birindya, Konkula, and Adargai formations and the latter comprising the Gonam, Omakhta, and Ennin formations.

(2) As is established for the first time, the Uyan Group rests with a considerable hiatus and discordance on different horizons of the Upper Karelian Ulkan group or on metamorphic rocks of the Aldan shield basement, overlying the weathering crust that originated on their surface.

(3) The Konkula Formation is not a local lithofacies of the Gonam Formation of the Uchur Group, as it was suggested before. This is an individual stratigraphic unit of the Lower Riphean in the Uchur–Maya region.

(4) The newly recognized Adargai Formation crowning the Uyan Group succession is composed of carbonate–terrigenous sediments.

(5) The Gonam Formation of the Uchur Group rests with a hiatus and discordance on deposits of the Uyan Group (the Konkula Formation included). Its basal beds bear pebbles of stromatolitic dolomites typical of the underlying Adargai Formation of the Uyan Group.

(6) Boundary between the Ulkan and Uyan groups is coeval to the time of considerable tectonic restructuring in the study region and separates here terminal stages of the Late Karelian acid and alkaline magmatism (the Ulkan intrusive complex) from the incipient stage of the platform cover accumulation. It marks the principal turning point in the geological history of the Uchur River region. This level remarkable in geological aspect is close in age to the Riphean base that is accepted to be 1650 ± 50 Ma old in the Precambrian stratigraphic scale of Russia (Semikhatov *et al.*, 1991). In general, our results demonstrate that the Uchur–Maya region is of prime significance for a deeper insight into the Lower Riphean stratigraphy.

ACKNOWLEDGMENTS

We are grateful to M.A. Semikhatov and V.V. Khomentovskii for valuable advices and critical remarks, which helped us to improve the manuscript.

Reviewers M.A. Semikhatov
and V.V. Khomentovskii

REFERENCES

Alekseev, V.R., Baranova, I.S., Gamaleya, Yu.N., *et al.*, New Data on Stratigraphy of Sinian Deposits in the Southeastern Margin of the Aldan Shield, *Soveshchanie po stratigrafii pozdnego dokembriya Sibiri i Dal'nego Vostoka* (Conference on the Upper Precambrian Stratigraphy in Siberia and the Far East), Novosibirsk, 1962, pp. 59–61.

Basharin, A.K., *Vostochno-Verkhoyanskaya epicratonnaya geosinklinal'* (The East Verkhoyansk Epicontinental Geosyncline), Moscow: Nauka, 1967.

Efremova, S.V. and Stafeev, K.G., *Petrokhimicheskie metody issledovaniya porod: spravochnoe posobie* (Petrochemical Methods of Rocks' Investigations: Reference Manual), Moscow: Nedra, 1985.

Gamaleya, Yu.N., Formation Analysis and Evolution of the Southeastern Siberian Platform during the Precambrian, *Geotektonika*, 1968, no. 6, pp. 34–45.

Gamaleya, Yu.N., Losev, A.G., and Popov, M. Ya., On Oldest Deposits of Sedimentary Cover in the Southeastern Siberian Platform, *Sov. Geol.*, 1969, no. 4, pp. 137–144.

Gur'yanov, V.A. and Karsakov, L.P., The Lower Precambrian Stratigraphy of the Southeastern Siberian Platform, in *Stratigrafiya nizhnego dokembriya Dal'nego Vostoka* (The Lower Precambrian Stratigraphy of the Far East), Vladivostok: DVO AN SSSR, 1990, pp. 18–30.

Knoll, A.H. and Semikhatov, M.A., The Genesis and Time Distribution of Two Distinctive Proterozoic Stromatolite Microstructures, *Palaios*, 1998, vol. 13, pp. 408–422.

Komar, V.A., Semikhatov, M.A., and Serebryakov, S.N., A Stratigraphic Scale for Riphean Deposits in the Uchur–Maya Region, *Sov. Geol.*, 1977, no. 8, pp. 32–49.

Konstantinovskii, A.A., The Middle Proterozoic Ulkan and Bilyakchan Grabens in the Southeastern Siberian Platform, *Izv. Akad. Nauk SSSR, Ser. Geol.*, 1974, no. 4, pp. 72–84.

Larin, A.M., Amelin, Yu.V., Neymark, L.A., and Krimsky, R.Sh., The Origin of the 1.73 Ga Anorogenic Ulkan Volcano-Plutonic Complex, Siberian Platform, Russia: Inferences from Geochronological, Geochemical and Nd–Sr–Pb Isotopic Data, *Anais. Acad. Brasil. Ciênei.*, 1997, vol. 69, no. 3, pp. 295–312.

Mokshantsev, K.B., Nuzhnov, S.B., and Timofeev, V.I., The Lower Boundary of the Riphean and Stratigraphic Position of the Konkula Formation in the Southern Aldan Shield, in *Tektonika, stratigrafiya i litologiya osadochnykh formatsii Yakutii* (Tectonics, Stratigraphy, and Lithology of Sedimentary Formations in Yakutia), Yakutsk: Yakut. Kn. Izd., 1968, pp. 86–90.

Nevolin, B.S., Potapov, S.V., and Stavtsev, A.L., The Upper Proterozoic (Riphean) and Lower Cambrian of the Southeastern Margin of the Siberian Platform, in *Novoe v stratigrafii i paleontologii posdnego dokembriya vostochnykh i severnykh raionov Sibiri* (New Data on the Upper Precambrian stratigraphy and Paleontology in Eastern and Northern Areas of Siberia), Novosibirsk: Sib. Otd. Akad. Nauk SSSR, 1978, pp. 21–63.

Nuzhnov, S.V., *Rifeiskie otlozheniya yugo-vostoka Sibirskoi platformy* (Riphean Deposits in the southeast of the Siberian Platform), Moscow: Nauka, 1967.

Nuzhnov, S.V. and Yarmolyuk, V.A., The Late Precambrian in the Southeastern Margin of the Siberian Platform, *Sov. Geol.*, 1959, no. 7, pp. 21–31.

Resheniya Chetvertogo mezhvedomstvennogo regional'nogo stratigraficheskogo soveshchaniya po dokembriyu i fanerozoyu yuga Dal'nego Vostoka i Vostochnogo Zabaikal'ya (Resolutions of the Fourth Interdepartmental Regional Stratigraphic Conference on the Precambrian and Phanerozoic in southern Areas of the Far East and Eastern Transbaikal Region), Khabarovsk: KhGGGP, 1994.

Semikhatov, M.A., *Stratigrafiya i geokhronologiya proterozoya* (Stratigraphy and Geochronology of the Proterozoic), Moscow: Nauka, 1974.

Semikhatov, M.A., Relationships between the Lower Riphean and Underlying Deposits in Continental Reference Sections), in *The Lower Boundary of the Riphean and Stromatolites of the Aphebian*, Moscow: Nauka, 1978, pp. 9–34.

Semikhatov, M.A. and Serebryakov, S.N., *Sibirskii gipostratotip rifeya* (The Siberian Hypostratotype of the Riphean), Moscow: Nauka, 1983.

Semikhatov, M.A., Shurkin, K.A., Aksenov, E.I., *et al.*, New Precambrian Stratigraphic Scale in the USSR), *Izv. Akad. Nauk SSSR, Ser. Geol.*, 1991, no. 12, pp. 3–13.

Shenfil', V.Yu., *Pozdnii dokembrii Sibirskoi platformy* (The Late Precambrian of the Siberian Platform), Novosibirsk: Nauka, 1991.

Stolyar, M.Ya., *Geologiya i zolotonosnost' Uchuro-Chul'binskogo raiona Yakutskoi ASSR* (Geology and Gold Mineralization in the Uchur– Chul'ba Region of the Yakut ASSR), Moscow: Gorno-Geol. Izd., 1934.

Yarmolyuk, V.A., The Proterozoic of Eastern Areas of the Aldan Plate, in *Materialy po geologii i poleznym iskopaemym Dal'nego Vostoka* (Data on Geology and Mineral Resources of the Far East), Khabarovsk: Gosgeoltekhizdat, 1946, pp. 121–129.

Yarmolyuk, V.A., A Stratigraphic Scheme for the Precambrian and Cambrian of the Uchur–Maya Region, *Soveshchanie po razrabotke unifitsirivannykh stratigraficheskikh skhem Dal'nego Vostoka* (Conference on the Unified Stratigraphic Schemes for the Far East), Khabarovsk: Gosgeoltekhizdat, 1956, pp. 9–13.

Zabrodin, V.E., On Early Stages of Sedimentary Cover Evolution in the Southeastern Siberian Platform, *Izv. Akad. Nauk SSSR, Ser. Geol.*, 1966, no. 3, pp. 121–125.

Zlenko, N.D., Nuzhnov, S.V., and Shpak, N.S., The Late Precambrian Volcanism and Stratigraphy of the Southeastern Siberian Platform, in *Stratigrafiya pozdnego dokembriya i kembriya* (Stratigraphy of the Upper Precambrian and Cambrian), Moscow: Akad. Nauk. SSSR, 1960, pp. 64–70.

Stratigraphy and Geological Correlation, Vol. 10, No. 1, 2002, pp. 57–68. Translated from Stratigrafiya. Geologicheskaya Korrelyatsiya, Vol. 10, No. 1, 2002, pp. 62–74.
Original Russian Text Copyright © 2002 by Mamedov.
English Translation Copyright © 2002 by MAIK "Nauka/Interperiodica" (Russia).

The Famennian Stage of the Southern Transcaucasia

A. B. Mamedov

Institute of Geology, Azerbaijani Academy of Sciences, pr. Guseina Dzhavida 29a, Baku, 370143 Azerbaijan

Received December 10, 1999

Abstract—The Famennian sediments of the southern Transcaucasia are described. The Noravank and Ertich formations are referred to the lower substage of the Famennian, the Kadrli and Shamamidzor formations, to the middle one, and the Gortun and Arshakiakhbyur formations, to the upper substage. The Devonian-Carboniferous boundary was placed at the base of the Gerankalasy Formation in accord with resolution of the ISC Commission on the Devonian and Carboniferous (Minsk, 1986). All groups of organic remains encountered in the Famennian sediments of the Transcaucasia are analyzed.

Key words: Famennian, stratigraphy, brachiopods, conodonts, algae, southern Transcaucasia.

A complete succession of the Famennian sediments represented by marine carbonate and terrigenous facies, occurs in the southern Transcaucasia within the Nakhichevan' Autonomous Republic of Azerbaijan and the adjacent part of Armenia. The sections are nowadays thoroughly studied, and the detailed stratigraphic scheme was developed for them.

Frech and Arthaber (1900), Rzhonsnitskaya (1948, 1964), Abramyan (1957, 1964), Mamedov (1962), Arakelyan (1964), and others suggested subdivision schemes for Famennian sediments of the southern Transcaucasia mostly in accord with distribution of brachiopods.

Abramyan distinguished the succession of beds (horizons) with particular brachiopod assemblages and suggested the most detailed biostratigraphic subdivision of these deposits. Arakelyan elaborated nomenclature of regional stratigraphic units (formations). Subsequently, his scheme was revised with due regard to composition of brachiopod assemblages and brachiopod generic names, and the faunal beds were ranked as zones (Aristov *et al.*, 1979; Grechishnikova *et al.*, 1982, 1988; Mamedov, 1980, 1992; Rzhonsnitskaya *et al.*, 1984; Rzhonsnitskaya and Mamedov, 1988; Mamedov and Rzhonsnitskaya, 1985).

Recently, I studied all sedimentary layers that represent the Famennian regional stratigraphic units and brachiopod zones in order to refine positions of their boundaries with regard to distribution of the following faunal groups: conodonts studied by V.A. Aristov and V.G. Khalymbadzha; corals identified by N.Ya. Spasskii; bivalve mollusks investigated by V.F. Kulikova; trilobites analyzed by Ya.N. Spasskii; foraminifers described by E.A. Reitlinger and N.B. Gibshman; and ostracodes studied by V.A. Chizhova.

According to the present-day regional scheme, sediments of the Famennian Stage of the Upper Devonian are subdivided into three substages and six local units: Noravank, Ertich, Kadrli, Shamamidzor, Gortun, and Arshakiakhbyur formations (see the table).

THE LOWER FAMENNIAN SUBSTAGE

The Noravank Formation (Arakelyan, 1964) is accepted in the range of the *Mesoplica meisteri* Zone. Its stratotype is situated within the Amagu-Gnishk anticline, exactly in the Gnishk River gorge below the Noravank Monastery. The lower boundary is defined by appearance of zonal index species in association with *Cyrtospirifer asiaticus* Brice (=*C. archiaci* Murchison, 1840 *sensu* Verneuil, 1845) and other species of the assemblage.

In addition to the type section, sediments of the Noravank Formation are exposed in the Ertich and Yaidzhi (parastratotype) sections and in the low reaches of the Bagarsykh-Deresi River.

The formation consists of light, often sugar-like quartzites and black to brownish black shales with intercalations of dark gray sandy limestones and light blue siltstones. The formation is 60 to 152 m thick. Its maximum thickness is recorded in the Yaidzhi parastratotype (Figs. 1 and 2) and the minimum one in the Bagarsykh-Deresi region, where this unit is incompletely exposed. In the Ertich section, the formation is 105 m thick.

Limestone interbeds commonly bear remains of brachiopods, foraminifers, conodonts, algae, and some other fossils.

Brachiopods of the Noravank Formation are represented by *Mesoplica tasadyrica* (Nal.), *M. meisteri* (Peetz), *M.* cf. *praelonga* (Sow.), *M. kayseri* Khalfin, *Ripidiorhynchus griasica* Nal., *Cyrtospirifer* ex gr. *verneuili* (Murch.), *C. asiaticus* Brice, *C.* ex gr. *wesgensis* Zeiba, *Tenticospirifer* cf. *tenticulum* (Vern. *sensu* Tien,

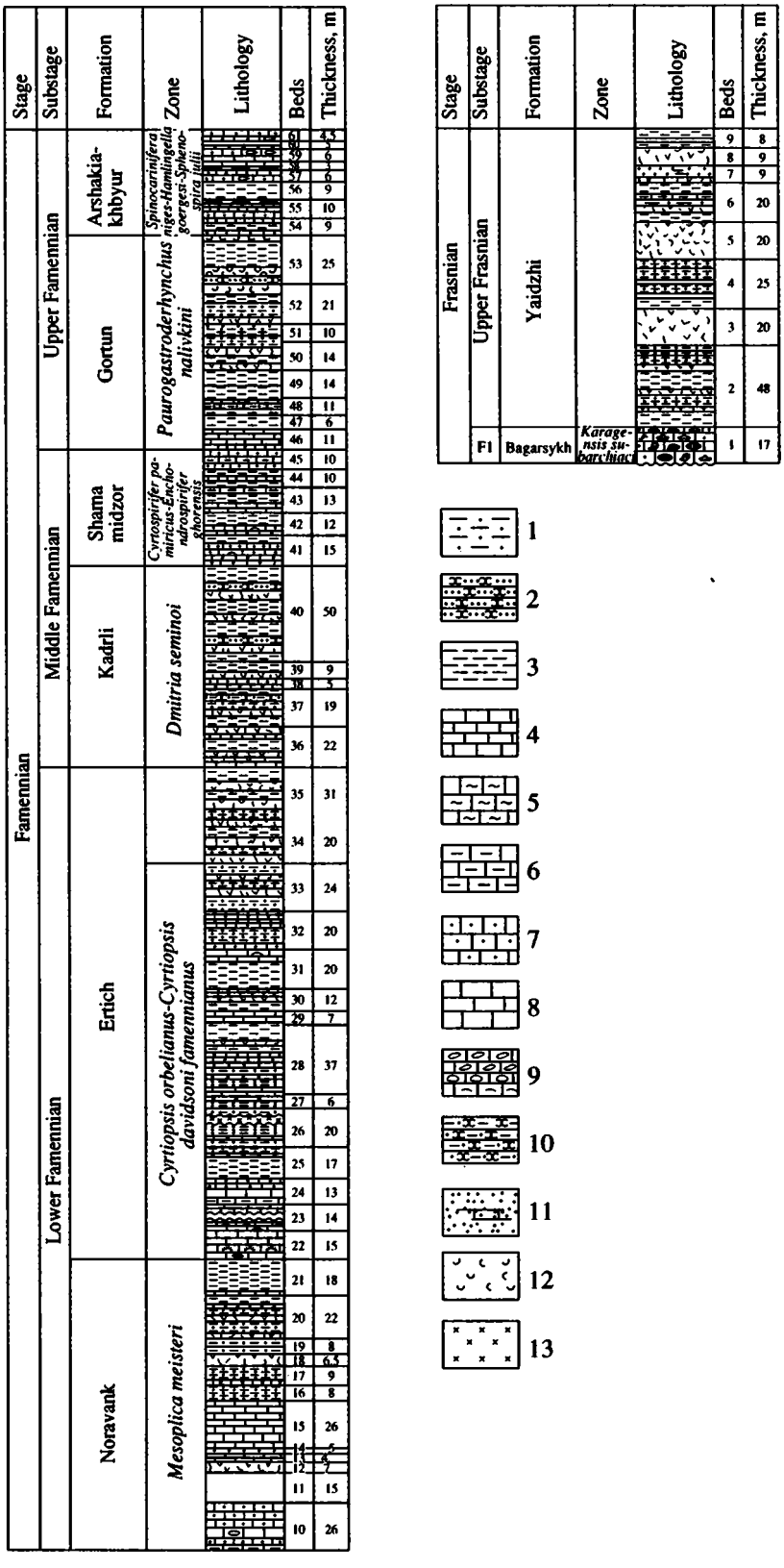

Fig. 1. The Upper Devonian section near the Ashagy Yaidzhi Village: (1) siltstones; (2) sandstones; (3) argillites; (4) limestones; (5) siliceous limestone; (6) clayey (lumpy) limestone; (7) sandy limestone; (8) biohermal limestone; (9) organogenic limestone; (10) silty sandstone; (11) calcareous sandstone; (12) quartzite; (13) intrusive rocks.

Subdivision of the Upper Devonian sediments of southern Transcaucasia, Nakhichevan' Autonomous Republic and southern Armenia (after A.B. Mamedov)

Standard stratigraphic scale of the Devonian proposed by SDS			Series	Stages	Substages	Formations (after Arakelyan, 1964; Abramyan, 1964; Mamedov, 1979, 1980, 1992; Mamedov and Rzhonsnitskaja, 1985)	Brachiopod zones (after Abramyan, 1957; Mamedov, 1962, 1980, 1983, 1992; with additions of Grechishnikova, 1979, 1982)	Conodont zones (after Aristov, 1979, 1982; Ovnatanova and Aristov, 1984)
Series	Stage	Standard conodont zones						
Upper	Famennian	*Protognathodus*	Upper	Famennian	upper	Arshakiakhbyur	*Spinocarinifera niger–Hamlingella goergesi–Sphenospira julii*	*Costatus*
		Unzoned						
		Costatus U M L						
		Styriacus U M L				Gortun	*Paurogastroderhunchus nalivkini*	*Styriacus*
		Velifer U M L			middle	Shamamidzor	*Cyrtospirifer pamiricus–Euchondrospirifer ghorensis*	*Velifer*
		Marginifa U M L				Kadrli	*Dmitria seminoi*	*Marginifera*
		Rhomboidea U M L						*Rhomboidea*
		Crepida U M L			lower	Ertich	*Cyrtiopsis orbelianus–Cyrtiopsis davidsoni famenniana*	*Crepida*
		Triangularis U M L				Noravank	*Mesoplica meisteri*	*Pal. triangularis*
	Frasnian	*Gigas* U M L		Frasnian	upper	Yaidzhi		*Gigas*
		Anc. triangularis						*Anc. triangularis*
		Unzoned						
		Asymmetricus U M L			lower	Bagarsykh	*Cyphoterhynchus koraghensis–Cyrtospirifer subarchiasi*	*Asymmetricus* Upper / Middle / Lower

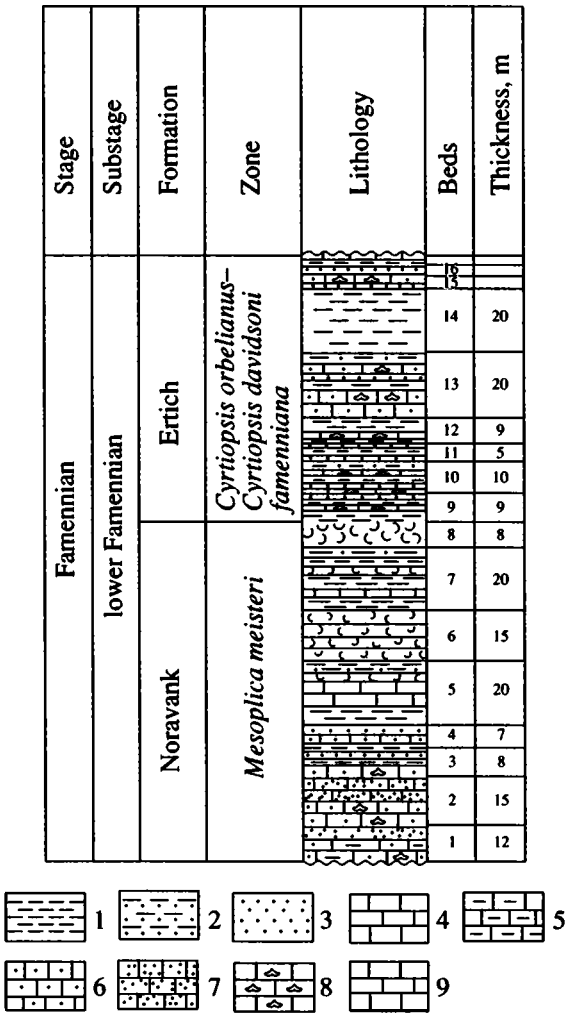

Fig. 2. The lower Famennian section near the former Ertich Village on the left bank of the Vostochnyi Arpachai River: (1) shale; (2) siltstone; (3) sand; (4) limestone; (5) clayey limestone; (6) sandy limestone; (7) detrital limestone; (8) organogenic limestone, mainly bearing brachiopods; (9) quartzite.

1938), and *Cyrtiopsis* sp. (cf. *C. intermedia* Grabau). Species *Mesoplica meisteri* (Peetz) is the guide fossil of the lower Famennian *meisteri* beds in Kazakhstan. Another form *M. tasadyrica* (Nal.) was described by Nalivkin (1937) from the so-called Tasadyr flinty limestones occupying the upper part of *meisteri* beds in central Kazakhstan. *M. praelonga praelonga* is of a wide distribution range and occurs either in the upper Famennian, or in transitional Devonian–Carboniferous (Etroeungtian) sediments. In the Rudnyi Altai, this form is typical of the Tarkhansk Formation. In Kazakhstan, it was encountered in the *sulcifera* Beds, and in England it was first described from the Pilton Beds. The form in question is also known from the Famennian sediments of the Urals, Central Asia, and Siberia. The rhynchonelloid *Ripidiorhynchus griasica* Nal. is an index species for the Elets Horizon (lower Famennian) of the Russian platform, though it first occurrence is confined to the Zadonsk Horizon.

The *Cyrtospirifer verneuili* (Murch.) type species was recorded in France in the upper Frasnian Ferques Limestone. In the Kuznetsk basin, this species is characteristic of the lower Famennian deposits. This is a form widespread across the whole Upper Devonian. *Cyrtospirifer asiaticus* Brice is one of the lower Famennian index species in many regions. In the central Russian platform, it occurs in the Zadonsk Horizon; it is known from the upper part of the *meisteri* Beds in Kazakhstan and from the lower Famennian in Afghanistan. *Tenticospirifer tenticulum* (Vern.) originated from the Buregi Beds (Frasnian) in the Il'men' Lake region, though different forms were described under this name. Biernat (1983) cited it from the Famennian of the Swietokrzyskie Mountains in Poland, and Tien (1938) identified it the Upper Devonian of South China.

Thus, almost all brachiopod species listed above indicate the early Famennian age of the Noravank Formation of Transcaucasia.

In addition to a series of new forms, V.G. Khalymbadzha identified in sediments of the Noravank Formation the following conodont species: *Icriodus cornutus* Sannem., *I. alternatus* (Br. et Mehl), *I. subterminus* Young., *I.* sp. (aff. *I. subterminus* Young.), *Polygnathus* aff. *decorosus* Stauffer, *P. streeli* Dressen *et al.*, *P. szulcewskii* Matyia, *P. guttulus* Khalym. *et al.*, *P. procerus* Br. et Mehl, and *P.* sp. that is likely a juvenile specimen of *P. procerus* Br. et Mehl. The typical *P. decorosus* Stauffer was found in the Frasnian Chrakhana Formation of the study region. Four of species listed above pass into the overlying Ertich Formation and even higher, but all others are characteristic of the Noravank Formation only. According to Khalymbadzha, all the species, excluding *P. streeli* Dressen *et al.*, are most common in the lower Famennian. The excepted form was originally described from the uppermost Famennian, but its wider distribution range cannot be ruled out. Khalymbadzha believed that the Noravank Formation corresponds most likely to the upper subzone of the *triangularis* Zone.

In the Noravank Formation of the Nakhichevan' district, Aristov identified conodonts *Polygnathus* ex gr. *politus* Ovnat., *P. normalis* Mill. et Young, *P. brevilaminus* Br. et Mehl, *Icriodus expansus* Br. et Mehl, *Palmatolepis triangularis* Sannem., and referred this assemblage to the conodont *triangularis* Zone. According to Gibshman who studied my collection, the Noravank deposits yield foraminifers *Nanicella tchernyshevae* Lip., *N. bella* Byk., *N. eugeni* Byk., *N. evoluta* Reitl., *N.* cf. *ovata* Reitl., and algae *Girvanella* aff. *ducii* Weth., *G.* sp., *Umbella pughatchovensis* Byk., and *U. orbicularis* Berchenko. All the identified algae forms, excluding *U. orbicularis* Berchenko, pass into the younger Famennian deposits.

The foraminifer and algae assemblages are incompatible with the early Famennian age of the Noravank

Formation. According to Gibshman, the foraminifer and algae species listed above are characteristic of the upper Frasnian sediments in the Russian platform, the Urals and northeastern Salair Ridge. It is unclear yet why the age determination based on foraminifers differs from that based on brachiopods and conodonts.

The formation under consideration corresponds to the Zadonsk Horizon of the Russian platform, to the lower part of the Izhma Formation in the southern Timan, to the Ionishkis Formation of Lithuania, to the Makarovsk Horizon of the Urals' western slope, to the *meisteri* beds of northeastern Kazakhstan, and to the Kogolysai Horizon of the central Tien Shan.

The Noravank Formation can be also correlated with the lower part of the Senzeille Beds in Belgium (Fa1a), with the lower part of the Nehden Formation in the Rhine region, and with the lower part of the so-called with *Cyrtospirifer asiaticus* Zone 9 in Afghanistan (Brice, 1970).

The *Ertich Formation* (Arakelyan, 1964) is accepted in the range of the *Cyrtiopsis orbelianus–Cyrtiopsis davidsoni famenniana* Zone. Its stratotype is situated at the left bank of the Vostochnyi Arpachai River, near the ruined Ertich Village (Fig. 2). The lower boundary is defined by the appearance of index species in association with brachiopods *Ptychomalotoechia omaliusi* (Goss.), *Centrorhynchus baitalensis* Reed, and others. Sediments of the formation exposed in the Vostochnyi Arpachai River basin were studied in the Ertich (stratotype) and Yaidzhi (parastratotype) sections. A sequence 78 m thick that we conventionally refer to the Ertich Formation according to its stratigraphic position underlies the middle Famennian Kadrli Formation in the central part of the Shamamidzor gorge.

The Ertich Formation consists of limestones, quartzites, and black or brownish black clayey shales. Its thickness is 82.5 m in the type section and 256 m (maximum value) in the Yaidzhi section.

Limestones, especially their sandy varieties, yield the diverse fauna dominated by brachiopods. Several beds and layers completely composed of calcareous algae remains occur within the formation. Fifty seven brachiopod taxa are known from the Ertich sediments. Most characteristic among them are *Schuchertella chemungensis* Conrad, *Productella lachrymosa* Hall, *P. pamirica* Reed, *P. baitalensis* Reed, *Mesoplica tasadyrica* (Nal.), *M. kayseri* Khalfin, *Praewaagenoconcha speciosa* (Hall), *Ripidiorhynchus* (?) ex gr. *kotalensis* Brice, *Ptychomalotoechia omaliusi* (Goss.), *P. depradi* (Mansuy), *P. charakensis* Brice, *Centrorhynchus baitalensis* (Reed), *Eoparophorhynchus triaqualis* (Goss.), *Paryphorhynchus* cf. *fatima* Nal., *"Camarotoechia"* ex gr. *sobrina* Stainb., *Cyrtospirifer verneuili yunnanensis* (Mansuy), *C. verneuili syringothyriformis* Paeck., *C. whitneyi* (Hall), *C. pellizoriformis* (Grabau), *C. subextensis* (Martelli), *C. tschernyschewi* Khalfin, *Cyrtopsis orbelianus* (Abich), *C. davidsoni famenniana* Paeck., *C. intermedia* Grabau, *Athyris gurdoni* (Reed), *Cleiothyridina reticulata* Stainb., etc.

The majority of these brachiopod species is known from the Famennian of Eurasia and North America, mainly from lower beds of the stage. Thus, the Ertich Formation should be of the corresponding age. For instance, *Schuchertella chemungensis* Conrad is known from the Chemung beds of the Upper Devonian in North America and from the lower Famennian *meisteri* Beds of Kazakhstan. *Productella lachrymosa lachrymosa* Hall is the guide species of the Zadonsk Horizon in the Russian platform. Typical representatives of this taxon were first described from the Chemung beds of North America, where they occur together with subspecies *P. lachrymosa stigmata* Hall and *P. lachrymosa lima* Conrad, and with *P. rarispira* Hall. *Praewaagenoconcha speciosa* (Hall) is known from the Chemung beds and *meisteri* beds of Kazakhstan as well. Rhynchonelloid *Ptychomalotoechia omaliusi* (Goss.) is characteristic of Famennian deposits in Western Europe (Senzeille beds in Belgium), Central Asia, and Kazakhstan. *Ptychomalotoechia depardi* (Mansuy) was found in Famennian strata of the Karatau, central and southeastern Asia, whereas *P. charakensis* Brice characterizes these strata in Afghanistan. At the same time, *Centrorhynchus letiensis* (Goss.) is characteristic of the upper Famennian, including the Etroeungtian beds in the France-Belgium basin. *Eoparaphorhynchus triaqualis* (Goss.) is recorded in the Famennian of Western Europe, the Urals, Central Asia, and Kazakhstan. *Paraphorhynchus fatima* Nal. was described from the *meisteri* Beds of Kazakhstan. Other species, among them *Cyrtospirifer asiaticus* Brice, *C. wesgensis* Zeiba, *C. tschernyschewi* Khalfin, *Cyrtopsis orbelianus* (Abich), and *C. davidsoni famenniana* Paeck., are characteristic of the lower Famennian in many other regions of Europe and Asia.

Conodonts identified by Khalymbadzha from the Ertich Formation are *Icriodus cornutus* Sannem., *I. alternatus* (Br. et Mehl), *Polygnathus streeli* Dreesen *et al.*, *Pelekysgnathus peejayi* Druce, *Spathognathodus disparilis* (Br. et Mehl), and *Palmatolepis subperlobata* Sannem. The former two species are typical of the lower Famennian and do not occur above the upper *marginifera* Subzone. At the same time, *Pelekysgnathus peejayi* Druce was detected in the upper Famennian, and *Polygnathus streeli* Dreesen *et al.* in the uppermost Famennian. Evidently, this conodont assemblage is somewhat younger than that from the Noravank Formation, but Khalymbadzha was unable to attribute it to any standard zone. At the same time, slightly above the top of the Ertich Formation in the Yaidzhi section (Bed 39), there was found *Pelekysgnathus* aff. *nodosus* Thomas widespread in the lower part of the upper Famennian, if we divide this substage into two subunits. Accordingly, we may assume that the conodont assemblage of the Ertich Formation is of the early Famennian age, not younger, and the formation

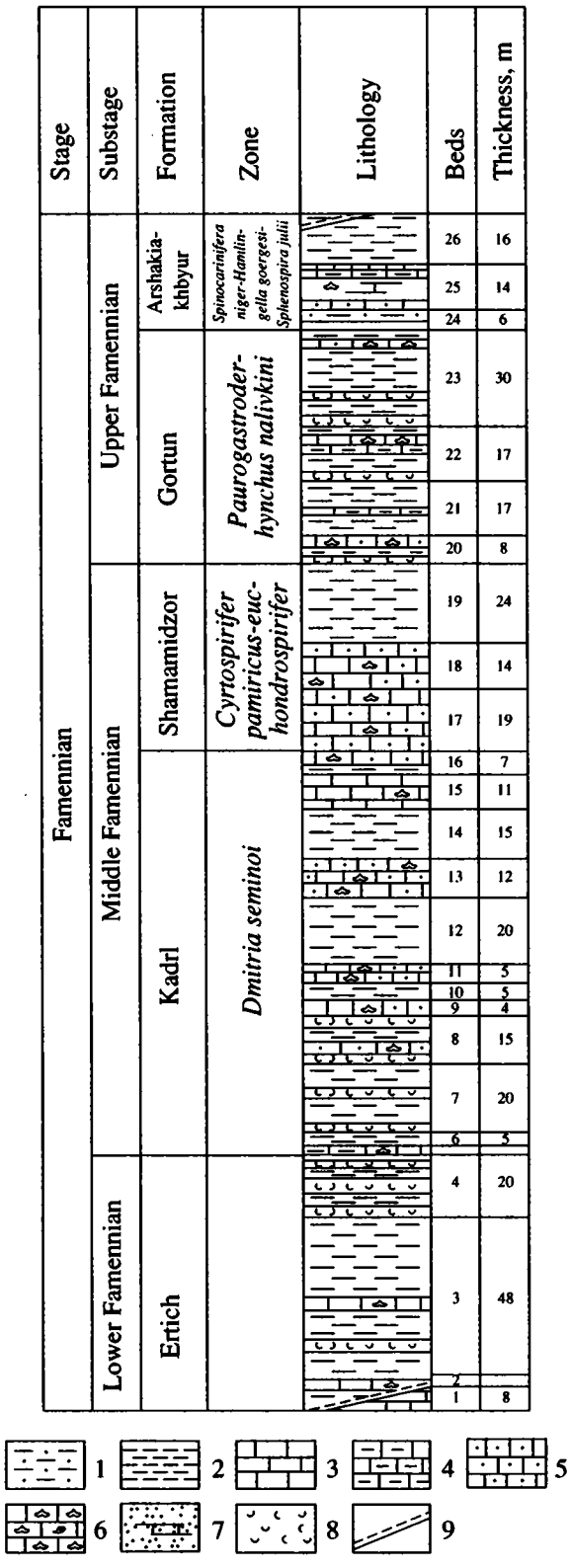

Fig. 3. Section of the Famennian sediments in the Shamamidzor gorge within the Kadrli anticline: (1) siltstones; (2) argillites; (3) limestones; (4) clayey limestone; (5) sandy limestone; (6) organogenic limestone, bearing brachiopods and corals; (7) calcareous sandstone; (8) quartzite; (9) tectonic contact.

thus corresponds to the upper part of the lower Famennian.

Aristov *et al.* (1979) reported on the following conodonts from this interval of the section: *Polygnathus normalis* Mill. et Young., *P. brevilaminus* Br. et Mehl, *Icriodus expansus* Br. et Mehl, *I. rectus* Young. et Pet., and *I. alternatus* Br. et Mehl. The assemblage was referred to the *crepida* Zone.

In 1984, Ovnatanova and Aristov described even more diverse conodont assemblage from the Ertich Formation of the study region. This one includes *Palmatolepis triangularis* Sannem., *P. delicatula* Br. et Mehl, *P. minuta* Br. et Mehl, *P. subperelobata* Br. et Mehl, *Ancyrognathus sinelaminus* (Br. et Mehl), *Nothognathella typicalis* Br. et Mehl, *Icriodus iowaensis* Young. et Pet., *I. cornutus* Sannem., *I. rectus* Young. et Pet., *I. expansus* Br. et Mehl, and *I. alternatus* Br. et Mehl. The coexistence of *Palmatolepis triangularis* Sannem. with *P. delicatula* Br. et Mehl, *P. subperlobata* Br. et Mehl., *P. minuta* Br. et Mehl., and *Ancyrognathus sinelaminus* (Br. et Mehl) suggests that the Ertich Formation is correlative to the uppermost part of the *triangularis* Zone or to the *crepida* Zone. The Ertich Formation also yields calcareous algae *Umbella pughatschovensis* Byk. and species *Leptodesma pamiricus* Reed of bivalve mollusks.

The Ertich Formation is correlative with the Elets Horizon of the Russian platform (evidently together with the uppermost beds of the Zadonsk Horizon), with the upper part of the *meisteri* Beds of northeastern Kazakhstan, and with the Makarovo Horizon of the Urals. This is supported by presence of brachiopods *Schuchertella chemungensis* Conrad, *Praewaagenoconcha speciosa* (Hall), *P. oreliana* (Moeller), *Ptychomalotoechia omaliusi* (Goss.), *Paryphorhynchus fatima* Nal., *Cyrtospirifer asiaticus* Brice, and *C. wesgensis* Zeiba.

As for its counterparts in the France-Belgium basin, the formation most likely corresponds to the upper part of the Senzeille Beds(Fa1a) and to the Mariembourg Beds (Fa1b) bearing a characteristic form *Ptychomalotoechia omaliusi* (Goss.). In the Rhine region, its analog is the middle (most thick) part of the Nehden Formation, and in Afghanistan, this is the upper part of the so-called Zone 9 that yields *Cyrtospirifer asiaticus* Brice and *C. quadratus* Nal.

THE MIDDLE FAMENNIAN SUBSTAGE

The Kadrli Formation (Arakelyan, 1964) is accepted in the range of the *Dmitria seminoi* Zone of the Abramyan's (1957) scheme. Its stratotype is exposed within the Kadrli anticline, in the Shamamidzor gorge not far away from the Kadrli Village (Fig. 3). The lower boundary of the formation is defined by the index species appearance in the section.

The deposits of the Kadrli Formation are widespread in Armenia, mostly in the Shamamidzor gorge

(stratotype), within the Amagu–Gnishk anticline in the Chrakhana River gorge (left tributary of the Gnishk River), to the southwest of the Gnishk Village, within the Khorvirap anticline in the Vedi region, on the bank of the Araks River near the Shikhlar Village, on one of isolated hills in the Nakhichevan' district in the vicinity of the Nizhnii Yaidzhi Village (parastratotype), and in the vast area between the Bagarsykh-Deresi River in the east and the Dzhaanam-Deresi River in the west, closer to the watershed part of the Bagarsykh Ridge.

The formation is composed of alternating limestone, sandstone, quartzite, and argillite members, the latter two predominant. In the Shamamidzor stratotype and Yaidzhi parastratotype, the formation is 106 and 105 m thick, respectively.

The Kadrli sediments yield brachiopods, conodonts, foraminifers, and corals. Twenty four brachiopod species were encountered, among them *Schizophoria* ex gr. *impressa* (Hall), *Schellwienella* cf. *percha* Stainb., *Productella* cf. *herminae* Frech, *Whidbornella caperatiformis* (Abr.), *Mesoplica* aff. *arctirostratum* (Hall), *M. simplicator* (Whidborne), *Ptychomalotoechia omaliusi* (Goss.), *Centrorhynchus letiensis* (Goss.), *Eoparophorhynchus triaqualis* (Goss.), *Cyrtospirifer sinensis* mut. *alfa* (Grabau), *C. pellizzorii* (Grabau), *Dmitria seminoi* (Viq.), *Eobrachythyris strunianus strunianus* (Goss.) sensu Brice, 1970, *Athyris pseudoglobularis* (Reed), *Cleiothyridina reticulata* Stainb., and others.

The distribution of many of them was discussed above. Species *Dmitria seminoi* (Viq.) that appears in the Kadrli Formation is known from the Upper Devonian of Iran. In Afghanistan, it occurs in the *archiaci* and *Ptychomalotoechia (?) turanica* zones of the upper Famennian, if the two-fold subdivision of the substage is given. *Schizophoria impressa* Hall is recorded in the Chemung Beds of North America and in the *sulcifera* Beds of Kazakhstan. *Schellwienella percha* Stainb. was described from the Percha Formation of New Mexico, North America and from the upper Famennian of Afghanistan. *Productella herminae* Frech is characteristic of the lower Famennian in the Carnian Alps, of the Frasnian of Poland, and of the Elets Horizon in the Russian platform. *Mesoplica simplicior* (Whidborne) was described from the Pilton Beds of England. In central Kazakhstan, this form is common in the *sulcifera* Beds; it occurs as well in the Tarkhansk Formation of the Rudnyi Altai. *Eobrachythyris strunianus* is known from the upper Famennian of the Rhine region and from the Etroeungtian deposits of the Anti Atlas, Morocco. In Afghanistan, this species is recorded in the upper Famennian and Etroeungtian deposits. Finally *Cleiothyridina reticulata* Stainb. was first described from the Percha Formation of North America; it was encountered in the upper Famennian and Etroeungtian deposits of Afghanistan.

Thus, many brachiopods found in the Kadrli Formation appear in the lower Famennian, being also known from the upper Famennian in different parts of the world. Accordingly, the joint occurrence of many early and late Famennian species can be considered as argument in favor of attributing the Kadrli Formation to the lower part of the middle Famennian, provided the three-fold subdivision of the stage.

Khalymbadzha identified in the Kadrli Formation the conodont species *Pelekysgnathus* aff. *nodosus* Thomas that is widespread in the lower upper Famennian. According to Aristov (1979), conodonts are scarce in both the carbonate and terrigenous parts of the formation section. He identified *Polygnathus semicostatus* Br. et Mehl, *P. communis communis* Br. et Mehl, *Icriodus cornutus* Sannem., spathognathids, and simple cone-shaped forms.

Later on, Ovnatanova and Aristov (1984) described the Kadrli assemblage of conodonts *Polygnathus semicostatus* Br. et Mehl., *P.* ex gr. *communis* Br. et Mehl, *Icriodus cornutus* Sannem., and *Spathognathodus crassidentatus* (Br. et Mehl). They assumed that the base of the *seminoi* Zone coincides with the appearance level of *P. semicostatus*. This species is known to be characteristic of shallow-water Famennian sediments, ranging from the middle part of the conodont *crepida* Zone to the *styriacus* Zone inclusive. It is impossible to correlate directly the conodont assemblage of the *seminoi* Zone with the standard scale, but, according to its position in the section, the distinguished assemblage may correspond to the *rhomboidea* and *marginifera* zones (Ovnatanova and Aristov, 1984).

Deposits of the Kadrli Formation yield tetracorals *Hexagonaria hexagona* (Goldf.) known from the Frasnian (identification by Spasskii), and algae *Girvanella* aff. *ducii* Weth. and *Umbella* sp. (identifications by Gibshman). According to Gibshman, *G. ducii* is characteristic of the upper Frasnian.

Ostracodes encountered in the Kadrli Formation are represented by species of genera *Zaninaella* and *Selebratina*, and by Quasillitidae forms. The *Cavellina* species are especially numerous and diverse. According to Chizhova (see in Aristov *et al.*, 1979), the ostracode assemblage suggests that the studied formation is correlative with the lower part of the Dankov-Lebedyan' beds of the Russian platform.

With due regard to the general composition of its fauna, the Kadrli Formation may be evidently correlated with the lowermost *sulcifera* Beds of Kazakhstan, with the Lebedyan' Horizon, and apparently with the lower part of the Dankov Horizon (Mtsensk beds) of the Russian platform. In the South Urals, the lower part of the Murzakaevo Horizon, which also corresponds to the conodont *rhomboidea* and *marginifera* zones, is a likely analogue of the Kadrli Formation. In the France-Belgium basin, the formation analogues are the Esneux (Fa1c) and Souverain-Pre (Fa2a) beds with *Centrorhynchus letiensis* (Goss.), and also other units referred to the conodont *rhomboidea* and *marginifera* zones. The Kadrli Formation of the Transcaucasia can be correlated with the upper part of the Nehden Formation

(Fa1c-Fa2a) and with lowermost horizons of the Hemberg Formation (Fa2b) in Germany. It may correspond as well to the so-called Zone 10 with *Dmitria seminoi* in Afghanistan.

The *Shamamidzor Formation* (Arakelyan, 1964) is accepted in the range of the *Cyrtospirifer pamiricus–Euchondrospirifer ghorensis* Zone. Its type section is situated in the Shamamidzor gorge within the Kadrli anticline (Fig. 3). The lower boundary is defined by the appearance level of zonal index species in association with many characteristic representatives of genera *Sentosia, Araratella, Syntectirostrum*, and others. The Shamamidzor rocks conformably overlie deposits of the Kadrli Formation wherever their contact is exposed. Additional excellent exposures of the Shamamidzor sediments are situated in the Danzik Village region, not far from the Mamadasan ruins (Site 49), in the low reaches of the Bagarsykh-Deresi River, near the Makhmudkend Village (Site 13). Partial sections of the formation are known at the southwestern foot of the Mt. Tezhgar (Site 54a).

The formation consists of alternating limestones, argillites, siltstones, and quartzites. Sandy limestones are overfilled with organic remains, mainly with those of brachiopods. Fossils also occur in the finely laminated sandstones. Black laminated shales are often intercalated with sandy limestones and bedded siltstones and sandstones. Quartzite members are not thick. The total thickness of the formation is 33 to 60 m, with its maximum value in the Nizhnii Yaidzhi site, and with the minimum one in the Shamamidzor gorge. In other studied sections, deposits of the formation are incompletely exposed.

The formation rich in paleontological remains yielded 49 brachiopod species and subspecies. Most characteristic among them are *Aulacella* cf. *interlineata* (Sow.), *Schuchertella chemungensis* Conrad, *Schellwienella* cf. *percha* Stainb., *Productella herminae* Frech, *P. baitalensis* Reed, *Leioproductus* ex gr. *pamiricus* Karapetov, *Semiproductus* cf. *angustus* (Hall), *Planoproductus hillsboroensis* (Kindle), *Sentosia retiformis* (Kr. et Karp.), *Ptychomalotoechia omaliusi* (Goss.), *Centrorhynchus letiensis* (Goss.), *Eoparophorhynchus triaqualis* (Goss.), *Parophorhynchus zuleika* Nal., *Syntectirostrum delicatocostatum* (Abr.), *Araratella dichotomians dichotomians* Abr., *A. dichotomians assimulata* Abr., *"Camarotoechia" sobrina* Stainb., *"C." tenisica* Martynova, *Cyrtospirifer verneuili syringothyriformis* Paeck., *C. tarbagataicus* (Vas.), *C. chaui* (Grabau), *C. pamiricus* Reed, *Cyrtiopsis graciosus chakhaensis* Brice, *Euchondrospirifer ghorensis* Brice, *Athyris sulcifera sulcifera* Nal., *A. sulcifera intermedia* Nal., *Cleiothyridina reticulata* Stainb., and others. Among species that appear in the Shamamidzor Formation, there is *Aulacella interlineata* (Sow.) occurring in the Upper Devonian Pilton Beds of England. It is rather common in Famennian strata of the Urals and Kazakhstan, namely, in the *meisteri* and *sulcifera* beds. In the Pamirs, this species was found in the coaly shale member of the uppermost Famennian substage. *Semiproductus angustus* (Hall) was described from the Chemung Beds of North America. Its scarce specimens occur in the Karakingir Beds of central Kazakhstan. *Leioproductus pamiricus* Karapetov was recorded in the lower Famennian of the eastern Pamirs (the Tugurek-Bashi River basin). *Planoproductus hillsbroensis* (Kindle) is known from the Percha Beds in North America, New Mexico. *Sentosia retiformis* (Kr. et Karp.) was described from the Kynov Horizon of the Urals. *"Camarotoechia" tenisica* Mart. occurs in the Karakingir Beds and likely in the upper part of the *sulcifera* Beds of central Kazakhstan. *Cyrtospirifer tarbagataicus* (Vas.) is widespread in the Famennian sediments of Tarbagatai, Kazakhstan (lowermost "Neodevonian," according to Vasil'evskii). *C. procumbens* Sim. was described by Simorin from the Etroeungtian beds of northern Kazakhstan. In the Rudnyi Altai, it occurs in the Tarkhansk Formation. *C. crassiplicatus cyrtinaeformis* Brice was described from the upper Famennian and Etroeungtian deposits of central Afghanistan. *C. pamiricus* Reed is known from the Famennian in the Ak-Baitala region of the Pamirs. *Euchondrospirifer ghorensis* Brice occurs in the upper Famennian of central Afghanistan, provided the two-fold subdivision of the stage. *Athyris intermedius* Nal. was recorded in Afghanistan at the same level; it is also widespread together with *A. sulcifera* in the *sulcifera* Beds of Kazakhstan. Therefore, the majority of brachiopod species clearly indicate the late Famennian age of the Shamamidzor Formation, provided the two-fold subdivision of the stage.

Seven conodont species were identified by Khalymbadzha in the formation under consideration. These are *Icriodus cornutus* Sannem, *Polygnathus streeli* Dressen *et al.*, *P. communis communis* Br. et Mehl, *P. communis collinsoni* Druce, *Pelekysgnathus inclinatus* Thomas, *P.* sp., and *Spathognathodus acidentatus* (E.R. Brans.). Four of these species and subspecies appear first exactly in this formation. The range of *P. communis collinsoni* spans the *styriacus* and *costatus* zones. *Pelekysgnathus inclinatus* is distributed from the *velifer* Zone to the lower subzone of the *costatus* Zone. *Spathognathodus acidentatus* is known within the *velifer-costatus* zone of the upper Famennian provided the two-fold subdivision of the latter. The assemblage includes species that commonly do not occur above the *velifer* Zone and associate with elements of the lowermost *styriacus* Zone. Thus, Khalymbadzha referred the discussed conodont assemblage to the *velifer-styriacus* Superzone.

Ovnatanova and Aristov described the conodont assemblage of the Shamamidzor Formation as follows: "limestones of the brachiopod *Euchondrospirifer ghorensis* Zone (the Shamamidzor Formation) are characterized by abundant conodonts. The assemblage includes *Scaphignathus velifer* Helms, *Polygnathus diversus* Helms, and *P. nodoundatus* Helms. *Pelekysg-*

nathus nodosus (Thomas) and *Spathognathodus varians* Br. et Mehl, which appear here and occur above in the section. *Spathognathodus semicostatus* Br. et Mehl, *P.* ex gr. *communis* Br. et Mehl, and *Icriodus cornutus* Sannem are the transient species in the interval. The occurrence of *Scaphignathus velifer* Helms in the assemblage permits correlation of the *ghorensis* Zone (Shamamidzor Formation) with the *velifer* Zone, and the late Famennian age of the formation is thus beyond question." (Ovnatanova and Aristov, 1984, p. 66). It is necessary to keep in mind that when they speak about the late Famennian age of the Shamamidzor Formation, meaning the two-fold subdivision of the stage. However, the three-fold subdivision of the Famennian is accepted nowadays after the joint conference of the ISC Commissions on Devonian and Carboniferous (Minsk, 1986).

Chizhova encountered numerous ostracodes in the Shamamidzor formation (Aristov *et al.*, 1979), though most of them are identified in the open nomenclature. These are *Selebratina* ex gr. *rjauzakensis* Tschig., *Kozlowskiella (Ilativella)* sp., *Shemonaella* sp., *Cavellina* sp., *Armenella* sp., *Akidellina (?)* sp., and Beyrichiacea. In her opinion the assemblage enables correlation of the formation with the upper part of the Famennian.

In my opinion, the Shamamidzor Formation corresponds to the uppermost middle Famennian. It is corresponding to the middle part of the Dankov Horizon (Kiselevo-Nikol'skoe, Orel-Saburovo, and likely Turgenevo beds) of the central Russian Platform and to the greater upper part of the Murzakaevo Horizon of the Urals. It could be apparently correlated with the middle part of the *sulcifera* Horizon of northeastern Kazakhstan and with its stratigraphic analogues. This is evident from joint occurrence of index species and *Planoproductus hillsboroensis* (Kindle), *"Camarotoechia" tenisica* Mart., *Planatoavetirostrum planovatus* Nal., *Cyrtospirifer procumbens* Sim., and some other forms.

The conodont assemblage of the Shamamidzor Formation suggests that it may be correlated with the Monfort (Fa2b) and lowermost Evieux beds (Fa2c) corresponding to the *Scaphignathus velifer* Zone in the France-Belgium basin. The unit is also correlative with the uppermost Hemberg Formation (Fa2b) of Germany and with the so-called Zone 11 in Afghanistan bearing *Araratella, Euchondrospirifer, Dichospirifer*, and other forms, in particular the index species. The deposits of the Shamamidzor Formation are conformably overlain by rocks of the Gortun Formation.

UPPER FAMENNIAN SUBSTAGE

The Gortun Formation (Arakelyan, 1964) is accepted in the range of the *Paurogastroderhynchus nalivkini* Zone distinguished by Abramyan (1957). Its type section is exposed in the Aratso River gorge to the south of the Gortun Village, within the Chanakhchi anticline. The lower boundary is defined by the appear-

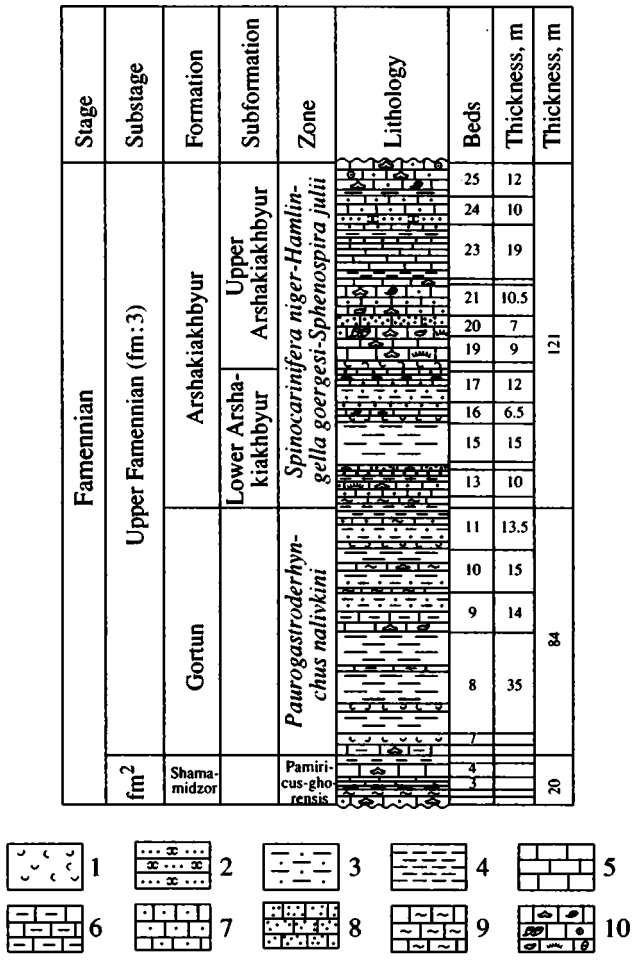

Fig. 4. Upper Famennian section on the western slope of the Tezhgar Mountain: (1) quartzites; (2) sandstones; (3) siltstones; (4) argillites; (5) limestones; (6) clayey limestone; (7) sandy limestone; (8) detrital limestone; (9) siliceous limestone; (10) organogenic limestone.

ance level of zonal index species in the section and by a sudden decrease of fauna diversity parallel to the facies change.

In addition to the type section, the Gortun Formation is exposed in southern areas of the Vostochnyi Arpachai River basin: near the Nizhnii Yaidzhi Village, at the northern foot of the Mt. Gerankalasy (parastratotype), on the east- northeastern ridge crowned by the Mt. Myunkh-Bala-Ogly, in the low reaches of the Bagarsykh-Deresi River, to the south of the Kabakhdag Mountain, at the western and southwestern foot of the Mt. Tezhgar (Fig. 4), on the Mt. Birali-Kuzei foothills, and in the Shamamidzor gorge.

The formation is composed of terrigenous rocks represented by variegated shales and siltstones enclosing beds and members of ferruginous micaceous, often platy limestones colored brownish-gray or brownish. The sequence also includes fine- to medium-bedded quartzite strata brownish at the surface. Shales are free

of carbonate. The best exposure of the Gortun Formation is at the Yaidzhi site (parastratotype). The thickness of the unit ranges from 28 m in the type section to 112 m in the Yaidzhi section.

Limestones of the Gortun Formation commonly yield numerous brachiopod shells, mainly isolated valves of *Paurogastroderhynchus nalivkini* (Abr.). The taxonomic composition of the brachiopod assemblage is impoverished. The assemblage includes *Whidbornella caperatiformis* (Abr.), *Planoproductus hillsboroensis* (Kindle), *Bagrasia chonetiformis* (Kr. et Karp.), *Buxtonia scabricula* (Martin), *Ptychomalotoechia omaliusi* (Goss.), *P.* ex gr. *turanica* (Rom.), *P.* cf. *gonthieri* (Goss.), *Centrorhynchus letiensis* (Goss.), *Syntectirostrus* cf. *delicatocostatum* (Abr.), *Araratella dichotomians dichotomians* Abr., *Pugnas pugnus* (Martin), *"Camarotoechia" sobrina* Stainb., *Cyrtospirifer procumbens* Simorin, *C. latus* Abr., *C. kindlei* Stainb., *C. insulcifer lectus* Martynova, *C. krestovnikovi* Nal., *Spirifer pseudosuavis* Kr. et Karp., *S.(?)* cf. *distans* (Sow.), *Athyris sulcifera sulcifera* Nal., *Actinoconchus* aff. *struniensis* (Dehee), *Cleiothyridina* cf. *reticulata* Stainb., and others. Twelve of these species first appear in the Gortun Formation.

Bagrasia chonetiformis (Kr. et Karp.) from the last group is widespread in the uppermost Famennian and Etroeungtian beds of the Urals. *B. scabricula* (Martin) occurs in the Upper Devonian and Lower Carboniferous of England, Ardennes, and some Asian regions, Afghanistan included. The sediments of the Gortun and lowermost Arshakiakhbyur formations also bear *Cyrtospirifer latus* Abr. and *C. kindlei* Stainb., the latter recorded in the Percha Formation of North America. *C. insulcifer lectus* Mart. was described from the upper *sulcifera* Beds of central Kazakhstan. *C. krestovnikovi* Nal., *Spirifer distans* Sow., and *S. pseudosuavis* Kr et Karp. are known from the Etroeungtian coquinas of the Urals. *Athyris squamigra* Kon. and *Actinoconchus struniensis* (Dehee) were described from the Etroeungtian level of the France-Belgium basin. Therefore, many species that appeared in the middle Famennian occur in the Gortun Formation, whereas newcomers of the latter are also characteristic of the transitional Devonian–Carboniferous beds. In addition, the Kulikova identified bivalves *Parallelodon* cf. *subcarinatus* (Dehee) and *Aviculopecten* sp. in the unit under consideration.

Aristov *et al.* (1979) and Grechishnikova *et al.* (1982) described the following conodonts of the unit: *Acodina curvata* Stauff., *Spathognathodus crassidentatus* (Br. et Mehl), *Polygnathodus semicostatus* Br. et Mehl, *P. communis communis* Br. et Mehl, *Pelekysgnathus nodosus* Thomas, *Icriodus cornutus* Sannem., *Bisphathodus stabilis* Br et Mehl., *Angulodus walrathi* (Hibb.), *A. demissus* Huddle, and others. In their opinion, the formation lacking zonal species cannot be directly correlated with the standard scale. However, its position immediately above sediments bearing *Scaphignathus velifer* suggests correspondence to the *styriacus* Zone.

Numerous ostracodes found in the formation have not been identified at the species level, though Chizhova concluded that they resemble the assemblage of the *Carborimitia turgenevi–Tchizhovaella primula–Marternella hemisphaerica* Zone. This zone corresponds to the uppermost *Clymenia* and *Woklumeria* zones and to Fa2c-Fa2d units of the France-Belgium basin.

I refer the Gortun Formation to the lowermost upper Famennian keeping in mind its three-fold subdivision. The formation is apparently correlative with the uppermost part of the Dankov Horizon, namely with the following units: the Kudeyarovka Beds of the Russian platform; the upper Zelenets Horizon of the Timan-Pechora province; the Ust' Karaganda Beds and the lower part of the Simorin Horizon of Kazakhstan; the Kushelga Horizon of the Urals, and with their analogues in other regions.

As for the France-Belgium basin, the formation most likely corresponds to the ammonoid *Gonioclymenia speciosa, Kalloclymenia subarmata*, and *Wocklumeria sphaeroides* zones or to the upper Evieux (Fa2c) and Comblain-au-Pont (Fa2d) Beds, at least to their lower part. The Gortun Formation can be correlated with the Dasberg Formation of the Eifel Mountains (Fa2c) and with the lower part of the so-called Voklum Beds (Fa2d). It also corresponds to the so-called zone 12 of Afghanistan that bears *Paurogastroderhynchus nalivkini* (Abr.), *Buxtonia scabricula* (Sow.), and others, and to the Percha Formation of North America, or at least to its lowermost half with *Schellwienella percha* Stainb., *"Camarotoechia" sobrina* Stainb., *Cyrtospirifer kindlei* Stainb., and others.

The Arshakiakhbyur Formation (Abramyan, 1964) is accepted in the range of the brachiopod *Spinocarinifera niger–Hamlingella goergesi–Sphenospira julii* Zone. Its type section is situated in the Arshakiakhbyur River gorge at the southwestern flank of the Kadrli anticline. The lower boundary of the unit is rather distinct, corresponding to the transgressive sedimentation cycle that begins with appearance of sandy-clayey, slightly lumpy reddish brown limestones bearing abundant brachiopods *Spinocarinifera niger* (Goss.), *Mesoplica praelonga* (Sow.), and *Sphenospira julii* (Dehee) along with other characteristic species. The upper boundary is placed at the base of the shale member enclosing thin-platy layers of sandy and sandy-clayey limestones of the Gerankalasy Formation. The last rock varieties yield *Rhipidomella micheilini* (L'Ev.), *Unispirifer* ex gr. *tornacensis* (Kon.), *U. ussuensis* Tolm., *U. taidonensis* Tolm., *Camarotoechia panderi* (Sem. et Moell.), *Syringothyris* cf. *hannibalensis*, and others.

Sediments of the Arshakiakhbyur Formation occur in many sites of the Vostochnyi Arpachai River basin: on the northern slope of the Mt. Gerankalasy; on eastern and northern slopes of the Mt. Myunkh-Bala-Ogly; in the Biralichai River basin; western and southern slopes of the

Mt. Tezhgar (parastratotype); and on the western slope of the Mt. Birali-Kuzei. Other exposures are known in the Shamamidzor and Arshakiakhbyur gorges near the Kadrli Village, and in the Bagarsykh-Deresi region on the western slope and foothills of the Mt. Kabakhdag. The Tezhgar and Gerankalasy sections are the richest in paleontological remains and most thoroughly studied.

The formation is represented by alternated members of yellowish-gray sandy limestones and black clayey shales, which are intercalated with sandstone and quartzite interbeds. Limestones and some calcareous sandstones are crammed with organic remains, especially with brachiopods and tetracorals. The formation is 60 to 100 m thick.

The diverse brachiopods are represented by 93 species and subspecies. The most characteristic forms are *Aulacella interlineata* (Sow.), *Schuchertella planumba planumba* (Weller), *Mesoplica praelonga* (Sow.), *Sentosia retiformis* (Kr. et Karp.), *Hamlingella goorgesi* Paeck., *Spinocarinifera niger* (Goss.), *Paruphorhynchus striatocostatum* (Meek et Worthen), *Syntectirostrum delicatocostatum* (Abr.), *Araratella dichotomians dichotomians* Abr., *A. araratica araratica* Abr., *A. araratica schamamensis* Abr., *"Camarotoechia" tenisica* Martynova, *"C." panderi* (Sem. et Moell.), *"C." quadriplex* (Tolm.), *Cyrtospirifer latus* Abr., *C. kindlei* Stainb., *C. siganensis* Kr. et Karp., *Eobrachythyris strunianus* (Goss.), *Sphenospira julii* (Dehee), *Unispirifer ventricosus* (Kon.), *U. striatoconvolutus* (Benson et Dun), *Spirifer pseudosuavis* Kr. et Karp., *Torynifera cooperensis* (Swall.), *Cleiothyridina prouti* (Swall.), *C. tenuilineata* (Rowley), *Lamellosathyris lamellosus* (L'Ev.), *Retzia tykhtensis* Besn., and others.

The brachiopod assemblage clearly indicates the Etroeungtian age of the Arshakiakhbyur Formation. It is similar to the assemblage from the upper part of the Comblain-au-Pont and Etroeungtian (Tn1a) beds and from the lowermost Astieux Beds (Tn1b) of the France-Belgium basin, which are nowadays referred to the Strunian Substage of the Famennian. The distribution of many species inherited from underlying deposits was discussed above. As for 60 forms newly appeared in the formation, almost all of them are associated in other regions with the Etroeungtian sediments or their analogues. All the data available show the correspondence of the Arshakiakhbyur sediments to the Etroeungtian strata of the Dinant basin.

Coral fauna of the unit is mainly represented by solitary tetracorals. The Arshakiakhbyur Formation yields ten their species identified by N.Ya. Spasskii: *Caninia* cf. *dorlodoti* Salee, *C.* aff. *juddi* (Thomson), *C.* cf. *coajuncta* Gorsky, *C.* aff. *cornucopia* Hich., *Siphonophyllum* ex gr. *cylindrica* Scouler, *Siphonella* sp., *Michelinia tenuisepta* (Phillips), *Campophyllum* sp., *Bothrophyllum pater* Jvnsky, and *Syshaelasma* sp. According to Spasskii, the joint occurrence of these species is characteristic of the Tournaisian.

The conodont assemblage described by Khalymbadzha includes *Bispathodus aculeatus plumulus* Rhodes *et al.*, *Polygnathus communis communis* Br. et Mehl, *Icriodus costatus* (Thomas), *Pelekysgnathus* cf. *inclinatus* Thomas, *Pseudopolygnathus nodomarginatus* (E.R. Brans.), *Spathognathodus acidentatus* (Br. et Mehl), and *S. crassidentatus* (Br. et Mehl). Khalymbadzha assigned the assemblage to the middle and upper subzones of the *costatus* Zone.

Aristov who also studied conodonts from the Arshakiakhbyur Formation (Aristov *et al.*, 1979; Ovnatanova and Aristov, 1984) considered their assemblage as corresponding to that from the upper part of the *costatus* Zone. He listed 32 conodont species.

In the discussed sediments, Chizhova (see in Aristov *et al.*, 1979; Grechishnikova *et al.*, 1982) identified ostracodes *Armenites quaseitus* Tschig., *Favorites proprius* Tschig., *Quasiknoxiella reverenda* Tschig., *Knoxiella reducta* Tschig., *K. praeclara* Tschig., *Kloedenellina* aff. *indistincta* Tschig., *Cavellina aolida* Tschig., *C. munda* Tschig., *Shishaella ferax* Tschig., *Armenella intracta* Tschig., *Bairdia zaninae* Posn., *Acutiungulata* sp., *Coryellina dinga* Tschig., and others.

Analyzing the assemblage, Chizhova (Grechishnikova *et al.*, 1982) stated that its composition suggests a conventional correlation with the *Richterina latior–Maternella hemisphaerica–Cryptophyllus* sp.–*Shishaella okeni* Zone, which in turn corresponds to the Chekmagush beds in the Russian platform and to the Tn1a and possibly Tn1b units of the France-Belgium basin.

Gibshman studied foraminifers, calcisphaeres, and algae from the discussed deposits. She identified foraminifer species *Tuberetina maljavkini* Mikh., *Paracaligella antropovi* Lip., *Septatournayella (Eoseptatournayella) praesegmentata* Bog. et Jut., *Septaglomospiranella nana* Reitl., *Bisphaera malevkensis* Bir., *B. minuta* Bir., *B. comperra* Reitl., *Parathurammina cushmani* Sal., *P. suleimanovi* Lip., *Earlandia minima* Bir., *Vicinesphaera squalida* Antr.; calcisphaeres *Calcisphaera plavskensis* Reitl., *C. transporanta* Reitl., *Polyderma chovanensis* Reitl., *Radiosphaera basifica* Reitl.; and algae *Girvanella maslovi* Shuysky, *Kamaena delicata* Antr., *Quasiumbella* ex gr. *globula* Reitl., and *Lagenumbella lageniformis* Reitl.

According to Gibshman, the assemblage is similar to that of the Zavolga Horizon of the Russian platform, namely, to the fauna with common *Quasiendothyra konensis* and *Q. kobeitusana*, though the *Quasiendothyra* species are missing in Transcaucasia.

In shales of the Arshakiakhbyur Formation, Chibrikova identified miospores of the *lepidophytus-explanatus* Zone. This also confirms the Etroeungtian age of the formation.

Trilobites encountered in the lower part of the Arshakiakhbyur Formation are represented by the characteristic Etroeungtian species *Phacops (Omegops) accipitrinus* (Phill.). According to Ya.N. Spasskii, who identified this form, it is the last representative of the Devonian genus *Phacops*.

The joint conference of the ISC Commissions on Devonian and Carboniferous (Minsk, 1986) suggested to transfer the analogues of the Etroeungtian from the lowermost Carboniferous to the upper part of the Famennian, and the Devonian Commission recommended to adopt the three-fold subdivision of the Famennian in the former USSR. As a result, I assign the Arshakiakhbyur Formation to the upper part of the upper Famennian Substage.

The formation appears to correspond to the Lytvino Horizon of the South Urals, to the ore-bearing beds of the Liman Formation of the Dnieper–Donets depression, to the lower and middle Tarkhansk subformations of the Rudnyi Altai, and to the upper greater part of the Simorin Horizon of Kazakhstan. The Arshakiakhbyur Formation is correlated with the Zavolga Horizon of the Russian platform and with the Abyshevo Horizon of the Kuznetsk depression. It apparently corresponds to the Etroeungtian (Tn1a) and the lowermost Astieux beds (Tn1b) of the France-Belgium basin. Other correlative units are the upper half of the Voklum beds in Germany (Tn1a) and sediments of the Etroeungtian level in Iran and Afghanistan. In Afghanistan, these sediments are constituents of the so-called Zone 12. The Arshakiakhbyur Formation may be also correlated with the upper part of the Percha Formation of New Mexico, North America, and with the lower (Bushberg and Hannibal) beds of the Kinderhook Series in the Missouri River basin.

The limestones of the Arshakiakhbyur Formation are conformably, with a gradual transition overlain by sediments of the Carboniferous Gerankalasy Formation that is composed of terrigenous and carbonate rocks with rich and diverse fauna represented by the typical Tournaisian species and genera devoid of Devonian elements.

Reviewer A.S. Alekseev

REFERENCES

Abramyan, M.S., *Brakhiopody verkhnefamenskikh i Etroeungtianskikh otlozhenii yugo-zapadnoi Armenii* (Brachiopods from the Upper Famennian and Etroeungtian Sediments of Southwestern Armenia), Erevan: Akad. Nauk ArmSSR, 1957.

Abramyan, M.S., Carboniferous, in *Geologiya Armyanskoi SSR*. T. 11. *Stratigrafiya* (Geology of Armyanskaya SSR. Vol. 11. Stratigraphy), Erevan: Akad. Nauk ArmSSR, 1964, pp. 96–117.

Arakelyan, R.A., Devonian, in *Geologiya Armyanskoi SSR*. T. 11. *Stratigrafiya* (Geology of Armyanskaya SSR. Vol. 11. Stratigraphy), Erevan: Akad. Nauk ArmSSR, 1964, pp. 46–96.

Aristov, V.A., Grechishnikova, I.A., Chizhova, V.A., and Feliks, V.P., Subdivision and Correlation of the Famennian and Lower Tournaisian Sediments of Transcaucasia, the Nakhichevan' ASSR (According to Brachiopods, Conodonts, and Ostracodes), *Serv. Geol. de Belgique. Prof. Pap.*, 1979, no. 161, pp. 87–95.

Biernat, G., Ramienionogi z utworow Famenu jablonnej, gory Swietokrzyskie, *Biul. Inst. Geol.*, 1983, vol. XIV, no. 345, pp. 135–153.

Brice, D., Etude paleontologique et stratigraphique du Devonien de l'Afghanistan, *Notes et Mem. Moyen-Orient*, 1970, vol. 11, pp. 1–364.

Frech, F. and Arthaber, H.B., Uber das Palaozoicum in Hocharmenien und Persien mit einem Anhang uber die Kreide von Sirab in Persien, *Beitr. zur Palaont. und Geol. Oster.-Ung. und Orients*, 1900, vol. 12, no. 4, pp. 161–208.

Grechishnikova, I.A., Aristov, V.A., Reitlinger, E.A., and Chizhova, V.A., *Biostratigrafiya pogranichnykh otlozhenii devona i karbona Zakavkaz'ya (opornye razrezy)* (Biostratigraphy of the Devonian-Carboniferous Boundary Sediments of Transcaucasia (Reference Sections)), Magadan: SVKNII DVNTs Akad. Nauk SSSR, 1982.

Grechishnikova, I.A., Aristov, V.A., Reitlinger, E.A., and Chizhova, V.A., Reference Section of the Border Devonian-Carboniferous Sediments of Transcaucasia (the Nakhichevan' ASSR), in *Granitsa devona i karbona na territorii SSSR* (Devonian-Carboniferous Boundary in the Territory of the USSR), Minsk: Nauka i Tekhnika, 1988, pp. 137–145.

Mamedov, A.B., Stratigraphy and Brachiopod Fauna of the Devonian Danzik Formation of the Nakhichevan' ASSR, *Cand. Sc. (Geol.–Min.) Dissertation*, Baku: Azizbekov Inst. of Oil and Chemistry, 1962, p. 16.

Mamedov, A.B., Zonal Subdivision of the Tournaisian Stage of the Lower Carboniferous in the Nakhichevan' ASSR, *Dokl. Akad. Nauk SSSR*, 1980, vol. 36, no. 12, pp. 53–57.

Mamedov, A.B., Devonian Stratigraphy and Brachiopods of the Nakhichevan' ASSR, Southern Transcaucasia, *Doctoral (Geol.–Min.) Dissertation*, Baku: Inst. Geol. Akad. Sci. AzerSSR, 1992, p. 57.

Mamedov, A.B., *Opisanie opornogo razreza verkhnego Devona po profilyu sel. Nizhnii Yaidzhi–g. Gerankalasy (razrez 94)* (Description of the Upper Devonian Reference Section along the Nizhnii Yaidzhi–Gerankalasy Profile Site 94), Available from VINITI, 1993, Baku, no. 966-B94.

Mamedov, A.B. and Rzhonsnitskaya, M.A., Devonian of the South Transcaucasia (Zonal Subdivision, Boundaries of Series and Stages, Correlation), *Cour. Forsch.-Inst. Senckenberg*, 1985, no. 75, pp. 135–156.

Ovnatanova, N.S. and Aristov, V.A., Conodont Biostratigraphy of the Upper Devonian of Transcaucasia, *Izv. Akad. Nauk SSSR, Ser. Geol.*, 1984, no. 5, pp. 61–68.

Rzhonsnitskaya, M.A., Devonian Sediments of Transcaucasia, *Dokl. Akad. Nauk SSSR*, 1948, vol. 59, no. 8, pp. 1477–1480.

Rzhonsnitskaya, M.A., Devonian Stratigraphy and Brachiopods of the Kuznetsk Basin Margins, *Doctoral (Geol.–Min.) Dissertation*, Leningrad: VSEGEI, 1964, p. 48.

Rzhonsnitskaya, M.A., Chegodaev, L.D., Mamedov, A.B., *et al.*, Devonian of the Caucasus. Excursion 097, in *27 Mezhdunarodnyi geologicheskii kongress. Kavkaz i Vostochnyi Donbass. Svodnyi putevoditel' ekskursii* (27th International Geological Congress. Caucasus and Eastern Donbass. Guidebook for Excursions), Moscow: Nauka, 1984, pp. 69–91.

Rzhonsnitskaya, M.A. and Mamedov, A.B., Devonian-Carboniferous Boundary Sediments in Southern Transcaucasia, in *Granitsa devona i karbona na territorii SSSR* (Devonian-Carboniferous Boundary in the USSR), Minsk: Nauka i Tekhnika, 1988, pp. 124–137.

Tien, C., Devonian Brachiopoda of Hunan, *Acta Palaeontol. Sinica. New Ser.*, 1938, no. 4, p. 192.

Stratigraphy and Geological Correlation, Vol. 10, No. 1, 2002, pp. 69–76. Translated from Stratigrafiya. Geologicheskaya Korrelyatsiya, Vol. 10, No. 1, 2002, pp. 75–82.
Original Russian Text Copyright © 2002 by Kazintsova.
English Translation Copyright © 2002 by MAIK "Nauka/Interperiodica" (Russia).

Correlation of Albian Radiolarian Assemblages from the Greater Caucasus, Europe, and Mediterranean

L. I. Kazintsova

All-Russia Research Institute of Geology (VSEGEI), Srednii pr. 74, St. Petersburg, 199106 Russia

Received July 26, 1999; in final form, December 20, 1999

Abstract—Generalized data on Albian radiolarians from the Greater Caucasus refine composition of their *Spongostichomitra elatica* (middle Albian) and *Dictyomitra disparlita–Crolanium triangulare* (upper Albian) assemblages. The assemblages are correlated with coeval (or close in age) radiolarian faunas of the Crimea, Russian platform, Poland, Czechoslovakia, Romania, Yugoslavia, Italy, Spain, and Tunisia. The correlation revealed many species in common. These species suggest that above regional basins were interconnected and offer a possibility for a broad correlation of late Albian–Cenomanian deposits of the Greater Caucasus, Crimea, Russian platform, and Mediterranean region. Late Albian radiolarians of the Greater Caucasus are pictured under scanning microscope for the first time.

Key words: Greater Caucasus, Europe, Mediterranean Sea, Albian, Cenomanian, radiolarians, assemblage, association, correlation.

In the last decade, researchers have published in Russia and abroad a series of works, which show that many Albian radiolarian species, previously described by Aliev (1960–1976) in the Greater Caucasus, occur in other regions.

In addition, O'Dogherty (1994) who studied well-preserved fossils from Spain and Italy revised the former taxonomy of Caucasian radiolarians and of some Italian species, known from publications by S. Squinabol and D. Rüst. As a result, he identified, instead of 29 taxa described by Aliev, the following 14 species:

(1) *Cryptamphorella clivosa* (Aliev) = *Tricolocapsa clivosa* Aliev;

(2) *Dictyomitra communis* (Squin.) = *D. orginala* Aliev, *D. ordinaria* Aliev, *D. margarita* Aliev, *D. mutabila* Aliev, *Lithocampe lipmanae* Aliev;

(3) *Dictyomitra montisserei* (Squin.) = *D. ornata* Aliev, *Lithocampe chalilovi* Aliev;

(4) *Thanarla brouweri* (Tan) = *Dictyomitra momentaria* Aliev, *Lithocampe strelkovi* Aliev;

(5) *Stichomitra communis* Squin. = *Dictyomitra ferosia* Aliev, *D. konachkendensis* Aliev, *D. albiensis* Aliev, *D. tekschaensis* Aliev, *Cyrtocapsa ambifaria* Aliev, *Stichomitra hemisphaera* Aliev, *Lithocampe rotunda* Aliev, *Stichocapsa rüsti* Aliev;

(6) *Stichomitra simplex* (Smirn. et Aliev) = *Theocampe simplex* Smirn. et Aliev;

(7) *Spongostichomitra elatica* (Aliev) = *Dictyomitra elatica* Aliev;

(8) *Pseudodictyomitra paronai* (Aliev) = *Stichomitra paronai* Aliev;

(9) *Ps. pseudomacrocephala* (Squin.) = *Dictyomitra sagitafera* Aliev;

(10) *Xitus clava* (Parona) = *Dictyomitra clivosa* Aliev;

(11) *Rhopalosyringium mosquense* (Smirn. et Aliev) = *Sethocyrtis mosquensis* Smirn. et Aliev;

(12) *Trisyringium echitonicum* (Aliev) = *Tricolocapsa echitonica* Aliev;

(13) *Obeliscoites perspicuus* (Squin.) = *Dictyomitra producta* Aliev, *Cyrtocapsa turritica* Aliev;

(14) *Obeliscoites giganteus* (Aliev) = *Cyrtocapsa gigantea* Aliev.

I agree with the results of revision, and new taxon names are used in this work.

First information on Albian radiolarians from the Greater Caucasus is presented in the work by Dzhafarov and Agalarova (1949). Studying microfauna in northeastern Azerbaijan, they noted presence of radiolarians in several exposures of the Kyulyuli Formation (upper Albian). These were the Mt. Kyzyl-Kayadag (Village of Zarat), Sovetabad, Mt. Kamennaya (Village of Altyhagach), and Mt. Dibrar localities of southeastern Caucasus, and the Akushi locality in the northern slope of the Greater Caucasus (Fig. 1).

Studying Aptian and Albian foraminifers in the same areas of northeastern Azerbaijan, Tairov (1959) established also presence of radiolarians in the upper Albian beds (Kyulyuli and *Aucellina* horizons). He points out that these radiolarians vary in size from larger to intermediate and smaller, and that they have spherical, discoidal, and turriculated skeletons. Identi-

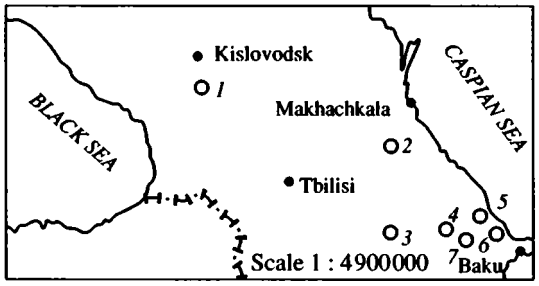

Fig. 1. Localities of sections with Albian radiolarians in the Greater Caucasus: (*1*) northern outskirts of the Podkumok village; (2) Village of Akusha; (*3*) Mt. Kelevudag (Village of Konakhkend); (*4*) Mt. Dibrar (southern slope); (*5*) Mt. Kyzyl-Koyadag (Village of Zarat); (*6*) Village of Sovetabad; (*7*) Mt. Kamennaya (Village of Altygach).

fied among them were *Cenosphaera* sp., *Porodiscus* sp., *Spongodiscus* sp., and *Lithocampe* sp.

Since 1960, Aliev has published a series of works on radiolarians from Lower Cretaceous deposits of NE Azerbaijan and the Caspian Sea region (Mts. Atachai, Keshchai, Tegchai rivers, Kelevudag and Dibrar). He was first to describe in detail the Albian radiolarians: 30 new species and several forms similar to those known from Italy (Aliev, 1965, 1967, 1968, 1969, 1976). He also distinguished the middle and upper Albian radiolarian assemblages. In the lower Albian deposits (the lower part of the Altyhagach Formation), Aliev identified single thin-walled skeletons of poorly preserved radiolarians belonging to genera *Cenosphaera, Cenodiscus, Euchitonia*, and *Dictyomitra.*

The middle Albian radiolarians were found in the upper part of the Altyhagach Formation (exposures of the Atachai, Keshchai, and Tegchai rivers, and near the Village of Konakhkend). The formation is composed of reddish brown to greenish gray and gray sandy clay with interlayers of compact (to different extent) and laminated fine-grained sandstone and gray siltstone. The thickness of the formation is 90 m. Along with radiolarians, there were discovered foraminifers of the *Gavelinella biinvoluta* Zone (Azizbekova and Abbasov, 1990) and belemnites *Neohibolites minimus* (List.), *N. pinguis* Stoll., *N. attenuatus djimiensis* Ak. Aliz., and *N. styloides* Renng. (*Melovaya sistema...*, 1988). Radiolarians, not abundant at this level, include such species as *Hexastylus aculeatus* Aliev, *Acanthosphaera atatschaica* Aliev, and *Spongostichomitra elatica* (Aliev). Other species occur not at this level only, but in overlying deposits as well. For the sake of convenience, I distinguished this radiolarian fauna as the *Spongostichomitra elatica* (former *Dictyomitra elatica*) assemblage (Kazintsova, 1990).

The upper Albian includes the Kyulyuli Formation and Autselli Horizon (Akushi, Zarat, Konakhkend, Sovetabad and Mt. Dibrar localities). The Kyulyuli Formation 5 to10 m thick is composed of alternating beds of gray (light greenish gray in places) fine-grained sandstone and dark gray, slightly calcareous clay. The *Aucellina* Horizon represents a flyschoid alternation of dark gray carbonaceous clay, mudstone, and greenish gray siltstone with rare interlayers of whitish marls. Its thickness at the Mt. Kelevudag locality is 30 m. Foraminifers found along with radiolarians are species of the *Hedbergella infracretacea* Zone (Azizbekova and Abbasov, 1990). Associated belemnites *Neohibolites styloides* Renng. and *N. subtitles* Krum. coexist with bivalves *Aucellina aptiensis* (d'Orb.) Pomp., *A. pavlovi* Sok., *A. nassibianzi* Sok., *A. gryphaeoides* Sow., *A. rengarteni* Sok., *A. pompeckyi* Pavl., and *A. anthulai* Pavl. (*Melovaya sistema...*, 1988). Radiolarian species encountered in this interval only are *Tricolocapsa kelevudacika* Aliev, *Lithostrobus parvicus* Aliev, *Pseudodictyomitra paronai* (Aliev), *Crolanium triangulare* (Aliev), and others. In my nomenclature, this is the *Dictyomitra disparlita–Crolanium triangulare* assemblage (Kazintsova, 1990).

Aliev argued that some species of the upper Albian assemblage were found in the Kemishdag Formation of the Cenomanian age (Konakhkend and Mt. Dibrar localities), and their stratigraphic range thus exceeds the Albian interval. The Kemishdag Formation represents a flyschoid sequence of gray fine-grained sandstone, limestone, foliated marl, and gray (greenish gray in places) soft carbonaceous clay. At the Mt. Kelevudag locality, the formation thickness is 50 m. Encountered along with radiolarians are foraminifers *Praeglobotruncana stephani* (Gand.), *Thalmanninella appenninica* (Renz), *Guembelitria cenomana* (Kell.), *Schackoina cenomanica* (Schacko), and others and also belemnite *Neohibolites ultimus* d'Orb (Aliev, 1965; *Melovaya sistema...*, 1988). In his paleontological plates published in the period of 1965–1976, Aliev presented only drawings of radiolarians from two Albian assemblages mentioned above.

Aliev kindly donated his collection of radiolarians from the *Aucellina* Horizon of the Mt. Kelevudag section (near the Village of Konakhkend) to my colleague G.E. Kozlova. Thus, all the specimens, we had at our disposal, were pictured under the scanning microscope (plates I and II) for the first time, and we had an opportunity to revise their taxonomy in accord with present-day classification.

Radiolarians from the same regions of northeastern Azerbaijan were studied later on by Abbasov (1987). He noted that radiolarians of the region were in the plentitude since the late Albian, and that the *Crolanium triangulare* assemblage is of that time. The assemblage includes *Cenosphaera albiensis* Aliev, *Conosphaera haeckeli* Aliev, *Porodiscus kavilkinensis* Aliev, *Crolanium triangulare* (Aliev), *Cr. cuneatum* (Smirn. et Aliev), *Obeliscoites perspicuus* (Squin.), *Xitus asymbatos* (Forman), and other species.

According to data by Agarkov and Vishnevskaya (Agarkov and Vishnevskaya, 1990; Vishnevskaya *et al.*, 1990), Albian radiolarians occur not only in the east,

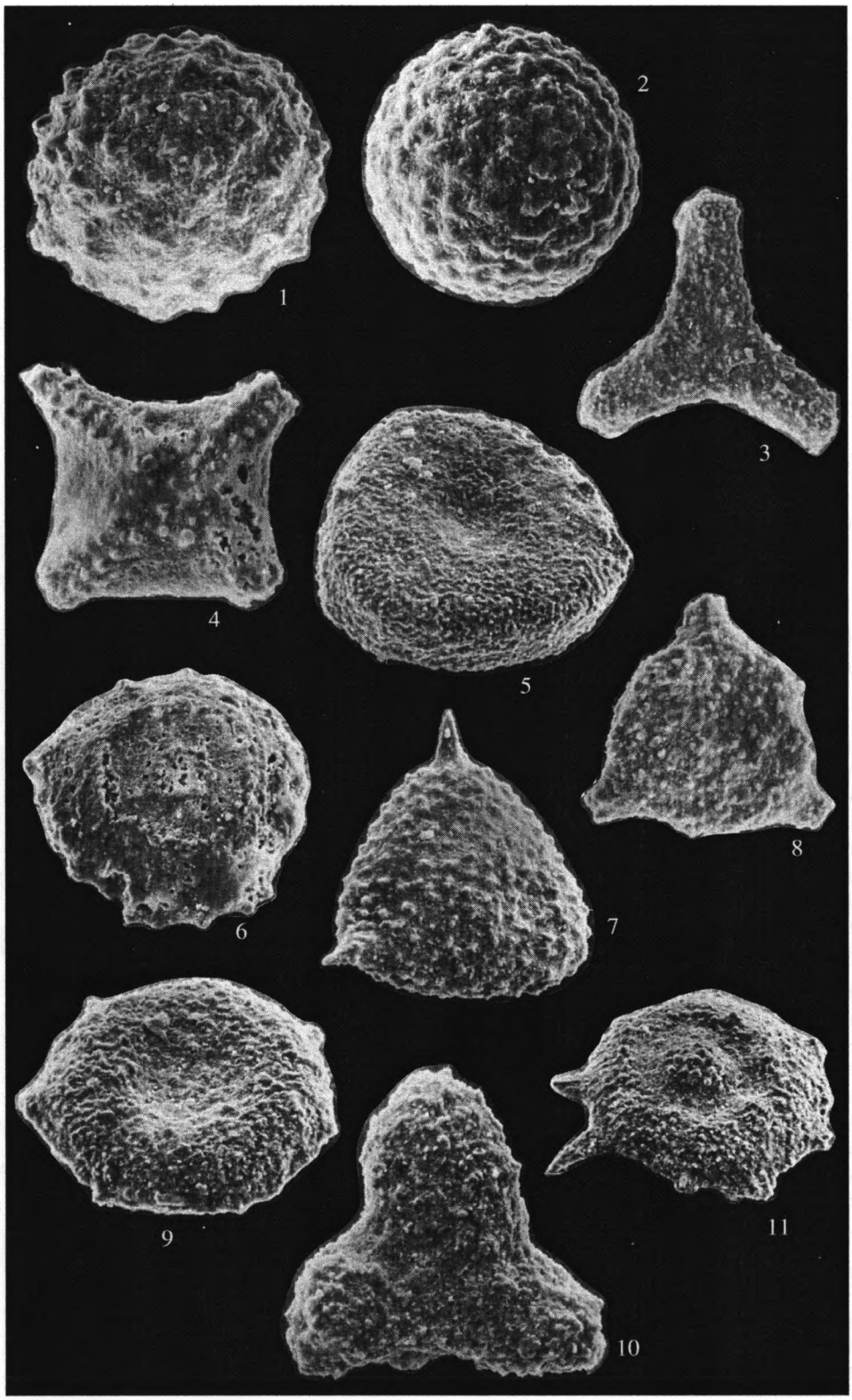

Plate I. *Dictyomitra disparlita–Crolanium triangulare* assemblage (late Albian, Greater Caucasus, Konakhkend site)
(1) *Conosphaera haeckeli* Aliev, ×215; (2) *Conosphaera sphaeroconus* Rüst, ×250; (3) *Pessagnobrachia fabiani* (Squin.), ×130; (4) *Crucella* aff. *espartoensis* Pess., ×440; (5) *Orbiculiforma* sp., ×140; (6) *Phacodiscus* sp. 1 Aliev, ×185; (7) *Alievium murphyi* Pess., ×185; (8) *Euchitonia* sp. 1 Aliev, ×220; (9) *Orbiculiforma multangula* Pess., ×185; (10) *Patulibracchium* ex gr. *obesum* Pess., ×215; (11) *Pseudoaulophacus lenticulatus* (White), ×430.

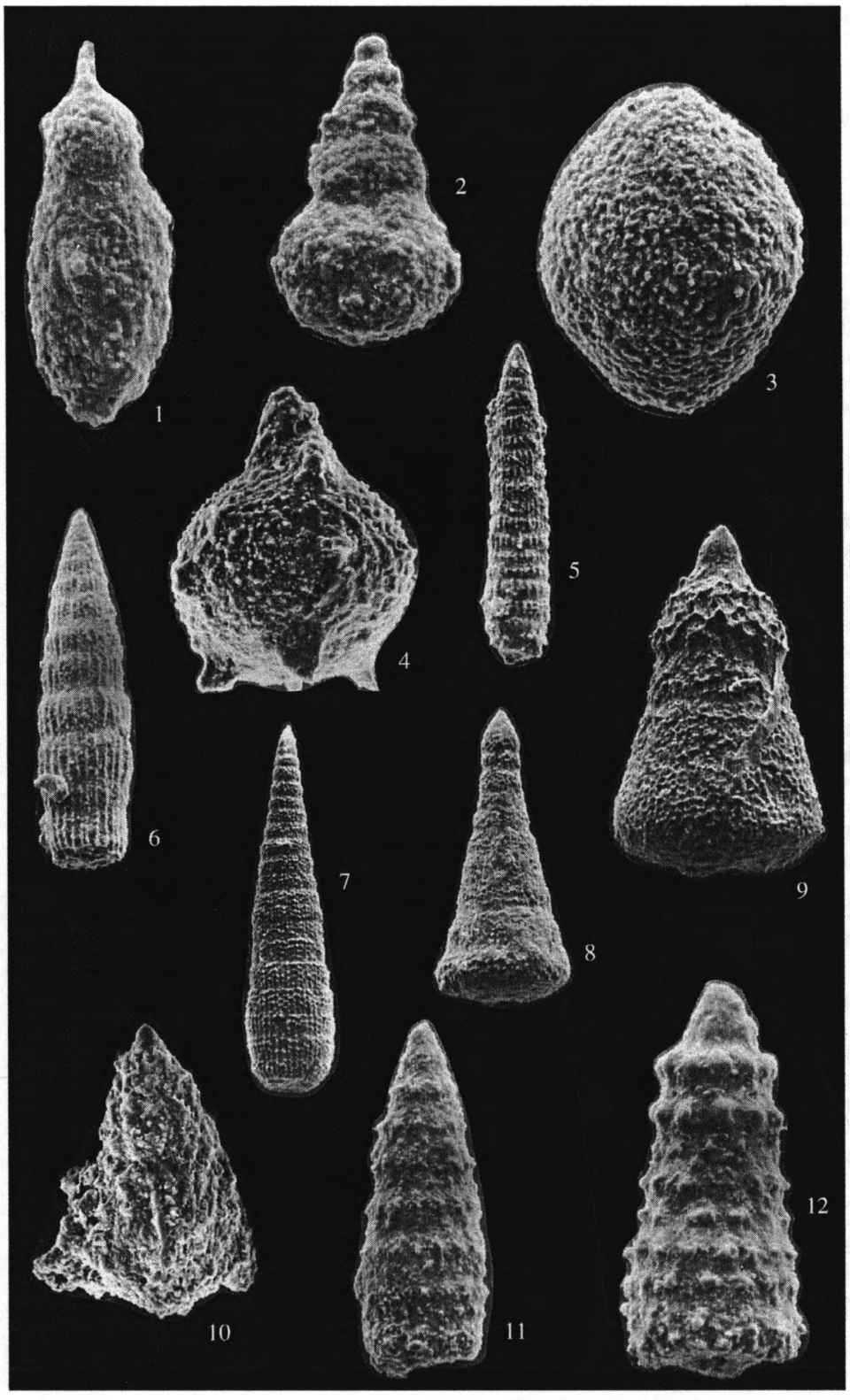

Plate II. *Dictyomitra disparlita–Crolanium triangulare* assemblage (late Albian, Greater Caucasus, Konakhkend site).
(1) *Diacanthocapsa euganea* Squin., ×250; (2) *Stichocapsa piriformis* (Tan), ×250; (3) *Cenodiscus cenomanicus* Aliev, ×215; (4) *Trisyringium echitonicum* (Aliev), ×220; (5) *Pseudodictyiomitra paronai* (Aliev), ×90; (6) *Dictyomitra montisserei* (Squin.), ×325; (7) *Obeliscoites perspicuus* (Squin.), ×45; (8) *Obeliscoites giganteus* (Aliev), ×215; (9) *Spongocapsula (?) zamoraensis* (Pess.), ×215; (10) *Crolanium triangulare* (Aliev), ×160; (11) *Xitus spicularius* (Aliev), ×145; (12) *Xitus mclaughlini* (Pess.), ×180.

but also in western and northern areas of the Caucasus. For instance, they macerated single radiolarian skeletons from light limestone of the southeastern slope of the Borgustan Range (northern outskirts of the Village of Podkumok) that is located in western spurs of the Greater Caucasus. Late Albian–early Cenomanian radiolarian species *Pseudodictyomitra pseudomacrocephala* (Squin.), *Stichomitra communis* Squin., and *Xitus spicularius* (Aliev) were also found in a small amount in cherty limestone of the same area. The researchers reported that radiolarians are poorly preserved, scanty, and much less abundant than in the eastern slope.

Summing up data on composition of middle and upper Albian radiolarian assemblages of the Greater Caucasus, we can see their distinctions and similarities. The *Spongostichomitra elatica* assemblage of the middle Albian consists of 22 species, nine of which belong to spumellarians and thirteen to nassellarians. Radiolarians are scarce and poorly preserved; most of them pass in overlying strata. The late Albian *Dictyomitra disparlita–Crolanium triangulare* assemblage includes 45 species, 16 spumellarians and 29 nassellarians. Radiolarians of the assemblage are diverse and well preserved. Some species are inherited from the underlying assemblage, whereas others cross the lower Cenomanian boundary. Eleven species are common for the middle and late Albian, and 18 species for the late Albian and Cenomanian (table).

The upper Albian and Cenomanian deposits that yield common species are frequently similar in lithology (flysch and cherty deposits) and considered integrally in many regions. Accordingly, the Cenomanian species are also considered here for comparison.

Analyzing published data on Albian and Albian–Cenomanian radiolarians in neighboring regions, I found out that species in various regions of Europe appear to be in common with the Caucasian ones (Fig. 2).

Many Caucasian radiolarians are also known from the late Albian *Orbiculiforma nevadaensis–Dictyomitra konachkendensis* assemblage of Crimea (southeastern outskirts of Simferopol) and occur together with foraminifers, ammonites, and belemnites (Gorbachik and Kazintsova, 1998). For these two regions, species in common are *Conosphaera sphaeroconus* Rüst, *C. haeckeli* Aliev, *Porodiscus kavilkinensis* Aliev, *Cenodiscus cenomanicus* Aliev, *Orbiculiforma multangula* Pess., *Patulibracchium* ex gr. *obesum* Pess., *Diacanthocapsa euganea* Squin., *Tricolocapsa kelevudacika* Aliev, *Holocryptocanium barbui* Dum., *Rhopalosyringium mosquense* (Smirn. et Aliev), *Trisyringium echitonicum* (Aliev), *Theocampe cylindrica* Smirn. et Aliev, *Stichomitra communis* (Squin.), *Crolanium cuneatum* (Smirn. et Aliev), *Cr. triangulare* (Aliev), *Obeliscoites perspicuus* (Squin.), and *Spongocapsula (?) zamoraensis* (Pess.).

Many Caucasian species were recognized in the late Albian *Porodiscus kavilkinensis–Crolanium cuneatum*

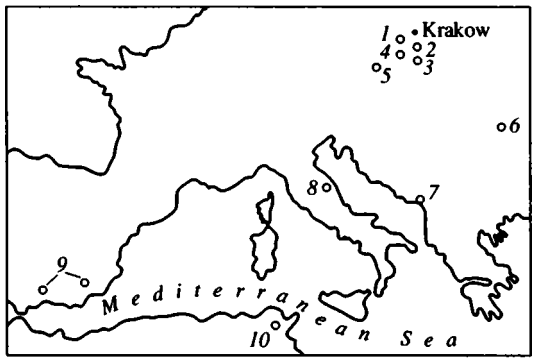

Scale
1 : 40600000

Fig. 2. Localities of sections in Western Europe, which yield radiolarian species in common with Caucasian ones: (*1*) Lipnik, (*2*) Czorsztyn, (*3*) Niedzica, and (*4*) Branisko sections Poland; (*5*) borehole Smolenske-17 in Slovakia; (*6*) Podul Dimbovitei section of Romania; (*7*) Budva section of Yugoslavia; (*8*) Scaglia Bianca Formation of Italy; (*9*) Capas Blancas Formation of Spain; (*10*) Hammam Mellgue section of Tunisia.

assemblage typical of the Paramonovo Formation of the Russian platform, where they also coexist with foraminifers (Aliev and Smirnova, 1969; Kazintsova and Olfer'ev, 1997). In this case, species in common are *Cenosphaera adornata* Aliev, *C. orginala* Aliev, *Conosphaera haeckeli* Aliev, *Porodiscus kavilkinensis* Aliev, *P. inflatus* Smirn. et Aliev, *Orbiculiforma multangula* Pess., *Diacanthocapsa euganea* Squin., *Theocampe cylindrica* Smirn. et Aliev, *Rhopalosyringium mosquense* (Smirn. et Aliev), *Dictyomitra disparlita* Aliev, *D. montisserei* (Squin.), *Stichomitra communis* Squin., *S. simplex* (Smirn. et Aliev), *Crolanium cuneatum* (Smirn. et Aliev), and *Cr. triangulare* (Aliev).

In Poland (south of Krakow, near the boundary with Slovakia), radiolarian species identical to Caucasian forms were found in several exposures of Cretaceous deposits in the Pieniny Klippen Belt of the Carpathians. Single radiolarians and associated foraminifers in the lower Albian deposits (samples L 50 and L 53, the lower part of the Lgota Beds) of the Lipnik section (near Bielsko-Biata). *Crolanium cuneatum* (Smirn. et Aliev) is identified among them (Gorka and Geroch, 1989).

The Albian–Cenomanian *Holocryptocanium barbui–H. geysersensis* assemblage of radiolarians that associates with foraminifers is established in the Branisco. This one includes the following species identical to Caucasian forms: *Holocryptocanium barbui* Dum., *Hemicryptocapsa praepolyhedra* Dum., *Stichomitra communis* Squin., *Xitus mclaughlini* (Pess.), and *Spongocapsula (?) zamoraensis* (Pess.) (Bak, 1995). The upper Albian–Turonian marls of the Niedzica section (Bak, 1996) yield foraminifers and associated radiolarians of the *Obesacapsula somphedia* assemblage, in which *Holocryptocanium barbui* Dum., *Pseudodictyo-*

Stratigraphic ranges of radiolarians in Albian–Cenomanian deposits of the Greater Caucasus

Radiolaria species	Albian		Cenomanian
	middle	late	
Hexastylus aculeatus Aliev	----------		
Acanthosphaera atatschaica Aliev	----------		
Spongostichomitra elatica (Aliev)	----------		
Cenosphaera albiensis Aliev	----------	----------	
Porodiscus kavilkinensis Aliev	----------	----------	
P. inflatus Smirn. et Aliev	----------	----------	
Trisyringium echitonicum (Aliev)	----------	----------	
Rhopalosyringium mosquense (Smirn. et Aliev)	----------	----------	
Theocampe cylindrica Smirn. et Aliev	----------	----------	
Stichomitra simplex (Smirn. et Aliev)	----------	----------	
Dictyomitra disparlita Aliev	----------	----------	
D. polycamerata Aliev	----------	----------	
Obeliscoites giganteus (Aliev)	----------	----------	
Crolanium cuneatum (Smirn. et Aliev)	----------	----------	
Pessagnobrachia cf. *fabiani* (Squinabol)		----------	
Alievium murphyi Pessagno		----------	
Pseudoaulophacus lenticulatus (White)		----------	
Orbiculiforma multangula Pessagno		----------	
Patulibracchium ex gr. *obesum* Pessagno		----------	
Crucella aff. *espartoensis* Pessagno		----------	
Tricolocapsa kelevudacika Aliev		----------	
Hemicryptocapsa cf. *praepolyhedra* Dumitrica		----------	
Diacanthocapsa euganea Squinabol		----------	
Lithostrobus parvicus Aliev		----------	
Stichocapsa piriformis (Tan)		----------	
Pseudodictyomitra paronai (Aliev)		----------	
Xitus mclaugliti (Pessagno)		----------	
Crolanium triangulare (Aliev)		----------	
Amphipyndax alamedaensis (Campb. et Clark)		----------	
Spongocapsula (?) *zamoraensis* (Pessagno)		----------	
Cenosphaera adornata Aliev		----------	----------
Conosphaera sphaeroconus Rust		----------	----------
Cenodiscus cenomanicus Aliev		----------	----------
Holocryptocanium barbui Dumitrica		----------	----------
Dictyomitra malleola Aliev		----------	----------
D. costata Aliev		----------	----------
D. communis (Squinabol)		----------	----------
Sethocapsa arca (Foreman)		----------	----------
Xitus spicularius (Aliev)		----------	----------
X. asymbatos (Foreman)		----------	----------
Cenosphaera orginala Aliev	----------	----------	----------
C. konachkendensis Aliev	----------	----------	----------
Conosphaera haeckeli Aliev	----------	----------	----------
Cenodiscaella nummulitica Aliev	----------	----------	----------
Dictyomitra montisserei (Squinabol)	----------	----------	----------
Stichomitra communis Squinabol	----------	----------	----------
Pseudodictyomitra pseudomacrocephala (Squinabol)	----------	----------	----------
Obeliscoites perspicuus (Squinabol)	----------	----------	----------

mitra pseudomacrocephala (Squin.), *Stichomitra communis* Squin., and *Xitus mclaughlini* (Pess.) are species in common with the Caucasian assemblages.

The *Acaeniotyle umbilicata* radiolarian assemblage (late Albian–early Cenomanian) from marls of the Czorsztyn section again coexists with foraminifers. Species of this assemblage, which are similar to Caucasian ones, are *Pseudodictyomitra pseudomacrocephala* (Squin.), *Spongocapsula (?) zamoraensis* (Pess.), *Stichomitra communis* Squin., *Holocryptocanium barbui* Dum., and *Xitus mclaughlini* (Pess.) (Bak, 1993).

In Slovakia, the Albian sequence of clayey limestone, marly shale, and limestone with radiolarians, ostracodes, and foraminifers was penetrated by the borehole Smolenske-17 (the Vienna Basin) in the depth interval of 1399–1605 m. Species *Holocryptocanium barbui* Dum. and *Xitus spicularius* (Aliev) from these rocks occur as well among Caucasian radiolarians (Ozvoldova, 1990).

In Romania, abundant and well-preserved radiolarians were found in the Cenomanian marl–mudstone horizon of the Podul Dimbovitei section that is exposed along the highway Rukar–Bran. Associated fossils here are foraminifers and sponge spicules. *Holocryptocanium barbui* Dum., *Hemicryptocapsa prepolyhedra* Dum., *Pseudodictyiomitra pseudomacrocephala* (Squin.), and *Xitus asymbatos* (For.) are species in common with Caucasian radiolarians (Dumitrica, 1975).

In Yugoslavia, well-preserved radiolarians were found in the middle Albian–lowermost Cenomanian siliceous rocks of the Budva zone (Montenegro coast of southern Crna Gora). Species *Holocryptocanium barbui* Dum., *Stichomitra communis* Squin., *Pseudodictyomitra pseudomacrocephala* (Squin.), and *Xitus mclaughlini* (Pess.), which occur here, are known from the Caucasus as well (Gorican, 1987, 1994).

Other regions, where Caucasian radiolarian species were found in association with foraminifers and nannoplankton, are Spain and Italy (O'Dogherty, 1994). In Spain (southeastern coast), the late Albian to early Cenomanian radiolarians are confined to white marl and marly limestone of the Capas Blancas Formation of the external zone of the Betic Cordilleras (the westernmost chain of the European Alps). In Italy (the area of the Adriatic Cape), the late Albian to early Cenomanian radiolarians are described from grayish white limestone of the Scaglia Bianca Formation in the Umbria–Marche zone (southernmost chain of the northern Apennines). O'Dogherty considers both formations as equivalents. Species originally identified by Aliev are plentiful in the above-mentioned deposits of Spain and Italy. The radiolarian *Spoletoensis* Zone (middle Albian–early Turonian) that is distinguished here includes the *Romanus, Missilis*, and *Anisa* subzones. Radiolarians of that zone, which represent species in common with Caucasian forms, are *Pessagnobrachia fabiani* (Squin.), *Trisyringium echitonicum* (Aliev), *Rhopalosyringium mosquense* (Smirn. et Aliev), *Dictyomitra montisserei* (Squin.), *Pseudodictyomitra pseudomacrocephala* (Squin.), *Ps. paronai* (Aliev), *Stichomitra communis* Squin., *St. simplex* (Smirn. et Aliev), *Xitus spicularius* (Aliev), *X. mclaughlini* (Pess.), *Spongostichomitra elatica* (Aliev), *Obeliscoites perspicuus* (Squin.), *Ob. giganteus* (Aliev), *Crolanium cuneatum* (Smirn. et Aliev), and *Cr. triangulare* (Aliev).

In 1987, A. Ormiston sent to me images of radiolarians the Fahdene Formation of Tunisia (the Hammam Mellgue section, Sample 12881). Ormiston arbitrarily referred these radiolarians to the *Obesacapsula somphedia* Foreman Zone of the late Albian–Cenomanian. In this case, species in common with Caucasian radiolarians are *Crucella espartoensis* Pess., *Holocryptocanium barbui* Dum., *Dictyomitra malleola* Aliev, *D. montisserei* (Squin.), *Xitus spicularius* (Aliev), *X. mclaughlini* (Pess.), *Pseudodictyomitra pseudomacrocephala* (Squin.), *Stichomitra communis* (Squin.), *Obeliscoites giganteus* (Aliev), and *Spongocapsula (?) zamoraensis* (Pess.).

Thus, the materials presented above show that many species in common occur in Albian radiolarian assemblages, which include 48 species in the Greater Caucasus, 17 species in the Crimea, 15 species in the Russian platform, and 19 species in the Mediterranean region. This is a clear indication of broad connections between Boreal and Tethyan seas in the late Albian–Cenomanian time, that offers a possibility of stratigraphic correlation between the above regions.

Reviewers V.S. Vishnevskaya and I.A. Basov

REFERENCES

Abbasov, A.B., Cretaceous Radiolarian Assemblages from the Southeastern Greater Caucasus, *Radiolyarii i biostratigrafiya (Informatsionnye materialy)* (Radiolarians and Biostratigraphy: Information Materials), Sverdlovsk: Ural. Otd. Akad. Nauk SSSR, 1987, pp. 3–5.

Agarkov, Yu.V. and Vishnevskaya, V.S., Late Jurassic to Cretaceous Radiolarians from the Western Slope of the Greater Caucasus, *Tez. dokl. devyatogo Vsesoyuzn. seminara po radiolyariyam* (Abstracts of the 9th All-Union Seminar on Radiolarians), Ufa: Bashkirgeologiya, 1990, pp. 5–8.

Aliev, Kh.S., *Radiolyarii nizhnemelovykh otlozhenii Severo-Vostochnogo Azerbaidzhana* (Radiolarians from Lower Cretaceous Sediments of Northeastern Azerbaijan), Baku: Akad. Nauk Azerb. SSR, 1965.

Aliev, Kh.S., New Radiolarian Species of the Valanginian and Albian Stages from Northeastern Azerbaijan, *Melovye otlozheniya Vostochnogo Kavkaza i prilegayushchikh oblastei* (Cretaceous Sediments in the Eastern Caucasus and Adjacent Areas), Moscow: Nauka, 1967, pp. 23–30.

Aliev, Kh.S., New Species of Subfamily Lithocampinae from Albian and Cenomanian Sediments of Northeastern Azerbaijan, *Izv. Akad. Nauk AzerbSSR. Ser. Nauki o Zemle*, 1968, no. 2, pp. 26–32.

Aliev, Kh.S., Distribution of Radiolarians in the Lower Cretaceous Sediments of the Southeastern Caucasus (Azer-

baijan), *Iskopaemye i sovremennye radiolarii* (Fossil and Recent Radiolarians), L'vov: L'vov Univ., 1969, pp. 45–61.

Aliev, Kh.S., New Radiolarian Species of the Lower Cretaceous from the Caspian Region of Azerbaijan, *Voprosy paleontologii i stratigrafii Azerbaidzhana* (Problems of Paleontology and Stratigraphy in Azerbaijan), Baku: Elm, 1976, pp. 114–122.

Aliev, Kh.S. and Smirnova, R.F., New Radiolarian Species of the Albian Stage from Sediments of Central Russia, *Iskopaemye i sovremennye radiolyarii* (Fossil and Recent Radiolarians), L'vov: L'vov. Univ., 1969, pp. 62–72.

Azizbekova, A.R. and Abbasov, A.B., Populations of Planktonic Microorganisms in Albian–Cenomanian Boundary Deposits of the Southeastern Caucasus, *Problemy sovremennoi mikropaleontologii. Tr. XXXIV sessii VPO* (Problems of Modern Micropaleontology, Proc. XXXIV Session of All-Union Paleontological Society), Leningrad: Nauka, 1990, pp. 179–185.

Bak, M., Late Albian–Early Cenomanian Radiolaria from the Czorsztyn Succession, Pieniny Klippen Belt, Carpathians, *Studia Geol. Polonica* (Krakow), 1993, vol. 102, pp. 177–207.

Bak, M., Mid-Cretaceous Radiolaria from the Pieniny Klippen Belt, Carpathians Poland, *Cretaceous Res.*, 1995, vol. 16, no. 1, pp. 1–23.

Bak, M., Cretaceous Radiolaria from Niedzica Succession of the Pieniny Klippen Belt in Polish Carpathians, *Acta Paleontol. Polonica*, 1996, vol. 41, no. 1, pp. 91–110.

Dumitrica, P., Cenomanian Radiolaria at Podul Dimbovitei, *14th European Micropaleontol. Colloquium, Romania,* 1975, pp. 87–89.

Dzhafarov, D.I. and Agalarova, D.A., *Mikrofauna al'bskikh otlozhenii Azerbaidzhana* (Microfauna from Albian Sediments of Azerbaijan), Baku: Aznefteizdat, 1949.

Gorbachik, T.N. and Kazintsova, L.I., Late Albian Radiolarians and Foraminifers from the Mar'ino Section (Outskirts of Simferopol, Crimea): Taxonomic Composition and Stratigraphic Position, *Stratigr. Geol. Korrelyatsiya*, 1998, vol. 6, no. 6, pp. 44–51.

Gorican, S., Jurassic and Cretaceous Radiolarians from the Budva Zone (Montenegro, Yugoslavia), *Rev. Micropaleontol.*, 1987, vol. 30, no. 3, pp. 177–196.

Gorican, S., Jurassic and Cretaceous Radiolarian Biostratigraphy and Sedimentary Evolution of the Budva Zone (Dinarides, Montenegro), *Mem. Geol. (Lausanne)*, 1994, no. 18.

Gorka, H. and Geroch, S., Radiolarians from a Lower Cretaceous Section at Lipnik Near Bielsko-Biata (Carpathians, Poland), *Ann. Soc. Geol. Poloniae*, 1989, vol. 59, pp. 183–195.

Kazintsova, L.I., Albian Radiolarians in the Soviet Union *Tez. dokl. devyatogo Vsesoyuzn. seminara po radiolyariyam* (Abstracts of Papers of the 9th All-Union Seminar on Radiolarians), Ufa: Bashkirgeologiya, 1990, pp. 37–41.

Kazintsova, L.I. and Olfer'ev, A.G., The Paramonovo Formation of the Albian in the European Part of Russia and Its Age as Indicated by Microfauna, *Stratigr. Geol. Korrelyatsiya*, 1997, vol. 5, no. 4, pp. 27–34.

Melovaya sistema Azerbaidzhana (Cretaceous System of Azerbaijan), Baku: Elm, 1988.

O'Dogherty, L., Biochronology and Paleontology of Mid-Cretaceous Radiolarians from Northern Apennines (Italy) and Betic Cordillera (Spain), *Mem. Geol. (Lausanne)*, 1994, no 21.

Ozvoldova, L., Occurrence of Albanian Radiolaria in the Underlier of the Vienna Basin, *Geol. Carpathica*, 1990, vol. 41, no. 2, pp. 137–153.

Tairov, Ch.A., Distribution of Foraminifers in Aptian and Albian Sediments Stages Northeastern Azerbaijan and Their Stratigraphic Significance, *Voprosy paleobiologii i biostratigrafii. Tr. II Cessii VPO* (Problems of Paleobiology and Biostratigraphy, Proc. II Session of All-Union Paleontological Society), Moscow: Gosgeolizdat, 1959, pp. 88–95.

Vishnevskaya, V.S., Agarkov, Yu.V., Zakariadze, G.S., and Sedaeva, K.M., Late Jurassic Radiolarians from the Greater Caucasus as Key Fossils Determining Age and Formation Settings of Ophiolites in the Lesser Caucasus, *Dokl. Akad. Nauk SSSR*, 1990, vol. 310, no. 6, pp. 1417–1421.

Stratigraphy and Geological Correlation, Vol. 10, No. 1, 2002, pp. 77–87. Translated from Stratigrafiya. Geologicheskaya Korrelyatsiya, Vol. 10, No. 1, 2002, pp. 83–93.
Original Russian Text Copyright © 2002 by Bugrova, Zakrevskaya, Tabachnikova.
English Translation Copyright © 2002 by MAIK "Nauka/Interperiodica" (Russia).

New Data on Paleogene Biostratigraphy of the Eastern Crimea

E. M. Bugrova*, E. Yu. Zakrevskaya, and I. P. Tabachnikova***

**All-Russia Scientific Research Geological Institute, Srednii pr. 74, St. Petersburg, 199026 Russia*

***V.I. Vernadskii State Geological Museum, Russian Academy of Sciences, ul. Mokhovaya 11, Moscow, 103009 Russia*

Received December 28, 1999; in final form, November 22, 2000

Abstract—New data on different organic remains and biostratigraphy of the Paleocene–lowermost Eocene type section in the Indol structural–facies zone of the Indol–Kuban' depression of the Eastern Crimea are discussed. The section demonstrates a succession of different faunal types from the shallow-water accumulation zone of carbonates (the southwestern Crimea) to relatively deep-water zone of pelagic sedimentation (the northern Caucasus). According to distribution of planktonic foraminifers, the section is subdivided into *Acarinina acarinata, Morozovella subbotinae* (s.l.), *Morozovella aragonensis*, and *Acarinina bullbrooki* zones, the standard units of the Paleogene scale elaborated for southern regions of the former USSR. Discocyclins discovered from the Paleocene interval of the section characterize the SBZ3, SBZ10, and SBZ11 zones of the Tethyan zonation of larger foraminifers. Nannoplankton assemblages studied for the first time in this section correspond, entirely or partly, to those of *Heliolithus kleinpelli* (NP6), *Heliolithus riedeli* (NP8), *Discoaster multiradiatus* (NP9), *Discoaster lodoensis* (NP13) and *Discoaster sublodoensis* (NP14) zones. Smaller foraminifers allowed subdivision of the section into new *Anomalina danica, Karreriella zolkaensis, Asterigerina bartoniana kaasschieteri,* and *Pseudogaudryina pseudonavarroana* (with two subzones) local zones correlated with regional zones of this faunal group. Transformations of the basin ecosystem and correlation with sections of neighboring regions are briefly discussed.

Key words: Paleocene, Eocene, nummulitids, smaller foraminifers, nannoplankton, zonal subdivision, correlation, ecosystem transformations.

INTRODUCTION

The section in the Nasypkoi Ravine (6 km west of Feodosiya, Fig. 1) is most complete among other Paleogene sections in the eastern part of the Crimea Peninsula. It was accepted as a type section of the Indol structural–facies zone (Fig. 2) of the Indol–Kuban' depression (Shutskaya, 1970; *Paleogenovaya systema*, 1975). The structure of the section is described in detail (Maimin, 1951; Shutskaya, 1960, 1970; Nemkov and Barkhatova 1961; Gorbach, 1972).

The composition of organic remains and their distribution throughout the section is, however, insufficiently studied. Moreover, various faunal groups are investigated to a different extent in both the Paleocene and lower Eocene parts of the section. Composition of mollusks, brachiopods, and echinoderms from the terrigenous–carbonate flyschoid sequence in the lowermost part of the section (Danian Stage) is known sufficiently well (Makarenko, 1961; Gorbach, 1972). Rare rotaliids and anomalinids were also found here (Shutskaya, 1960; Gorbach, 1972). Biostratigraphic subdivision of the upper part of the section (upper Paleocene–Eocene) was based on planktonic foraminifers, occurring throughout and best studied in the Eocene interval (Shutskaya, 1970). Analyzing planktonic foraminifers, Shutskaya referred to the *Acarinina acarinata* Zone the lower sequence of alternating sandstones and clays, which are carbonate-free or slightly calcareous in the lower part, but calcareous and intercalated with limy interbeds above. She reported on the assemblage of arenaceous benthic foraminifers occurring in these sediments and similar in composition to foraminifers from the Goryachii Klyuch Formation of the North Caucasus. Nemkov and Barkhatova (1961) noted rare discocyclins of the *Discocyclina archaici* group in conglomerate-like detrital limestones of the basal part of the sequence. In the uppermost beds, this group is associated with single nummulites of the *Nummulites planulatus* group. According to occurrence of these larger foraminifers, the entire sequence was referred to the lower Eocene that contradicted data on distribution of smaller foraminifers.

The member of black carbonate-free clays was reported to enclose a diverse nannofossil assemblage correlated with the lowermost Eocene (the *Globorotalia aequa* Zone) and rare *Nummulites planulatus* (determination by G.I. Nemkov). The overlying calcareous clays with interbeds of nummulitic limestone (the *Nummulites planulatus* Zone) are correlated with the uppermost Bakhchisarai Formation (or Bakhchisaraian regional stage) exposed in the eponymous area. Higher, the *Globorotalia aragonensis* and *Acarinina bullbrooki* (*Acarinina crassaformis* after Shutskaya) zones were defined in calcareous clays and marls.

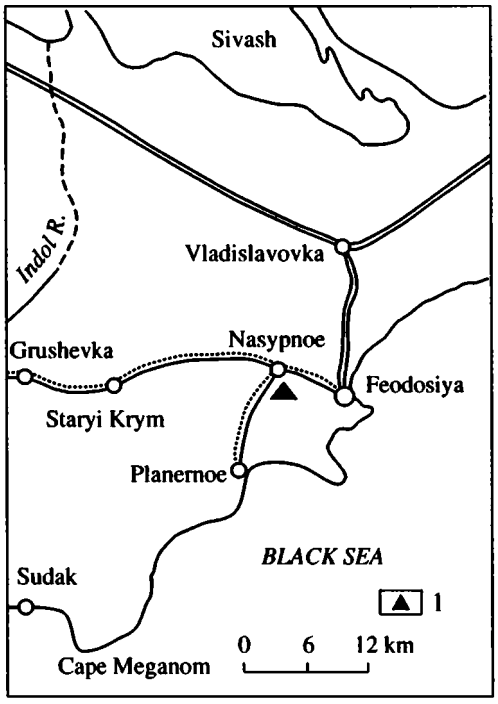

Fig. 1. Geographic location of the studied Nasypkoi section (1).

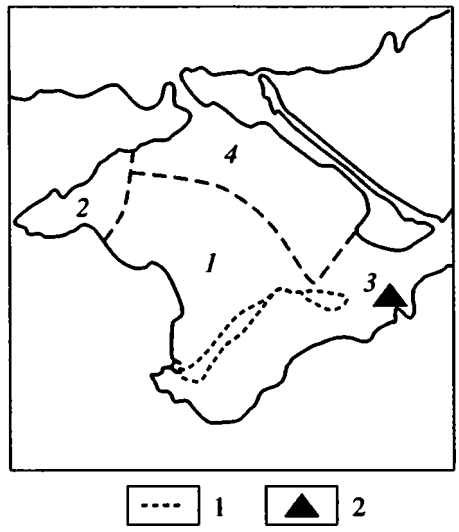

Fig. 2. Schematic structural–facies zoning of the Crimea during the Paleogene time (modified after Shutskaya, 1970): (1) area of exposures of Paleocene and Eocene rocks; (2) Nasypkoi section. Structural–facies zones: (*1*) Al'ma, (2) Tarkhankut, (*3*) Indol, (*4*) Sivash.

Data on distribution of smaller benthic foraminifers are very scarce. The rotaliid genus *Cibicides* and large anomalinids were found in the lower Paleocene part of the section (Shutskaya, 1960; Gorbach, 1972). Shutskaya reported on the occurrence of an assemblage of arenaceous foraminifers of the North Caucasian type in the upper Paleocene interval. Several species were detected in the basal Eocene layers, and almost complete absence of benthic foraminifers was noted in younger sediments. Three early Eocene nummulitid species and 11 *Discocyclina* and *Asterocyclina* species were listed amid larger foraminifers (Nemkov and Barkhatova, 1961; Nemkov and Portnaya, 1969; Portnaya, 1969), but this faunal group have not been used for the detailed stratigraphic subdivision. Nannofossils from the Nasypkoi section have never been studied.

The complex study of the material sampled by Zakrevskaya in 1997 provided new data on distribution of nummulitids and discocyclinids (determinations by Zakrevskaya), nannofossils (determinations by Tabachnikova), and smaller benthic and planktonic foraminifers (determinations by Bugrova). Simultaneously, new data were used for interpretation of ecosystem transformations in the basin during the Paleocene–initial Eocene.

Because of a poor exposition, it is difficult to compile the continuous Paleocene–Eocene succession. Therefore we pay main attention to paleontological characteristics of successive levels in the section (Fig. 3) and to discrimination of biostratigraphic units on the basis of changes in foraminiferal and nannoplankton assemblages. Using the original materials and published data, were also compared the composition of faunal assemblages from the investigated section with those from neighboring regions and correlated the corresponding sections.

PALEONTOLOGICAL CHARACTERISTIC AND BIOSTRATIGRAPHY OF THE SECTION

Paleocene

Flyschoid terrigenous–carbonate deposits in the lower Paleocene part (about 130 m thick) of the section were most thoroughly described by Gorbach (1972) who referred the lower 30-m-thick interval to the Danian Stage and upper 100 m, to the Montian Stage according to stratigraphic distribution of bivalves and brachiopods. Our own observations showed that the uppermost part of the sequence is composed of relatively deep-water facies of an open sea basin, which are represented by obscurely bedded fine-grained to microgranular clayey limestones with an admixture of silty material. The detrital component consists of fragments of foraminiferal tests, echinoid spines, and sponge spicules. Also present are rare whole shells of small rotaliids and globigerinids (Samples 31, 32; Fig. 3).

The flyschoid sequence is overlain, with erosion marks, by a member of calcareous and calcareous–terrigenous rocks 6 m thick (Samples 33–37; Fig. 3). Its basal part is composed of brecciated coarse-grained algal limestones with glauconite and phosphorite nodules and with large (2–8 cm) fragments of underlying clayey limestone and fragments or accumulations of non-carbonate clays, the alteration products after ashy tuffs.

Organic remains from the matrix are *Lithotamnium* algae and bryozoans. In addition, we recognized fragments of echinoids, crinoids, bivalves, serpulids, smooth ostracod carapaces, benthic and planktonic foraminifers. In the fragments of calcareous clay, organic remains are represented by abundant *Globigerina* tests. Higher in the section, there is a thin bed of fine-grained recrystallized limestone with small benthic and planktonic foraminifers (Bed 3, Sample 35; Fig. 3).

The upper part of the member is composed of alternating calcareous sandstones and clayey rocks. These glauconite–quartz fine-grained sandstones contain abundant detritus of *Lithotamnium* algae, Bryozoa, and foraminifers. Foraminifers from compact organogenic limestones of the lower part of the member (samples were studied in thin sections) are mainly represented by benthic species, prevalent among which are small smooth-walled rotaloid forms of the *Cibicidoides, Gyroidina*, and *Brotzenella* genera (Samples 33–35). Arenaceous forms appear in upper (terrigenous) layers. The calcareous sandstones yield the assemblage of following, poorly preserved smaller foraminifers: *Globigerina* sp., *G.* ex gr. *varianta* Subb., *Gaudryina* aff. *gigantica* (Subb.), *Marssonella* sp., *Ataxophragmium variabile* (d'Orb.), *Nodosaria* sp., *N.* ex gr. *latejugata* Gumb., *Pseudonodosaria radicula* (Linne), *Dentalina* sp., *Robulus* sp., *Astacolus* sp., *Globulina* sp., *Anomalina danica* (Brotz.), *Cibicidoides* sp., *C. spiropunctatus* (Gall. et Morrey), and *Buliminella* sp. Representatives of the *Cibicidoides* genus are prevalent. Found single tests belonging to the miliolid genus *Triloculina* (Sample 33) are characteristic of Paleogene lagoonal facies. The base of the member (Sample 34) is marked by the first occurrence of single discocyclins from the *Discocyclina archaici* group, and more abundant *Discocyclina seunesi* (Douv.) occur in its upper part. In the zonal scale of Tethyan larger foraminifers, the range of this species corresponds to the SBZ3 zone attributed to the late Selandian–early Thanetian (Less, 1987; Serra-Kiel *et al.*, 1998). This species is noted at the Montian–Thanetian boundary in the Western Carpathian section of algal limestones (Samuel, *et al.*, 1972) and in the upper Paleocene of Abkhaziya (Mrevlishvili, 1978). Similar facies with *Discocyclina seunesi* are referred to the Thanetian Stage (Zernetskii, 1977) in the adjacent area of the Mokryi Indol River (Deredzhilga valley).

In composition and its ecological type, the above assemblage of smaller foraminifers is close to that from the Danian *Anomalina danica–Mississippina binkhorsti* local zone of the southwestern Crimea (Preobrazhenskii *et al.*, 1998). This zone is traceable away from the Bakhchisarai area, because its characteristic species *Mississippina binkhorsti, Pararotalia tuberculifera*, and *Rosalina brotzeni* are known from the Tarkhankut Peninsula as well (reference borehole 1, depth interval of 314.95–314.90 m; collection by V.G. Morozova, Moscow State University).

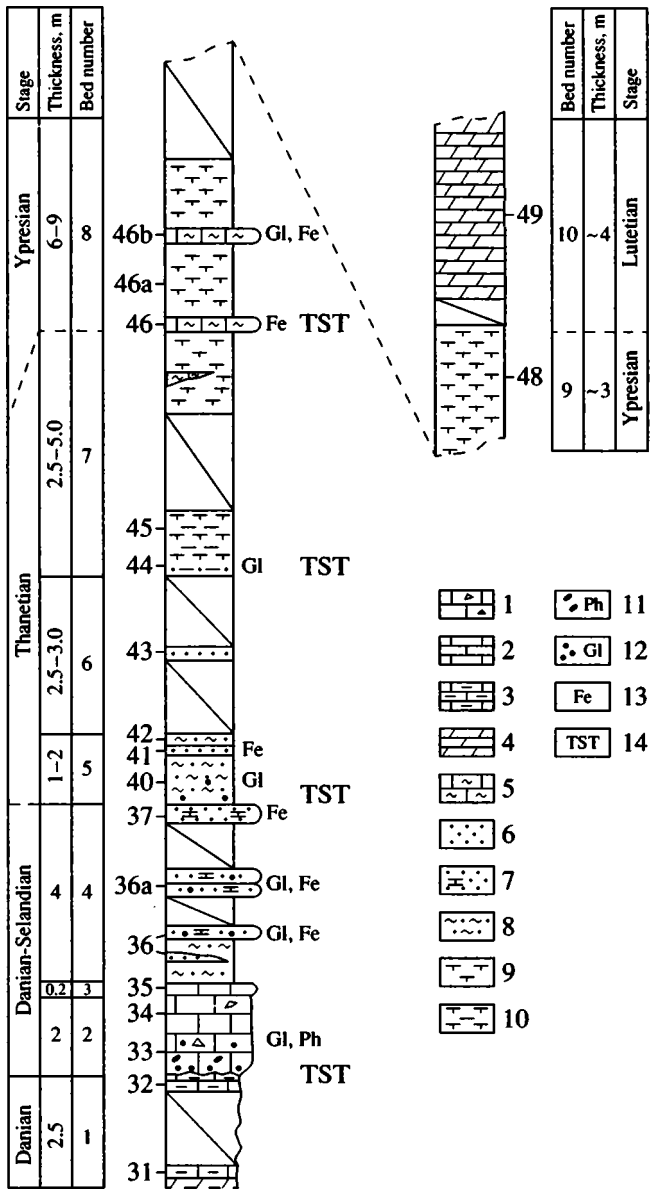

Fig. 3. Schematic uppermost Paleocene–lowermost Eocene section in the Nasypkoi Ravine: (1) brecciated coarse-detrital or algal, (2) fine-detrital, (3) fine-detrital or clayey, and (5) nummulitic limestone; (4) marl; (6) carbonate-free sandstone and silt; (7) calcareous sandstone; (8) sandy–silty carbonate-free, (9) carbonate, and (10) slightly calcareous clay; (11) phosphorite; (12) glauconite; (13) Fe hydroxides; (14) signs of the transgressive tract (sample numbers are designated right of the column).

None of species typical of the Montian Stage or Inkerman regional stage was found in the considered section. Nevertheless, Gorbach (1972, p. 37, Fig. 7) notes that underlying limestones with remains of mollusks *Solemya pavlovi* Arkh., *Phacoides* cf. *montensis* Cossm., and *Miltha contorta* Defr. enclose also "rare anomalinid tests up to 0.5 cm across." In the southwestern Crimea, rotaliids of large dimensions, anomalinids included, are characteristic of the assemblage from ree-

fal facies of the uppermost Danian *Stomatorbina imnkermanica* local zone (Preobrazhenskii *et al.*, 1998). In addition, *Stomatorbina inkermanica* (Schutzk.), *Pararotalia* sp. (test up to 0.625 mm in size), *Viveja beaumontiana* (d'Orb.), *Anomalina danica* (Brotz.), *Ataxophragmoides* sp., *Rosalina* sp., *Cibicidoides* spp., and others (10 species and 10 genera in total) were found in bryozoan limestones overlying Danian sandstones in the upper part of the lower Paleocene sequence that is exposed to the west, in the central Crimea (the Ak-Kaya section, collection by E.Yu. Zakrevskaya). Thus, we do not rule out possible presence of the *Stomatorbina inkermanica* Zone in the Nasypkoi section. Similarly to sections of the southwestern Crimea, smaller foraminifers were not found in this section.

In general, we have different views on the age of the considered part of the section. Bugrova believes that the entire member is correlative with the Belokamenskii Horizon (*Stratigraficheskaya skhema...*, 1987) that includes the Danian Stage and Inkerman Formation. According to Zakrevskaya, discocyclins of the member suggest its late Paleocene (probably, late Selandian–initial Thanetian) age, and the unit can be correlated with similar facies of *Lithotamnium* Limestone that yields *Discocyclina seunesi* in the Deredzhilga valley (the Mokryi Indol River basin, central Crimea). Finally, the opinion of Shutskaya that the member of algal limestones and sandstones should be referred to the upper Thanetian *Acarinina acarinata* Zone finds no confirmation in our material.

The considered section is visually lacking unconformities except for that well manifested one between flyschoid (Bed 1) and shallow-water (Bed 2) deposits and noted by previous researchers. However, the lithological analysis revealed erosional surfaces also within the upper Paleocene–lower Eocene calcareous–clayey sequence, which point to the unstable deposition regime. Transgressive phases of sedimentation are distinguished at the levels of Beds 2, 5, 7, and 8 (Fig. 3). In general, sedimentary cycles defined in the Nasypkoi Ravine section correspond to those in the southwestern Crimea.

Calcareous sandstones of Bed 4 are overlain by sandy–silty non-carbonate and low-carbonate clays about 5 m thick (Beds 5–6, Samples 40–43, Fig. 3). Their basal part encloses thin interbeds (lenses) of loose fine-grained quartz sandstones and (or) siltstones with an admixture of glauconite and Fe hydroxides. Rounded fragments of fish teeth and (Samples 42, 43) coprolites also occur here. These sediments represent a transgressive tract similar to that well expressed at the beginning of sedimentation cycle V (Thanetian) in the southwestern part of the Crimean basin. Single tests of planktonic genera *Globigerina* and *Acarinina*, and nannofossils of the *Heliolihus kleinpelli* Zone (determination by N.G. Muzylev) are registered only in the siltstone bed of the lower part of the clayey sequence (Sample 40). Its remaining part is characterized by the assemblage of benthic, mainly arenaceous foraminifers. Shutskaya (1970) reported on 18 species from these sediments. In fact, the assemblage is more diverse and consists of many species belonging to 28 genera. These are mainly primitive tests of *Rhizammina, Rhabdammina, Saccammina, Bathysiphon, Hyperammina, Proteonella, Caudina, Bogdanowiczella, Spirillina, Glomospirella, Usbekistania, Nodellum, Reophax, Haplophragmoides, Trochammina*, and others. They associate with *Rhizammina indivisa* Brady, *Rhabdammina cylindrica* Glaessn., *Bathysiphon nodosariaformis* Subb., *Lituotuba bucharica* Suleim., *Repmanina charoides* (Jones et Park.), *Ammodiscus incertus* d'Orb., *Ammodiscoides kumaensis* Schutzk., *Nodellum velascoense* Cushm., *Trochamminoides irregularis* Cushm., *T. planulatus* Schutzk., *Haplophragmoides caucasicus* Schutzk., *H. kubanensis* Schutzk., *Kolchidina* sp., *Textularia plummerae* (Lalick.), *Bolivinopsis kurtishensis* Balakhm., *Vulvulina* aff. *fursenkoi* Moroz., *Clavulinoides* sp., *Bigenerina plana* Subb., *Arenobulimina presli* Reuss, *Gaudryina* aff. *pyramidata* Cushm., *Martinottiella* sp., *Marssonella oxycona* Reuss, *Karreriella kabardinensis* (Schutzk.), and *K. zolkaensis* (Schutzk.). Foraminifers with a calcareous test are rare and include *Nodosaria* sp., *Cibicidoides* sp., *Stensioeina caucasica* (Subb.), and *Bulimina golubjatnikovi* Moroz.

After unexposed interval of 2 m, silty clays of Bed 6 are replaced by slightly calcareous variegated clays (Bed 7, Samples 44–45). The latter grade into lower Eocene calcareous clays with interbeds and lenses of nummulitic limestones (Bed 8). The base of Bed 7 corresponds to the erosion surface marked by occurrence of glauconite grains, rounded fish teeth, and reworked foraminifers of the *Stomatorbina* genus. This boundary also marks a sharp change in composition of smaller foraminifers. Because of the increased carbonate content in sediments, abundance of arenaceous foraminifers decreases, although their characteristic species still occur. Simultaneously, calcareous forms appear in Bed 7 including representatives of genera *Vaginulina, Dentalina, Nodosaria*, and species *Eponides obtusus* (Burr. et Holl.), *Karreria* sp., *Osangularia plummerae* (Brotz.) *Brotzenella* ex gr. *acuta* (Plumm.), *Anomalinoides* aff. *welleri* (Plumm.), *Intricatus spiropunctatus* (Gall. et Morrey), *Bulimina midwayensis* Plumm., *B. golubjatnikovi* Morz., and *Reussela paleocenica* (Brotz.). In the top layer (Sample 45), small tests of *Asterigerina* ex gr. *bartoniana* ten Dam are found as single specimens, but they become widespread in higher stratigraphic horizons. According to species composition, these sediments are referred to the *Karreriella zolkaensis* regional zone of the Thanetian Stage (*Zonal'naya stratigrafiya...*, 1991).

Planktonic foraminifers characteristic of a deeper basin zone are *Acarinina acarinata* Subb., *A. intermedia* Subb., *Globigerina velascoensis* Cushm., *G. nana* Chal., *G. pileata* Chal., and first *Morozovella aequa*

(Cushm. et Renz) (Sample 44). This assemblage is correlative with that of the *Acarinina acarinata* Zone crowning the Paleocene section.

Composition of nannofossils also points to the Thanetian age of host deposits. For instance, basal layers of the interval under consideration (Sample 42) yield an impoverished assemblage of the *Heliolithus kleinpelli–Heliolithus riedeli* Zone that consists of single *Discoaster* cf. *lenticularis* Br. et Sull. and *Heliolithus* sp. The assemblage of the *Heliolithus riedeli* Zone is distinguished higher in the section (Samples 43–44). It consists of *Heliolithus riedeli* Br. et. Sull., *H.* sp. *Chiasmolithus bidens* Br. et Sull., *Discoaster* sp., *D.* cf. *lenticularis* Br. et Sull., and *Toweius* spp. Higher (Sample 45), it is replaced by an impoverished assemblage of the *Discoaster multiradiatus* Zone, which includes, in addition to the zonal species, also *Discoaster megastypus* Br. et Sull., *D. delicatus* Br. et Sull., *D. falcatus* Br. et Sull., *D. lenticularis* Br. et Sull., *Toweius* spp., and *Facsiculithus* spp. As is known, sediments of the *Discoaster multiradiatus* Zone are absent in the Bakhchisarai stratotype section (Muzylev, 1980), where the terminal Thanetian corresponds to a hiatus.

The noteworthy fact is the appearance of *Morozovella aequa* (Cuhm. et Renz) (Sample 45) in *Discoaster multiradiatus* (NP9) nannoplankton zone or *Acarinina acarinata* foraminiferal zone of the terminal Paleocene. Concurrent arenaceous foraminifers include representatives of the *Kolchidina* genus, which are unknown from Eocene sediments.

Morozovella aequa was macerated from another sample of dark gray clays that was collected approximately at the same level 50 m away from Sample 45 along the strike of Bed 7. The foraminiferal assemblage from this sample is dominated by arenaceous forms of the *Karreriella zolkaensis* zone: *Bathysiphon nodosariaformis* Subb., *Budashevaella* sp., *Repmanina charoides* (Park. et Jones), *Spirillina* sp., *Glomospirella* sp., *Trochamminoides irregularis* Cushm., *T. planulatus* Schutzk., *Haplophragmoides kubanensis* Schutzk., *Kolchidina* sp., *Boliviniodes spectabilis* Grzyb., *Textularia plummerae* (Lalick.), and *Karreriella zolkaensis* (Schutzk.). The associated calcareous species are *Tappanina selmensis* (Cushm.), *Osangularia plummerae* (Brotz.), *Pseudoparella modica* Subb., *Nittallides trumpyi* (Nutt.), *Loxostomoides applinae* (Plumm.), *Bulimina golubjatnikovi* Moroz., *B. midwayensis* Plumm., *B.* aff. *aksuatica* Moroz., and *Globocassidulina caucasica* (Subb.). Planktonic foraminifers are represented by *Globigerina nana* Chal. (abundant), *G. bacuana* Chal., rare *G. eocaenica* Terq., *Acarinina intermedia* Subb.), *Morozovella aequa* (Cuhm. et Renz) (two specimens), *Pseudohastigerina eocenica* (Berggr.), and minute *Chiloguembelina* sp. Poorly preserved spherical radiolarians (pyritized casts) are present as well.

According to Shutskaya (1970), species *Globigerina nana, G. bacuana*, and *Acarinina intermedia* appear in the uppermost Thanetian Stage and transit into the Eocene, whereas *Morozovella aequa (=Globorotalia aequa)* characterizes only the synonymous zone of the lowermost Eocene. This is true for shallow-water sections of the southwestern Crimea, where this zone was first defined. Nevertheless, according to many publications, the biozone of this species is wider and spans the uppermost Paleocene–lowermost Eocene. Therefore, in absence of indicative accompanying assemblage of Eocene foraminifers, we do not accept the appearance level of this species as indicative of the Eocene boundary.

The *Karreriella zolkaensis* Zone of the Nasypkoi section is hardly correlative with the synchronous *Anomalina fera* local zone of the southwestern Crimea. In this area, marls of the Kacha Formation enclose an assemblage of the different type: abundant planktonic and diverse secretory benthic species, among which anomalinids is a dominant group. For instance, about 15% of the assemblage from the reference section of Borehole 1 (Bakhchisarai) are represented by planktonic forms. Prevalent amid benthic foraminifers (23 species of 20 genera) are secretory forms (43.6% of rotaliids, 20% of nodosariids); arenaceous species compose only 14% of the assemblage.

The assemblage of agglutinated foraminifers similar to that from the Nasypkoi section is established (Voloshina and Denega, 1969) only in the Kerchenskii Peninsula (Kuibyshevo and Moshkar'evka localities), being unknown elsewhere in the Crimea. In species composition, the Nasypkoi assemblage is analogous to that from slightly calcareous and carbonate-free sediments of the Goryachii Klyuch Formation in the northwestern Caucasus and central Ciscaucasia region (Subbotina, 1950; Shutskaya, 1956, Bugrova *et al.*, 1988; and others). Par example, in sections exposed along the Kuban' and Kheu rivers, arenaceous foraminifers are confined to sediments of the *Acarinina subspherica* and *Acarinina acarinata* zones. In these rocks, they are represented by species of 23 genera, and carbonate layers yield calcareous forms (10 genera) of the same composition. Further to the east, in the Malyi Balkhan and western Kopetdag, a similar assemblage occurs only in deep-water sediments of the upper Paleocene. Development of such assemblages is usually thought to be related to the oxygen deficiency in bottom waters. It is apparent that changes in hydrodynamic environments in the initial Thanetian time affected a significant area. In future, a particular attention should probably be paid to the study of microfossils from the basal part of the clayey sequence with nannoplankton assemblage of the *Heliolithus kleinpelli–Heliolithus riedeli* zones (NP6–9).

Eocene

The lower Eocene section about 15 m thick in total is composed of yellowish gray calcareous clay with interbeds 0.2–0.5 m thick, lenses, and blocks of nummulitic limestones. Its rocks rest upon the eroded sur-

face of the Paleocene deposits. The limestone bed with nummulites occurring at the base of the section (Bed 8, Sample 46) encloses the reworked Late Cretaceous specimens of *Stensioeina pomerrana* Brotzen, Paleocene species *Morozovella* cf. *angulata* (White), fragments of fish teeth, and sponge spicules. An insignificant hiatus is recorded at the base of the overlying limestone layer with nummulites (Sample 46b), Late Cretaceous *Globotruncana* sp. and *Globorotalites michelenianus* d'Orb., fish teeth, bryozoan fragments, and sponge spicules.

Thus, despite the absence of distinct hiatuses in this part of the section, the redeposited fauna and some lithological features of sediment reworking point to transgressive moments in the early Eocene sedimentation. The distinct transgressive onlap of similar nummulitic limestones is established approximately 0.5 km upstream, in the Nasypkoi Ravine right side (Sample 20–23). At this site, nummulitic limestones with thin basal interbed (0.2 m) of oncolitic limestone overlie with an angular unconformity the lower Paleocene flyschoid sequence that is uplifted approximately by 50 m relative to the section under consideration.

Nummulitic limestones (Samples 46, 46b) with the grainstone texture are of organogenic–detrital type. Unlike nummulitic limestones of the southwestern and central Crimea, they contain rather abundant fragments of *Lithotamnium* algae, bryozoans, and echinoderms. The assemblage of larger foraminifers from the Nasypkoi section shows the following peculiar features: the almost complete absence of forms belonging to microspherical generation, low species diversity of nummulitids and discocyclinids, absence of the *Assilina* genus and large nummulite species, and high diversity and abundance of asterocyclinids, prevalent among which are inflated and asteroid forms of the *Orbitoclypeus* genus. Similar features are characteristic of the North Caucasian nummulitid and discocyclinid assemblages. These features differ the Nasypkoi assemblage from the Bakhchisarai one. The lower bed (Sample 46) yields preponderant *Nummulites planulatus* (Lam.) (A) and *N.* aff. *laxus* Schaub (A, B) in association with less common *N. pustulosus* (Donc.) (A), *N. praelucasi* Douv. (A), *N. escheri* Schaub (A), and *Operculina karreri* Pen. (A, B). Rare discocyclinids are represented by *Discocyclina archaici* (Schlum.) *staroseliensis* Less, *D. archaici archaici* (Schlum.), *D. pseudoaugustae* Port., *D. dispansa* (Sow.) *taurica* Less, and *Nemkovella evae* Less. More abundant asterocuyclinids include *Orbitoclypeus varians* (Kauf.) *horsarrieuensis* Less, *O. varians* (Kauf.) *angoumensis* Less, *O. ramaraoi* (Sam.) *suvlukayensis* Less, *O. ramaraoi* (Sam.) *crimensis* Less, *O. douvillei douvillei* (Schlum.), *O. bayani* (Mun.-Chalm.), *O. bayani* (Mun.-Chalm.) sp. nov., and *Asterocyclina stella taramellii* (Mun.-Chalm.) These fossils are characteristic of the upper part of the lower Ypresian (lower Cuisian in the Mediterranean scale)—SBZ10 Zone, which corresponds to the *Assilina plana* (Zakrevskaya, 1993) or *Assilina placentula–Nummulites nemkovi* (Nemkov and Barkhatova, 1961) zones (the interval of the upper Bakhchisarai Formation–basal Simferopol' Beds).

A clay bed intercalated with nummulitic limestones (Sample 46a) yields single discocyclinids *Nemkovella strophiolata* (Gumb.) *fermonti* Less. In the upper layer (Sample 46b), composition of the nummulitid assemblage changes: *Nummulites nitidus* de la Harpe (A, B) appears to become abundant; species *N. pustulosus* Donc., *N. planulatus* (Lam.) and *N. escheri* Schaub are rare; small *Operculina karreri* Pen. and *O.* aff. *parva* Douv. are accompanied by large *O. escheri* Hott. and *O. marinelli* Dain. *Discocyclina fortisi* (d'Arch.) *simferopolensis* Less and *D. trabayensis trabayensis* Neum. are determined amid discocyclins in addition to *D. archaici archaici* that characterizes the higher stratigraphic level. Asterocyclinids are represented by *Orbitoclypeus chudeaui chudeaui* (Schlum.), *O. ramaraoi* (Sam.) *crimensis* Less, *O. varians* (Kauf.) *angoumensis* Less, *O. bayani* (Mun.-Chalm.) sp. nov., *Asterocyclina stella taramelli* (Mun.-Chalm.), and *A.* aff. *alticostata* (Nutt.). This assemblage reliably indicates the middle Cuisian (the initial late Ypresian) age of enclosing sediments, which are thus correlative with the Zone SBZ11. In sections of the southwestern Crimea, this level corresponds to the *Nummulites distans* Zone of the Simferopol' Beds.

Owing to the general shoaling of the basin in the early Eocene, corresponding sediments (Bed 8, Samples 46, 46a) contain abundant planktonic foraminifers that compose up to 98% of smaller foraminifers. Foraminifers occur in association with rare spherical and discoid radiolarians. The limestone bed at the base of the section (Sample 46) yields abundant *Pseudohastigerina eocaenica* (Bergg.) and common *Globigerina compressaeformis* Chal., *G. velascoensis* Cushm., *G.* ex gr. *bacuana* Chal., *G. zuensis* Schutzk., and *G. incisa* Hillebr. These forms coexist with rare specimens of *Acarinina pseudotopilensis* Subb., *A. camerata* Chal., and *A. acarinata* Subb., and with small tests of *Globorotalia perclara* Loebl. et Tapp., *Morozovella wilcoxensis* Cushm. et Pont., and others. This foraminiferal assemblage correlates enclosing sediments with the lower Eocene *Morozovella subbotinae* s. l. Zone of the Crimean–Caucasian stratigraphic scale. According to Schutskaya (1970), the zonal species proper do not occur in the section under consideration. The range of this species may correspond to the gap in observations, although it is not inconceivable that the section includes only the upper part of the zone, where *M. subbotinae* can be missing (Table).

The benthic group includes species that are absent in underlying beds. These are *Siphotextularia plana* Bugr., *Asterigerina bartoniana kaasschieteri* Tzaneva, *Pararotalia rotaliaformis* (Davidz.), *Euuvigerina praecompacta* (Balakhm.), *Aragonia aragonensis* (Nutt.), and others. In addition, Shutskaya (1970) found *Pseudogaudryina externa* Bugr. (determined as *Gaud-*

Correlation of biostratigraphic units defined in the Paleogene Nasypkoi section with zones of the Crimean-Caucasian and Tethyan standard scales

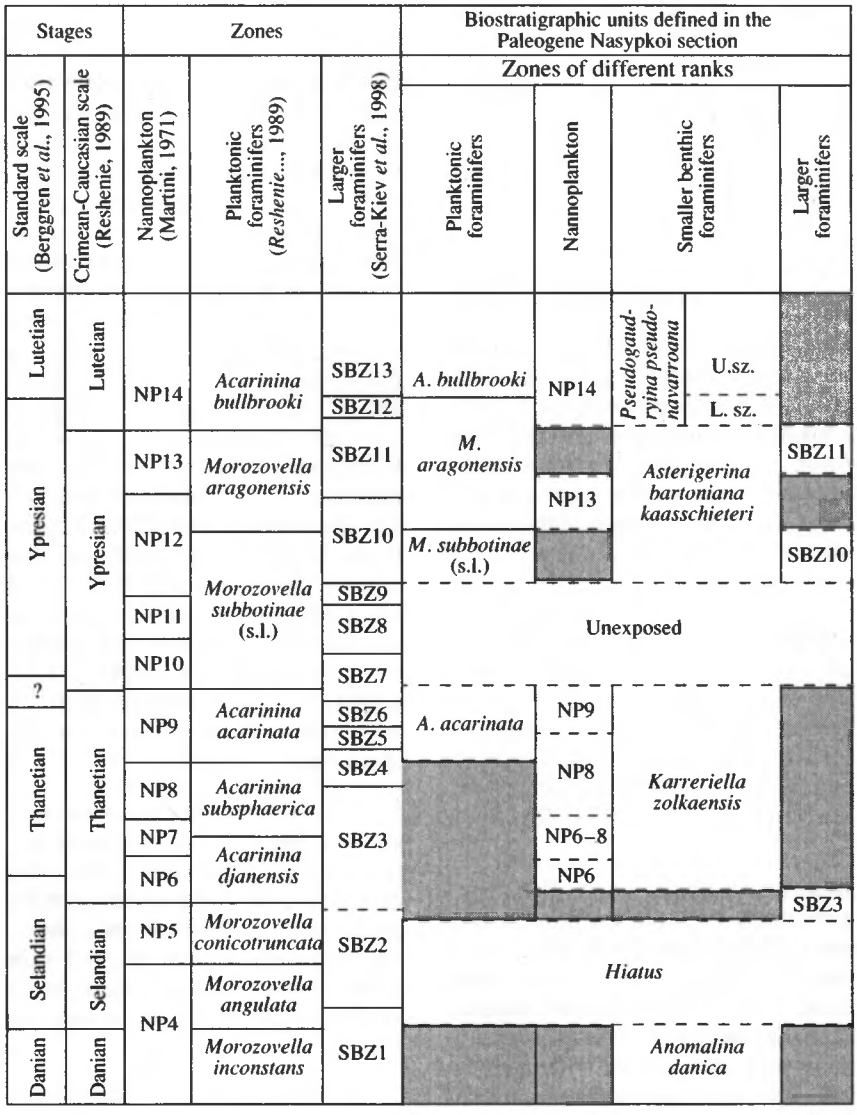

Note. Hatched areas indicate the absence of microfossils or their zonal assemblages. (U.sz.) upper subzone, (L. sz.) lower subzone.

ryina navarroana Cushm.) and *Marginulinopsis eofragaria* Balakhm., which characterize, along with the aforementioned species the *Pseudogaudryina externa* regional zone (*Zonal'naya stratigrafiya...*, 1991). According to composition of smaller foraminifers, this part of the section can be reliably correlated with the *Asterigerina kaasschieteri* local zone of Bakhchisarai Formation of the southwestern Crimea (Bugrova, 1988). This zone is also defined in the Nasypkoi section. A similar foraminiferal assemblage is distinguished in the Gaurdak–Kugitang area of southeastern Turkmenia.

Higher in the section (Sample 46a), the composition of planktonic foraminifers changes: *Pseudohastigerina eocaenica* (Bergg.) is still abundant here and coexists with *Acarinina pseudotopilensis*, but *Morozovella aragonensis* (Nutt.), *M.* sp., and *Acarinina interposita* Subb. appear for the first time. This part of the section corresponds to the higher *Morozovella aragonensis* Zone of the Crimean–Caucasian scale.

The composition of benthic foraminifers also slightly changes at this level. Despite their low abundance, they become diverse and represented by 30 species of 28 genera (Samples 46a, 46b). The assemblage includes arenaceous species of genera *Textularia, Spiroplectammina, Clavulinoides, Martinottiella, Haplophragmoides, Trochammina*, and others (10 genera in total), but secretory forms are more abundant and diverse. Species occasionally occurring in the lower part of this interval (Sample 46a) are *Asterigerina bar-*

toniana kaasschieteri Tzaneva, **Pararotalia rotaliaformis* (Davidz.), **Euuvigerina praecompacta* (Balakhm.), **Sphaerogypsina antiqua* Bugr., **Angulogerina wilcoxensis* (Cushm. et Pont.), *Siphogeneroides elegantus* (Plumm.), **Bolivina crenulata* Cushm., *B. wilcoxensis* Cushm., *Aragonia aragonensis* (Nutt.), *Pleurostomella subnodosa* Reuss, **Siphonina wilcoxensis* Cuschm., *Osangularia* sp., *Nuttallides* aff. *trumpyi* (Nutt.,), *Stilostomella* sp., *Bulimina aksuatica* Moroz., **Globimorphina conica* (Cushm. et Todd), and also rare specimens of genera *Lagena, Dentalina, Globorotalites, Discorbis, Rosalina, Cibicidoides, Pleurostomella, Stilostomella*, and *Fursenkoina.*

The asterisk marks species characteristic of the *Asterigerina bartoniana kaasschieteri* local zone of the Bakhchisarai Formation in the southwestern Crimea (Bugrova, 1988). It should be noted that some of them (*Siphotextularia plana, Pararotalia rotaliaformis, Sphaerogypsina antiqua*) appear in the upper part of this formation, and this fact may point to a hiatus in the Nasypkoi Ravine section. Thus, benthic foraminifers of the *Asterigerina bartoniana kaasschieteri* Zone are distributed, in addition to the *Morozovella subbotinae* s.l. Zone, also in the basal part of the *Morozovella aragonensis* Zone of the Nasypkoi Ravine section. The lower part of the Simferopol' Beds in the Bakhchisarai section contains some species of the *Asterigerina kaasschieteri* Zone, although other assemblages present there characterize units of the bed rank because of a different facies confinement (Kraeva, 1972; Bugrova, 1988).

The nannoplankton assemblage from this level (Sample 46a) is represented by species of the *Discoaster lodoensis* Zone (NP13 Zone after E. Martini). It includes approximately 15 species, six of which belong to the *Discoaster* genus. These are *Discoaster lodoensis* Br. et Ried., *D.* cf. *sublodoensis* Br. et Sull. (transitional forms), *D. binodosus* Mart., *Rhabdosphaera crebra* (Defl.) Br. et Sull., small *Reticulofenestra* ex gr. *umbilica* (Lev.) Mart. et Ritzk., and others. The upper part of the clayey sequence (about 5 m) is unexposed.

After the unexposed interval of about 10 m, we observed a bed of light gray calcareous silty clay about 3 m thick (Bed 9, Sample 48). Planktonic foraminifers representing about 90% of the assemblage considerably differ in composition from their assemblage in underlying strata. Prevalent among them are *Planorotalites* species appearing for the first time: *P. planoconica* (Subb.), *P. elongatus* (Glaessn.), and *P. pseudoscitula* (Glaessn.). They are accompanied by abundant *Globigerina pseudoeocena pseudoeocena* Subb., *G. transversa* Chal., *G.* ex gr. *varianta* Subb., *Pseudohastigerina eocaenica* (Bergg.), and by less common *Globigerina inaequispira* Subb. and *Acarinina pseudotopilensis* Subb. Other organic remains are first *Acarinina pentacamerata* (Subb.), *A. marksi.* (Martin), *A. interposita* Subb., and *A. triplex* Subb., single specimens of *Morozovella caucasica* (Glaessn.), and radiolarians. According to composition of planktonic foraminifers, this part of the section is referred to the uppermost *Morozovella aragonensis* Zone (Table).

Benthic foraminifers are also of different composition at the level in question. They become more diverse, represented by 38 genera, 13 of which belong to arenaceous forms. The level marks disappearance of shallow-water ornamented *Pararotalia rotaliaformis*, granulated *Asterogerina* forms, and *Sphaerogypsina antiqua.* Species inherited from underlying sediments are *Siphogeneroides elegantus, Angulogerina wilcoxensis, Siphonina wilcoxensis, Aragonia aragonensis, Bulimina aksuatica, Loxostomoides applinae*, and *Globimorphina conica.* The newly appeared forms are *Pseudogaudryina* sp., *P. pseudonavarroana* (Balakhm.), *Fursenkoina* aff. *dibollensis* (Cushm. et Appl.), *Spiroplectammina* aff. *carinatiformis* Moroz., *Vulvulina* sp., *Dorothia postbulletta* Balakhm., *Silicosigmoilina* sp., *Robulus laticostatus* (Tutkow.), *Gyroidina* aff. *depressaeformis* N. Byk., *Anomalina* aff. *calymene* (Gumb.), *Brotzenella* aff. *discoidea* (Balakhm.), *Cibicidoides* aff. *hadjibulakensis* (N. Byk.), *Asterigerina* sp. nov., *Hopkinsina compacta* Balakhm., *Sporobulimina eocena* N. Byk., *Bulimina mitgarziana* Balakhm., *B.* aff. *vermiformis* N. Byk., *Uvigerina muralis* (Terq.), *Kolesnikovella elongata* (Halk.), and others. Species of nodosariids genera *Lagena, Robulus*, and *Dentalina* are abundant.

In addition, we discovered infusoria *Aubertianella taurica* Bugr. and new species of this genus. The former taxon was described from uppermost strata of the Bakhchisarai Formation and lowermost Simferopol' Beds of the Bakhchisarai area. The assemblage of benthic foraminifers of such composition is untypical of sections in the southwestern Crimea, where this level is characterized by shallow-water facies with nummulites.

Species *Pseudogaudryina pseodonavarroana, Bulimina mitgarziana, Hopkinsina compacta, Kolesnikovella elongata, Sporobulimina eaocena*, and others found in the Nasypkoi section characterize the lower subzone of the regional *Pseudogaudryina pseodonavarroana* Zone, the index species of which is *Bulimina mitgarziana* (*Zonal'naya stratifrafiya...*, 1991). Other forms, usually occurring in the upper subzone, imply that this part of the section corresponds to the uppermost part of the lower subzone.

The diverse and abundant nannoplankton occurring here includes *Discoaster lodoensis* Br. et Ried., *D.* cf. *sublodoensis* Br. et Sill., *D. bifax* Bukry, *D. wemmelensis* Ach. et Strad., *D. binodosus* Mart., *D. barbadiensis* Tan, *D. kuepperi* Strad., *D. cruciformis* Mart., *Micrantholithus pinguis* Br. et Sull., *Helicosphaera lophota* (Br. et Sull.) Haq, *H. seminulum* (Br. et Sull.) Roth, *Chiasmolithus grandis* (Br. et Sull.) Rad., *Zigrhablithus crassus* Strad., *Z. bijugatus* (Defl.) Defl., *Reticulofenestra* ex gr. *umbilica* (Lev.) Mart. et Ritzk., *Rhab-*

dosphaera crebra P.-N., *Rh. vitrea* (Defl.) Br. et Sull., and others.

Accordingly, host sediments can be correlated with the lower subzone of the *Discoaster sublodoensis* Zone (NP14) in the scale by Martini (1971), or with the XI intrazonal unit in the scale by Steurbant (1988). Most characteristic species of the unit are *Discoaster wemmelensis, D. bifax*, and *Zigrhablithus crassus*. The unit corresponds to the lower part of the NP14 Zone and terminates the Ypresian Stage in the International stratigraphic scale. In the Crimean–Caucasian region, the NP14 Zone is referred to the middle Eocene (*Reshenie...*, 1989).

Spherical and discoidal radiolarians occurring as single specimens are unknown at this level in sections of the southwestern Crimea and northern Caucasus.

Clays are overlain by light gray marls (apparent thickness 4 m) with abundant remains of pelagic organisms (Sample 49), which are represented predominantly by planktonic foraminifers (51%), to a lesser extent by radiolarians (37%), and by less abundant (11–13%) benthic forms. Species of two *Globigerina* and *Acarinina* genera compose approximately a half of the planktonic foraminifer assemblage. Persistent components are *Globigerina pseudoeocaena* Subb., *G. inaequispira* Subb., *G. karabogasica* Kopev., *Acarinina pseudotopilensis* Subb., *A. intermedia* Subb., and *Planorotalites pseudoscitula* (Glaessn.). Less common accompanying forms are *A. pentacamerata* (Subb.), *A.* aff. *gravelli* (Bronn.), *A. bullbrooki* (Bolli), and single specimens of *Morozovella caucasica* (Glaessn.). Host deposits of this assemblage are correlated with the basal part of the *Acarinina bullbrooki* Zone in the standard stratigraphic scale. Thus, planktonic foraminifers and nannoplankton imply, like in the standard scale, slightly different levels of the lower boundary of the Lutetian Stage.

Despite their low abundance, benthic foraminifers are highly diverse, represented by 36 genera. Arenaceous forms are rare (*Spiroplectammina, Textularia, Vulvulina*, and *Dorothia* genera), and prevalent secretory species show a peculiar composition. Many of them could not be determined at the species level. The identifiable species are *Dorothia postbulletta* Balakhm., *Spiroplectammina carinatiformis* Moroz., *Chrysalogonium eocenicum* Cushm. et Todd, small thin-walled flattened *Asterigerina* sp. nov., *Osangularia pteromphalus* Hagn, *Valvulineria filaeprincipes* Hagn, *Cibicidina dampelae* (N. Byk. et Chram.), *Sporobulimina eocena* N. Byk., *Uvigerina muralis* Terq., *Hopkinsina* aff. *compacta* Balakhm., *Kolesnikovella elongata* (Halk.), *Pleurostomella* aff. *acuta* Hantk., *Fursenkoina* aff. *dibollensis* (Cushm. et Appl.), and others. Despite the absence of zonal species, this deep-water assemblage is correlative with that of the upper subzone of the regional *Pseudogaudryina pseudonavarroana* Zone that corresponds to the basal part of the Lutetian Stage.

In addition to spherical and discoidal radiolarians, their assemblage includes representatives of Sponguridae and Nasselaria, which appear for the first time at this level.

Changes in the species composition and dominant morphotypes of benthic foraminifers are remarkable. Their thin-walled unornamented tests became widespread instead of earlier biconvex and flattened-convex, frequently ornamented rotaloid forms. They associate species with subcylindrical tests, which are also abundant (genera *Dentalina, Chrysalogonium, Kolesnikovella, Stilostomella, Pleurostomella, Cuneus, Trifarina, Bolivina*, and *Fursenkoina*). Taxa of such morphology usually characterize the oxygen deficiency in the bottom water layer (Kaiho, 1990) and, probably, in the surface muddy sediments. Taking into consideration the occurrence of radiolarians and sponge spicules, the water chemistry also slightly changed and became enriched in silica. The studied part of the section is terminated with light-colored marls of the *Hantkenina alabamensis* Zone.

CONCLUSION

The study of microfaunal assemblages in the Paleocene–lowermost Eocene sequence, the Nasypkoi Ravine locality, provided an opportunity to define biostratigraphic units of foraminifer and nannoplankton zonal scales. We distinguished the Paleogene zones of planktonic foraminifers, which are accepted as unified for southern areas of the former Soviet Union. These are *Acarinina acarinata, Morozovella subbotinae* s. l., *Morozovella aragonensis*, and *Acarinina bullbrooki* zones that were established earlier by Shutskaya. In distinction from her scheme, we failed to define the *"Globorotalia aequa"* Zone as an autonomous unit in the basal part of the Eocene, because its index species occurs also in the foraminiferal *Acarinina acarinata* and nannoplankton *Discoaster multiradiatus* zones of the Paleocene. In addition, this species coexists with the assemblage of arenaceous foraminifers similar to those from the uppermost Paleocene of the northern Caucasus.

Nannoplankton assemblages, which have not been studied before, allowed recognition of *Heliolithus kleinpelli, Heliolithus riedeli, Discoaster multiradiatus*, uppermost *Discoaster lodoensis*, and lowermost *Discoaster sublodoensis* zones in the investigated section. Dissimilarly to sections of the southwestern Crimea, planktonic foraminifer and nannoplankton assemblages reveal presence of the uppermost Thanetian layers in the study area. We also established that lower boundaries of the foraminiferal *Acarinina bullbrooki* and nannoplankton *Discoaster sublodoensis* zones do not correspond to their levels in the acknowledged Crimean–Caucasian scale.

Smaller benthic foraminifers that are studied for the first time enabled subdivision of the section into differ-

ent-rank units. These are the following units: the local *Anomalina danica* Zone known also in the Danian of the southwestern Crimea; the regional *Karreriella zolkaensis* Zone with an assemblage characteristic of the uppermost Paleocene (Thanetian Stage) in the northern Caucasus, southern East European platform, and Central Asia; the local *Asterigerina bartoniana kaasschieteri* Zone of the basal Eocene that was earlier defined in the southwestern Crimea; and the regional *Pseudogaudryina pseudonavarroana* Zone with two subzones, the boundary between which coincides with that between the Ypresian and Lutetian stages. Depending on the facies confinement, this fauna occurring at different levels is close in composition to assemblages from either the southwestern Crimea, or northern Caucasus. Such a dependence is important for detailed correlation of Paleogene sections not only in these regions, but in more distant areas as well.

The studied species composition of oldest discocyclins implies the initial late Paleocene (late Selandian, time of the SBZ3 Zone) age of enclosing sediments. Based on composition of nummulitids and dicocyclinids, two stratigraphic intervals are defined for the first time in the lower Eocene interval of the section: the lower Cuisian (SBZ10 Zone) corresponding to the upper part of the Bakhchisarai Formation and the middle Cuisian (SBZ11 Zone) correlative with the middle part of the Simferopol' Beds. It is established also that the generic and species composition of larger Eocene foraminifer assemblages is similar to that of assemblages from the northwestern Caucasus. In addition, we suspect that sedimentation during the late Paleocene–early Eocene was unstable due to hydrodynamic changes in response to tectonic activity in the region.

Reviewers V.A. Krasheninnikov and I.A. Basov

REFERENCES

Berggren, W.A., Kent, D.V., Swisher, C.C., and Aubry, M.-P., A Revised Cenozoic Geochronology and Chronostratigraphy, *Geochronology Time Scale and Global Stratigraphic Correlation, SEPM Spec. Publ.*, Berggren, W.A. *et al.*, Eds., 1995, vol. 54, pp. 129–212.

Bugrova, E.M., Nikolaeva, I.A., Panova, L.A., and Tabachnikova, I.P., To Zonal Subdivisions of the Paleogene in Southern Regions of the Soviet Union, *Sov. Geol.*, 1988, no. 4, pp. 96–107.

Bugrova, E.M., Zonal Subdivisions of the Eocene in the Bakhchisarai District of the Crimea, Data on Smaller Foraminifers, *Izv. Akad. Nauk SSSR, Ser. Geol.*, 1988, no. 1, pp. 82–91.

Gorbach, L.P., *Stratigrafiya i fauna mollyuskov rannego paleotsena Kryma* (Stratigraphy and Molluscan Fauna, the Early Paleocene of the Crimea), Moscow: Nedra, 1972.

Kaiho, K., Global Changes of Paleogene Aerobic/Anaerobic Benthic Foraminifera and Deep-Sea Circulation, *Palaeogeogr., Palaeoclimatol., Palaeoecol.*, 1991, vol. 83, nos. 1–3, pp. 65–85.

Kraeva, E.Ya., Stratigraphic Distribution of Benthic Foraminifera in Eocene and Oligocene Sediments of the Crimean Borehole Stratotype, *Tektonika i stratigrafiya*, 1972, no. 4, pp. 91–106.

Less, G., *Az Europai Orthophragminak oslenytana es retegtana*, Budapest: Geol. Hung., Ser. Paleontol., Fasc. 511, 1987.

Maimin, Z.L., *Tretichnye otlozheniya Kryma* (Tertiary Sediments of the Crimea), Moscow: Gostoptekhizdat, 1951.

Makarenko, D.E., Mollyuski paleotsenovikh vidkladiv v Krimu, *Tr. Inst. Geol. Nauk Akad. Nauk UkrRSR. Ser. Stratigr., Paleontol.*, 1961, vol. 40.

Martini, E., Standard Tertiary and Quaternary Calcareous Nannoplankton Zonation, *Proc. II Plank. Confer. (Roma, 1970), pt. V.II.*, Roma, 1971, pp. 739–785.

Mrevlishvili, N.I., *Nummulity Gruzii i ikh stratigraficheskoe znachenie* (Nummulites from Georgia and Their Stratigraphic Significance), Tbilisi: Tbil. Univ., 1978.

Muzylev, N.G., *Stratigrafiya paleogena yuga SSSR po nannoplanktonu (Severnyi Kavkaz i Krym)* (Nannoplankton-Based Stratigraphy of the Paleogene in the Southern Soviet Union, Northern Caucasus and Crimea), Moscow: Nauka, 1980.

Nemkov, G.I. and Barkhatova, N.N., *Nummulity, assiliny i operkuliny Kryma* (Nummulites, Assilins, and Operculins from Crimea), Moscow: Muzei Karpinskogo, 1961.

Nemkov, G.I. and Portnaya, E.L., Asterocyclins from the Lower Eocene Sediments of the Southeastern Crimea, *Izv. Vyssh. Uchebn. Zaved., Geol. Razved.*, 1969, no. 4, pp. 33–40.

Portnaya, V.L., *Diskotsiklinidy eotsenovykh otlozhenii Kryma i ikh biostratigraficheskoe znachenie* (Discocyclinidae of the Eocene Sediments and Their Biostratigraphic Significance), Moscow: Mosk. Gos. Univ., 1974.

Preobrazhenskii, M.B., Bugrova, E.M., and Nikolaeva, I.A., Ecosystem Transformation in the Carbonate Sedimentation Zone of the Paleocene Crimean Basin: Data of Microfacies Analysis, *Tez. dokl. XLIV sessii Paleont. obshchestva* (Abstracts of XLIV Session of Paleontological Society), Petersburg, 1998, pp. 80–82.

Resolution of XVI Plenary Session of the Paleogene Commission, VSEGEI, April 6–12,1987, *Postanovleniya MSK i ego postoyannykh komissii* (Resolutions of International Stratigraphic Committee and Its Permanent Commissions), Leningrad: Vses. Geol. Inst., 1989, no. 24, pp. 51–54.

Samuel, O., Borza, K., and Kohler, E., *Microfauna and Lithostratigraphy of the Paleogene and Adjacent Cretaceous of the Middle Van Valley (West Carpathian)*, Bratislava: Geol. Ust. D. Stura., 1972.

Serra-Kiel, J., Hottinger, L., Caus, E., *et al.*, Larger Foraminiferal Biostratigraphy of the Tethyan Paleocene and Eocene, *Bull. Soc Geol. France*, 1998, vol. 169, no. 2, pp. 281–299.

Shutskaya, E.K., Stratigraphy of the Lower Paleogene Horizons in the Central Cis-Caucasus, *Tr. Inst. Geol. Nauk Akad. Nauk SSSR*, 1956, issue 164, Geol. Ser. (no. 71), pp. 3–119.

Shutskaya, E.K., Stratigraphy of the Lower Paleogene in the Northern Cis-Caucasus and Crimea, *Paleogenovye otlozheniya yuga Evropeiskoi chasti SSSR* (Paleogene Sediments in the Southern European Part of the Soviet Union), Moscow: Akad. Nauk SSSR, 1960, pp. 207–229.

Shutskaya, E.K., *Stratigrafiya, foraminifery i paleogeografiya nizhnego paleogena Kryma, Predkavkaz'ya i zapadnoi chasti Srednei Azii* (The Lower Paleogene Stratig-

raphy, Foraminifers, and Paleogeography of the Crimea, Cis-Caucasus, and Western Part of Central Asia), Moscow: Nedra, 1970.

Steurbant, E., New Early and Middle Eocene Calcareous-Nannoplankton Events and Correlation in Middle to High Latitudes of the Northern Hemisphere, *Newslett. Stratigr.*, 1988, vol. 18, no. 2, pp. 99–115.

Stratigraficheskaya skhema paleogenovykh otlozhenii Ukrainy (unifitsirovannaya) (Unified Stratigraphic Scheme for Paleogene Sediments of Ukraine), Kiev: Nauk. Dumka, 1987.

Stratigrafiya SSSR. Paleogenovaya sistema (Stratigraphy of the USSR, Paleogene System), Moscow: Nedra, 1975, pp. 5–524.

Subbotina, N.N., Microfauna and Stratigraphy of the El'burgan and Goryachii Klyuch Horizons, *Tr. Vses. Nauchno-Issled. Geol.-Razved. Inst., Nov. Ser.*, 1950, vol. 51, pp. 5–112.

Voloshina, A.M. and Denega, B.I., Stratigraphic Subdivision of Paleocene to Eocene Deposits of the Kerchenskii Peninsula, *Dop. Akad. Nauk UkrRSR, Ser. B., Geol., Geofiz., Khimiya, Biol.*, 1969, no. 4, pp. 294–298.

Zakrevskaya, E.Yu., *Assiliny, operkuliny i ranikotalii Kryma i ikh biostratigraficheskoe znachenie* (Assilinae, Operculinae, and Ranicotaliae of the Crimea and Their Biostratigraphic Significance), Moscow: Nauka, 1993.

Zernetskii, B.F., Paleocene Discocyclinidae First Found in the Crimea, *Materiali do paleontologii kainozoyu Ukraini* (Materials on the Cenozoic Paleontology of the Ukraine), Kiiv: Nauk. Dumka, 1977, pp. 55–59.

Zonal'naya stratigrafiya fanerozoya SSSR (spravochnoe posobie) (Zonal Stratigraphy of the Phanerozoic in the Soviet Union, Guide Book), Koren', T.N., Ed., Moscow: Nedra, 1991.

Stratigraphy and Geological Correlation, Vol. 10, No. 1, 2002, pp. 88–96. Translated from Stratigrafiya. Geologicheskaya Korrelyatsiya, Vol. 10, No. 1, 2002, pp. 94–103.
Original Russian Text Copyright © 2002 by Tarasov, Dorofeyuk, Vipper.
English Translation Copyright © 2002 by MAIK "Nauka/Interperiodica" (Russia).

The Holocene Dynamics of Vegetation in Buryatia

P. E. Tarasov*, N. I. Dorofeyuk, and P. B. Vipper**†**

**Moscow State University, Geographical Department, Vorob'evy gory, Moscow, 119899 Russia*
***A. N. Severstov Institute of Ecology and Evolution Problems, Russian Academy of Sciences, Leninskii pr. 33, Moscow, 117071 Russia*

Received March 15, 1999; in final form, October 29, 1999

Abstract—Bottom deposits of four lakes in the central part of Buryatia (51–54°N, 106–112°E) were subjected to the pollen and radiocarbon analyses. The data obtained elucidate development of regional and local Holocene vegetation in response to climatic changes. As far as 10600–10000 years ago, the Kotokel' Lake depression was covered by the forest tundra and cryophilic forest-steppe vegetation. The summer temperature rise and some increase in aridity 10000–9000 years ago widened steppe areas, which were replaced by forests 9000 years ago. The interval of 8500–8000 years ago was characterized by the distribution maximum of spruce forests in Buryatia. Birch and spruce were widespread in forest communities till 6000 year ago. The dispersal of spruce suggests a more humid and less continental climate of the mid-Holocene time. Climatic conditions optimal for fir growth on the ridge slopes facing the Lake Baikal existed 3000–6000 years ago. The pine and larch forests, which became dominant in the vegetation cover during the last 3000 years, characterize the period of less humid and more continental climate in the region.

Key words: lakes, bottom deposits, pollen analysis, radiocarbon dates, pollen diagrams, vegetation changes, paleoclimate, Holocene.

INTRODUCTION

The pollen analysis of lacustrine-boggy deposits provides the bulk of information on regional and global changes in the Pleistocene–Holocene vegetation and climate, and is widely used for paleogeographic reconstruction, geological correlation, and for testing global climatic and biological models.

At present, only scarce radiometric dates are known for the Holocene vegetation in the Transbaikal region, particularly in Buryatia (Vipper, 1968; Vipper and Golubeva, 1976; Savina, 1982). The present article is aimed to partly compensate the information deficiency by presenting unpublished results of the pollen and radiocarbon analyses of bottom deposits in the Chernoe, Bol'shoe Eravnoe, and Dukhovoe lakes.

The comprehensively studied core section of bottom sediments in the Kotokel' Lake (Vipper, 1968; Korde, 1968) is the most complete, elucidating the vegetation dynamics in Buryatia during the late Pleistocene–Holocene. The analysis of publications (Vipper, 1968; Korde, 1968; Khotinskii, 1977; Savina, 1982) shows, however, a considerable difference in interpretations of chronology of vegetation changes and factors, which caused them. We made an attempt to settle up the discrepancies by comparing the former information with recently obtained palynological and geochronological data on the Transbaikal region and northern Mongolia (Kulagina and Trofimov, 1992; Tarasov *et al.*, 1994; Dorofeyuk and Tarasov, 1998; Gunin *et al.*, 1999). To facilitate the correlation of the reconstructed events, we present the pollen diagram for the Kotokel' Lake in the same form, as for other sections considered in the article.

The field work, sampling and description of plant remains from drilling sites, and the laboratory treatment of samples were supervised by Vipper, who took an active part in all procedures. This article is a memorial to him.

NATURAL ENVIRONMENTS IN THE REGION STUDIED

We studied bottom deposits of the lakes located in the central Buryatia between 106 and 112°E (Fig. 1). The region under consideration is bounded by the Baikal Lake in the north and northwest and by the Russia–Mongolia state boundary in the south. Dominating landforms here are mountain ridges up to 1700 m high above the sea level and intermontane depressions stretching from the southwest to northeast.

The climate is continental, with cold winter and relatively warm summer. The mean temperature of January could be as low as –27°C, and that of July ranges from 18 to 20°C (Nogina, 1964). The mean annual precipitation is 250–350 mm in depressions and up to 700 mm and more at the tops of ridges (Zhukov, 1965). The most humid conditions are characteristic of July and August, when the meridional circulation of air

† Deceased.

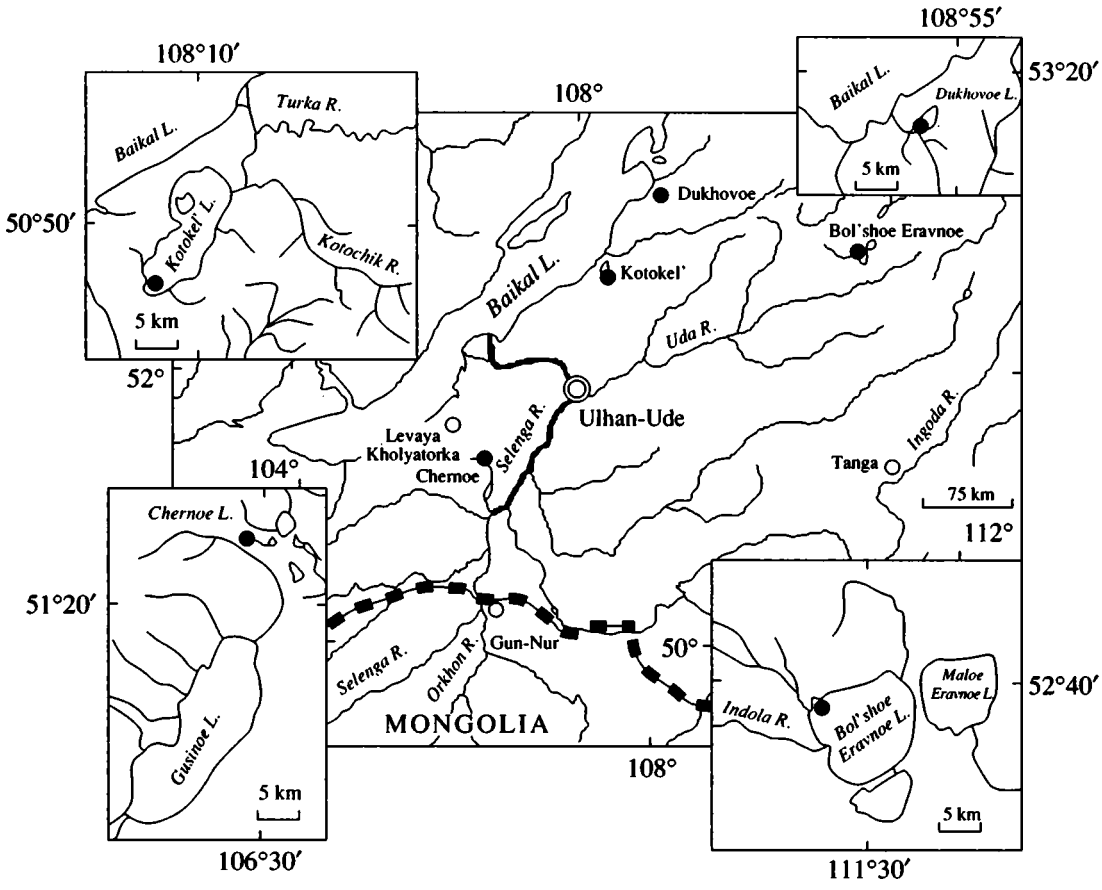

Fig. 1. Sketch map of the study region showing position of lakes mentioned in the article. Sections described in this work and other publications are denoted by solid and open circles, respectively.

masses and the polar cyclone activity prevail over the atmospheric transport from the west. Cyclones transport warm and relatively humid tropical air masses from the southeast to northwest, causing heavy and long-lasting rains. Thus, the summer precipitation in the Transbaikal region is mostly related to the monsoon-type air circulation (Zhukov, 1965). The minor autumn and winter precipitation confined to the polar front is connected with the Atlantic air masses.

The severe climatic conditions are responsible for a limited distribution of thermo- and hydrophilic plants. Dark coniferous forests (Siberian pine, spruce, and fir) occupy mainly the ridge slopes facing the Lake Baikal. Pine, larch and birch forests are most widespread. The forest steppe areas occur in the south and southeast. Steppe vegetation mainly covers flat intermontane depressions.

METHODS OF INVESTIGATIONS

The lacustrine deposits, predominantly gyttja, were sampled using the piston and mechanical bore corers. Samples for pollen and radiocarbon analyses were selected in the field. Pollen and spores extracted by the standard procedure of acetolysis (Grichuk and Zaklinskaya, 1948) were identified by A.K. Nedoseeva. In the pollen diagrams, percentages of individual taxa are calculated relative to a sum of arboreal and herbaceous pollen in a spectrum, taken for 100%.

Pollen zones distinguishable from the diagrams are chronologically allocated according to 12 radiocarbon dates. In the pollen diagram for sediments of the Dukhovoe Lake, the dates are extrapolated from those characterizing sediments of the Kotokel' Lake that is situated 62 km to the southwest. Ages of the pollen zones in the corresponding diagrams are calculated using the Tilia-Tilia.graph computer program.

The results obtained are interpreted with due account for the following trends established by analysis of surface pollen spectra from Northern Eurasia and Mongolia (Peterson, 1993; Tarasov *et al.*, 1998).

(1) In the forest steppe zone, spectra from forestless areas usually contain not more than 50% of arboreal pollen.

(2) When *Picea* and *Abies* pollen represents more than 5% of a spectrum, it is a reliable indicator of spruce and fir forests situated in the immediate proximity to the sampling site.

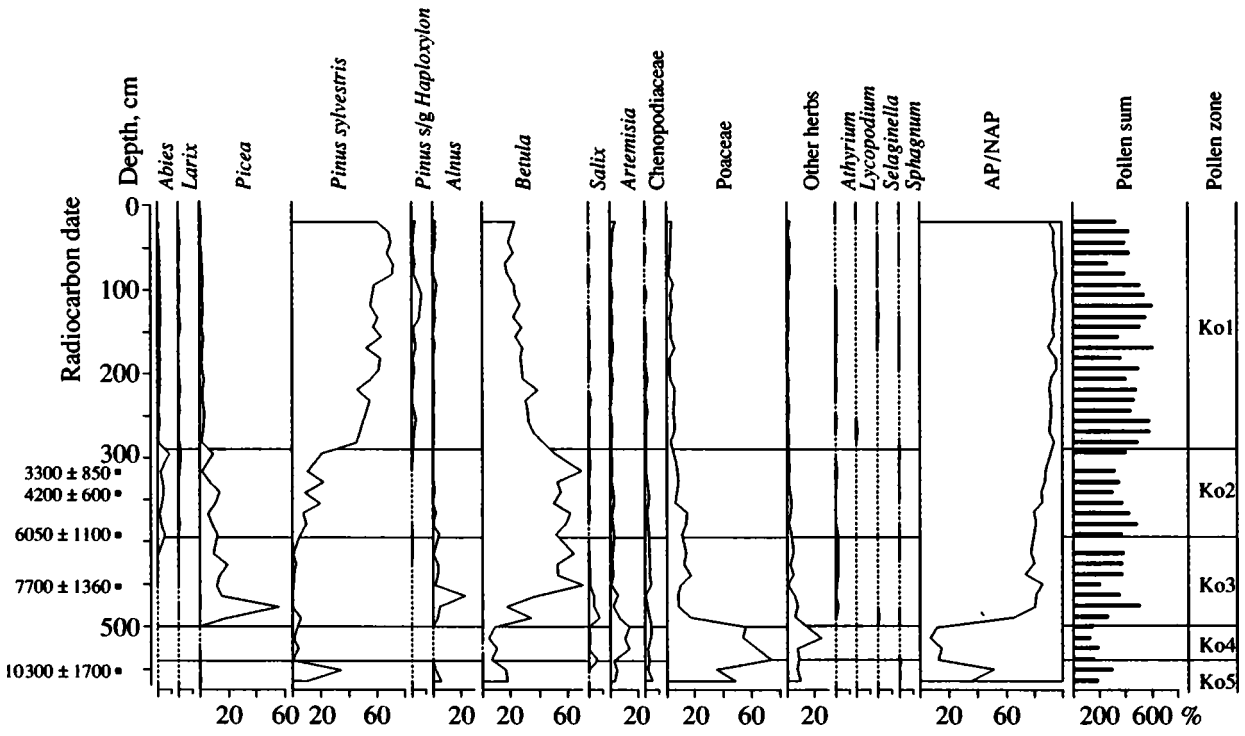

Fig. 2. Pollen diagram for the core section of bottom sediments of the Kotokel' Lake (in all figures, AP/NAP curve shows relative percentages of arboreal and non-arboreal pollen).

(3) Pollen of *Larix*, poorly surviving fossilization, and be transported not farther than 200–350 m away from a tree-producer (Savina and Burenina, 1981). Accordingly, even single pollen grains of larch in lacustrine-boggy or alluvial deposits evidence for its local origination. The same is characteristic of the *Salix* pollen (Sladkov, 1967).

(4) An insignificant amount (less than 5%) of *Pinus* pollen may be brought by wind, and this possibility should be taken into consideration by the palynological reconstruction of vegetation.

The paleoclimatic interpretation of the vegetation changes in Buryatia is based on the ecologically evaluated modern vegetation–climate relationships (Prentice *et al.*, 1992).

ANALYTICAL RESULTS AND PALEORECONSTRUCTIONS

The Kotokel' Lake (52°46′ N, 108°06′ E, 458 m above the sea level) is situated 2 km away from Baikal (Fig. 1), being separated from the latter by a low mountain ridge (maximal altitude 729 m). The lake area is 67 km^2, and the maximal depth is 12.5 m (Tarasov *et al.*, 1994). Its banks are covered with pine forest having an admixture of larch, birch, and aspen. To the east of the lake, there are forests of Siberian pine with a larch admixture and mountain forests consisting of spruce, Siberian pine, and fir (*Rastitel'nost'*, 1967). In the upper mountain zone, tundra vegetation is associated with overgrowth of dwarf-cedar elfin wood and with thin birch or larch forests. The mean January temperature in the lake region is –18.5°C, and that of July is 14.3°C. The mean annual precipitation here reaches 450 mm.

The borehole was drilled in the southern part of the lake, 1 km away from the bank (Fig. 1), where the water depth is 2.6 m. The recovered bottom deposits 565 cm thick are mostly represented by gyttja. Two basal interbeds of fine-grained sand rich in organic matter (depth intervals 555–565 and 494–499 cm) are separated by an interbed of peaty gyttja (499–555 cm).

The pollen diagram (Fig. 2) shows five zones corresponding to the main stages in the vegetation development around the lake beginning from the terminal Pleistocene.

Zone Ko5 (540–565 cm) is characterized by a moderate abundance (35–50%) of arboreal pollen that mostly represents *Pinus sylvestris* (10–35%), *Betula* (15–20%), and *Alnus* (1–5%). Dominant in the fruticose and herbaceous spectrum is pollen of Poaceae (35–50%), and that of *Artemisia*, Chenopodiaceae, and motley grass represents not more than 25% in sum. The zone range is estimated to be 10000–10600 years by means of linear extrapolation of sedimentation rate.

Zone Ko4 (500–540 cm; 9000–10000 years) shows the decreased content of arboreal pollen (5–15%). Only *Betula* (7–10%) and *Salix* (1–5%) can be considered as

local taxa. The non-arboreal spectrum mostly consisting of *Poaceae* (55–75%) show an increased abundance of *Artemisia* pollen (11–15%).

Spectra of Zone Ko3 (395–500 cm, 6000–9000 years) differ from the preceding ones. Abundance of arboreal pollen increased here (up to 75–85%), and this group is dominated by *Betula* (35–70%) and *Picea*; the maximum content of the latter (60%) is recorded in the depth interval of 475–480 cm (8000–8500 years). All spectra include pollen of *Alnus* and *Salix* and single grains of *Larix*. The content of Poaceae decreased to 10–17%.

Zone Ko2 (290–395 cm; 3000–6000 years) is still dominated by pollen of *Betula*, but content of *Picea* pollen here does not exceed 5–15%. Abundance of *Abies* and *Pinus sylvestris* pollen increases at this level up to 5–8 and 10–22%, respectively.

Spectra of Zone Ko1 (0–290 cm; 0–3000 years) show the abundance maximum of arboreal pollen (90–95%). While percentage of *Betula* pollen gradually decreases down to 15–20% within this interval, the content of *Pinus sylvestris* pollen increases up to 60–73%, and the abundance maximum of *Pinus* s/g *Haploxylon* (5–7%) is recorded at the depth interval of 100–140 cm. Pollen of *Picea, Abies, Larix*, and *Alnus* is a permanent but minor component of the spectra.

The described changes in the spectra characterize the vegetation development in the Kotokel' Lake basin. At the time of Pleistocene–Holocene boundary (10000–10600 years), the vegetation was most likely similar to the recent forest tundra or to cold forest steppe, as it is evident from presence of pollen of birch and alder represented mostly by shrub forms (Vipper, 1968; Korde, 1968). Coexisting spores of sphagnum moss and predominance of Gramineae pollen lead to the same conclusion. Thin birch and pine forests played a subordinate role in the arboreal vegetation. Spruces occurred as single specimens according to scarcity of their pollen. These features suggest cold and relatively arid climatic conditions.

In the early Holocene (9000–10000 years), there were significant changes in the vegetation. Scarcity of pine pollen in spectra indicates a virtual absence of forests around the lake. Shrub forms of birch and willow whose pollen represents an insignificant percentage of spectra could grow on the swamped banks. The increased abundance of Gramineae, wormwoods, and herbs suggests the distribution of steppe coenoses in the lake basin. These changes may result from a rise of summer temperatures and related increase in aridity. The latter is evident from the low abundance of arboreal pollen, especially of conifers occurring as accessory components only.

The arboreal vegetation spread rapidly in the lake basin beginning from 9000 years ago. Birch and spruce forests played a noticeable role in the period of 6000–8500 years. The interval of 8000–8500 years was characterized by the maximal distribution of pine and by increasing role of larch, pollen of which was found in all samples. These changes in vegetation, as well as rapid spruce distribution, indicate a period of more humid and milder climate, when winter time was not too cold, and summer not too hot.

Approximately in the interval of 3000–6000 years, fir was most widespread in the dark coniferous forests of the Holocene. Fir is more sensitive than spruce to the temperature regime (Prentice *et al.*, 1992), moisture content and soil fertility (Gunin *et al.*, 1999), and the above time interval corresponded to the optimal combination of these parameters. Beginning from 6000 years ago, pine, an undemanding and highly competitive tree, spread steadily.

The pine participation in the forests was especially noticeable in the last 3000 years, when spruce and fir gave their place to pine, Siberian pine and larch. The late Holocene degradation of spruce and fir forests, as well as the pine expansion, may represent a response to deterioration of climate, which became more arid and continental. Heavy forest fires, which are frequent now in the Transbaikal region (Dylis *et al.*, 1965), could be also of significance. They destroyed the moss cover, thus increasing the depth of seasonal soil defrosting. This favored the expansion of pine that has thick vertical, but not only subsurface roots. In opinion of Savina (1982), the oppression and degradation of spruce forests in the valleys of the Baikal region, which took place 7000–8000 years ago, and subsequent expansion of pine and larch forests could be caused by a rise of ground water level in response to the increased moisture content and peculiar bog formation.

The interpreted paleoclimatic changes in the vegetation of the Kotokel' depression show correlation with the changeable lake levels, reflecting the sedimentation–evaporation ratio (Tarasov *et al.*, 1994). The low level stand (8500–10600 years) coincided with the minimum abundance of forest vegetation in the lake depression. Medium and high levels are recorded in the middle and late Holocene, when taiga spread widely in the region under consideration.

The Dukhovoe Lake (53°18′ N., 108°53′ E.; 514 m) is situated 3 km away from the Lake Baikal (Fig. 1) and separated by a low (843 m) mountain ridge. Aspen and thin larch forests with a minor admixture of spruce cover the low coastal zone. Thin pine forests with single larches and abundant birches and aspens occupy the mountain slopes. Siberian pine and fir occur along the Baikal coast, dwarf-cedar elfin wood is characteristic of sandy dunes. The Barguzin weather station, located in a more arid area, recorded the mean temperature of −26.7°C for January and +18.3°C for July (Nogina, 1964).

Two cores of bottom sediments were selected for palynological analysis. Their pollen diagrams are very similar, and we consider here one of them (Fig. 3), characterizing the longer section. The borehole was drilled 1 km away from the southern coast, in the lake

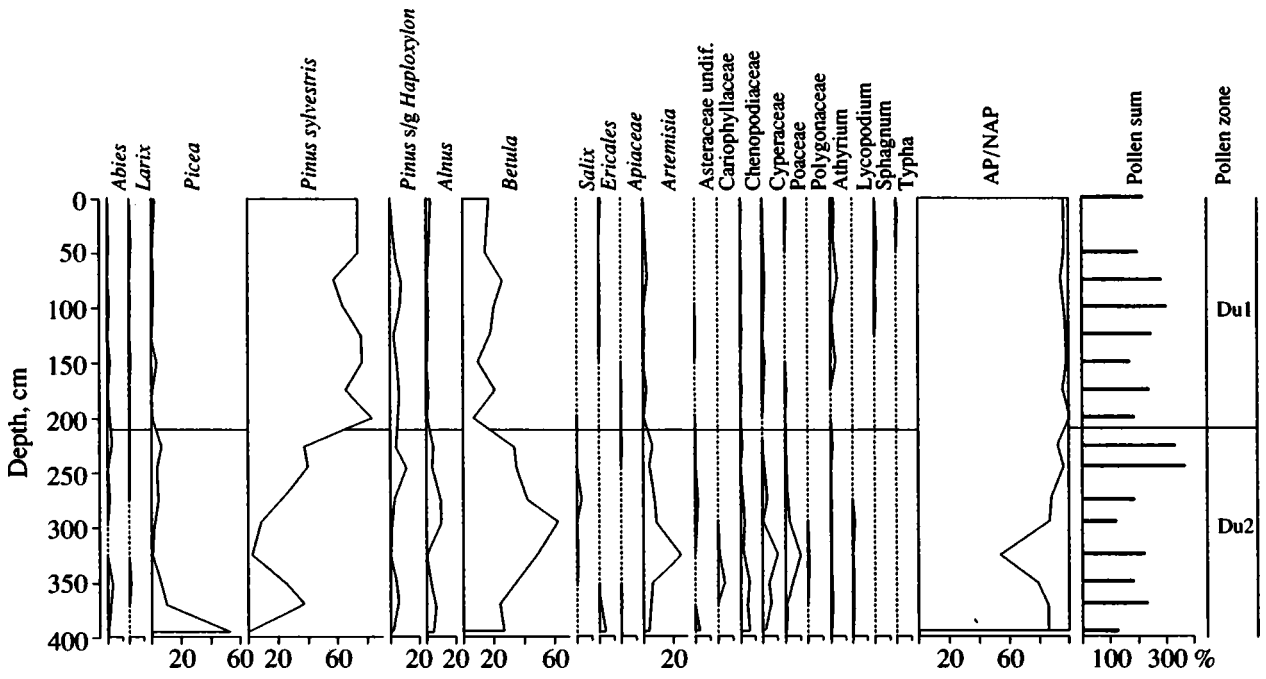

Fig. 3. Pollen diagram for the core section of bottom sediments of the Dukhovoe Lake.

area, where water depth is 1.8 m. It penetrated the 395-cm-thick gyttja underlain by sand. Because these deposits are lacking radiocarbon dates, they were dated by correlation with the nearest sequence of the Kotokel' Lake (Figs. 1 and 2). The comparison of pollen diagrams shows that the spruce pollen is most abundant in the Dukhovoe Lake section within the interval that accumulated 8000–8500 years ago. The increase in abundance of pine pollen is recorded here at the depth of 200 cm and appears to be simultaneous with the analogous event in the Kotokel' Lake deposits that happened about 3000 years ago. These two chronostratigraphic levels allowed us to date boundaries of the pollen zones in the Dukhovoe Lake section.

In Zone Du2 (210–400 cm; 3000–8500 years), arboreal pollen represents 75–85% of pollen assemblage. Pollen of *Betula* (25–65%) and *Pinus sylvestris* (up to 45%) dominates. Permanent components of pollen spectra are *Pinus* s/g *Haploxylon* (up to 10%), *Alnus* (up to 10%), *Abies* and *Larix* (1–3%). Abundance of *Picea* pollen decreases from 55 to 5–7% upward in the section. A single spectrum (level of 325 cm) contains up to 45% of fruticose and herbaceous pollen, mostly that of *Artemisia*, Poaceae, and Cyperaceae.

In Zone Du1 (0–210 cm), percentage of arboreal pollen is 95–100%. Pine pollen represents up to 85%, whereas abundance of other taxa, except for larch and Siberian pine, decreases.

Development of vegetation in the Dukhovoe Lake area was similar to that of the Kotokel' Lake basin. Spruce forests were most widespread in the interval of 8000–8500 years. However, the most thermo- and hydrophilic dark coniferous species (spruce and, especially, fir) had limited abundance in the period of 3000–8000 years. In the mid-Holocene, forests, which included birch, pine, spruce, fir, Siberian pine, and larch, were typical of the Dukhovoe Lake basin. Abundance of dark coniferous species that was greater than at present evidences for more humid and less continental climate. A sharp abundance decrease of arboreal pollen (in particular, that of pine) and growing content of wormwood, Gramineae, and sedge pollen is established in the sample from the depth interval of 320–330 cm, and this level may indicate a temporary expansion of steppe into forest zone around the lake. In our opinion, this event recorded in both core sections was caused by local factors (for instance, by a big fire) rather than by a regional climatic change. Recent observations (Dylis *et al.*, 1965) show that fires are frequent in pine forests, and that new trees grow slowly and irregularly in the burned places.

The vegetation of the last 3000 years was similar to the recent one. This period was characterized by a very rapid expansion of pine forests in the region.

The Chernoe Lake (51°24′30″ N, 106°29′20″ E; 550 m) is located at the left edge of a large linear depression (Fig. 1). A small river that takes origin in the Soldatskii Ridge to the northwest flows into the Chernoe Lake to connect it with the Krugloe Lake. Coastal ramparts 15 m high are covered by pea-shrubs, Gramineae, and wormwood. Birch, rare larch and spruce grow in the depression. The spruce forest of the Soldatskii Ridge reaches the lake. There are some massifs of Siberian pine with sporadic larches (*Rasti-*

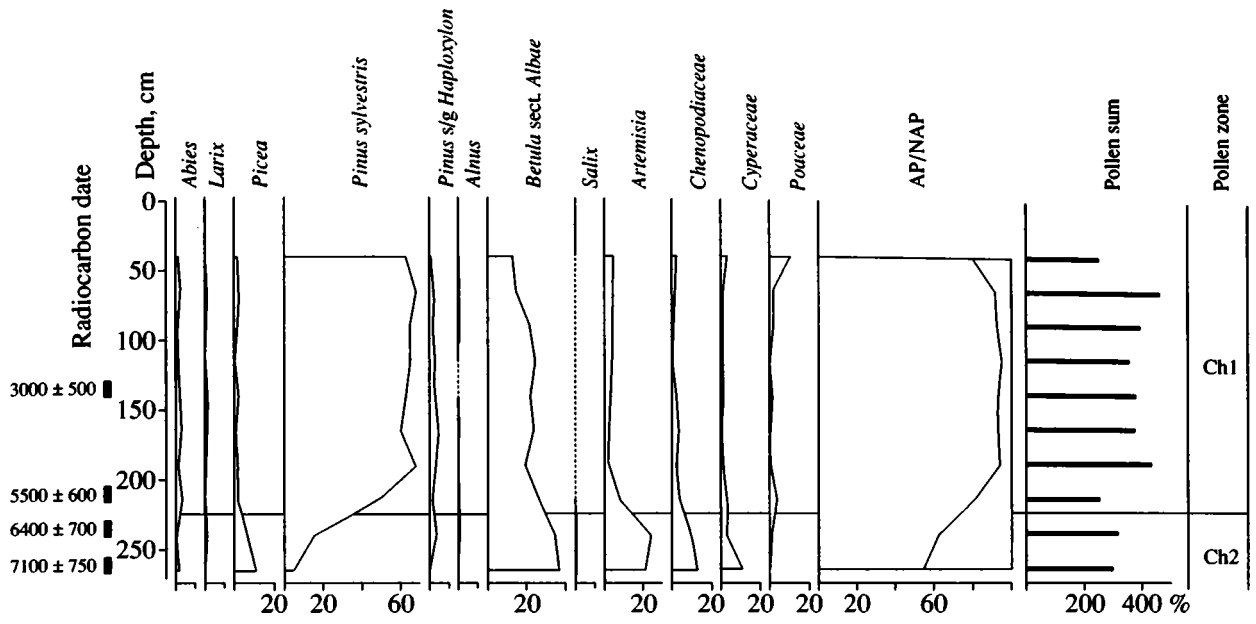

Fig. 4. Pollen diagram for the core section of bottom sediments of the Chernoe Lake.

tel'nost', 1967). According to data of the Novo-Selenginsk weather station (Nogina, 1964), the mean temperature is –26.2°C for January and +19.9°C for July; the mean annual precipitation is 255 mm.

The borehole was drilled 250 m away from the coast in the middle of the lake, where the water depth is 2.15 m. The penetrated gyttja bed 265 cm thick yields abundant shells of small mollusks and plant detritus. The pollen diagram (Fig. 4) shows two distinct zones. Zone Ch2 (225–270 cm; 6000–7400 years) is characterized by a relatively low content of arboreal pollen (55–65%), representing dominant *Betula* sect. *Albae* (35%), subordinate *Pinus sylvestris* (5–15%) and *Picea* (7–12%), and scarce other taxa (*Pinus* s/g *Haploxylon, Abies, Larix, Alnus, Salix*). Main non-arboreal components are *Artemisia* (22–25%), Chenopodiaceae (10–13%), and Cyperaceae (3–11%).

Zone Ch1 (0–225 cm; 0–6000 years) is characterized by the absolute predominance of arboreal pollen (up to 95%). The dominant taxon is *Pinus sylvestris* (60–68%). The zone shows a noticeable decrease in abundance of birch (12–25%) and spruce (1–2%) pollen. The non-arboreal group has not been changed in composition, but it includes not more than few percent of each taxon.

The composition of spectra (high percentages of wormwood and Chenopodiaceae pollen) confidently suggests the forest steppe type of vegetation in the depression 6000–7400 years ago. Spruce–birch and larch forests were most widespread at that time. Pine and fir were minor components. Nevertheless, the climatic conditions were fairly favorable for the dark coniferous taiga. The presence of willow pollen and the increased content of Cyperaceae suggest swamping of the lake banks owing to a risen level of ground water, or to a high humidity of climate. This indirectly confirms the previous conclusion. The alternative explanation is the lake shoaling and distribution of bog vegetation in the littoral zone.

Since 6000 years ago, the eurythermal pine, birch and larch forests became widespread. According to the pollen analysis, larch, in contrast to spruce, retained its significant role in the regional vegetation. Spruce needs a higher moisture than pine and birch, and the reduced abundance of its pollen may point to some increase in aridity. The higher content of arboreal pollen in the late Holocene spectra does not evidence for a greater significance of forests than in the mid-Holocene. The spectra are dominated by pine pollen that is of a higher productivity and has better aerodynamic properties than pollen of other species.

The Bol'shoe Eravnoe Lake (52°40′ N., 111°32′ E; 948 m) is situated in the Vitim Upland (Fig. 1). In the lake depression, steppe areas neighbor upon the larch, pine–larch and birch forests. According to data of the Chita weather station (Nogina) located near the lake, the mean temperature of January is –26.8°C, that of July is +18.5°C, and the mean annual precipitation is 300 mm.

The borehole at the site that is located 500 m away from the north-northwestern coast (Fig. 1) and has water depth of 2.57 m penetrated the 285-cm-thick gyttja deposits. The pollen diagram (Fig. 5) shows a great similarity to that of the Chernoe Lake site(Fig. 4).

In Zone Be2 (225–285 cm; 6000–7000 years), arboreal taxa represent 65–70% of pollen assemblage show-

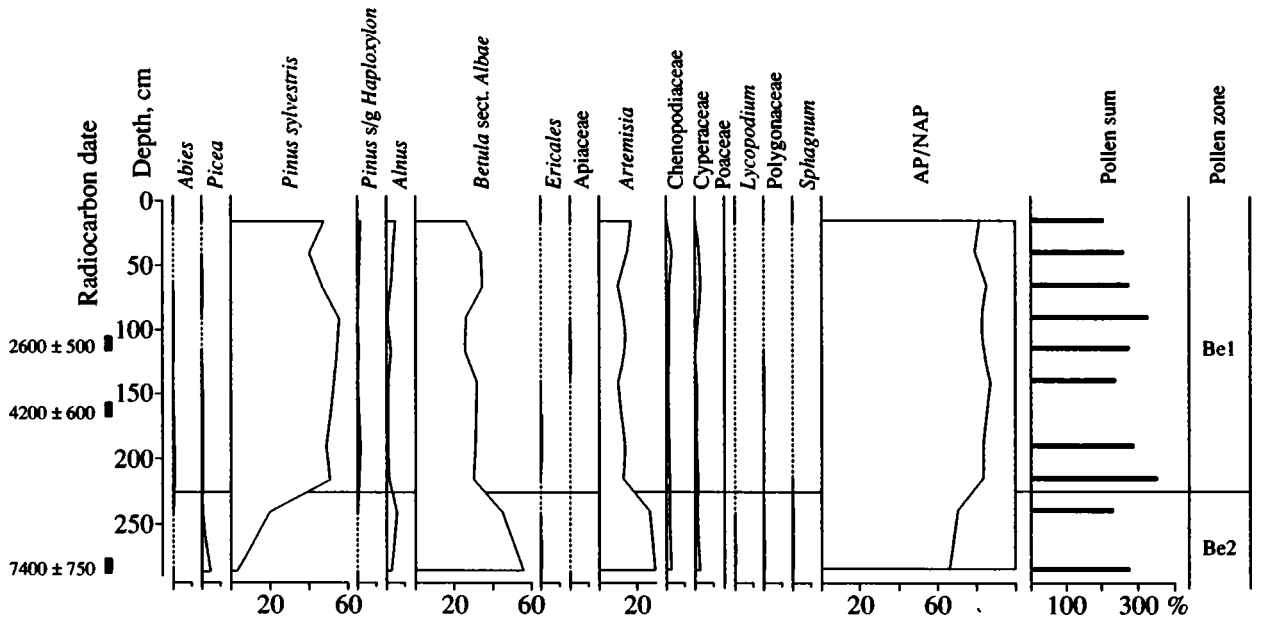

Fig. 5. Pollen diagram for the core section of bottom sediments of the Bol'shoe Eravnoe Lake.

ing predominance of *Betula* sect. *Albae* (45–55%). Content of *Pinus sylvestris* pollen increases upward in the section from 4 to 25%. The highest content of *Picea* pollen (4%) was found in the lower sample. The non-arboreal group is dominated by pollen of *Artemisia* (30%).

Zone Be1 (0–225 cm) is characterized by the increased content (85%) of arboreal pollen. The dominant pollen of *Pinus sylvestris* is associated with less abundant (30–35%) of pollen of *Betula* sect. *Albae*, and with single pollen grains of dark coniferous *Abies, Picea*, and *Pinus* s/g *Haploxylon*. Against the background of persistently low content of Chenopodiaceae and Cyperaceae, the share of *Artemisia* is reduced down to 10–15% in the zone.

The composition of pollen spectra suggests that forests prevailed in the lake basin during the last 7600 years despite the changes in plant communities. Beginning since 6000 years ago, the widespread birch forests associated with pine forests. The absence of larch pollen in the spectra does not mean that this taxon was missing from the forests, if we take into consideration the large size of the lake and the long distance of the drilling site from the coast. The stable occurrence of single pollen grains of spruce, fir and Siberian pine in the spectra of the second half of Holocene proves their presence in the region. The relatively high content of spruce pollen in the lower sample indicates the increased role of this taxon in the regional vegetation about 7500 years ago. This is in good agreement with the data on other lakes (Figs. 2–4).

DISCUSSION

One of the ways to check the reliability of our inferences is to compare them with the published reconstructions of Holocene vegetation and climate in the Transbaikal region and adjacent areas of Mongolia. Palynological data for the Gun-Nur Lake area (Fig. 1), where the pine–larch forest steppe is widespread now, indicate predominance of steppe landscapes and insignificant abundance of trees (mostly of birch) 8700–9600 years ago (Dorofeyuk and Tarasov, 1998). However, the forest area was noticeably enlarged in that region owing to the intense expansion of *Pinus sylvestris* 8000 years ago. The predominance of the forest steppe similar to the recent one was characteristic of the middle and late Holocene. The steppe expansion coincided with periods of the low lake-level stand, which were established by lithological and diatom analyses (Dorofeyuk and Tarasov, 1998). The high level stand of the Gun-Nur Lake was typical of the interval of 3300–8300 years, whereas the terminal Holocene was a time of predominantly medium level stand.

As for several lakes of the Chita region, where palynology of lacustrine deposits was studied (Vipper and Golubeva, 1976), radiocarbon dates are available only for sediments of the Tanga Lake (Fig. 1) surrounded by mountainous forest steppe with participation of pine, birch, and larch. The pollen diagram includes a zone, the upper boundary of which is dated at 7560 ± 250 years. The zonal spectrum includes 50–70% of non-arboreal pollen (mostly, of *Artemisia* pollen). The spectrum composition suggests its connection prior to 8000 years ago with a forest steppe, where woods consisted of birch and spruce. The expansion of

trees and bushes took place here about 7500 years ago. Birch and spruce, pollen of which was very abundant until 7000 years ago (below the mark of 6500 ± 200 years in the diagram), were dominant, and then their abundance was sharply reduced. Spectra characterizing the second half of the Holocene reveal predominance of common and Siberian pine and an increased abundance of larch. In our opinion, this phase began about 6000 years ago, i.e., simultaneously with the analogous vegetation changes in Buryatia.

When interpreting the pollen diagram for the Kotokel' Lake and discarding the radiocarbon dates owing to their significant error, Khotinskii (1977) referred the break in sedimentation to the Preboreal period (9000–10200 years ago) and concluded that forestless period corresponded to the Younger Drias. The recent palynological results and radiocarbon dates for the Verkhnyaya Angara valley (Kulagina and Trofimov, 1992) and for Gun-Nur (Dorofeyuk and Tarasov, 1998) and Khoton-Nur (Gunin *et al.*, 1999) lakes imply a broad distribution of woodless landscapes in the initial Holocene (10000–9000 years) over the large territory of the Transbaikal region, northwestern and northern Mongolia. This phase was followed everywhere by an intense dispersal of tree vegetation virtually during the entire Holocene. These data are in agreement with our inferences for Buryatia. Accordingly, we can speak about similar trends in development of vegetation and climate, taking into account the synchronous Holocene phases of steppe progradation and aridity growth and of forest expansion and humidification in the regions under discussion.

Speaking about common trends of landscape development in the Transbaikal region and northern Mongolia, we should emphasize some regional differences related to the geographic position, orography and climatic peculiarities of separate areas. For instance, pine occupied positions similar to the recent ones about 8000 years ago in the Lake Gun-Nur basin near the Mongolian boundary, about 5000–6000 years ago in central Buryatia and the western Chita region, and 3000 years ago in the immediate proximity to the Lake Baikal. The Boreal maximum of pine distribution that was established by palynological analyses in different Siberian regions (Khotinskii, 1977) and northern Mongolia (Gunin *et al.*, 1999) is also distinguishable in Buryatia and indicates thus a significant climatic deterioration in Northern Asia in that period. On the other hand, the opinion of Khotinskii (1977) on the climate deterioration in the Transbaikal region at the time of Atlantic–Subboreal boundary (about 4500 years ago) of the Holocene sometimes finds no confirmation from palynological data and radiocarbon dating results. In particular, data on the Kotokel' Lake basin and Levaya Kholyatorka River valley (Savina, 1982; Fig. 1) show that the fir abundance in the forests of the Baikal mountain ridges was at the maximum in the period of 5500–3500 years ago. In terms of plant ecology, the increasing abundance of fir is indicative of humidification and of winter temperatures rise (Vipper, 1962; Vipper and Golubeva, 1976; Savina, 1982; Prentice *et al.*, 1992). However, sections located far away from the Baikal depression (basins of the Chernoe, Bol'shoe Eravnoe, and Tanga lakes) do nor reveal records of the late Holocene humidification. This inconsistency may be related to changes in atmospheric circulation, particularly to the increased or reduced influence of the Atlantic (latitudinal) and monsoon (submeridional) air masses on the regional climate.

CONCLUSIONS

The analysis of bottom deposits in the Buryat lakes situated at the relatively low hypsometric levels (up to 1000 m) revealed synchronism of main evolutionary phases of forest and steppe vegetation in the Transbaikal region and northern Mongolia. It points as well to the great influence of climatic factor on vegetation.

Relative proportions of main forest components in the vegetation noticeably changed from the north to the south and from the west to the east. Accordingly, the interregional correlations in the Transbaikal region and Mongolia are insufficiently reliable, when they are based only on palynological data without due regard for radiocarbon dating.

Materials that are considered in this work allow us to specify and partially revise the former understanding of development of the Holocene vegetation and climate in the western Transbaikal region. However, a special study and modeling of general atmospheric circulation is needed to explain the mechanism of the reconstructed changes in vegetation.

Reviewers N.Yu. Filippova and M.A. Akhmet'ev

REFERENCES

Dorofeyuk, N.I. and Tarasov, P.E., Vegetation and Lake Levels in Northern Mongolia in the Last 12500 years as Indicated by Data of Pollen and Diatom Analyses), *Stratigr. Geol. Korrelyatsiya*, 1998, vol. 6, no. 1, pp. 73–87.

Dylis, N.V., Reshchikov, L.I., and Malyshev, L.I., Vegetation, *Predbaikal'e i Zabaikal'e* (Cis- and Transbaikal Regions), Moscow: Nauka, 1965, pp. 225–281.

Grichuk, V.P. and Zaklinskaya, E.D., *Analiz iskopaemykh pyl'tsy i spor i ego primenenie v palinologii* (Analysis of Fossil Pollen and Spores and Its Application to Palynology), Moscow: Geografgiz, 1948.

Gunin, P.D., Dorofeyuk, N.I., Vostokova, E.A., *et al.*, *Vegetation Dynamics of Mongolia*, Dordrecht: Kluwer, 1999.

Khotinskii, N.A., *Golotsen Severnoi Evrazii* (The Holocene of Northern Eurasia), Moscow: Nauka, 1977.

Korde, N.V., Biostratigraphy of Sediments in the Lake Kotokel', *Mezozoiskie i kainozoiskie ozera Sibiri* (Mesozoic and Cenozoic Lakes of Siberia), Moscow: Nauka, 1968, pp. 150–170.

Kulagina, N.V. and Trofimov, A.G., The Holocene of the Verkhnyaya Angara River Valley (Northern Baikal Region), *Izv. Akad. Nauk SSSR, Ser. Geol.*, 1992, no. 12, pp. 156–160.

Nogina, N.A., *Pochvy Zabaikal'ya* (Soils of the Transbaikal Region), Moscow: Nauka, 1964.

Peterson, G.M., Vegetational and Climatic History of the Western Former Soviet Union, *Global Climates since the Last Glacial Maximum*, Minneapolis: Univ. Minnesota, 1993, pp. 169–193.

Prentice, I.C., Cramer, W., Harrison, S.P., *et al.*, A Global Biome Model Based on Plant Physiology and Dominance, Soil Properties and Climate, *J. Biogeography*, 1992, vol. 19, pp. 117–134.

Savina, L.N., Tendencies in Evolution of Coastal Landscapes around the Lake Baikal, *Pozdnekainozoiskaya istoriya ozer v SSSR* (Late Cenozoic History of Lakes in the Soviet Union), Novosibirsk: Nauka, 1982, pp. 42–52.

Savina, L.N. and Burenina, T.A., Preservation degree of Larch Pollen in Forest Soils and Larch Forests of Mongolia as Represented in Recent Spectra, *Paleobotanicheskie issledovaniya v lesakh Severnoi Azii* (Palebotanical Studies in Forests of Northern Asia), Novosibirsk: Nauka, 1981, pp. 62–83.

Sladkov, A.N., *Vvedenie v sporovo-pyl'tsevoi analiz* (Introduction into Palynological Analysis), Moscow: Nauka, 1967.

Tarasov, P.E., Harrison, S.P., Saarse, L., *et al.*, *Lake Status Records from the Former Soviet Union and Mongolia: Data Base Documentation. NOAA Paleoclimatology Publications Series Report 2*, Boulder, 1994.

Tarasov, P.E., Webb III T., Andreev, A.A., *et al.*, Present-Day and Mid-Holocene Biomes Reconstructed from Pollen and Plant Macrofossil Data from the Former Soviet Union and Mongolia, *J. Biogeography*, 1998, vol. 25, no. 6, pp. 1029–1054.

Vegetation, *Atlas Zabaikal'ya (Buryatskaya ASSR i Chitinskaya oblast')* (Atlas of the Transbaikal Region, Buryat ASSR and Chita District), Moscow: GUGK, 1967, pp. 58–59.

Vipper, P.B. and Golubeva, L.V., To the History of Holocene Vegetation in the Southwestern Transbaikal Region, *Byull. Komis. Izuch. Chetv. Per.*, 1976, no. 45, pp. 45–55.

Vipper, P.B., Postglacial History of Landscapes in Transbaikal Region, *Dokl. Akad. Nauk SSSR*, 1962, vol. 146, no. 4, pp. 871–874.

Vipper, P.B., Relationships between Forest and Steppe in Mountain Areas of Southwestern Transbaikal Region, *Botan. Zh.*, 1968, vol. 53, no. 4, pp. 491–504.

Zhukov, V.M., Climate, *Predbaikal'e i Zabaikal'e* (Cis- and Transbaikal Region), Moscow: Nauka, 1965, pp. 91–126.

Stratigraphy and Geological Correlation, Vol. 10, No. 1, 2002, pp. 97–101. Translated from Stratigrafiya. Geologicheskaya Korrelyatsiya, Vol. 10, No. 1, 2002, pp. 104–109.
Original Russian Text Copyright © 2002 by Sokolov, Fedonkin.
English Translation Copyright © 2002 by MAIK "Nauka/Interperiodica" (Russia).

Academician M.A. Semikhatov and Proterozoic Geology (on the Occasion of His 70th Birthday)

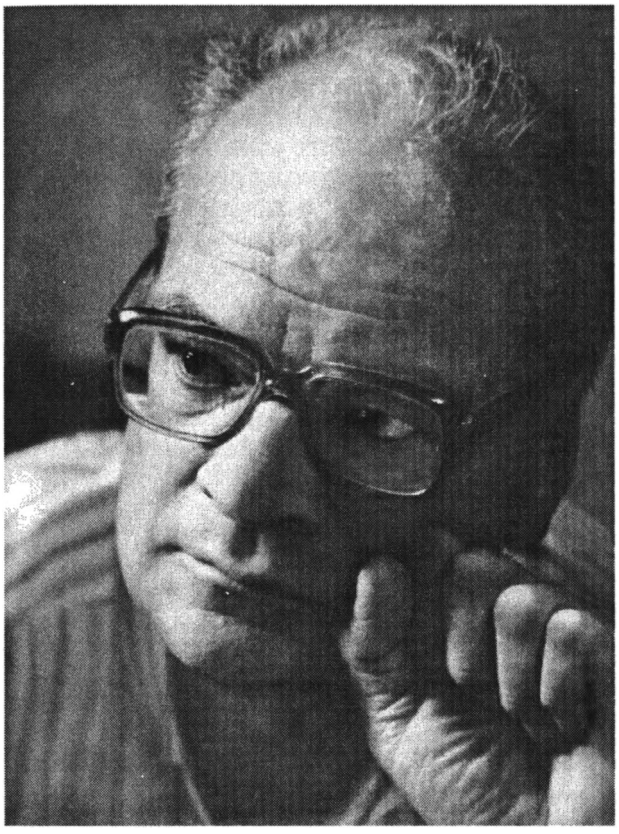

Mikhail Aleksandrovich Semikhatov is undoubtedly among most prominent Russian geologists who dedicated their life to the study of the Precambrian, the longest period of the Earth history that comprises at least 3 billion years and is simultaneously most difficult for investigation. All the tendencies in development of the Precambrian geology and dramatic turns of ideas and approaches to this young, but rapidly developing natural science found their place in the scientific life of M.A. Semikhatov. Both in Russia and abroad, he is justly acknowledged as the most outstanding connoisseur of the Precambrian geology in all its variable aspects: regional stratigraphy, isotopic geochronology, chemostratigraphy, and biosphere characteristics. An immense experience of research virtually in all continents brought him a glory of an expert of the world class. His personal qualities, such as wide erudition, inexhaustible interest to natural enigmas, organizational talent, and well-meaning strictness of judgments attracts to him colleagues everywhere, in the Academy of Sciences, in expeditions to remote regions, and in multilingual international conferences.

His striving for comprehensive education and passion to the intellectual work Semikhatov inherited from his remarkable parents. His mother, professor Sof'ya Viktorovna Semikhatova, born Karpova (1889–1973), was a brilliant paleontologist and biostratigrapher who was first to distinguish the Bashkirian Stage of the Carboniferous System. She was well-educated purposeful woman with a strong and independent character. The father, professor Aleksandr Nikolaevich Semikhatov (1882–1956) was an outstanding hydrogeologist, the founder of hydrogeology in Russia who introduced a new culture of 20th century into study of endogenic and ground waters. They both were typical representatives of the well-educated Russian intelligentsia of the 19th–initial 20th centuries, always devoted to their domestic and professional duties, to perfection of knowledge and education, and to good breeding of their three children at the hard time of initial 1930s. Maintaining of the family spirit, its warm and strict traditions, and protection from the unacceptable influences of time demanded a particular attention and wisdom from parents. A.N and S.V. Semikhatovs managed to overcome these difficulties successfully and brought their children as well-educated and highly ethical persons. Taking into consideration their devotion to the professional duty, this was a heroic deed.

Mikhail Aleksandrovich was the late (third) child in the family (he was born February 21, 1932) and inherited best qualities from his parents: their inexhaustible diligence and purposefulness, devotion to selected affair, unhurried discipline and obligingness, innate culture and wisdom, and, what is most important, a keen interest for "inflammatory ideas" that was noted by B.M. Keller, one of his first preceptors. In addition to his natural intellect and keenness to observation, this heritage was a valuable gift for the future researcher. Like many people during the war, Semikhatovs have suffered hardships and poverty of the evacuation life, but their son gained the full-fledged education despite all difficulties of the war and postwar time.

In 1949, young Semikhatov joined the geological faculty of the Moscow University, where soon he began to study geology of the North Caucasus in the chair of historical geology under supervision of M.M. Moskvin. The first scientific article, he prepared together with M.M. Moskvin in 1956, was dedicated to submarine sliding dislocations in Upper Cretaceous and Paleogene

sequences of Dagestan. He joined the chair of historical geology under the influence of A.A. Bogdanov, G.P. Leonov, N.M. Strakhov, and M.M. Moskvin, the brilliant scientists with wide erudition who had a peculiar gift to get insight into the prospect of geological research.

The Caucasian geological experience was undoubtedly useful for Semikhatov, although decisive for selection of his further scientific activity was another period. In 1954, he joined the Institute of Geological Sciences of the USSR Academy of Sciences, which was divided a year later into two autonomous institutes. One of them, the Geological Institute proper, was headed since 1956 by Academician N.S. Schatsky, a scientist who had extremely wide interests and was full of new ideas and creative fascination that particularly attracted young and ambitious researchers. Precisely here, in the department of stratigraphy headed by V.V. Menner, Semikhatov found once and forever his avocation and joined the creative group, which became a core of the future Laboratory of Upper Precambrian Stratigraphy organized in 1958 under guidance of professor B.M. Keller.

Practical needs of the postwar time required accumulation of new factual material and critical revision of the available theoretical geological basis. Earth sciences distinctly entered the turning epoch in their development, they needed new concepts, fresh facts, and modern generalizations of the available knowledge. Precambrian geology was one of the branches in Earth sciences, for which this was particularly crucial.

Craving for renewal was a natural consequence of victory in the Patriotic War. In addition to the active older generation, academic institutes received a lot of young, fervent, and creative persons who either went through the war or experienced this war in their childhood. To a large measure, daring searches of new ways in the science were connected precisely with this generation. The "golden age" of geology was approaching. Already during the war time there was a sharp need in new data on the Precambrian history of the Earth, on the ore and hydrocarbon potential of the earth crust as a whole, and on early stages of biosphere evolution. This need was soon materialized in unprecedented programs of deep reference drilling and field research of Precambrian sequences in foldbelts and platform structures. An avalanche of new data resulted in appearance of absolutely new approaches to solution of problems in Precambrian geology and triggered the complete revision of existing views on early stages of Earth evolution.

Of top priority in the Precambrian geology were stratigraphy and methods of subdivision and correlation of ancient "barren" sequences, which represented new scientific problems. At that time, the Riphean Group was already established in the Urals (Schatsky, 1945) and Vendian rocks were defined soon after in the uppermost Precambrian of the East European platform (Sokolov, 1950, 1952). The acute polemics concerning relationships of these units between each other and with the Cambrian System was largely a consequence of biostratigraphic data absence. The phrase "Precambrian biostratigraphy" sounded at that time as a nonsense for many geologists. Silicified microfossils about 2 Ga old discovered in Canada in 1920s were considered as inorganic structures or artifacts. In Russia, geologists disputed the redeposited versus in situ occurrence of organic-walled fossils first discovered in the Vendian. Absence of unified opinion on these problems was characteristic of the Geological Institute as well. Schatsky was a proponent of historical–geological substantiation of boundaries between the Precambrian subdivisions and considered the paleontological method as inappropriate for the Proterozoic. On the other hand, Menner who leaned upon works by V.P. Maslov argued for the thorough study of stromatolites, which were abundant in carbonate sequences of the Urals and Siberia and sometimes accompanied by microfossils as well. The study of Riphean and Vendian stromatolites was initiated in 1958 by a group of young enthusiasts headed by Academician Menner and professor Keller. Together with Semikhatov, participants of the group were I.N. Krylov, V.A. Komar, M.E. Raaben, S.V. Nuzhnov, and later on S.N. Serebryakov.

Investigation of stromatolite nature and elaboration of their taxonomy were time-consuming and difficult, but this research avenue was crowned by a great success from both the stratigraphic and biologic standpoints. Now, we can confidently state that such intellectual attack of extremely difficult paleontological and stratigraphic problems of Precambrian geology can hardly be expected again either in Russia or abroad. Most acute debates and frenzied conflicts of scientific opinions took place at that time among true companions involved into the common deed. Dozens of expeditions to Siberia, the Urals, Karelia, and best sections in other countries, elaboration of new methods of studying and classifying stromatolites, and documentation of their spatial and temporal distribution laid the groundwork for the Russian school of Precambrian stratigraphy that received a worldwide acknowledgment and many followers. The article by P.E. Cloud and M.A. Semikhatov "Proterozoic stromatolite zonation" published in "American Journal of Science" in 1969 can be considered as a symbolic event. In this article, P.E. Cloud, one of the most experienced American researchers of Precambrian geology who rejected classification and stratigraphic significance of stromatolites for many years revised his views, highly appraised the stratigraphic potential of these unusual fossils, and accepted Russian classification of stromatolites, according to which higher taxons are defined using peculiar features of their general morphology, whereas lower taxons are recognized on the basis of their microstructures. Precisely this approach prevails nowadays in the world literature on stromatolites.

Although Semikhatov did not formally head the laboratory in 1970s, he was a beginner of many important projects and involved colleagues into the sphere of his own interests. This sphere was very broad: elaboration of non-conflicting stratigraphic scales and telecorrelation of Precambrian sequences made it necessary to analyze data obtained in different branches of science. Since 1984, Semikhatov headed the Laboratory of Upper Precambrian Stratigraphy at the Geological Institute. Since that time, the laboratory widened significantly a spectrum of research methods and scientific problems, thus following the world tendencies in Precambrian studies, but retaining simultaneously its leading position in the study of stromatolites and Proterozoic stratigraphy.

The progress in stratigraphic–paleontological studies is well manifested in several first-class monographs published by Semikhatov in addition to his most important methodological and theoretical articles of last two decades. These were books entitled "Stratigraphy of Precambrian and Lower Paleozoic deposits of the western part of Eastern Sayan" (1960, in collaboration), "The Riphean and Lower Cambrian of the Yenisei Range" (1962, Candidate dissertation), "Reference Riphean sections of continents" (1968, in collaboration with B.M. Keller), "The Yudoma Complex of the stratotype region", 1970 (with co-authors), "Proterozoic Stratigraphy and Geochronology" (1974, Doctorate dissertation), "Siberian Riphean hypostratotype" (1983, in collaboration with S.N. Serebryakov), and "General problems of Proterozoic stratigraphy in the USSR" (1991, published in United States). These publications important by themselves are remarkable by persistent application of chronostratigraphic principles for elaboration of general Proterozoic scales, by new biochronological evaluation of Precambrian events, and by a complex approach to solution of newly appearing problems.

Semikhatov is indisputably one of prominent researchers of Upper Precambrian stratigraphy. He is well-acquainted with international historical–geological and paleogeographic materials, and this knowledge leans, to al large extent, upon his own experience gained during the study of sections in Northern Eurasia, China, North America, North Africa, and Australia. He reported his results to many Russian and international conference and symposia, where the reports received always a high appreciation of listeners owing, to a significant extent, of his excellent knowledge of English. All his works are marked by an extremely thorough analysis, strict treatment of initial data and own results, and clear presentation. His scientific interests are extraordinary broad, going far beyond ordinary objectives of Earth sciences.

Regional stratigraphy and geology occupy a particular place in investigations of Semikhatov. They represent not only a reliable basis for the analysis of spatial and temporal distribution of organic remains and for determination of their position in the facies succession, but elucidate as well principal features of geological history in a given region, which must be known for the correct interpretation of isotopic dates obtained from sedimentary chronometers and their geological significance, and for evaluation of Sr- and C-isotope chemostratigraphic data. The long-term period of field studies allowed Semikhatov to get a deeper insight into the structure and geological history of the Riphean, Vendian, and Lower Cambrian in several regions of Siberia, to create a basis for the modern Upper Riphean–Vendian stratigraphic scale of the Yenisei Range, to contribute much to the knowledge of structural features of the Yudomian, the Siberian equivalent of the Vendian, and to substantiate, together with Serebryakov, the structure and status of the Siberian hypostratotype of the Riphean. Using the comparative–historical analysis of Proterozoic sequences of different continents, Semikhatov established several general regularities in their development and the global geological significance of pre-Riphean historical–geological boundary. He also showed that the four-member subdivision of the Upper Precambrian (three Riphean and one Vendian subdivisions) that is established in Russia can be applied, based on paleontological and isotopic–geochronological data, to reference sections in other continents.

Despite the biosedimentary origin of stromatolites, which are biogenic but not biological structures, first achievements in Riphean biostratigraphy were connected precisely with these organic remains. The tremendous efforts of Semikhatov, Krylov, Komar, Raaben, and Nuzhnov yielded as a result the peculiar classification of stromatolites and substantiation of their position amid fossils of biological origin that rooted out the prejudice to this group of organic remains. The stratigraphic significance of stromatolites was demonstrated by two empirical facts: (1) in Riphean sequences of North Eurasia, stromatolites are grouped into three successive taxonomically different assemblages whose composition is generally sustained at a interregional scale; and (2) close values of K–Ar glauconite age characterize stromatolite assemblages occupying the same position in the succession. These data, published in 1960 by Keller, Kazakov, Krylov, Nuzhnov, and Semikhatov were supplemented later on by new materials, which showed the autonomous position of the Vendian (Yudomian) stromatolite assemblage and substantiated the stromatolite-based four-member subdivision of the Upper Precambrian. The experience of the Russian school in stratigraphic application of stromatolites received immediately a resonance in the world and was used in North America, Australia, and Africa. This was to a significant extent a merit of Semikhatov and other scientists from the Geological Institute.

Later on, Semikhatov proved, using materials from North America and Karelian as an example, the autonomous taxonomic status of the Early Proterozoic (Aphabian) stromatolite assemblage, which was con-

sidered by Canadian researchers to be close, in some morphological features of buildups, to the Late Riphean one, thus discarding the validity of the Precambrian stromatolite-based stratigraphy. In addition, Semikhatov established the provincial status of Proterozoic (in particular Lower Proterozoic) stromatolite assemblages, which restricts to some extent their correlation potential. Recently, he and A.H. Knoll defined, using most demonstrative examples, two contrasting types of stromatolite microstructures: (1) biogenic ones whose stratigraphic position was controlled by parallel evolution of microbial communities and global environments of carbonate deposition and diagenesis; and (2) mechanogenic structures, which have no stratigraphic value and originate by cementation of clastic particles by cyanobacterial mats. These conclusions will be of undoubted significance for understanding of the early history of the Earth biosphere.

The established direct influence of paleosettings on composition of stromatolite assemblages and organic-walled microorganisms was also an extremely important step in investigation of ancient paleontological remains. Investigations of this kind, initiated about 20 years ago by Semikhatov together with Serebryakov (stromatolites), and A.F. Veis (microfossils), were recently carried out at a new level by scientists from the Laboratory of Precambrian Stratigraphy of the Geological Institute (A.F. Veis, P.Yu. Petrov, and V.N. Sergeev) and resulted in the detailed reconstruction of facies–ecological structure of ancient microbial communities.

Striving for a complex substantiation of stratigraphic interpretations in Precambrian geology and for evaluation of strong and weak points of every method was always important for Semikhatov. Focusing his interest on different isotopic–geochronological systems since 1960s, he appeared to be among first Russian researchers who analyzed factors responsible for disturbances of these systems in various, mostly sedimentary geochronometers.

Together with I.M. Gorokhov (Institute of Precambrian Geology and Geochronology), Semikhatov organized and headed the interdisciplinary research group that elaborated a new methodology for dating sedimentary successions. At the beginning of new dating procedures, the main attention is paid to the following steps: (1) determination of position of studied objects in the geochronological scale; (2) thorough compositional, structural, and crystallochemical analyses of samples subjected to isotopic analysis; (3) evaluation of their preservation degree using different criteria; (4) identification and discrimination of non-cogenetic mineral phases of epigenetic carbonates, when dating carbonate rocks by the U–Pb and Pb–Pb method, and of size-variable submicron fractions of structurally different illite, when dating shales by the Rb–Sr and K–Ar method; and (5) application of different reagents for separation of non-cogenetic phases, the isotopic systems of which differ from each other and from that of the primary phase. Important at the final stage is critical analysis of all geological, biostratigraphic, chemostratigraphic, and geochemical data characterizing the rock succession under dating. This analysis should evaluate the geological significance of every isotopic date obtained for sedimentary minerals, their different fractions, and/or crystallochemical varieties, which differ in the Rb–Sr and K–Ar systems, were formed at different stages of lithogenesis, and date different events in the diagenetic history. The works performed revealed real possibilities of sedimentary geochronometers in particular geological settings and substantially increased data on the isotopic age of Riphean and Vendian successions in Russia. They also showed confidently that the distortion of isotopic–geochronological systems of sedimentary geochronometers is a consequence of low-temperature catagenesis caused by migration of meteoric or ground waters and basinal fluids.

The same group of researchers has contributed much to the adequate understanding of variation of Sr isotopic ratio in the Riphean ocean. As early as in 1995, when they studied, applying the improved treatment method, the least altered rock samples from Siberia, which were selected on the basis strict criteria in the field and laboratory, the researchers showed that the $^{87}Sr/^{86}Sr$ ratio in Riphean seawater was substantially lower than that accepted previously. Recently, the increased data base, stiffening of geochemical criteria for selection of "best" samples, and application of previously elaborated method that partially removes secondary carbonate phases led them to nontrivial conclusion. It was shown that, in contrast to Pan-African events marking Gondwana formation, the Grenville orogenic cycle and formation of Rodinia were not accompanied by a substantial elevation of the $^{87}Sr/^{86}Sr$ ratio in the ocean, and that this ratio gradually decreased in the early Late Riphean time. The thorough geological analysis allowed Semikhatov to elucidate factors responsible for this phenomenon. He demonstrated that the mantle flux into the World Ocean prevailed during the long Riphean history over the continental runoff, and that, from this standpoint, the pre-Vendian collision and accretionary orogenic structures were principally different from the later ones.

In addition to aforementioned investigations, Semikhatov and scientists from the Institute of Precambrian Geology and Geochronology RAS studied, together with American geologists, the dynamics of changes of carbonate carbon isotope composition in the key Riphean and Vendian sections of Siberia and the Urals, including the Uralian stratotype and Uchur–Maya hypostratotype of the Riphean. This study yielded results principally important for correlation and stratigraphy of the Vendian–Cambrian boundary deposits in the southeastern, northern, and central Siberia. It also revealed stratigraphic incompleteness of upper horizons in the Upper Riphean stratotype of the Urals, and demonstrated a variable resolution ability of C-isotope chemostratigraphy for different intervals of the Riph-

ean and Vendian section. These works widened substantially the available C-isotope chemostratigraphic data on the Riphean and Vendian deposits of Russia and created basis for the practical use of chemostratigraphy in correlation.

The articles by Semikhatov, which were published during last three decades, contribute much to development of the chronostratigraphic principle of general subdivision of Precambrian and are of a paramount significance for elaboration of the modern Proterozoic stratigraphic scale of Northern Eurasia. The three-member subdivision of the Riphean that was substantiated in 1960 by Keller, Kazakov, Krylov, Nuzhnov, and Semikhatov with due account for data on stromatolites represented a first attempt to create the Precambrian chronostratigraphic scale. Nevertheless, the general scales of the Precambrian, which were officially accepted in the former USSR, were based on the chronometric principle until 1964: boundaries in those scales were determined by statistical maximums of isotope dates without any consideration concerning the particular sections. The 1st All-Union Meeting on General Problems of Precambrian Subdivision (Ufa, 1978) was a turning event, because it accepted with some modifications the general stratigraphic scale of the Proterozoic that was proposed by Semikhatov in 1974, and that was based on the analysis of the global materials. This scale that was grounded on real successions of supracrustal rocks, on stratotypes of subdivisions, and on stromatolite or microfossil assemblages and isotope-geochronological data satisfied the chronostratigraphic requirements in general and was used in domestic geological practice for a long period.

Semikhatov made a decisive contribution also to elaboration of a new Precambrian scale (Ufa, 1990) that is based on the chronostratigraphic principle as well, but is more detailed than the previous one. The same concerns the new Lower Precambrian stratigraphic scale of Russia approved in Apatity in 2000. Thus, it is evident that the chronostratigraphic principle of subdividing the Precambrian is prevailing one in our country, and this is, to a significant extent, a merit of Semikhatov. Modern Precambrian chronostratigraphic scales, in which boundaries are calibrated in accord with isotopic dates, are of particular value for geologists and biologists because they give a new view of duration and rates of most important abiotic and biotic events in the Precambrian.

The remarkable achievements of last two–three decades in Precambrian paleontology not only revealed the biostratigraphic potentialities of Proterozoic fossils, but discovered, probably, a most important chapter in the history of formation of the Earth biosphere. Recently, Semikhatov pays increasingly more attention to cyanobacterial communities that formed stromatolites and Precambrian cyanobacterial ecosystems. This line of his research sheds light on development of the early biosphere of the planet with its characteristic biogeochemical cycles. Semikhatov established several, previously unknown global reorganizations in Proterozoic ecosystems. Using as an example the positive isotopic anomaly of carbonate carbon, the largest one in the Earth history that occurred 2.3–2.06 Ga ago, he drew a conclusion about the direct influence of abundance and distribution range of cyanobacterial ecosystems on the global biogeochemical cycle of carbon. Revision of abundant planetary data on stromatolites, which he published together with Raaben in several large articles, discovered the three-modal dynamics of these biogenic structures during the Archean and Proterozoic and some other phenomena and major events in the Precambrian biosphere. These and other publications by Semikhatov are based on the synthesis of data obtained in different branches of the Earth science: in stratigraphy, paleontology, isotope geochronology, geochemistry, historical and regional geology. This approach is characteristic of many his works. What is most important, his synthesis always resulted in appearance of a new knowledge.

Semikhatov is well known as an outstanding researcher in many branches of Precambrian geology not only in Russia, but also in other countries, where he brilliantly presents a prominent experience of Russian geologists and his own achievements, which became already classical. Many years, he is the vice-chairman and member of the bureau of the Interdepartmental Stratigraphic Committee (ISC) in the USSR–Russia, chairman of the ISC Commission on Upper Precambrian, and member of several scientific councils of Russia on Precambrian geology and geochemistry. He is the authoritative scientist in important international bodies of the International Union of Geological Sciences and International Geological Correlation Program. Significant also is his role in edition of the bilingual journal "Stratigraphy and Geological Correlation" as he is the deputy editor-in-chief since the moment of the journal foundation. His prominent works published in Russia and abroad are marked by several academic, state, and social rewards. The total number of his publications is approaching three hundreds.

All friends and colleagues congratulate Mikhail Aleksandrovich Semikhatov with his 70th birthday and wish him good health and many years of creative work.

B.S. Sokolov and M.A. Fedonkin

GEOLOGY OF ORE DEPOSITS

Editor-in-Chief
Nikolai P. Laverov
Professor, Member of the Russian Academy of Sciences

GEOLOGY OF ORE DEPOSITS was founded in 1959. Since 1993 the journal has been published simultaneously in both Russian and English. The journal is one of a few special periodicals devoted to metallic minerals and the conditions of their formation and distribution. Since the advent of glasnost, many restrictions on publication of geological data have been lifted, making available more complete and concrete information on important deposits throughout the former USSR, including such unique ore districts as Noril'sk, Udokan, and Muruntau. Also included are articles submitted by foreign contributors on strategic deposits throughout the world.

Scope:

- *Economic Geology of Metal Ore Deposits*
- *New and Traditional Types of Nonmetallic Minerals*
- *Mineral Composition of Ores*
- *Experimental and Isotope Studies of Ore-Forming Systems*
- *Ore-Forming Processes and Their Physicochemical Parameters*
- *Geochronology of Ore-Forming Processes and Their Evolution*

2002 Volume 44 • ISSN 1075-7015 • Bimonthly
$1165 US/Canada
$1335 Rest of World

Tel: 800-633-4931
205-995-1567 (outside US and Canada)
Fax: 205-995-1588

INTERPERIODICA
Subscription Office
P.O. Box 1831
Birmingham, AL 35201

PETROLOGY

Editor-in-Chief
Vilen A. Zharikov
Member of the Russian Academy of Sciences

PETROLOGY is a journal of magmatic, metamorphic, and experimental petrology, mineralogy, and isotopic geochemistry. The journal offers comprehensive information on all multidisciplinary aspects of theoretical and experimental petrology. By giving special consideration to studies on the petrography of different regions of the former Soviet Union, **PETROLOGY** will provide all readers with a unique opportunity to refine their understanding of the geology of the vast territory of the Eurasian continent.

Scope:

- *Petrology of magmatic, metamorphic, and metasomatic rocks in continental and oceanic environments*
- *Experimental petrology and mineralogy*
- *Geothermobarometry*
- *Physicochemical analysis of mineral assemblages*
- *Isotopic geochemistry and geochronology*

2002 Volume 10 • ISSN 0869-5911 • Bimonthly
$1165 US/Canada
$1335 Rest of World

Tel: 800-633-4931
205-995-1567 (outside US and Canada)
Fax: 205-995-1588

INTERPERIODICA
Subscription Office
P.O. Box 1831
Birmingham, AL 35201

Subscribe to the journals from the Russian Academy of Sciences

Translated and Published by MAIK "Nauka / Interperiodica"
(International Academic Publishing Company "Nauka / Interperiodica")
Distributed Worldwide by INTERPERIODICA

Copy this form to mail or fax your order today

	TITLE	Volume	ISSN	ISSUES	RATE IN US DOLLARS US/CAN	RATE IN US DOLLARS INTERNATIONAL	YOUR ORDER
❑	Biophysics	47	0006-3509	6	$3,080	$3,210	$ _____
❑	Computational Mathematics and Mathematical Physics	42	0965-5425	12	$2,950	$3,590	$ _____
❑	Doklady Earth Sciences	382-387A	1028-334X	9	$3,455	$3,970	$ _____
❑	Doklady Mathematics	65-66	1064-5624	6	$1,690	$1,940	$ _____
❑	Entomological Review	82	0013-8738	9 + 2 Suppl.	$3,130	$3,560	$ _____
❑	Eurasian Soil Science	35	1064-2293	12 + 1 Suppl.	$2,605	$3,000	$ _____
❑	Geochemistry International	40	0016-7029	12 + 1 Suppl.	$2,940	$3,378	$ _____
❑	Geology of Ore Deposits	44	1075-7015	6	$1,165	$1,335	$ _____
❑	Geomagnetism and Aeronomy	42	0016-7932	6	$910	$1,045	$ _____
❑	Geotectonics	36	0016-8521	6	$710	$770	$ _____
❑	Herald of the Russian Academy of Sciences	72	1019-3316	6	$1,865	$2,370	$ _____
❑	Izvestiya, Atmospheric and Oceanic Physics	38	0001-4338	6 + 1 Suppl.	$1,155	$1,240	$ _____
❑	Izvestiya, Physics of the Solid Earth	38	1069-3513	12	$1,040	$1,150	$ _____
❑	Journal of Communications Technology and Electronics	47	1064-2269	12	$3,400	$3,910	$ _____
❑	Journal of Computer and Systems Sciences International	41	1064-2307	6	$2,500	$2,875	$ _____
❑	Journal of Ichthyology	42	0032-9452	9 + 2 Suppl.	$2,690	$3,095	$ _____
❑	Laser Physics	12	1054-660X	12	$2,095	$2,530	$ _____
❑	Oceanology	42	0001-4370	6 + 1 Suppl.	$1,034	$1,108	$ _____
❑	Paleontological Journal	36	0031-0301	6 + 6 Suppl.	$3,315	$3,820	$ _____
❑	Pattern Recognition & Image Analysis	12	1054-6618	4	$830	$950	$ _____
❑	Petroleum Chemistry	42	0965-5441	6	$3,375	$3,505	$ _____
❑	Petrology	10	0869-5911	6	$1,165	$1,335	$ _____
❑	The Physics of Metals and Metallography	93-94	0031-918X	12 + 2 Suppl.	$3,290	$3,790	$ _____
❑	Physics of Particles and Nuclei	33	1063-7796	6 + 1 Suppl.	$2,720	$2,890	$ _____
❑	Polymer Science. Series A	44	0965-545X	12	$3,125	$3,600	$ _____
❑	Polymer Science. Series B	44	1560-0904	6	—	—	$ _____
❑	Polymer Science. Series C	44	Pending	2	—	—	$ _____
	Polymer Science. Ser. A+B+C	44	—	20	$3,781	$4,371	$ _____
❑	Proceedings of the Steklov Institute of Mathematics	236-239	0081-5438	4 + 2 Suppl.	$1,700	$1,960	$ _____
❑	Russian Journal of Inorganic Chemistry	47	0036-0236	12 + 1 Suppl.	$3,711	$4,267	$ _____
❑	Russian Journal of Mathematical Physics	9	1061-9208	4	$730	$830	$ _____
❑	Russian Journal of Physical Chemistry	76	0036-0244	12 + 1 Suppl.	$3,710	$4,270	$ _____
❑	Russian Metallurgy (Metally)	—	0036-0295	6	$1,780	$1,940	$ _____
❑	Stratigraphy and Geological Correlation	10	0869-5938	6	$1,165	$1,335	$ _____
❑	Studies on Russian Economic Development	13	1075-7007	6	$850	$975	$ _____
❑	Thermal Engineering	49	0040-6015	12	$1,820	$2,090	$ _____
❑	Thermophysics and Aeromechanics (only distribution)	9	0869-8643	4	$780	$935	$ _____

TOTAL _____

❶ Name _____
Institution _____
Address _____
_____ State _____
City _____ Country _____
Zip/Postal Code _____
Telephone (_____)

Delivery is not made until payment is received

To order by phone call **1 800 633-4931**
or (205) 995-1567 outside the US and Canada

❷ ❑ My payment for $_____ is enclosed.
OR
❑ Bill me. My library's purchase order number is _____

❸ Send this order and payment to:
INTERPERIODICA
P.O. Box 1831
Birmingham, AL 35201-1831
Or fax this order form to (205) 995-1588

Order now for immediate delivery. All journals will be published in 2002!

MAIK "Nauka/Interperiodica" Publishing

is pleased to present to the international scientific community simultaneous Russian- and English-language publication of the journals of the Russian Academy of Sciences

MAIK "Nauka/Interperiodica" 2002 volumes include the following titles:

- *Biophysics*
- *Computational Mathematics and Mathematical Physics*
- *Doklady Earth Sciences*
- *Doklady Mathematics*
- *Entomological Review*
- *Eurasian Soil Science*
- *Geochemistry International*
- *Geology of Ore Deposits*
- *Geomagnetism and Aeronomy*
- *Geotectonics*
- *Herald of the Russian Academy of Sciences*
- *Izvestiya, Atmospheric and Oceanic Physics*
- *Izvestiya, Physics of the Solid Earth*
- *Journal of Communications Technology and Electronics*
- *Journal of Computer and Systems Sciences International*
- *Journal of Ichthyology*
- *Laser Physics*
- *Oceanology*
- *Paleontological Journal*
- *Pattern Recognition and Image Analysis*
- *Petroleum Chemistry*
- *Petrology*
- *Polymer Science, Series A*
- *Polymer Science, Series B*
- *Polymer Science, Series C*
- *Physics of Particles and Nuclei*
- *Proceedings of the Steklov Institute of Mathematics*
- *Russian Journal of Inorganic Chemistry*
- *Russian Journal of Mathematical Physics*
- *Russian Journal of Physical Chemistry*
- *Russian Metallurgy (Metally)*
- *Stratigraphy and Geological Correlation*
- *Studies on Russian Economic Development*
- *The Physics of Metals and Metallography*
- *Thermal Engineering*
- *Thermophysics and Aeromechanics**

* *Thermophysics and Aeromechanics* is only distributed by MAIK "Nauka/Interperiodica" Publishing

Please direct all inquiries about the above journals to: **INTERPERIODICA**, P.O. Box 1831, Birmingham, AL 35201-1831.
For faster service call toll-free (800) 633-4931 or (205) 995-1567 (outside US and Canada). Fax: (205) 995-1588, E-mail: interperiodica@ebsco.com

- *Applied Biochemistry and Microbiology*
- *Automation and Remote Control*
- *Biochemistry (Moscow)*
- *Biology Bulletin*
- *Colloid Journal*
- *Combustion, Explosion, and Shock Waves**
- *Cosmic Research*
- *Differential Equations*
- *Doklady Biochemistry and Biophysics*
- *Doklady Biological Sciences*
- *Doklady Chemistry*
- *Doklady Physical Chemistry*
- *Fluid Dynamics**
- *Functional Analysis and Its Applications**
- *Glass Physics and Chemistry*
- *High Energy Chemistry*
- *High Temperature*
- *Human Physiology*
- *Inorganic Materials*
- *Instruments and Experimental Techniques*
- *Journal of Analytical Chemistry*
- *Journal of Applied Mechanics and Technical Physics**
- *Journal of Evolutionary Biochemistry and Physiology*
- *Journal of Mining Science**
- *Journal of Structural Chemistry**
- *Kinetics and Catalysis*
- *Lithology and Mineral Resources*
- *Mathematical Notes**
- *Microbiology*
- *Molecular Biology*
- *Problems of Information Transmission*
- *Programming and Computer Software*
- *Protection of Metals*
- *Radiochemistry*
- *Russian Chemical Bulletin**
- *Russian Journal of Applied Chemistry*
- *Russian Journal of Bioorganic Chemistry*
- *Russian Journal of Coordination Chemistry*
- *Russian Journal of Developmental Biology*
- *Russian Journal of Ecology*
- *Russian Journal of Electrochemistry*
- *Russian Journal of General Chemistry*
- *Russian Journal of Genetics*
- *Russian Journal of Marine Biology*
- *Russian Journal of Nondestructive Testing*
- *Russian Journal of Organic Chemistry*
- *Russian Journal of Plant Physiology*
- *Russian Microelectronics*
- *Siberian Mathematical Journal**
- *Solar System Research*
- *Theoretical and Mathematical Physics**
- *Theoretical Foundations of Chemical Engineering*
- *Water Resources*

* *The journal* is produced under contracts between Plenum Publishing and the Russian Academy of Sciences and/or its divisions,the institutes, and the editorial boards, and under contract and subcontract between Kluwer Academic/Plenum Publishers and MAIK "Nauka/Interperiodica"

Please direct all inquiries about the above journals to: **Kluwer Academic/Plenum Publishers**, P.O. Box 322, 3300 AH Dordrecht, The Netherlands. Phone: (31 78) 639-2392. Fax: (31 78) 654-6474, E-mail: orderdept@wkap.nl

- *Acoustical Physics*
- *Astronomy Letters*
- *Astronomy Reports*
- *Crystallography Reports*
- *Doklady Physics*
- *JETP Letters*
- *Journal of Experimental and Theoretical Physics*
- *Optics and Spectroscopy**
- *Physics of Atomic Nuclei*
- *Physics of the Solid State*
- *Plasma Physics Reports*
- *Semiconductors*
- *Technical Physics*
- *Technical Physics Letters*

* *Optics and Spectroscopy*: Optical Society of America, 2010 Massachusetts Ave., NW, Washington, DC 20036-1023, Attn.: Publications Department. Tel. (202) 223-8130, (800) 582-0416. Fax: (202) 416-6140.

Please direct all inquiries about the above journals to: **American Institute of Physics**, Circulation and Fulfillment Services, Suite 1NO1, 2 Huntington Quadrangle, Melville, NY 11747-4502 USA. Tel. (516) 576-2270, 1-800-344-6902. Fax: (516) 349-9704, E-mail: subs@aip.org

International Academic Publishing Company "Nauka/Interperiodica" (MAIK "Nauka/Interperiodica")
Profsoyuznaya ul., 90, Moscow, 117997, Russia, Phone: 7 (095) 336-1600; Fax: 7 (095) 336-0666,
E-mail: compmg@maik.ru, http://www.maik.ru